Preclinical Testing of Bispecific T Cells Attracting Monoclonal Antibodies for Immunotherapy of Colorectal cancer

Norah Saad Alrishedan

Wolfson College

A thesis submitted to the Division of Medical Sciences, University of Oxford, in partial fulfilment of the requirements for the degree of Doctor of Philosophy in Oncology

Weatherall Institute of Molecular Medicine

University of Oxford

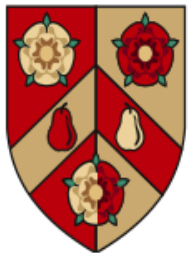

I dedicate this work to my amazing mother, who believes in me and who will always be there for me and being father and mother and best friend. To my father who passed away when I was child whom I wish he with me for this moment and be proud of me. To, my brothers Abdullah Dr. Faisal and Dr. Bandar whom taking care of me as their daughter since I was child, and to sweet and kind and my best friends my sisters Sarah, Dr.Tarfah, Mona, and Sahar.

Abstract:

Immunotherapy using bispecific monoclonal antibodies (BiMAb) is a promising cancer therapy. Such BiMAbs bind simultaneously to immune effector cells and to a cancer-specific antigen on tumour cells, resulting in killing of the latter.

The heterogeneity of tumour associated antigen (TAA) expression in a tumour as well as poor infiltration of the T cells into the tissue can pose challenges to the use of BiMAb in solid tumours, raising the need for mechanistic insights into the mode of BiMAb-dependent cell killing. It has been shown that IFNγ secreted by antigen specific T cells can act on bystander tumour cells resulting in contact independent cell killing; for efficient eradication of tumours a bystander effect is essential.

Placental alkaline phosphatase (PLAP) is an enzyme expressed on the cell surface only in the placenta not in other normal tissues. PLAP is ectopically expressed in some tumours such as ovarian tumours, seminomas, and about 20% of colon carcinoma, making it a good target for BiMAb immunotherapy.

Colorectal cancer (CRC) causes one of the highest numbers of cancer-related deaths worldwide. That emphasises the urgency to find an effective treatment to treat colon cancer. We have a collection of 116 different CRC cell lines in our lab, well characterised in terms of gene expression and mutations, providing a reliable tool to test potential therapeutic agents.

The specificity of an anti-PLAP monoclonal antibody (H17E2) produced by our lab was used to develop a BiMAb that binds to T cell co-receptor CD3ε chain and to PLAP (CD3 x PLAP BiMAb (RPLP3)).

Microarray analysis of our CRC cell lines showed that 21.5% of them express PLAP. Interestingly, immunofluorescence and FACS analysis showed that some of the lines are heterogeneous in their expression, with levels ranging from PLAP-negative to PLAP-high.

We found that the CD3-PLAP BiMAb induced specific killing of PLAP-positive colorectal cancer cell lines cultured with peripheral blood mononuclear cells (PBMCs) as source of T cells, and that the killing depends on PLAP expression.

Moreover, we found that the effect of CD3-PLAP BiMAb (RPLP3) treatment was extended to PLAP-negative cells, when co-cultured with PLAP-positive ones, indicated a bystander effect. The bystander effect on PLAP-negative cells is only visible after 48 hours of treatment, suggesting a different mechanism for the indirect killing. Understanding the mechanism behind the bystander killing would be key to improving antibody therapy for colorectal cancer. As well as understanding the cause of PLAP expression on CRC cell lines.

Acknowledgements

I am grateful to Sir Professor Walter Bodmer for his support and his being supervisor for my DPhil. I appreciate him giving me this opportunity. It is my great honour in life to be part of his team. Under Sir Prof Walter Bodmer's supervision, I learnt from his motivation and scientific insight. It would not have been possible to do this work without his generous guidance.

I am grateful to Prof. Ahmad Ahmad and Prof. Valentine Macaulay (May her soul rest in peace) for their guidance and support as second supervisors. As well I am very grateful to Dr. Vita Golubovskaya from our collaborator ProMab. As well I would like to thank sincerely my transfer and confirmation of status examiners Professor Len Seymour and Professor Ben Fairfax for their advice and suggestion which help a lot on shaping my work. I would like to thank Prof. Walter Bodmer lab members who helped me though my DPhil; specially Dr. Viorica Liebe Lastun and Dr. Ta Chun (Jeff) Liu, as well extremely thankful for Dr. Johanna Michl for her generosity and support. As well I would thank Prof. Ahmad Ahmad' lab members who warmly welcomed me and help me through my DPhil Aws Aldeka, Dr. Lili Wang, Dr. Nancy Zaarour, Dr.Amro Ahmed-Ebbiary, and Dr. May Sallam.I am very grateful for everyone in the MRC Weatherall Institute of Molecular Medicine (Oxford University & John Radcliffe Hospital) who always supported me for all the need for my research. Specially the flow cytometry facility members (Dr.Sally-Ann Clark, Dr. Craig Waugh, Dr. Kevin Clark, and Dr. Paul Sopp and health and safety DrKathryn Robson and Imaging facility Dr.Jana Koth. As well as Oncology facility members Dr. Caroline Fitchett and Dr. Andrew Mortimer. As well everyone at Wolfson College where I spent a lot of time it was memorable. I would like to thank the Ministry of Education Saudi Arabia and MISK foundation for their endless support and for sponsoring my Dphil through the scholarship. Lastly, I am grateful for my family for their unconditional love and support. Also, to all the amazing friends I met at the university of Oxford wishing them all successful happy life.

Author Declaration

I, Norah Alrishedan, hereby declare that the whole of this thesis is based on my original work at the Weatherall Institute of Molecular Medicine, University of Oxford Department of Oncology, and that neither the whole work nor any part of it has been, is being, or will be submitted for any other degree at this or any other university. The work is wholly original except as indicated by reference in the text.

Table of Contents

Preclinical Testing of Bispecific T Cells Attracting Monoclonal Antibodies for Immunotherapy of Colorectal cancer i

Abstract: iii

Acknowledgements v

Author Declaration vi

Table of Figures 12

Table of tables: 16

Chapter 1: General Introduction 17

1.1 Colorectal cancer CRC 18

1.1.1 Definition 18

1.1.2 Colorectal cancer incidence 18

1.1.3 Colorectal cancer causes 19

1.1.4 Colorectal cancer genetics 19

1.1.5 Different treatments used for colorectal cancer: 20

1.1.6 Challenges for colorectal cancer treatment 21

1.2 The immune system and cancer immunology 21

1.2.1 Cancer immunology 22

1.3 Types of Immunotherapies 23

1.3.1 Monoclonal antibody therapy for cancer (mAbs). 23

1.3.2 T cell engaging bispecific monoclonal antibody immunotherapy. 24

1.3.3 Chimeric Antigen Receptor T (CAR T) cell Immunotherapy: 29

1.3.4 T Cell Receptor Mimic Antibodies—TCRms immunotherapy: 31

1.4 T Lymphocytes 33

1.4.1 Cytotoxic T lymphocytes CD8+ T cells 35

1.4.2 Helper T cells CD4+ 36

1.4.3 γδ T cells 37

1.5 Apoptosis 38

1.5.1 Apoptotic perforin and granzyme pathway 39

1.5.2 Apoptotic intrinsic pathway 39

1.5.3 Apoptotic extrinsic pathway 40

1.5.4 Methods for apoptosis detection: 40

1.6 Proteins targeted by T cells engaging bispecific antibodies used in this thesis. 41

1.6.1 PLAP 41

1.6.2 Epithelial Cell Adhesion Molecule (EpCAM) 42

1.7 Colorectal cancer heterogeneity. 43

1.8 Aims 45
Chapter 2: Material and methods 46
2.1 List of reagents and chemicals 47
2.2 Methods of cell culture 47
2.2.1 Colorectal cancer cell lines 47
2.2.2 Peripheral blood mononuclear cell (PBMC) isolation and preparation. 49
2.2.3 CRC cell lines routine culture and maintenance. 50
2.2.4 Co-culture assay 51
2.2.5 Cell lines cryopreservation 51
2.2.6 Retrieving frozen cells. 52
2.2.7 Cell counting 52
2.2.8 Cell condition and contamination 52
2.2.9 5-Aza-2'Deoxycytidine (5-aza) Treatment 53
2.2.10 Phospholipase C treatment 53
2.2.11 Internalization assay 53
2.2.12 Transient siRNA transfection 54
2.2.13 Overexpression 55
2.3 Antibodies: 56
2.3.1 Antibodies used in immunofluorescence, Immunohistochemistry (IHC), and fluorescence-activated cell sorting (FACS)/Flow cytometry staining. 56
2.3.2 Bispecific monoclonal antibodies construct and mRNA-Lipid Nanoparticle (LNPs) 58
2.4 Immunofluorescence staining 58
2.5 Fluorescence-activated cell sorting (FACS) analysis: 60
2.5.1 Flow cytometry staining analysis 60
2.5.2 Flow cytometry sorting 60
2.6 Human Formalin-Fixed Paraffin-Embedded tissues (FFPE) staining 61
2.6.1 Immunofluorescence staining of human Formalin-Fixed Paraffin-Embedded tissues (FFPE) samples 61
2.6. 2 Immunohistochemistry (IHC) staining of human FFPE tissue samples 62
2.7 PLAP x CD3 BiMAb(RPLP3) and EPCAM x CD3 and LNPs mediated cell killing assays 64
2.7.1 BiMAbs and LNPs mediated cell killing assay by ELISA M30 64
2.7.2 Both BiMAbs and LNPs mediated cell killing assay by immunofluorescence. 64
2.7. 3 BiMAbs mediated cell killing assay by xCELLigence analyser 65
2.8 T cell subpopulation isolation 65
2.9 Statistical methods 65
2.9.1 Bimodal gene analysis by Gaussian Mixture Modeling (GMM) 65

2.9.2 Flow Jo and FACS Diva software v 8.0.3: 66
2.9.3 RTCA Software Pro: 66
2.9.4 Fiji and Qpath: 66
2.9.5 General data analysis: 66
Chapter 3: Placental alkaline phosphatase (ALPP) and placental-like 2 (ALPPL2) alkaline phosphatase expression in a panel of human colorectal cancer derived cell lines. 67
3.1 Introduction 68
3.2 Results: 70
3.2.1 ALPP and ALPPL2 expression on human colorectal cancers 70
3.2.2 The expression of *ALPP* and *ALPPL2* on colorectal cancer cell lines 72
3.2.3 Cleavage and internalization of PLAP 75
3.2.4 Internalization of anti PLAP antibody 77
3.2.5 In-house antibodies cross react with ALPPL2 and PLAP 79
3.2.6 PLAP protein expression on panel of CRC cell lines 88
3.3 Discussion: 91
Chapter 4: Testing PLAP-CD3 bispecific monoclonal antibody (RPLPh3) and EpCAM-CD3 bispecific monoclonal antibody as immunotherapy treatments for colorectal cancer. 94
4.1 Introduction 95
4.1.1 The Anti-PLAP-CD3 BiMAb (PLAPh3) and mRNA LNP delivered Anti-PLAP-CD3 BiMAb 96
4.1.2 The Anti-EpCAM-CD3 BiMAbs / mRNA LNP delivered Anti-EpCAM-CD3 BiMAb ... 97
4.2 Results 99
4.2.1 The specificity of mouse anti-PLAP antibody was used to design PLAP-CD3 BiMAb (RPLP3) 99
4.2.2 Human anti-PLAP (PLAP-CD3 BiMAb (RPLP3) binds competitively to same epitope site as Mouse anti PLAP (H17E2) 100
4.2.3. RPLP3 and H17E2 staining on colorectal cancer cell lines. 102
4.2.4 PLAP positive but not PLAP negative colorectal cancer cells lines were killed by T cells in the presence of RPLP3 105
4.2.5 PLAP positive but not PLAP negative colorectal cancer cells lines were killed by T cells in the presence of RPLP3 for 24 hours and 48 hours. 110
4.2.6 The Colorectal cancer cells lines that have ALPPL2 higher expression than ALPP were killed by T cells in the presence of RPLP3 for 24 hours and 48 hours. 112
4.2.7 The expression of EpCAM in colorectal cancer cell lines 114
4.2.8 EpCAM positive, but not the EpCAM negative colorectal cancer cell lines were killed by T cells in the presence of EpCAM antibody 115
4.2.9 PLAP CD3 BiMAb mRNA delivered to cells in a CRC cell line by LNPs shows antibody produced by the cells binds to PLAP on the cell's membrane. 118

4.2.10 EpCAM CD3 BiMAb mRNA delivered to cells in a CRC cell line by LNPs shows antibody produced by the cells binds to EpCAM on the cells in the cell line. 120

4.2.11 EpCAM positive, but not the EpCAM negative colorectal cancer cell lines were killed by T cells in the presence of LNP based delivery of mRNA coding for the antibody EpCAM BiMaB.....122

4.3 Discussion.....124

Chapter 5: Heterogeneity of PLAP expression on CRC cell lines 127

5.1 Introduction 128

5.2 Results.....129

5.2.1 Analysis of heterogeneity of PLAP expression within cell lines over time. 129

5.2.2 Analysis of PLAP expression on single cells sorted from heterogeneous CACO2. 132

5.2.3 Colony formation of sorted cells from heterogeneously PLAP expressing cell lines. 135

5.2.4 RPLP3 induces killing of low PLAP expressing cells in a CRC cell line with heterogeneous PLAP expression 141

5.3 Discussion:.....148

Chapter 6: RPLP3 (PLAP-CD3) and EpCAM CD3 BiMAb induce bystander killing on PLAP and EpCAM negative cell lines......150

6.1 Introduction: 151

6.2 Results.....153

6.2.1 Bystander killing of PLAP negative by RPLP3 153

6.2.2 Bystander killing combining RPLP3 and EpCAM CD3 BiMaB.....157

6.2.3 Killing assay using supernatant transfer of activated T cells or cell free medium.....172

6.2.4 Bystander killing by activated subtypes of T cells (CD4, CD8, Gama delta (γδ) T cells)176

6.2.5 IFNγ and TNFα induce the expression of ICAM and FAS on bystander cells. 180

6.2.6 IFNγ and TNFα released from activated T cells in the presence RPLP3 or EpCAM CD3 BiMaB induces the expression of ICAM and FAS on bystander non-target cells......183

6.2.7 Blocking bystander killing by blocking IFNγ or TNF alpha receptor and so blocking increased expression ICAM1 and FAS. 185

6.3 Discussion:.....187

Chapter 7: Expression of PLAP and EPCAM on Human FFPE tissue samples 189

7.1 Introduction: 190

7.2 Results: 191

7.2.1 PLAP is expressed in primary human colorectal cancer samples. 191

7.2.2 Quantification of PLAP expression on PLAP positive cancer patient tissue slides......195

7.2.3 Clinical outcome: 198

7.2.3 Expression of PLAP in Human normal lung tissues 200

7.2.4 PLAP expression in lung of cigarette smokers and non-smokers......202

7.3 Discussion:.....206

Chapter 8: What controls the ectopic expression of PLAP? 208
8.1 Introduction 209
8.2 Result: 210
8.2.1 5-azacytidine treatment effect on PLAP expression 210
8.2.2 Identifying candidate genes closely related to PLAP expression in CRC cell lines. 216
8.2.3 The VGLL1 association with ALPP expression in CRC cell lines. 220
8.2.4 The SLC2A3 association with ALPP expression in CRC cell lines. 222
8.3 Discussions 223
9. General discussion 225
9.1 Discussion 226
9.1.1 Placental alkaline phosphatase (PLAP) expression on colorectal cancer and other normal tissues. 226
9.1.2 Overcome Cancer antigen heterogeneity 228
9.1.3 Implication of BiMabs therapy 229
9.1.4 Future of Bispecific monoclonal antibody therapy 231
9.1.5 Concluding remarks: 233
Appendix 234
References: 239

Table of Figures

FIGURE 1.1: STRUCTURE OF THERAPEUTIC IGG 1LIKE BISPECIFIC ANTIBODIES. 26

FIGURE 1.2: DIAGRAM OF CD3 X CEA 1BISPECIFIC MONOCLONAL ANTIBODY. 27

FIGURE 1.3: THE THREE FORMATS 1OF THERAPEUTIC ANTIBODIES DEPENDING ON THEIR THERAPEUTIC PROCESS. 28

FIGURE 1.4: THE CART CELL IMMUNOTHERAPY 1PRODUCTION. 30

FIGURE 1.5: THE FUNDAMENTAL APPROACH OF 1 OF TCRMS IMMUNOTHERAPY MIMICKING THE RECOGNITION OF TCR OF T CELLS. 31

FIGURE 1.6: A. T CELL RECOGNIZES 1PEPTIDES ATTACHED TO HLA THROUGH A T CELL RECEPTOR (TCR). B. TCRM ANTIBODY RECOGNIZES THE PEPTIDE ATTACHED TO HLA SIMILARLY TO TCR RECOGNITION (D. LI ET AL., 2017B). 32

FIGURE 1.7: SCHEMATIC OVERVIEW OF 1 LYMPHOCYTE IMMUNE RESPONSE IN TWO DIMENSIONS. 34

FIGURE 3.1: ALPP AND ALPPL2 EXPRESSION OF COLORECTAL CANCER PATIENTS USING TCGA RNA-SEQ DATA. 71

FIGURE 3.2: ALPP AND ALPPL2 MRNA EXPRESSION OF PANEL OF OVER 100 COLORECTAL CANCER CELL LINES. 73

FIGURE 3.3: GMMCHI ANALYSIS OF ALPP, AND ALPPL2 CELL LINES. 74

FIGURE 3.4: PLAP CLEAVAGE BY PHOSPHOLIPASE C. 76

FIGURE 3.5: INTERNALIZATION OF ANTI PLAP ANTIBODY (H17E2). 78

FIGURE 3.6: THE AMINO ACID SEQUENCING ALIGNMENT OF HUMAN ALPP AND HUMAN ALPPL2 THE SEQUENCES OBTAINED FROM UNIPORT AND ALIGNED USING UNIPORT ALIGNMENT TOOL. 79

FIGURE 3.7: IMMUNOFLUORESCENCE CO-STAINING CRC CELL LINES WITH HD8B6 AND RPLP3 (HUMANIZED FORM OF H17E2) 80

FIGURE 3.8: SIALPP,AND SIALPPL2 KNOCKDOWN IN PLAP POSITIVE CELL LINE COLO678.SIALPP AND SIALPPL2 KNOCKDOWN EXPERIMENT IN COLO678. 83

FIGURE 3.9: OVER EXPRESSION OF ALPP AND ALPPL2 ON NEGATIVE CELL LINES (LS180, HT29). 86

FIGURE 3.10: HUMAN PLACENTA AND HUMAN TESTIS TISSUES STAINED WITH HD8B6 AND RPLP3 (HUMANIZED FORM OF H17E2) 87

FIGURE 3.11: PLAP EXPRESSION IN CRC CELL LINES BY IMMUNOFLUORESCENCE AND FACS. .. 90

FIGURE 4.1: DIAGRAM OF CD3 X EPCAM BISPECIFIC MONOCLONAL ANTIBODY FORMATS. 98

FIGURE 4.2: H17E2 AND RPLP3 STAINING SPECIFICITY FOR PLAP POSITIVE COLO678 CELLS BY FACS ANALYSIS 99

FIGURE 4.3: BINDING OF H17E2 AND RPLP3 ON THE SAME ANTIGENIC SITE. 101

FIGURE 4.4: 5 COLORECTAL CANCER CELL LINES PLAP STAINING WITH RPLP3. 104

FIGURE 4.5: PLAP-POSITIVE AND NOT PLAP-NEGATIVE COLORECTAL CANCER CELL LINES ARE KILLED BY T CELLS IN THE PRESENCE OF RPLP3. 107

FIGURE 4.6: PLAP-POSITIVE (LOVO, COLO678, DLD1) AND NOT PLAP-NEGATIVE COLORECTAL CANCER CELL LINES (HT29, LS180) ARE KILLED BY T CELLS IN THE PRESENCE OF RPLP3.109

FIGURE 4.7: PLAP-POSITIVE AND NOT PLAP-NEGATIVE COLORECTAL CANCER CELL LINES ARE KILLED BY T CELLS IN THE PRESENCE OF RPLP3 CRC CELL LINES WERE TREATED WITH 5NM RPLP3 AND CO CULTURE WITH PBMC IN RATIO EFFECTOR CELLS TO CANCER CELLS (1:10). 111

FIGURE 4.8. ALPP, ALPPL2 - POSITIVE AND 1AND NOT ALPP, ALPPL2-NEGATIVE COLORECTAL CANCER CELL LINES ARE KILLED BY T CELLS IN THE PRESENCE OF RPLP3. 113

FIGURE 4.9: THE ANALYSIS BY USING GAUSSIAN 1MIXTURE MODELING (GMM) TO DRAW THE DISTRIBUTION OF EXPRESSION AND THE IDENTIFICATION OF EPCAM NEGATIVE OR WEAKLY POSITIVE CELL LINES. 114

FIGURE 4.10: EPCAM-POSITIVE AND NOT EPCAM 1-NEGATIVE COLORECTAL CANCER CELL LINES ARE KILLED BY T CELLS IN THE PRESENCE OF EPCAM CD3 BIMAB. 116

FIGURE 4.11: EPCAM-POSITIVE DLD1 BUT NOT 1 EPCAM-NEGATIVE CC20 COLORECTAL CANCER CELLS ARE KILLED BY T CELLS IN THE PRESENCE OF EPCAM CD3 BIMAB. 117

FIGURE 4.12: COLORECTAL CANCER CELL LINES 1PLAP STAINING WITH PLAP-CD3 MRNA LNPS. 119

FIGURE 4. 13: COLORECTAL CANCER CELL LINES 1 EPCAM STAINING WITH EPCAM-CD3 MRNA LNPS. IMMUNOFLUORESCENCE STAINING USING MRNA LNPS DELIVERED EPCAM-CD3 BIMAB ON EPCAM POSITIVE HT29 AND EPCAM NEGATIVE CC20..... 121

FIGURE 4.14: A. EPCAM CD3 BIMAB MRNA LNP 1INDUCED KILLING IN THE EPCAM POSITIVE COLORECTAL CANCER CELL LINE (CCO7), BUT NOT IN EPCAM NEGATIVE CRC CELL LINE (CC20). 123

FIGURE 5.1: ANALYSIS OF HETEROGENEITY OF 1 PLAP EXPRESSION IN CACO2 AND OXCO3 CELL LINES OVER TIME. 131

FIGURE 5.2: ANALYSIS OF PLAP EXPRESSION 1 ON SINGLE CELL COLONIES FROM THE HETEROGENEITY OF PLAP EXPRESSING CACO2. 134

FIGURE 5.3: METHOD OF CELL SORTING BY FACS 1ON CACO2, DLD1 AND CCO7..... 137

FIGURE 5.4 THE COLONIES FORMATION OF SORTED 1SORTED CACO2. 138

FIGURE 5.5: THE COLONIES FORMATION OF SORTED CACO2 1. 139

FIGURE 5.6: COLONY FORMATION OF SORTED CCO7 1 CELLS. 140

FIGURE 5.7: RPLP3 INDUCED KILLING ON LOW 1PLAP EXPRESSING OR HETEROGENEOUS PLAP EXPRESSING CELL LINES, CACO2. 143

FIGURE 5.8: PLP3 INDUCED KILLING ON LOW 1PLAP EXPRESSING OR HETEROGENEOUS PLAP EXPRESSING CELL LINES, DLD1. 145

FIGURE 5.9: RPLP3 INDUCED KILLING ON LOW 1PLAP EXPRESSING OR HETEROGENEOUS PLAP EXPRESSING CELL LINE CCO7. 147

FIGURE 6.1: DIAGRAM OF BISPECIFIC MONOCLONAL 1MONOCLONAL ANTIBODY INDUCES KILLING OF TAA POSITIVE TUMOUR CELL AND LATER INDUCED BYSTANDER KILLING ON TAA NEGATIVE TUMOUR CELLS. 152

FIGURE 6.2: BYSTANDER KILLING MEDIATED BY 1RPLP3 MEASURED BY ELISA M30. 154

FIGURE 6.3. BYSTANDER CELL KILLING MEDIATED 1BY RPLP3 MEASURED BY IMMUNOFLUORESCENCE. 156

FIGURE 6.4 PLAP AND EPCAM STAINING ON DLD1 AND CC20 1. 160

FIGURE 6.5: BYSTANDER CELL KILLING MEDIATED BY RPLP3 MEASURED BY ELISA M30 1. 161

FIGURE 6.6 BYSTANDER KILLING MEDIATED BY 1RPLP3 BIMAB MEASURED BY IMMUNOFLUORESCENCE STAINING. 162

FIGURE 6.7 BYSTANDER CELL KILLING MEDIATED 1BY RPLP3, EPCAM CD3 BIMAB MEASURED BY XCELLIGENCE REAL-TIME CELL ANALYSIS. 167

FIGURE 6.8 BYSTANDER CELL KILLING MEDIATED 1BY RPLP3, EPCAM CD3 BIMAB MEASURED BY XCELLIGENCE REAL-TIME CELL ANALYSIS. 171

FIGURE 6.9 ACTIVATED T CELLS AND FILTERED 1MEDIUM TREATMENT OF NEGATIVE CELLS FOR 24 HOURS AND 48 HOURS. 174

FIGURE 6.10 KILLING BY ACTIVATED T CELL 1TREATMENT OF NEGATIVE CELLS FOR 48 HOURS ASSESSED BY CLEAVED CASPASE 3 STAINING. 175

FIGURE 6.11 SUGGESTED BYSTANDER KILLING 1MEASURED BY THE ELISA M30 ASSAY USING T CELL SUBSETS. DLD1 IS PLAP, EPCAM POSITIVE AND CC20 IS PLAP AND EPCAM NEGATIVE. 179

FIGURE 6.12 UPREGULATION OF FAS AND ICAM 1 ON CRC CELL LINE ON RESPONSE TO INCUBATION WITH IFNΓ AND TNFA. 181

FIGURE 6.13 UPREGULATION OF FAS AND ICAM 1ON CRC CC20 CELL LINE ON RESPONSE TO INCUBATION OF IFNΓ AND TNFA INCUBATION. 182

FIGURE 6.14: UPREGULATION OF FAS AND ICAM 1 ON CC20 WHEN IT WAS CO-CULTURED WITH DLD1 50% CC20 AND 50% DLD1 AND ANTIBODIES AND PBMCS. 184

FIGURE 6.15: THE EFFECT OF BLOCKING ICAM 1, FAS, IFNΓ OR TNFR ON SUGGESTED BYSTANDER KILLING OF CC20. 186

FIGURE 7.1: SUBSET OF HUMAN COLORECTAL CANCER 1FFPE SLIDES WHICH ARE POSITIVE FOR PLAP. 192

FIGURE 7.2: SUBSET OF HUMAN COLORECTAL CANCER 1FFPE SAMPLES WHICH ARE PLAP NEGATIVE. HUMAN NORMAL COLON IS PLAP NEGATIVE. 193

FIGURE 7.3: IHC STAINING FOR PLAP BY HD8B6 1ON HUMAN PLACENTA AND ON HUMAN COLORECTAL CANCER SAMPLES. 194

FIGURE 7.4: SINGLE CELLS EXPRESSION DATA 1FOR PLAP ON HUMAN TISSUES. IT SHOWS PLAP MRNA EXPRESSION ON ALVEOLAR CELL TYPE 1 IN LUNG (PONTÉN ET AL., 2008). THE DATA IS OBTAINED FROM HUMAN PROTEIN ATLAS. 200

FIGURE 7.5: HUMAN LUNG STAINING WITH RPLP3 1AND AUA1 IN DIFFERENT POSITIVE AREAS (A). (B) IS NEGATIVE CONTROL FOR STAINING ON HUMAN LUNG TISSUE SLIDES STAINED WITH SECONDARY ANTIBODIES ONLY (GOAT ANTI MOUSE ALEXA FLUOR 568 AND RABBIT ANTI HUMAN 488 ALEXA FLUOR). 201

FIGURE 7.6. IHC STAINING FOR PLAP USING 1ANTI-PLAP HD8B6 AND ANTI-EPCAM AUA1 ON HUMAN LUNG TISSUE. 201

FIGURE 7.7: FFPE SAMPLE OF HUMAN NORMAL 1LUNG. THE RED CIRCLES INDICATE THE AREA OF PLAP/ EPCAM EXPRESSION. PLAP IS GREEN AND STAINED WITH ANTI-PLAP MOUSE ANTI PLAP (HD8B6) AND SECONDARY ANTI MOUSE ALEXA FLUOR 488. 202

FIGURE 7.8 IMMUNOFLUORESCENCE STAINING OF 1PLAP/EPCAM ON HUMAN NORMAL LUNG OF SMOKER OR NONSMOKER SAMPLES. 205

FIGURE 8.1:5-AZA TREATMENT OF CC20 FOR DIFFERENT 1TIMES. FACS STAINING OF PLAP OF CC20 PLAP- NEGATIVE CELL LINE TREATED WITH 10UM OF 5-AZA AND AN UNTREATED CONTROL WITH ANTI-PLAP (H17E2). RED IS CONTROL AND BLUE IS 5- AZA TREATED. 211

FIGURE 8.2: 5-AZACYTIDINE TREATMENT OF CRC 1CELL LINES. IF STAINING OF PLAP ON CRC CELL LINES AFTER TREATMENT WITH 10UM 5AZA FOR 72 HOURS. 212

FIGURE 8.3: 5-AZACYTIDINE TREATMENT TO SUBSETS 1OF SORTED CELLS FROM HIGH, LOW, AND ORIGINAL POPULATION OF CRC CELL LINES. 215

FIGURE 8.4: VOLCANO PLOT OF GENES ASSOCIATES 1WITH ALPP AND ALPPL2 POSITIVE MRNA EXPRESSION (RIGHT HAND) VERSUS NEGATIVE EXPRESSION (LEFT HAND). GENES WITH STRONGLY ASSOCIATED EXPRESSION DIFFERENCE ARE ENCIRCLED. 218

FIGURE 8.5: GMMCHI OF GENES THAT ARE CORRELATED 1WITH PLAP. 219

FIGURE 8.6 5-AZA TREATMENT OF CRC CELL 1LINES FOR 72HOURS. FACS STAINING OF VGLL1 IN CRC CELL LINES TREATED WITH 10UM OF 5-AZA (BLUE) COMPARED WITH UNTREATED CONTROL (RED). 221

FIGURE 8.6 5-AZA TREATMENT OF CRC CELL 1LINES FOR 72HOURS. FACS STAINING OF VGLL1 IN CRC CELL LINES TREATED WITH 10UM OF 5-AZA (BLUE) COMPARED WITH UNTREATED CONTROL (RED). 221

FIGURE 8.7 VGLL1 SIRNA KNOCK DOWN ON PLAP 1POSITIVE COLO678. IF STAINING OF PLAP AND VGLL1 WITH SISCRAMBLE AS CONTROL. 222

FIGURE 9 1: GMMCHI OF MAGEA3. BLUE HASHED 1BARS ARE MAGEA3 POSITIVE CELL LINES. . 232

Table of tables:

TABLE 2.1: X CRC CELL LINES USED FOR PLAP 1 AND EPCAM KILLING ANALYSIS IN THIS THESIS AND THE ORIGINAL SOURCES. 48

TABLE 3.1 2X2 TABLE OBTAINED BY GMMCHI OF 2 TCGA RNA-SEQ DATA FOR BOTH GENES ALPP AND ALPPL2..... 71

TABLE 3 2: THE 2X2 TABLE OBTAINED BY GMMCHI 1 OF CRC CELL LINES MRNA DATA FOR THE ASSOCIATION BETWEEN ALPP AND ALPPL2 EXPRESSION. 75

TABLE 3 3: MRNA ALPP AND ALPPL2 EXPRESSION 1 IN A SELECTED SUBSET OF CRC CELL LINES. 89

TABLE 4.1 MRNA EXPRESSION OF ALPP, ALPPL2 1 ON SELECTED CRC CELL LINES. 108

TABLE 6.1: MRNA EXPRESSION (LOG2) OF ALPP 1 *EPCAM* IN CRC CELL LINES USED TO STUDY BYSTANDER KILLING..... 157

TABLE 6.2: MRNA EXPRESSION OF ICAM1 AND 1 FAS ON SELECTED CRC CELL LINES... 180

TABLE 7.1: TABLE SHOWS THE QUANTIFICATION OF 1 OF EPCAM AND PLAP EXPRESSION ON COLORECTAL CANCER PATIENTS' SAMPLES. IT SHOWS THE PERCENTAGE OF PLAP EXPRESSION OUT OF EPCAM POSITIVE STAINING. 196

TABLE7.2 CLINICAL DATA FOR PATIENT'S DONORS 1 199

TABLE 7.3: CLINICAL AND SMOKING DATA FROM 1 NORMAL LUNG DONORS OF FFPE SLIDES USED FOR PLAP STAINING..... 203

TABLE 8.1 CRC CELL LINE LISTS OF PLAP POSITIV1AND LOW/NEGATIVE PLAP CRC CELL LINES USED TO GENERATE THE VOLCANO PLOT..... 217

TABLE 8.2 GENES ARE 1 ARE ASSOCIATED WITH *ALPP POSITIVELY OR NEGATIVELY*. THE GENES POSITIVELY ASSOCIATED ARE SLC2A3 AND VGLL1 AND GENES NEGATIVELY ASSOCIATED ARE RNASE4, LRRC31, METTL7A, AGR3 AND OLFM4.... 218

Chapter 1: General Introduction

1.1 Colorectal cancer CRC

1.1.1 Definition

Colorectal cancer (CRC) is a cancer of the large bowel which can affect the colon, the rectosigmoid junction, and the rectum (Vieira et al., 2021) . Colorectal cancer is initiated from adenomas which can develop into carcinomas (Cappell, 2008a) . The colorectum is nearly five feet long and consist of four parts: the descending colon and the ascending colon, the transverse colon, and sigmoid colon and the cecum (Azzouz & Sharma, 2023).The main function of the colon as part of the gastrointestinal tract is metabolizing food as well as absorbing and producing vitamins, water, electrolytes and vitamins, and forming faeces (Sulaiman & Marciani, 2019)(Azzouz & Sharma, 2023).

1.1.2 Colorectal cancer incidence

Colorectal cancer is considered as the cancer with the third highest occurrence and is the second deadliest cancer worldwide (Bray et al., 2018). Colorectal cancer is ranked as the third most frequent cancer for men and the second most common for women (Maida et al., 2017). The percentages of death caused by colon or rectal cancer is estimated to increase to 60% of colon cancer, and to 71.5 % for rectal cancer by 2035 (Araghi et al., 2019a).

1.1.3 Colorectal cancer causes

Key factors which influence the incidence of colorectal cancer are age and environmental influences, especially diet (Dekker et al., 2019) . Family history showing genetic inheritance is also a factor that contributes to colorectal cancer incidence (Henrikson et al., 2015). Obesity has been suggested as a highly associated factor influencing the incidence of colorectal cancer in women (Thrift et al., 2015). To reduce the mortality rate caused by the disease, an early screening for colorectal cancer is strongly suggested (Ransohoff, 2005).

1.1.4 Colorectal cancer genetics

Common genetic mutations seen in sporadic colorectal cancer are in the *APC* (Adenomatous polyposis coli) gene, occurring with up to 70% being the first mutated gene in all colorectal cancers (Armaghany et al., 2012). Both *KRAS* (Kirsten rat sarcoma virus) and, *TP53* genes (Tumour Protein P53) being the next commonest (Armaghany et al., 2012) (W. F. Bodmer, 2006). Familial adenomatous polyposis (*FAP*) as a dominantly inherited susceptibility that occurs in about 1 per 8,000 of the population and so accounts for about 25% of all colorectal cancers and is caused by mutations in the *APC* gene (W. Bodmer & Bodmer, 1999; W. F. Bodmer, 2006;) . The *APC* gene is also the most mutated gene in non- familial sporadic colorectal cancer and due to *APC* mutations occurring in most Familial adenomatous polyposis and sporadic colorectal cancer patients, it is considered as primary factor for cancer formation (W. F. Bodmer, 2006). Other genes found in colorectal cancer that are relatively commonly mutated or methylated include: *CNNBT* (beta catenin), *CDH1* (E-Cadherin), *TCF7L2*, hMSH2, *hMSH6 ATM*, *CDKN2A, FBXW7*, *ERBB2* (W. Bodmer & Golubovskaya, 2023a).

1.1.5 Different treatments used for colorectal cancer:

The treatment of colorectal cancer depends on the stage of the disease (Araghi et al., 2019b). Different treatments are used for colorectal cancer, either surgical, radiotherapy, or targeted therapy (W. Zhao et al., 2022a). Surgery is often curative, if the colon cancer is not metastatic and at an early stage, by removing the tumour, including surrounding tissues around the colorectal cancer site (Biller & Schrag, 2021) (Thanikachalam & Khan, 2019). Laparoscopic surgery is now a commonly used method of surgical treatment for metastatic or primary cancer (Kuipers et al., 2015). Considering the patient's age or cancer's stage, doctors can select the type of treatment; patients with stage I and stage II are mostly treated and cured by surgery and, patients with stage III colorectal cancer can be treated with a combination of chemotherapy and surgery, metastatic cancer can be treated with chemotherapy alone or with a combination of therapies (Papamichael et al., 2015). The combination of two adjuvant therapies (levamisole and fluorouracil) is potent treatment to improve the survival of colorectal cancer patients with stage III by 33% and can lower the disease recurrence up to 41% (Moertel et al., 1990). Radiotherapy in combination with chemotherapy is a common method of treatment for CRC cancer patients in stage II/III, using radiotherapy is effective in reducing the size of tumour and reducing the recurrence of the tumour (Shi et al., 2023) (Benson et al., 2022). Immunotherapies is type of targeted therapy to a specific site of the tumours and the immune cells, it can be in form of nanoparticles, antibodies or cell-based therapy (Wang et al., 2017).

1.1.6 Challenges for colorectal cancer treatment

Early screening, detection, and treatment of colorectal cancer, for example by the removal of adenomatous polyps, can increase survival rate which reduce death caused by the disease, however, many countries lack the facilities to provide suitable health care (Araghi et al., 2019b). Due to the difficulties of diagnosing and screening colorectal cancer at early stages, many cancers are diagnosed at later stages when they have obvious symptoms, which limits the effectiveness of currently available treatments (W. Zhao et al., 2022b). There are also unpleasant side effects of current chemotherapy (André et al., 2004). All these factors urge the development of novel therapy. The mutations or epigenetic changes in tumour cells create the differences between cancer cells, and normal cells which can then be potentially targeted by targeted therapy such as immunotherapy(Mellman et al., 2023).

1.2 The immune system and cancer immunology

The immune system protects the body from pathogens carrying foreign antigens (Parkin & Cohen, 2001b; Tomar & De, 2014). The mammalian immune system consists of the innate and adaptive immune systems(Parkin & Cohen, 2001b; Tomar & De, 2014). The innates system usually attacks first by recognising features commonly found on different pathogens allowing time for the adaptive system to recognise particular foreign features on particular pathogens (Parkin & Cohen, 2001a). The innate immune system is rapid and fast to provide the initial defence against a new pathogen by making chemical, physical and cellular defence mechanism, while adaptive immune system takes time for developing its defence, its defence using B lymphocytes to produce antibodies to the foreign components and cytotoxic T cells to kill infected pathogens by recognising foreign antigens on the surfaces of infected cells (Parkin & Cohen, 2001a).The innate

immune system encompasses of physical barriers such as skin, gut and lung, as well cellular like polymorphonuclear leukocytes, mast cells and macrophages, their immune recognition to the antigens through pattern recognition receptors located on the bloodstream and on the cell surface or inside the cells (Janeway & Medzhitov, 2002).The adaptive immune system may also recognise foreign chemical features of cancers as if they were pathogens and so may play an important role in naturally attacking cancers and developing novel tools for the treatment of cancers (Netea et al., 2011)

1.2.1 Cancer immunology

The relation between the immune system and cancer has long been of interest (Mellman et al., 2023). To what extent does the adaptive immune system play a natural role in attacking cancers? (Ribas, 2015). There are many different mechanisms by which a cancer can escape immune attack so that in general the immune system does not protect much against cancers except for certain cancers that have large numbers of mutations, for example, due to the effects of sunlight on skin, of cigarette smoking on lung cells and mutations in certain types of DNA repair genes (Mellman et al., 2023) (Jiang et al., 2021; N. Liu et al., 2024) . There is different mechanism which cancer can trigger to attack or suppress the immune system activation, as well immune system can help in initiation or prognosis of the tumour through different mechanisms such chronic inflammation, or through dysfunctional humoral which help in cancer initiation or cancer prognosis, investigating the relation between them can improve the direction of immunotherapy (Prestwich et al., 2008). Immunotherapy in cancer principles started back in the 19th century, when William Coley started testing the idea in 1881 of used bacterial toxin as an immunotherapy on patient suffering from sarcoma (COLEY, 1891).

1.3 Types of Immunotherapies

1.3.1 Monoclonal antibody therapy for cancer (mAbs).

Monoclonal antibody (mAbs) therapies to treat cancer are diverse and designed to target different types of markers or trigger different immune cells to kill cancer cells (Samaranayake et al., 2009). The work on developing mAbs is promising and advances the scope for cancer treatment (Samaranayake et al., 2009).

Monoclonal antibody therapy has been used for cancer therapy either based on their ability, for example, to block key receptor functions, such as the interaction between the epithelial growth factor (EGF) and its receptor (EGFR), or on their ability to mediate immune-based killing of antibody targeted cancer cells by different populations of lymphocytes (Silberstein et al., 2015).

Most direct killing by straightforward humanized antibodies is mediated by NK cells, for example, the hPR1A3 anti- Carcinoembryonic antigen (CEA) antibody has been shown to mediate antibody-dependent cellular cytotoxicity on panel of colorectal cancer cell lines (Conaghan et al., 2008). Recently a newer type of immunotherapy, pembrolizumab, which is a humanized antibody that acts as an anti- PD-1 immune check point inhibitor, gives promising results for mismatch repair defective colorectal cancers, these are CRCs with genetic mutations leading to microsatellite DNA instability caused by accumulating of various somatic mutations comparing to mismatch proficient colorectal cancer which has a lower respond to pembrolizumab (Le et al., 2015).

Vascular endothelial growth factor monoclonal antibody immunotherapy (Bevacizumab) has also shown positive effects in the treatment of colorectal cancer in combination with chemotherapy (Hurwitz et al., 2004) (Cappell, 2008b). Immune checkpoint blocking by mAbs such as anti-CTLA4 and anti-PD-L1 increase anti-tumour activity (Iwai et al., 2002) (Leach et al., 1996). The Anti- CTLA4 mAbs ipilimumab and tremelimumab have been approved by the FDA as anti-tumour treatments (Pardoll, 2012).

The advancement of mAb-based cancer treatment faces challenges such as mAb production costs and choice of novel mAb targets (Samaranayake et al., 2009). There are also side effects due to unwanted immunoreactions, but these are not usually very serious (Silberstein et al., 2015). With a wide variety of new methods for engineering mAbs, more advanced antibodies can, for example, be engineered to bind to more than one epitope, as described in the next section (Hosseini et al., 2021).

1.3.2 T cell engaging bispecific monoclonal antibody immunotherapy.

The first engineered monoclonal antibody approved for the human therapeutics of transplanted rejection was muromonab-CD3 (OKT3) in 1985, followed by the monoclonal anti CD20 (+), rituximab, for non-Hodgkin lymphoma treatment in 1997 (Kyriakidis et al., 2021). There are now more than 27 antibodies approved for the treatment of different types of diseases (Z. Wu & Cheung, 2018).

Monoclonal antibody production in the mouse by the hybridoma technology was invented by Hans Kohler and Caesar Milstein (Köhler & Milstein, 1975). Alfred Nisonoff had earlier initiated the idea of engineering the antibody antigenic binding sites (Nisonoff & Rivers, 1961). Antibody engineering, including for example humanisation of mouse monoclonal antibodies is now applied in a wide variety of ways to the development of

bispecific antibody designs with multiple binding and recognition sites (Fischer et al., 2004).

Bispecific T cell attracting monoclonal antibodies (BiMAb) are antibodies that bind a cancer target antigen, for example, CEA, and a T cell attracting target, usually the epsilon chain of CD3(CD3ε) found on nearly all T cells (Bacac et al., 2016a). The T cells are in this way attracted to the immediate vicinity of the target tumour cells and are thereby activated to kill the tumour cells not dependent on a T cell receptor TCR engagement signal, or a co-stimulation signal (Klinger et al., 2016a) . At the T cells and cancer cell synapse, the T cell activation releases cytolytic granules and induces apoptosis of cancer cells, this mechanism is explained in following section (Huehls et al., 2014a). The structures of such bispecific antibodies can be engineered in a variety of ways Figure 1-1 (Hosseini et al., 2021b) (Runcie et al., 2018a).

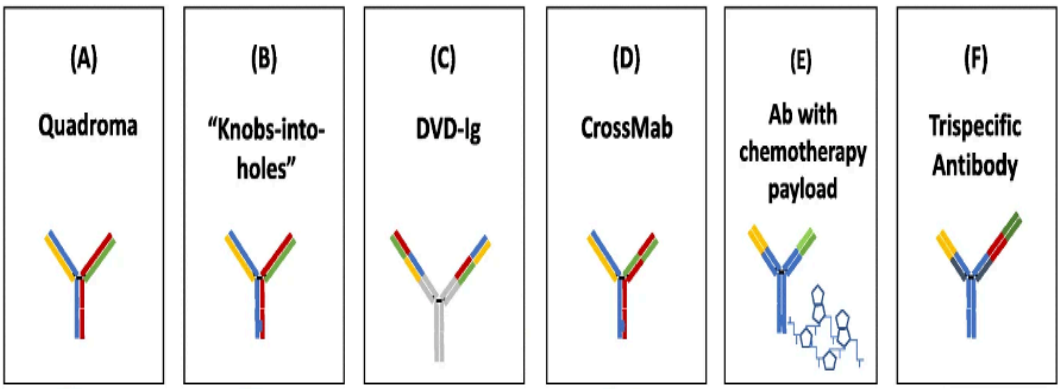

Figure 1.1: Structure of therapeutic IgG like bispecific antibodies.
A. Quadroma formatted by fusing heavy chain and light chain of two monoclonal antibodies. (B) Knobs into holes is technology design by inserting mutation on CH3 used to format the bispecific antibody with preventing the mispairing chains in bispecific antibody production. (C) Dual-Specific Antibody is a format of bispecific antibody that has dual specificity due to fusing two variable domains of two antibodies. (D) CrossMab is technology to format the bispecific antibody for enhancing the light chain interaction by swapping CH1 and the constant domain. (E) Bispecific antibody with chemotherapy payload has two unique antigen-binding sites and a chemotherapy payload attached to the constant domain (F) A Trispecific antibody is formatted to have three antigenic binding sites (Runcie et al., 2018b).

There are over 60 formats for designing therapeutic bispecific antibodies (Spiess et al., 2015). They are usually first derived from a suitable mouse anti-human target, such as CEA (CEACAM5), whose antigen recognition sequences are incorporated into a human framework antibody (Bacac et al., 2016a). This is then engineered to include an anti-human CD3ε antibody and mutations in the Fc portion of the overall structure to prevent unwanted Fc mediated activity (Bacac et al., 2016a). (See Figure 1.2 A). The simultaneous binding of BiMAbs to a tumour associated antigen on cancer cells and to CD3ε on T cells results in redirection and activation of T cells and subsequent tumour cell cytotoxicity as illustrated in (Figure 1-2 A) (Bacac et al., 2016b) (Klinger et al., 2016b).

Almost 30 antibodies have been approved by the Food and Drug Administration (FDA) of the USA as cancer treatment (Suurs et al., 2019a). Blinatumomab is a type of targeted immunotherapy showing higher survival by 31% compared to chemotherapy 12% on adult patients with relapsed or refractory B-cell precursor ALL (Kantarjian et al., 2017). Catumaxomab is an example of a bispecific antibody immunotherapy at first approved for cancer therapy, it is designed to bind to Epithelial cell adhesion molecule (EpCAM) on one arm and bind to CD3 on another arm but removed from use following unacceptable side effects. (Seimetz et al., 2010).

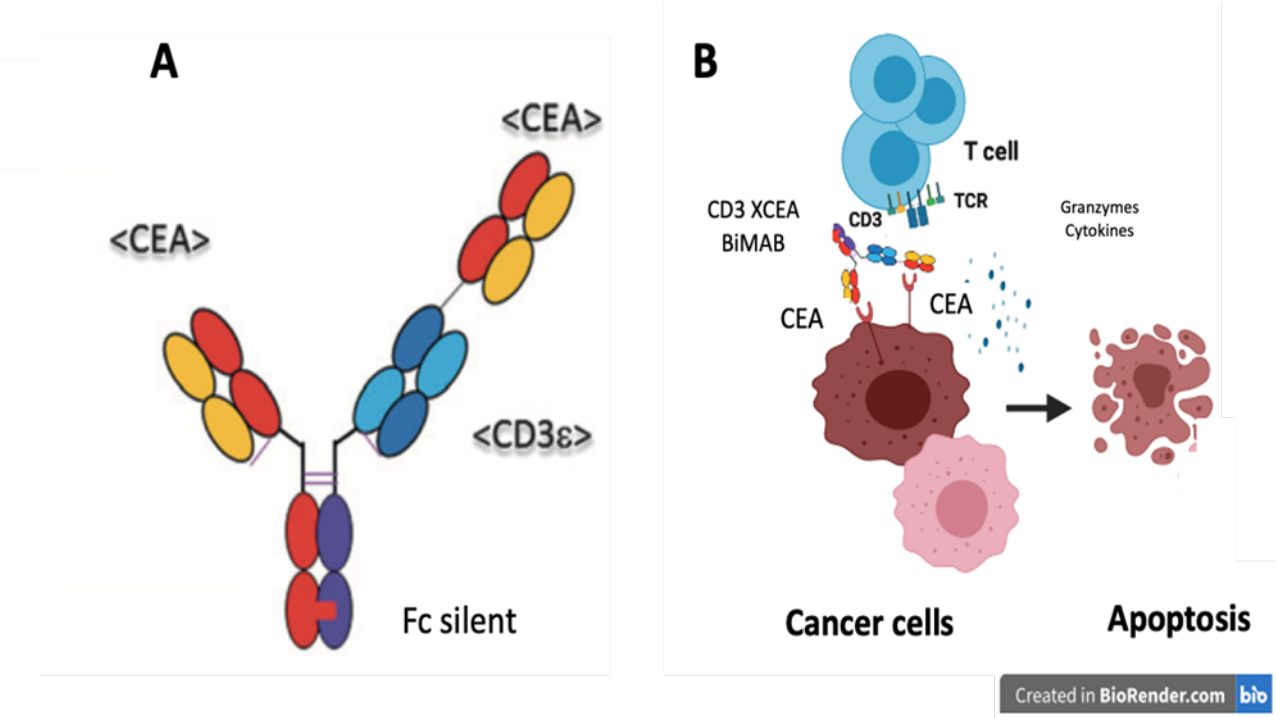

Figure 1.2: Diagram of CD3 X CEA bispecific monoclonal antibody.
A.CD3 X CEA BiMAb has one CD3-, two CEA-binding sites, and an engineered silent Fc region. It consists of four peptides; two (red) heavy chains bind to CEA. Its specificity comes from CEA (CEACAM5) (Bacac et al.,2016a). The blue part of the heavy chains from CEA (CEACAM5) and anti CD3 antibodies. B. CD3 X CEA BiMAb recruits T cells to CEA positive cancer cells, resulting in T cell activation, release of cytolytic granules and subsequent apoptosis of CEA Positive cancer cells (Bacac et al., 2016b).

Therapeutic antibodies can be formatted to be antibodies, which target one antigen or target two antigens on two different cells cancer cells and T cells and named as T cell engagers, or they can be formatted to target two antigens on the same cell, called non T cell engager such as Amlvantamab which binds to EGFR (epidermal growth factor receptor) and MET (Hepatocyte growth factor receptor), or therapeutic antibodies ca be conjugated with toxin or radioisotopes for their therapeutic function (Figure 1.3) (Paul et al., 2024).

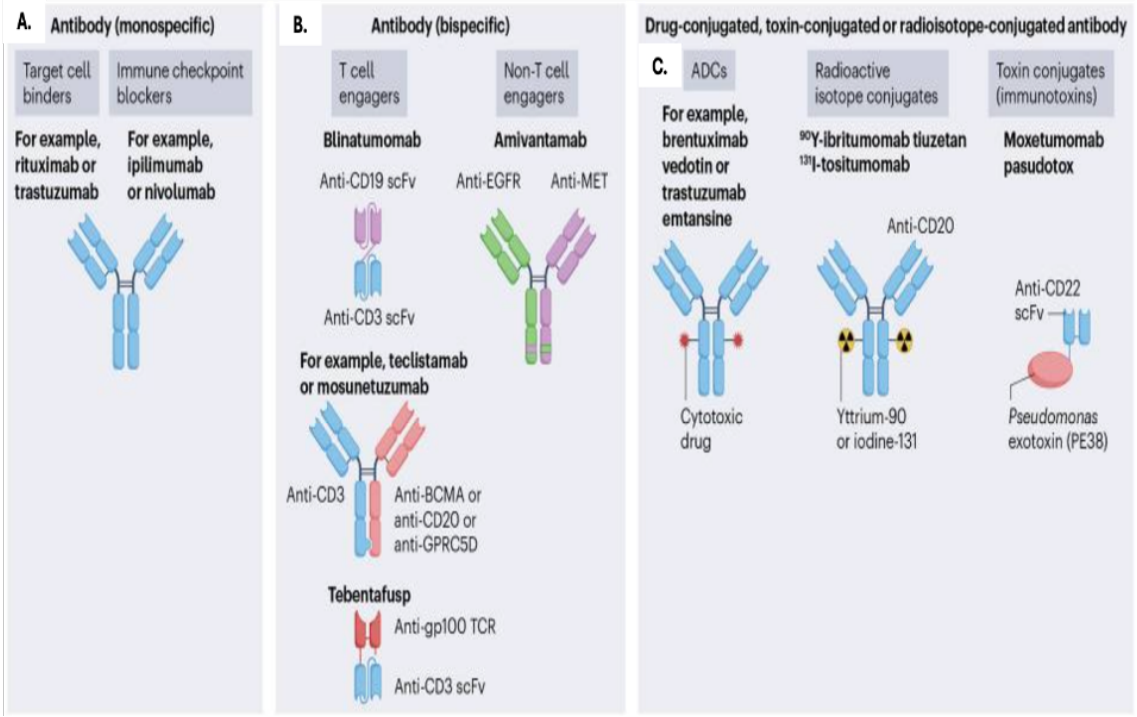

Figure 1.3: The three formats of therapeutic antibodies depending on their therapeutic process.
A. Monospecific antibodies. B. Bispecific antibodies, C. Drug-conjugated, toxin-conjugated or radioisotope-conjugated antibodies (Paul et al., 2024).

1.3.3 Chimeric Antigen Receptor T (CAR T) cell Immunotherapy:

The Chimeric Antigen Receptor T (CAR T) cell immunotherapy innovation is a personalized therapy, which is based on utilizing patients' immune cells to induce killing of cancer cells, that by introducing genetic engineering changes on patients' T cells by attaching the recognition portion of a monoclonal antibody which has specificity to an antigen on certain cancer cells (W. Bodmer & Golubovskaya, 2023b). This recognition induces immune-mediated tumour killing instead of the usual T cell receptor antigenic recognition of cells which is dependent on HLA- associated peptide recognition (Figure 1.4) (W. Bodmer & Golubovskaya, 2023c). The first generation of CAR T cells involve has one intracellular domain (CD3ζ), the second generation of CART cells has one additional costimulatory domain, and third generation CART cell has two costimulatory domains (Maus et al., 2014). CAR T cell therapy has proved to be potent treating blood cancer but not solid cancers (Golubovskaya & Wu, 2016). There are CAR T cell therapies already undergoing clinical study including CART cells targeting of Le-Y, CD7, CD33, CD38, CD70, CD123, CLL-1, FLT3, CD44, NKG2D, NKG2D ligand, and CD33 (Putnam et al., 2023). Although, CART cell therapy is potent therapy, it has limitations including cost and manufacture production and lack of effectiveness so far on solid tumors (Sterner & Sterner, 2021)s (Maus et al., 2014).

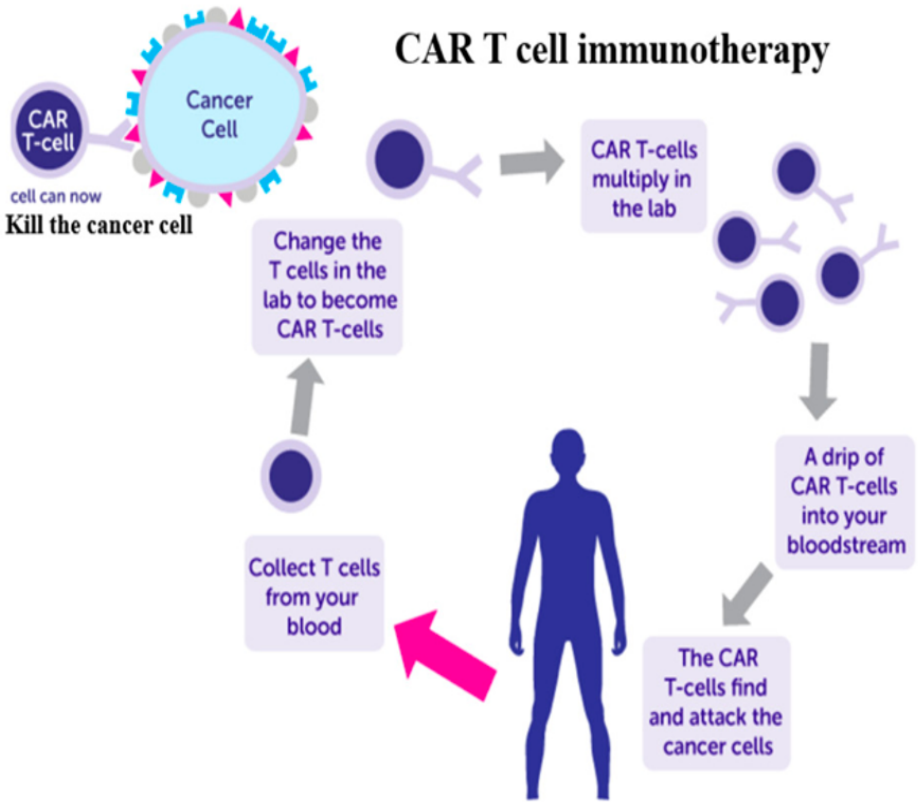

Figure 1.4: The CART cell immunotherapy production.
(W. Bodmer & Golubovskaya, 2023c) **.**

1.3.4 T Cell Receptor Mimic Antibodies—TCRms immunotherapy:

T Cell Receptor Mimic Antibody (TCRms) immunotherapy is targeted therapy designed to target intra-cellular cancer antigens which are recognised on the cell surface through peptides derived from the intra-cellular protein that are attached to the surface HLA proteins (Dubrovsky et al., 2015). This works by having TCRms antibodies that recognise the combination of peptide with HLA protein on the cell surface (Dubrovsky et al., 2015). These antibodies can then be used, as already described, to engineer T cell engaging of cancer cells (W. Bodmer & Golubovskaya, 2023c). The antigens which are located inside the cell are processed to be expressed on the surface of the cancer cells as shown in figure 1.5 (Chang et al., 2016). The TCRms recognize the cancer antigen mimicking the recognition by TCR on T cells as shown in figure 1.6 A and B (D. Li et al., 2017a).

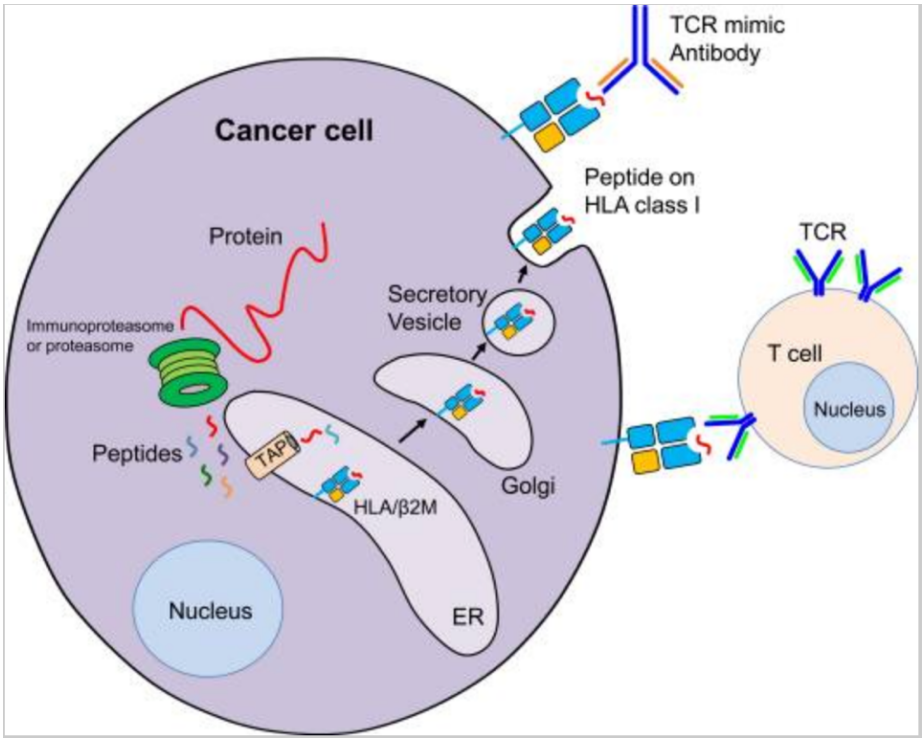

Figure 1.5: The fundamental approach of TCRms immunotherapy mimicking the recognition of TCR of T cells.
(Chang et al., 2016).

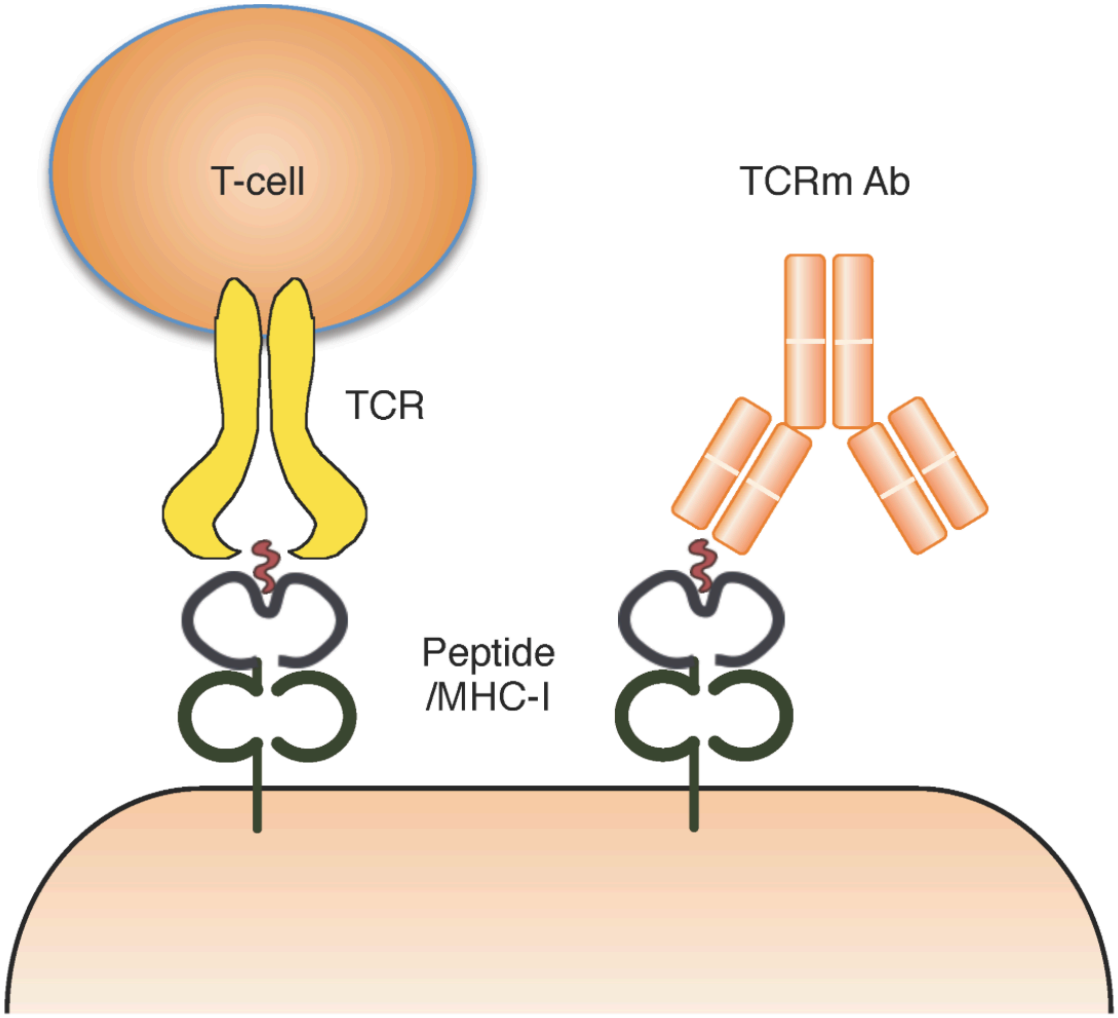

Figure 1.6: A. T cell recognizes peptides attached to MHC-1 through a T cell receptor (TCR). B. TCRm antibody recognizes the peptide attached to MHC-1 similarly to TCR recognition (D. Li et al., 2017b).

1.4 T Lymphocytes

T Lymphocytes (T cells) are a key part of adaptive immune system (Medzhitov, 2007b). T cell development and production occur in the bone marrow (BM) and the thymus (Sun et al., 2023a). The T cell activation and functions are triggered by binding to antigen presenting cells (APC) through T cell antigen receptor (TCR) and antigenic peptide incorporated in human leukocyte antigens (HLA) (Murphy, 2017).

Naïve T cells differentiate to specialized T cells either regulatory, or memory cells (Sallusto et al., 2004). Specialized effector T lymphocytes such as CD8+ after antigen recognition proliferate and eliminate the pathogens by TCR recognition or secretion of cytokines directly inducing death, and specialized CD4+ T helper cells coordinate the immune invasion(Sun et al., 2023b). Subsets of T cells become long lived memory cells which turn out to be faster and better performing in fighting pathogens when later exposed to the same pathogen Figure 1-7 (Yatim & Lakkis, 2015).

T cell antigen receptor (TCR) on T cells is the responsible part of T cell activation, proliferation or resting in combinations of cofactor molecules CD3 (Wange & Samelson, 1996). CD3 is a key component of nearly all T cells that controls their recognition of antigens by the T cell receptor, It consists of 4 polypeptides CD3 ε, δ, γ and ζ which are important for TCR expression on the cell surface of T cells and for signal transduction due to their immunoreceptor tyrosine-based activation motifs (ITAMs) (Guy & Vignali, 2009).T cells induce death of virus infected cells by different methods: through granule exocytosis releasing perforin and granzymes which induce pores on the membrane of infected cells, and by releasing death ligands, such as FAS ligand (FASL) or TNF related apoptosis inducing ligand (Sutton et al., 2000). The main subtypes of T cells are the

cytotoxic CD8+ T cells, the helper T cells CD4+, and γδ T cells, each type having a different main function (Ashby & Hogquist, 2023).

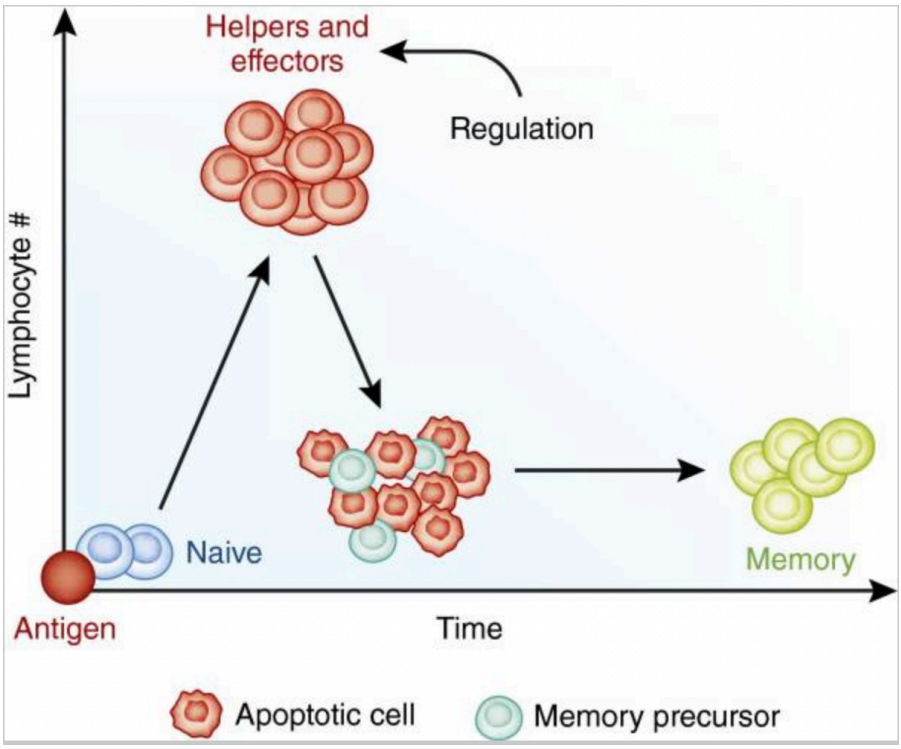

Figure 1.7: Schematic overview of lymphocyte immune response in two dimensions.
Firstly, lymphocytes are exposed to antigens, causing activation and proliferation and specialization to be either helper T cells or effector T cells. Secondly, after elimination of the pathogen, the majority of lymphocytes undergo programmed cell death and some become memory lymphocytes (Yatim & Lakkis, 2015)

1.4.1 Cytotoxic T lymphocytes CD8+ T cells

Cytotoxic T lymphocytes are powerful effector cells and are targeted to help in the field of cancer immunotherapy (Sun et al., 2023b). The development and selection of CD8+ cells targets occur in the thymus (Ashby & Hogquist, 2023). The immature CD8+ become mature CD8+ or active through Interleukin 2 (IL2) activation, which leads to CD8+ proliferation, and the activation of CD8+ is induced through the recognition of antigenic peptide bound to MHC type I on antigen presenting cells like dendric cells (Ashby & Hogquist, 2023) (Vacca et al., 2018). CD8+ Cytotoxic T lymphocytes (CTLs) cells clear abnormal cells such as virus-infected cells, or sometimes certain types of cancer cells, by inducing apoptosis through secreted cytokines such as tumour necrosis factor-alpha (TNF-α), and interferon-gamma (IFN-γ)(Vacca et al., 2018) (Kaech & Cui, 2012). The Second method of inducing apoptosis in infected cells is through their interaction with Fas ligand and Fas receptor, and the third, through the secretion of perforin and granzymes (Chen et al., 2024). After CD8+ cells have first killed infected a subset of the activated CD8+ cells become memory CD8+ T cells that can later induce killing of infected cells with the same pathogen and so produce long-term immunity against that pathogen (Reina-Campos et al., 2021). As CD8+ T cells are powerful in clearing infected cells, their activities cannot be indefinitely and can be regulated through inhibitory mechanisms such as inducing apoptosis to the active CD8+ cell or surrounding cells, inducing the expression of check point inhibitors, or inducting autophagy mechanism (Chen et al., 2024)

1.4.2 Helper T cells CD4+

CD4+ T cells called T helper cells (Th) recognise antigens on antigen-presenting cells through their T cell receptor restricted to recognising peptides attached to MHC II (Carpenter & Bosselut, 2010). The T CD4+T cells induce killing of infected cells indirectly through activation of other immune cells in the immune system, like macrophages, B cell antibody production, and CD8+T cells (Wik & Skålhegg, 2022).

The CD4+ T cells subtypes are Th1, Th2, Th9, Th17, Treg, and Tr1 and they differ in their function and secreted cytokines (Geginat et al., 2014). The development and specialization of naive CD4 T cell subtypes are regulated by the source of the pathogens (Zhu et al., 2010). The Th1 cells produce a high amount of interferon-γ (IFNγ) and interleukin (IL)-2, IL-10, and tumour-necrosis factor (TNF), while the Th2 cells produce IL-4, IL-5, IL-6, IL-13, IL-10 (Abbas et al., 1996). The Th9 cells secrete IL9.(J. Li et al., 2017).

The CD4+ induction of apoptosis of infected cells works through the binding FAS and FAS ligand, and through secretion of perforin and granzymes (Juno et al., 2017).The subtype of CD4+ Treg cells that express FOXP3 help in inhibiting the autoimmunity against self-antigen (Fontenot et al., 2003). They also help in reducing the autoimmunity by C8+ cells by expressing immunosuppressive secretion such as IL-10 and TGF-β (Chen et al., 2024).

1.4.3 γδ T cells

γδ T cells are a unique subset of T cells representing about 1-5% of the total CD3 T cells (Pistoia et al., 2018). The γδ T cells specialize or develop in the thymus to express the T cell receptor γδ (TCR γδ) (Prinz et al., 2013a). γδ TCR consist of γ chain and δ chain and γδ T cells have multiple subgroups depending on their function and their TCR chain combinations of γ chain and δ chain, δ chain has four types (δ1, δ2, δ3, δ5) each bind with the γ chain to make main four subgroups of γδ T cell (Y. Zhao et al., 2018). γδ T cells function is to recognize rapidly multiple antigens bypassing the recognition of MHCI or MHCII unlike αβ T cells which are restricted to MHC for their recognition (Prinz et al., 2013b). γδ T cells have been suggested to have useful activity against cancer cells as the cancer cells often lose or downregulate the expression of MHC I and MHC II as mechanism of immune scape, which is not needed for γδ T cells immune invasion since their target recognition does not depend on HLA(Hayday et al., 2024) (Smyth et al., 2006).

IFNγ or TNFα secretion, granzyme B and perforin generation, or membrane bound TRAIL and Fas (CD95) ligands are all approaches that have been suggested to be used by activated γδ T cell to induce killing of cancer cells (Saura-Esteller et al., 2022). However, other workers suggest different ways in which γδ T cells could influence tumour growth such as secretion of interleukin 17 (IL-17) or myeloid derived suppressor cells (MDSCs) which induce tumour advancement in colorectal cancer, breast cancer, oesophageal cancer, non-small cell lung carcinoma, gastric cancer, gall-bladder cancer, and many other types of tumours (Y. Zhao et al., 2018).

1.5 Apoptosis

Apoptosis is programmed cell death (Elmore, 2007a). It is an essential mechanism in the development of healthy tissues in the processes of building differentiated tissues or maintaining the balance between building healthy cells and destroying damaged cells (Elmore, 2007b). Apoptosis can be initiated by external or intracellular factors lead to morphological changes such cells shrinking or chromatin become pyknotic, and biochemical changes such as DNA breakage (Majno & Joris, 1995). Apoptosis is an irreversible process and considered as a cell defense mechanism which takes place during immune activity, disease, aging and development (Elmore, 2007a). There are many ways of inducing apoptosis such as by chemotherapy, radiation, hormones like corticosteroids (Elmore, 2007b).

Apoptosis is initiated through activation of a family of cystine protease enzymes called caspases (J. Li & Yuan, 2008). During of apoptosis, cell membranes change through phosphatidylserine (PS) exposure to the outer leaflet, this becomes a signal for phagocytosis by macrophages, which is used as an early signal of apoptosis by staining with Annexin V (Hengartner, 2001; Prestwich et al., 2008). Apoptosis is classified either as an extrinsic caspase pathway, an intrinsic mitochondria pathway, or perforin and granzyme pathway (Pistritto et al., 2016), (Kashyap et al., 2021).

1.5.1 Apoptotic perforin and granzyme pathway

The Apoptotic perforin and granzyme pathway initiated by granzyme A (GzmA) and granzyme B (GzmB), the serine protease granzymes which are secreted in the form of granules by cytotoxic T lymphocytes (CTLs) and natural killer cells (NK) as they immune attack unhealthy cells like cancer cells or virus infected cells (Kuhla et al., 2009) (Prager et al., 2019). Perforin helps this process by inducing pores on the cell membrane of unhealthy cells allowing the entrance of granzyme into the cells leading to cell apoptosis (Kashyap et al., 2021).

1.5.2 Apoptotic intrinsic pathway

The Apoptotic intrinsic pathway is initiated by factors that induce internal cellular signals, this is regulated by two groups of proteins: Proapoptotic which help inducing apoptosis such as BAX and BAK, and antiapoptotic proteins which inhibit apoptosis (Danial & Korsmeyer, 2004). The Apoptotic intrinsic pathway is initiated by attack of the mitochondrial transmembrane leading to release of cytochrome C to the cellular cytosol leading to activation of a cascade of caspases leading to cell death (Elmore, 2007c).

1.5.3 Apoptotic extrinsic pathway

The extrinsic pathway is initiated by extracellular factors through binding cellular receptors with the following ligands : tumor necrosis factor receptor (TNFR) binding to tumour necrosis factor (TNF), TNF-related apoptosis-inducing ligand receptor TRAILR binding to TNF-related apoptosis-inducing ligand (TRAIL), and FAS binding to its FAS ligand which induces the activation of inactive caspase 8 to active caspase 8, this in turn induces activation of caspase7 and caspase 3 which cleave cellular substrates leading to cell death (Igney & Krammer, 2002).

1.5.4 Methods for apoptosis detection:

There are different methods for studying apoptosis cell death as induced, for example, by BiMaB T cell immunotherapy (see section 1.3). One commonly used method is the quantitative measurement of caspase cleaved product keratin 18 (ccK18) by using the anti M30 antibody Apoptosense® ELISA (De Haas et al., 2008). The ccK18 is an early biomarker for cell apoptosis (Caulín et al., 1997). ccK18 is generated after caspase cleavage of protein Keratin 18, which is recognized by the antibody M30, ELISA M30 is used to measure the soluble cck18 released from dying cancer cells (De Haas et al., 2008).

An alternative method for detecting apoptosis is through the measurement of cell health and growth can also be carried out by xCELLigence Real-Time Cell Analysis (Ke et al., 2011). It measures the real-time killing of cancer cells mediated by effector T cells (Peper et al., 2014a). The principle of the method is by measuring the adherent cancer cells detachment from an E plate which is attached to an electrode and the detachment is measured as a cells index (CI.) This is a measured unit of the calculation of impedance recording the number and/ or the size of cells detached in each well, the reading is normalized by the background reading of the wells before adding the cells (Ke et al.,

2011) . Cancer cells are seeded on an E plate which is attached to an electrode at the bottom of each well, upon adherence of cancer cells, the electrical impedance increases, when the adherent cancer cells detach due to immune induced killing the electrical impedance decreases, and this is measured by xCELLigence Real-Time Cell Analyzer (Peper et al., 2014b).

Apoptosis can also be measured by detecting the cleaved Caspase-3 staining using by IF or FACS analysis. Procaspase 3 is cleaved into two subunits, one of which is the active form of caspase 3, formed when the cells undergo apoptosis (Nicholson et al., 1995).

1.6 Proteins targeted by T cells engaging bispecific antibodies used in this thesis.

1.6.1 PLAP

Placental alkaline phosphatase (PLAP), a plasma membrane-bound glycoprotein, is one of the four members of the alkaline phosphatase isozyme family (ALP) (Sharma et al., 2014). The four-isozymes are distinguished according to their tissues expression, 1) placenta alkaline phosphatase, ALPP 2) germ/testis cell alkaline phosphates, ALPPL2, 3) intestinal alkaline phosphatase and 4) the tissue non-specific liver bone kidney alkaline phosphatase (Millán, 2006). The testis-specific enzyme ALPPL2 is very similar to ALPP (Durbin et al., 1988) (Durbin, Tucker, et al., 1988) . Placenta alkaline phosphatase, testis alkaline phosphates, and intestinal alkaline phosphatase are closely linked genes on the same chromosome while the liver bone kidney enzyme is on a different chromosome (Le Du et al., 2001). PLAP is encoded by the ALPP gene at chromosome 2q37.1 (Reiswich et al., 2021). PLAP is glycolipid-bound membrane protein (Yekehfallah et al., 2022). It is a metalloenzyme that has two Zn2+ ions and one Mg2+ ion and its function is

hydrolysis of phosphomonoesters (Bassi et al., 2021). PLAP is expressed on syncytiotrophoblasts in placenta and has not been detected in other normal tissues (Tucker et al., 1985). It has been shown that PLAP is released into the serum of patients with PLAP expressing tumours such as testis tumours (Jacobsen & Norgaard-Pedersen, 1984; Lange PH, 1990).

When PLAP is expressed ectopically in cancers, such as ovarian or colon carcinomas, it is essentially cancer specific and therefore an excellent target for immune-based antibody therapy (Orsaria et al., 2016) (Harmenberg et al., 1991). PLAP was found in the blood circulation of smokers, where RNA expression of PLAP has been found at low levels in lung (Lonsdale et al., 2013; Williams et al., 1986).

CAR T cell immunotherapy targeting PLAP shows beneficial effects on colorectal cancer in vitro and in animal testing (X. Li et al., 2020). Monoclonal antibody anti-PLAP is a useful tool to stain and localise the tumours that express it (Koshida et al., 1998).

1.6.2 Epithelial Cell Adhesion Molecule (EpCAM)

The epithelial cell adhesion molecule (EpCAM) is 40 kDa intramembrane-expressed glycoprotein (Linnenbach et al., 1993)(Aiman Mohtar et al., 2020). EpCAM may help in cell-cell adhesion, but its function is not yet well defined (van der Gun et al., 2010). EpCAM is expressed on essentially all epithelial cells in all the different epithelial tissues (Gires et al., 2020). The first anti- EpCAM was generated in 1979 but was identified as anti- EpCAM by several investigators over the years (Herlyn et al., 1979) (Gires et al., 2020).The antibody used in our laboratory, AUA1, was first produced in 1980, first used

for pathology in 1982, and further characterised (Pervez et al., 1988) (Durbin et al., 1990) (Spurr et al., 1986).

EpCAM is expressed on different types of tumours and is found in normal epithelial tissue such as colon cancer, liver cancer, breast cancer, and prostate cancer (Went et al., 2004). Silencing EpCAM in breast cancer has a positive outcome of inhibiting or preventing the proliferation of breast cancer cells in vitro (Osta et al., 2004). A bispecific antibody CD3 - EpCAM Bispecific T-cell Engager (BiTE) to treat uterine and ovarian carcinosarcomas (CS) showed effective results on a chemotherapy resistant tumour (Ferrari et al., 2015). The EpCAM - specific BiTE (MT110) developed to kill pancreatic cancer showed positive effects in vitro and in animal models (Cioffi et al., 2012).

1.7 Colorectal cancer heterogeneity.

In cancers selected changes in the genome gene sequences and epigenetic changes are drivers of cancer progress, however, there are also huge numbers of gene mutations that have no significant functional effect found in any somatic cells including in cancers (Zellmer & Zhang, 2014). These can be cancer specific antigens that could be used for immunotherapy targeting though not for functional based therapies since in many cases they may be novel mutations in proteins derived peptides are presented on cell surface attached to HLA on cancer cells (Prestwich et al., 2008).

Cancer heterogeneity can be both intertumoural heterogeneity and intratumoural heterogeneity (Dagogo-Jack & Shaw, 2017). Intertumoural heterogeneity is the differences between cancer cells from different patients reflecting the variety of possible driver changes, and intratumor heterogeneity is the differences between cancer cells within a patient's tumour (Dagogo-Jack & Shaw, 2017). This tumour heterogeneity is mostly not caused by genomic instability and seems often to be variation in gene

expression that may, for example, be caused by transient methylation changes (Dagogo-Jack & Shaw, 2017)(Polyak, 2007). The tumour heterogeneity can be seen in the structural characteristics associated with differentiation or expansion of cancer cells within tumour (Hanahan & Weinberg, 2011).

Next generation DNA sequencing technology is tool used to understand the heterogeneity within a tumour due to different stages in the clonal outgrowth of tumours driven by different combinations of driver genetic changes (Gerlinger & Swanton, 2010a).

Tumour microenvironment has been suggested as factor influencing tumour heterogeneity, such as due to myofibroblasts influencing cancer growth patterns by released products such as TGFbeta (Bissell & Hines, 2011). The tumour heterogeneity causes clinical complications due to different intratumoural clones responding differently to potential therapies, this could sometime be dealt with by developing cancer therapies that target subpopulations of tumours (Gerlinger & Swanton, 2010b) (Fidler, 1989). Intratumoural heterogeneity may also arise from selection for genetic changes that resist a given treatment, such resistance is always a serious problem associated with any single treatment whether some form of chemotherapy or different forms of immunotherapy, as will be discussed later (Kwak et al., 2015)(Gerlinger & Swanton, 2010b).

1.8 Aims

The initial aims of the project were:

- Using our panel of colorectal cancer cell lines and the PLAPh3 BiMAb and EpCAM CD3 BiMab antibodies, study their immune mediated-killing ability as a function of level of the PLAP expression.
- Study to what extent PLAP3 BiMaB and EpCAM CD3 BiMaB can mediate killing of bystander cells (PLAP-negative cells or EpCAM-negative cells), and what is the underlying mechanism for this.
- Study the effect of T cell subtypes on BiMaB dependant cellular toxicity.
- Characterize the CRC cell lines in terms of PLAP expression and try to understand what regulates its expression.
- Study the expression of PLAP in Human normal lung tissues.

Chapter 2: Material and methods

2.1 List of reagents and chemicals

All the reagents and chemicals used throughout this work are specified in corresponding text, including the manufacturing details information.

2.2 Methods of cell culture

2.2.1 Colorectal cancer cell lines

The panel of colorectal cancer (CRC) cell lines used throughout this work was obtained from the source of the cryogenic storage of the Cancer and Immunogenetics Laboratory (CIL) at the Weatherall Institute of molecular medicine (WIMM) in Oxford, UK (Mouradov et al., 2014a).(Bacac et al., 2016b). The original sources of all the CRC cell lines used in this thesis are listed in Table 2.1. The pmCherry-C1(addgene:632524) mCherry stable transfected celllines CC20, HCT116 and LS180 were generated by Dr. Djamila Ouaret. The pLV-eGFP (addgene: 36083) stable transfected cell lines (DLD1 and COLO678) were generated by a collaborating laboratory (Swietach Group, Department of Physiology, Anatomy and Genetics, University of Oxford, Oxford).

Table 2.1: x CRC cell lines used for PLAP and EpCAM killing analysis in this thesis and the original sources.

Cell line name	Source
CACO2	Received from ATCC (American Type Culture Collection)
CC20	Received from A.R. Kinsella
CCO7	Received from JT Immunotech,USA
DLD1	Received from ATCC (American Type Culture Collection)
COLO678	Received from ATCC (American Type Culture Collection)
HCA7	Received from Dr. S.Kirkland, Royal Postgrad School, London
HCT116	Received from ATCC (American Type Culture Collection)
HT29	Received from ATCC (American Type Culture Collection)
LOVO	Received from ATCC (American Type Culture Collection)
LS180	Received from B.H.TOM, NW Uni Med Centre, Chicago
LS123	Received from ATCC (American Type Culture Collection)
OXCO3	Received from Prof. Vincenzo Cerundolo, Weatherall Institute of Molecular Medicine, University of Oxford, Oxford OX3 9DS ATCC
SW620	Received from ATCC (American Type Culture Collection)
OXCO1	Received from Prof. Vincenzo Cerundolo, Weatherall Institute of Molecular Medicine, University of Oxford, Oxford OX3 9DS
CL14	Received from ATCC (American Type Culture Collection)
ISCEROL	Received from Pr. Richard Hamelin, INSERM U434-CEPH, 75010 Paris, France
CAR1	Obtained by the W.F. Bodmer laboratory
PCJW	Received from Prof. Christos Paraskeva, Department of Pathology and Microbiology, University of Bristol, UK

C32	Obtained by the W.F. Bodmer laboratory
OUMS23	Obtained by the W.F. Bodmer laboratory
VACO429	Received from Dr Elizabeth Zborowska under an MTA, Case Western reserve University, Cleveland, Ohio
JHCOLOY1	Obtained by the W.F. Bodmer laboratory
C10	Obtained by the W.F. Bodmer laboratory
HCC2998	Received from NCI-FREDERICK CANCER DCTD tumor/cell line repository, vial designation: 0507244
HDC114	Received from Prof. Manfred Schwab under an MTA, DKFZ, Hedelberg, Germany
HDC8	Received from Prof. Manfred Schwab under an MTA, DKFZ, Hedelberg, Germany
RW2982	Received from Dr John Mariadason, Montefiore Medical Center, 111 E210th St. Department of Oncology, Bronx NY
HDC143	Received from Prof. Manfred Schwab under an MTA, DKFZ, Hedelberg, Germany
HDC9	Received from Prof. M, Schwab (DKFZ, Germany)
VACO4A	Received from Dr. J.A. McBain (University of Wisconsin School of Medicine, Madison, WI)

2.2.2 Peripheral blood mononuclear cell (PBMC) isolation and preparation.

The PBMCs used were isolated from whole blood leukocyte cones provided by the NHS Blood and Transplant john Radcliffe Hospital university of Oxford, Oxford. The PBMCs

isolation after recovery from the cones was carried out by using Ficoll-Paque PLUS density gradient media (catalogue number 17144002 Cytiva), according to the manufacturer's instructions. After PBMC purification, PBMCs were aliquoted in freezing medium (heat inactivated FBS+ 10% Dimethyl sulfoxide (DMSO)). PBMCs were cultured in Roswell Park Memorial Institute (RPMI) medium Gibco™ (catalogue number 11875093) supplemented with 10% heat inactivated Fetal Bovine Serum (FBS) (catalogue number A5256701) and 1% penicillin antibiotics penicillin 200 IU/ml and streptomycin 200ug/ml (Gibco/ Invitrogen) (catalogue number 15140122).

2.2.3 CRC cell lines routine culture and maintenance.

The CRC cell lines were cultured adherent in different sized cell culture plates (96, 24, 48 or 6 well-plates and in 100mm Corning dishes ®). Cells were grown in complete Dulbecco's Modified Eagle Medium (DMEM) Gibco™ (catalogue number 52100047) supplemented with 10% heat inactivated Fetal Bovine Serum (FBS) and 1% penicillin-streptomycin antibiotics in a humidified incubator with 10% CO_2 at 37°C. The cell lines were cultured and maintained in a sterile environment in a laminar flow hood. Passaging CRC cell lines was done when cells reached their 80% confluency, usually either split once or twice a week. Cells were passaged by washing with 1X PBS then added 0.5% Trypsin/Ethylenediaminetetraacetic acid (EDTA) (Sigma-Aldrich) (catalogue T4049) for 5-10 minutes at room temperature or at 37°C. Then, cells were collected in 10ml of complete media to neutralize the activation of trypsin and then centrifuged at 300 g for 5 minutes. The cell pellets were resuspended in fresh complete medium, and the cells counted for the experiment's purpose or passage in 1:5 or 1:3 ratios according to the growth rate of each cell line.

2.2.4 Co-culture assay

2.2.4.1 Co-culture of CRC cell lines

Different combinations of CRC cell lines were used CC20, DLD1, COLO678, HCT116 and LS180. Two CRC cell lines were cultured in varying proportions, based on the total cell number in each well. The PLAP/ EpCAM positive and PLAP/ EpCAM negative CRC cell lines were maintained each separately. Cells were washed by 1X PBS then trypsin EDTA added for 5-10 minutes and collected in a 15 ml tube in 10 ml complete medium. Cells were counted by a cell counter before seeding to cell culture plates in the desired percentage mixtures of the cell lines (50%, 50%), (25%, 75%), and (5%, 95%). The mixture of cells was aliquoted equally to each well in either 96 well or 24 well plates.

2.2.4.2 Co-culture of CRC cancer cell lines and PBMCs

The selected CRC cell line or the mixture of two CRC cell lines were seeded as described earlier for overnight. The frozen aliquoted PBMCs were defrosted in a quick manner. PBMCs were transferred to a 15 ml tube with warm complete RPMI. PBMCs centrifugation was for 10 minutes at 300g. PBMCs were counted and added to adherent CRC cells in the ratio of cancer cell to PBMC 1:10.

2.2.5 Cell lines cryopreservation

When the CRC cell lines were growing healthy and reached their 70-85% confluency, cells were washed with PBS and treated with 0.5% trypsin EDTA for 5-10 minutes, then the cells were collected by centrifugation for 5 minutes at 300 g. Cell pellets were collected in 1 ml of freezing medium (heat inactivated FBS+ 10% Dimethyl sulfoxide (DMSO Thermo Scientific Chemicals catalogue J66650.AE)). Cells were collected in the

cryovial tube (corning®), then placed at -80 °C freezer overnight. Cryovials were transferred for the long-term storage to the liquid nitrogen tank at -196 °C.

2.2.6 Retrieving frozen cells.

The frozen cells in cryovial tubes were defrosted quickly to maintain their viability. The cryovial tube was placed in a 37 °C water bath and gently swirled for less than a minute and immediately after defrosting the frozen cells transferred to 10 ml of warm complete medium in a 15 ml tube. Cells were collected by centrifugation for 5 minutes at 300 g and the medium was removed. The cell pellet was resuspended in new 10 ml complete media.

2.2.7 Cell counting

After cells were collected in 10 ml fresh medium, a 20 ul of the cell's solution was taken from the cell suspension and placed in a cell counting chamber and placed on a Cellometer Auto T4 cell counter (Nexcelom Biosciences, USA). This method determines the count of the number of cells per 1 ml.

2.2.8 Cell condition and contamination

Cells and cell cultures were routinely checked under microscope. Cells were tested for Mycoplasma contamination using mycoplasma chambers test (MycoStrip™ InviviGen mycoplasma detection Kit), following the manufacture's procedures.

2.2.9 5-Aza-2'Deoxycytidine (5-aza) Treatment

5-aza-2'deoxycytidine (sigma catalogue number A3656) was prepared by dissolving it into DMSO to make the stock concentration 5mM and stored at -20 °C. Cells were treated with 10 µM 5aza and control conditions were treated with DMSO for 24 hours, 48 hours and 72 hours. Every day of treatment the cells were treated with fresh 10 µM of 5-aza or control with DMSO. The cells were tested for the level of protein expression by flow cytometry or Immunofluorescence staining.

2.2.10 Phospholipase C treatment

COLO678 cells were seeded for treatment with 0.5 or 1 unit of phospholipase C (phospholipase C, phosphatidylinositol-specific, Sigma-Aldrich catalogue P8804) for 30 minutes or 1 hour at 37° C. The cells were washed with 1X PBS three times then fixed with 4% Paraformaldehyde fixative (PFA) (VWR Chemicals) for immunofluorescence staining.

2.2.11 Internalization assay

COLO678 and HT29 were cultured in a 96-well plate (10.000/ well) for overnight. Cells were incubated with in house Anti-PLAP for 1 hour at 37 °C in a humidified CO_2 cell culture incubator. Primary antibody washed by PBS three times and cells were incubated with secondary antibody Alexa fluor 488 (1:500) for 30 minutes. Secondary antibody was washed with PBS three times and fresh medium was added to cells. After 4 hours the cells were fixed with 4% Paraformaldehyde (PFA) (VWR Chemicals) for 20 minutes. The cells membranes were permeabilize by 0.2% triton X100 (Sigma-Aldrich, catalogue number 1.08643) in PBS for 5 minutes. Cells were washed three times with PBS. Cells were incubated with blocking solution (1% Bovine Serum Albumin (BSA), Sigma-Aldrich catalogue number A7030) for 1 hour at room temperature. Primary antibody (rabbit anti

human LAMP1) was then added for 1 hour at room temperature. After washing step, cells incubated with anti-rabbit secondary antibody Alexa fluor 568(1:500). DAPI (sigma D9542) (1:10000) added to cells for 5 minutes and then cells washed with PBS three times. The cells were imaged by using a Zeiss Observer z1, Carl Zeiss (ZEISS Axioscan 7 Microscope Slide Scanner, 2024.) (Oncology Microscopes, WIMM, University of Oxford).

2.2.12 Transient siRNA transfection

Cells were prepared for siRNA transfection by washing the cells with 1X PBS and then trypsinising with trypsin EDTA for 5 -10 minutes. For measuring the protein expression by immunofluorescence, $1x10^4$ cells seeded in a 96 well plate, or $1x10^5$ cells in 24 well plate for Flow cytometry assay.

Pre-designed sequences of siRNAs of ALPP, ALPPL2 and VGLL1 were used (shown in Table 2.2 (source and catalogue number)). The siRNAs were dissolved in RNAase free water on arrival. The stock prepared to 10 µM and stored at -20°C. The concentration used was 20nM siRNA (ALPP, ALPPL2, VGLL1) treated to the cells. The solution of mixture of 10 µl of siRNA (10 µM) and 10 µl of Lipofectamine® 2000 (Life Technologies/Thermo Fisher Scientific catalogue number: 11668019) was dissolved in 100µl Opti-MEM Gibco™ (catalogue number 31985062) then incubated for 10 minutes at room temperature, then added to 400 µl DMEM medium (no FBS or antibiotics). The mixture was added to the cells and incubated with cells for 6 hours. The DMEM medium (no FBS or antibiotics) was replaced with complete DMEM (with FBS and antibiotics). Protein expressions was analysed after 72 hours by immunofluorescence staining. Control of the transient siRNA transfection was scrambled siRNA.

Table 2. 2: siRNAs used in this work and their sources.

siRNA target	Source	Catalogue number	Assay ID number
siRNA ALPPL2	Thermo Fisher	AM16708	114955
siRNA ALPP	Thermo Fisher	4392420	s1301
siRNA VGLL1	Dharmacon™	017939-00-0005	51442
scrambled	Thermo Fisher	4351372	Dm01815567_s1

2.2.13 Overexpression

The ALPP plasmid (catalogue number RC210504) and ALPPL2 plasmid (catalogue number SC123000) were predesigned and received from OriGene Technologies, Inc. The plasmids were prepared by dissolving it in 100 µl distilled water on arrival to make the final concentration 100 ng/µl and then frozen in -20 °C.

The plasmid transfection to the cells was added to seeded cells overnight in 6 well plate (250.000 cells/ well). The 500 ng of total plasmid either, ALPP or ALPPL2 or both together mixed with Polyethylenimine (PEI, Sigma-Aldrich) in ratio 1:1 and added to 100 µl of DMEM medium without FBS or antibiotics. The mixture solution was incubated at room temperature for 10-15 minutes. The mixture was then added to 500 ul medium without FBS or antibiotics. The plasmid mixture was added to the cells for 6 hours in the cell culture incubator. The medium was replaced after 6 hours with complete medium (with FBS and antibiotics). Protein expression was measured after 72 hours by immunofluorescence staining.

2.3 Antibodies:

2.3.1 Antibodies used in immunofluorescence, Immunohistochemistry (IHC), and fluorescence-activated cell sorting (FACS)/Flow cytometry staining.

The list of antibodies including primary and secondary antibodies used in this work and their source and working concentration are given in Table 2 2: siRNAs used in this work and 2.

Table 2.3: Antibodies and their sources.

Antibody-Primary /Secondary	Source	Concentration
H17E2 (Mouse monoclonal antibody)	In house	1:100
HD8B6 (Mouse Monoclonal antibody)	In house	1:100
AUA1 (Mouse monoclonal antibody)	In house	1:200 or 1:200
Rabbit Anti-cleaved caspase 3 (Rabbit monoclonal antibody)	cell signalling technology (Catalogue number 9661T)	1:250
Isotype iGg mouse	BD pharmingen (Catalogue number 14-4714-82)	1:100
CD45 APC anti-human CD45 antibody	Biolegend (Catalog number 304011)	1:100
CD8 Alexa Flour 700 anti-human CD8 antibody	Biolegend (catalogue number 344723)	1:100

CD3 Brilliant Violet 711 anti Human CD3 antibody	Biolegend (catalogue number 317327)	1:100
CD4 Brilliant Violet 510 anti-human CD4 antibody	Biolegend (Catalogue number 300545)	1:100
PE/Cyanine7 anti-human CD94 Antibody	Biolegend (Catalogue number 305515)	1:100
ICAM Brilliant Violet 421 anti-mouse CD54	Biolegend Antibody (catalogue number 116141)	1:100
FAS PE anti-human CD95 (Fas) Antibody	Biolegend (Catalogue number 305607)	1:100
FAS-L PE/Cyanine7 anti-human CD178 (Fas-L)	Biolegend (Catalogue number 306417)	1:100
LFA-1 FITC anti-human CD11a/CD18 (LFA-1)	Biolegend Antibody-(catalogue number 363415)	1:100
Alexa flour 568 donkey anti rabbit	Invitrogen (Catalogue number A10042)	1:500

Alexa flour 488 goat anti mouse	Invitrogen (Catalogue number A-11001)	1:500
Alexa Fluor 488 Goat anti human	Invitrogen (Catalogue number A-11013)	1:500
LAMP-1 Rabbit polyclonal to LAMP1 - Lysosome Marker	Abcam (Catalogue number ab199946)	1:200
Goat anti-Mouse IgG (H+L) Secondary Antibody, HRP	Invitrogen (Catalogue number 31430)	1:500

2.3.2 Bispecific monoclonal antibodies construct and mRNA-Lipid Nanoparticle (LNPs)

The bispecific monoclonal antibodies for immunotherapy used in this work are PLAP-CD3 BiMAb(RPLP3) construct, received from our collaborators Roche and ProMab, which is a humanised engineered construct derived from H17E2. The EPCAM-CD3 BiMAb were received from Promab and humanised and engineered from AUA1. The LNPs used in this work either PLAP-CD3 BiMAb LNP, EPCAM-CD3 BiMAb LNP were received from Promab (Golubovskaya et al., 2023a).

2.4 Immunofluorescence staining

For immunofluorescence staining of the cells, they were first washed with 1X PBS three times. Cells were then treated with fixative solution 4% Paraformaldehyde (PFA) for 20 minutes. Cells were next washed with PBS three times and treated with 0.2% Triton X100 (Sigma-Aldrich, catalogue number: HFH10) in PBS for 5 minutes. Cells were then washed three times with PBS. Blocking solution (1% Bovine Serum Albumin (BSA), Sigma-Aldrich) in PBS was added to the cells for 1 hour at room temperature. Cells were then incubated with primary antibody in antibody solution (1% BSA in 1 XPBS), refer to table 2.3 for primary antibody concentrations used. Primary antibody was incubated for 1 hour. After cells were washed then were incubated with secondary antibody (refer to table 2.4). Cells were stained with DAPI ((4′,6-diamidino-2-phenylindole) thermoFisher (1:10000)) for 5 minutes, then washed with PBS three times. Cells were imaged by using Zeiss Observer z1, Carl Zeiss (Oncology Microscopes, WIMM, University of Oxford).

For immunofluorescence by LNPs or BiMAbs cells were incubated with BiMABs or LNPs at the treatment concentration for 1 or 4 hours or 1-3 days depending on the experimental purpose either in a 37 °C cell culture incubator or at room temperature. The BiMABbs or LNPs washed with PBS three times and cells were fixed with 4% PFA for 20 minutes. Cells were stained with secondary antibody (goat anti human alexa flour 488) for 30 minutes. After washing by PBS the cells were stained with DAPI for 5 minutes, then washed and imaged using Zeiss Observer z1, Carl Zeiss (Oncology Microscopes, WIMM, University of Oxford). The image was processed by FIJi (Schindelin et al., 2012)

.

2.5 Fluorescence-activated cell sorting (FACS) analysis:

2.5.1 Flow cytometry staining analysis

To stain protein for protein expression or for single cell sorting, cells were collected by trypsin EDTA and washed with PBS. Cells were counted by cell counter and then suspended in FACS solution (3% FBS in 1X PBS). Then cells were incubated on ice with primary antibody or IGg isotype or conjugated antibodies for 30 minutes at room temperature. Cells were then washed twice with FACS solution (3% FBS in PBS) and incubated with secondary antibody for 30 minutes. Cells were washed twice with FACS solution. Cells were stained with DAPI and analysed on Attune™ NxT Flow Cytometer. FlowJo software was used for data analysis FlowJo™ Software (Mac) [flowjo] Version10. Ashland, OR: Becton, Dickinson and Company; 2019.

2.5.2 Flow cytometry sorting

Cells were stained with primary antibodies for PLAP, EPCAM, or CD45 which are surface marker by washing the cells with PBS then cells were stained for preparation for FACS sorting. Cells were suspended in FACS solution (3% FBS in 1X PBS) then incubated with primary antibody for 30 minutes. Cells then washed with PBS and stained with secondary antibody in dark for 20 minutes. Cells washed with PBS for three times. Cells collected in fresh complete medium and sent to the FACS sorting facility to perform the sorting. The cell lines sorted were CACO2, CCO7, DLD1, CC20, and OXCO3, selected according to their protein expression. For PLAP sorting, cells were sorted were 10% high, 10% medium, and 10% low populations from their PLAP fluorescence level of expression in the whole cell line population. Cells were stained with H17E2, and

control stained with IGg mouse isotype. The sorted population was seeded in 96 well plate for the purpose of the experiment.

2.6 Human Formalin-Fixed Paraffin-Embedded tissues (FFPE) staining

2.6.1 Immunofluorescence staining of human Formalin-Fixed Paraffin-Embedded tissues (FFPE) samples

Pararafin embedded tissue slides (FFPE) were all obtained from company or other laboratories at the University of Oxford, refer to list in Table2.4. To process the protein staining on FFPE, dewaxing step was first carried out by immersing the slides in xylene for 10 minutes twice. Next, the rehydration process was done by immersing the slides in ethanol with different concentrations in the following order: 100% ethanol for 5 minutes, next 90% ethanol for 5 minutes, and lastly 70% ethanol for 5 minutes. The slides were washed with dH_2O for 5 min on a shaker three times. The antigen retrieval step was by incubating slides in retrieval solution (0.05% trypsin + 0.1 $CaCl_2$ at 37°C for 10 minutes). Tissue slides were then washed with dH_2O for 5 minutes three times. They were immersed in Sudan black B solution (Sigma Aldrich Catalogue number 26150) for 10 minutes. Washing steps were performed with dH_2O for 5 minutes three times.Circles were drawn around tissues on the slides for antibody incubation using a PAP Pen (Sigma-Aldrich Gillingham). The blocking solution, 10% Bovine serum albumin (BSA) in 1 X PBS, was added for 1 hour at room temperature.

The primary antibodies used were in-house AUA1 (1:500) antibody and anti-RPLP3 (PLAP X CD3 BiMaB) (5nM). The slides were incubated with the primary antibodies overnight at 4 °C. The stained tissue slides were then washed three times with 1X PBS and 0.1% TWEEN® sigma-Aldrich (PBST) for 5 minutes. The stained slides were then

incubated with secondary antibodies (Goat anti Mouse 647 Alexa fluor and Goat anti Human 488 Alexa fluor) (1:250).

Finally, mounting medium with DAPI (catalogue number ab104139) was added to the slides and cover slips. Tissues were scanned using ZEISS Axioscan and the scans were analysed using Qupath(*ZEISS Axioscan 7 Microscope Slide Scanner*, n.d.) (Bankhead et al., 2017) .

2.6. 2 Immunohistochemistry (IHC) staining of human FFPE tissue samples

The FFPE slide source is listed in Table 2-4 To dewax the paraffin embedded tissue sections, the slides were first incubated twice in two different containers of xylene for 10 minutes each. Slides were dehydrated by using 100% ethanol, then 90% ethanol, followed by 70% ethanol for 5 minutes each. Next, they were washed in dH_2O for 5 min three times. The 3% hydrogen peroxide solution sigma-aldrich (10 ml of 30% hydrogen peroxide in 90ml Methanol (Sigma Aldrich)) was then added to the FFPE tissue slides. Slides were washed on a shaker by dH_2O for 5 minutes three times. The slides were incubated with blocking solution (10% BSA in 1X PBS) for 1 hours.

The slides were incubated overnight with primary antibodies (AUA1 1:500) and (HD8B6 1:50) in 1% BSA in 1 X PBS at 4°C. The slides were washed with 0.1% tween in 1X PBS (PBST) three times for 5 minutes. The tissue slides were incubated with secondary antibody (HRP-conjugated goat anti mouse secondary antibody, Invitrogen) in 1% BSA/1X PBS for 1 hour at room temperature. The tissue slides were washed with PBST (Phosphate Buffered Saline and 0.1% Tween 20) three times each for 5 minutes. DAB (3,3′-diaminobenzidine tetrahydrochloride) (Abcam catalogue number 34002) was added to the slides and the oxidation reaction due to DAP and HRBP enzyme create insoluble brown precipitate which indicate the presence of our antigen of interest, which is PLAP

or EpCAM, this was monitored under the microscope, then stopped by immersing slides in dH_2O.

The nuclei were stained using haematoxylin (Thermo Scientific Chemicals Catalog number:047223.14) for 15 seconds then the slides were washed using dH_2O three times. A coverslip was added, and the tissue was scanned using Aperio slide scanner at the Oncology department (University of Oxford). Tissue staining scans were analysed using Qpath (Bankhead et al., 2017) (Anatomical Pathology Equipment & Workflow Solutions: Leica Biosystems, 2025.).

Table 2.4: The FFPE tissues and sources used in this work.

Tissue type	source
Human Placenta FFPE tissues	Prof. Manu Vatish University of Oxford, Women's Center John Radcliff Hospital, Oxford, UK
Normal Human Colon FFPE and Human colorectal cancer FFPE tissues patients' sample	Dr. David Church University of Oxford, Oxford, UK
Norma Human lung FFPE	SuperBioChips 62/M Catalogue number 0028000B
Norma Human testis FFPE	US Biomax Catalogue number: HuFPT151
Normal Human Lung (Smoker, Nonsmoker)	amsbio Catalogue number AMS28006-SC

2.7 PLAP x CD3 BiMAb(RPLP3) and EPCAM x CD3 and LNPs mediated cell killing assays

2.7.1 BiMAbs and LNPs mediated cell killing assay by ELISA M30

For testing cytotoxicity on CRC cell lines or bystander of co-culture of positive and negative cells in different ratios, cancer cells were seeded in 96 wells plates (3000 cells/well) and allowed to attach overnight. On the following day, the culture medium was replaced with RPMI containing PBMCs at a ratio of 1:10 (cancer cells: PBMCs) and treated with 20nM PLAP-CD3 BiMAb (RPLP4) or 8 nM EPCAM-CD3 BiMAb or 1 µl LNP in 100 µl total culture media for 24 hours or 48 hours.

Controls were used in different wells containing either cancer cells or cancer cells with PLAP-CD3 BiMAb, EPCAM-CD3 BiMAb or 1 µl LNP and cancer cells co-culture with PBMC. Cell killing was detected by measuring caspase cleaved Keratin 18 (K18) as an apoptosis marker by M30 Apoptosense® ELISA (PEVIVA®) and following the manufacturers' protocol.

2.7.2 Both BiMAbs and LNPs mediated cell killing assay by immunofluorescence.

For immunofluorescence, the staining protocol as described earlier was used. Killing was detected by staining for cleaved caspase 3 by anti- cleaved caspase 3 antibody and secondary antibody. Images for immunofluorescence were acquired by using a microscope Zeiss Observer z1, Carl Zeiss (Oncology Microscopes, WIMM, University of Oxford) and image processing by FIJi (Schindelin et al., 2012).

2.7. 3 BiMAbs mediated cell killing assay by xCELLigence analyser

Cells were seeded in a 96 well E PLATE (10.000 cells /well) overnight in xCELLigence Real-Time Cell Analysis - Multiple Plates (RTCA MP) from Agilent's analyser in the Oncology department, University of Oxford, Oxford (Ke et al., 2011b). The next day the cells were cocultured with PBMCs and treated with BiMAbs using the concentrations described earlier. Data generated was analysed using RTCA Software Pro (Ke et al., 2011b).

2.8 T cell subpopulation isolation

T cell subpopulations were used separately for some immune cell mediated cell killing assays. Isolation of T cell subpopulations (CD3 MicroBeads catalogue number 130-097-043, CD4 MicroBeads catalogue number 130-097-048, CD8 MicroBeads catalogue number 130-045-201, CDγ/δ MicroBead catalogue number 130-050-701) was carried out using MicroBeads for positive selection by direct magnetic beads from Miltenyi Biotec. The isolation was carried out according to the manufacturers' protocol. The T cells were then washed and resuspended in RPMI and co-cultured with CRC cell lines.

2.9 Statistical methods

2.9.1 Bimodal gene analysis by Gaussian Mixture Modeling (GMM)

Gaussian Mixture Modelling (GMM) is a probabilistic modelling using an expectation-maximization algorithm to show whether gene expression profiles of our cell line panel or human samples are unimodal or bimodal. If bimodal, the intersection of the two fitted normal distributions defines the dividing line between low or absent and high expression. The details of the GMMchi procedure as applied to the cell line and TCGA data are described by Liu et al 2022(T. C. Liu et al., 2022), briefly discerption added on the

figures. I am grateful to Dr.Jeff (Ta-Chun) Liu and his work for providing the GMMchi algorithm analysis used in this thesis.

2.9.2 Flow Jo and FACS Diva software v 8.0.3:

The analysis of the data obtained from flow cytometry were analysed by Flow Jo 10 software and FACS sorting data by FACS Diva software v 8.0.3 (BD Bioscience) FlowJo™ Software (Mac) [flowjo] Version10. Ashland, OR: Becton, Dickinson and Company; 2019.

2.9.3 RTCA Software Pro:

The analysis of data from using xCELLigence Real-Time Cell Analysis - Multiple Plates (RTCA MP) from Agilent's analyser was carried out using RTCA Software Pro (Ke et al., 2011b).

2.9.4 Fiji and Qpath:

Images obtained from IF or IHC staining were processed using Fiji and Qpath(Bankhead et al., 2017; Schindelin et al., 2012).

2.9.5 General data analysis:

All the data presented in this work are based on the mean of triplicate values and ± standard error mean (SEM). The standard t- Test was used to calculate P values and refer to ($p<0.05$) for significance when appropriate. The graphs were created using (Microsoft Excel 2021, Microsoft Corporation, USA).

Chapter 3: Placental alkaline phosphatase (ALPP) and placental-like 2 (ALPPL2) alkaline phosphatase expression in a panel of human colorectal cancer derived cell lines.

3.1 Introduction

PLAP is Glycosylphosphatidylinositol (GPI) anchored on the human trophoblast cell membrane, and it is an enzyme which has function toward phosphoethanolamine, pyridoxal 5'-phosphate and inorganic pyrophosphate, as well as the IgG transplacental transportation depends on it (Lin et al., 2005). Placental alkaline phosphatase (PLAP) is one of the four alkaline phosphatase isozyme family (Crofton, 1982) . The testis specific alkaline phosphatase isoenzyme, Alkaline phosphatase, placental-like 2 (*ALPPL2*), is very similar to the placenta specific alkaline phosphatase, PLAP (*ALPP*), and the anti-PLAP antibodies often cross react with ALPPL2, but that does not abrogate their cancer specificity (Su et al., 2020a). The protein Placental alkaline phosphatase PLAP is encoded by the *ALPP* gene and expressed in human normal placenta, and ALPPL2 is encoded by the gene *ALPPL2/ALPG* and expressed in human normal testis *(S. Liu et al., 2019; Yekehfallah et al., 2022b)*. *ALPP* and *ALPPL2* are located on chr 2 and have very similar gene and amino acid sequences (Raimondi et al., 1988; Su et al., 2020a).

Placental alkaline phosphatase and Alkaline phosphatase, placental-like 2 are ectopically expressed in colorectal cancer as well as a range of other adenocarcinomas, and so are potential targets for bispecific monoclonal antibody immunotherapy to treat cancer (Yekehfallah et al., 2022b) (Su et al., 2020b).

The focus of this chapter is on PLAP expression screening on colorectal cancer (CRC) and will mainly be based on mRNA and protein levels within a well characterised panel of over 100 colorectal cancer cell lines (Mouradov et al., 2014b). The Cancer Genome Atlas (TCGA) is collection of databases for cancer patients, including genetic, mutation, methylation and clinical information, TCGA databases are a useful tool to screen for cancer specific targets for bispecific antibody immunotherapy on a range human cancer patient, including CRC (Weinstein et al., 2013).

As PLAP is targeted by bispecific antibody therapy and for the therapy successes, testing the antibody against all normal tissues including testis is important. Since both enzymes have very similar amino acid sequences, this chapter focusses on the recognition of the in-house anti PLAP antibodies (H17E2 and HD8B6) to PLAP and ALPPL2 (Durbin, Milligan, et al., 1988; Travers & Bodmer, 1984a).

3.2 Results:

3.2.1 ALPP and ALPPL2 expression on human colorectal cancers

ALPP and *ALPPL2* expression was examined on panel of colorectal cancers using RNA-seq data provided by the TCGA database. The results shown here are in whole or part based upon data generated by the TCGA Research Network: https://www.cancer.gov/tcga. Kaplan-Meier survival curves show the effect of *ALPP* expression on colorectal cancer patients' survival by plotting *ALPP* 25% highest-expressing patients versus those with the 25% lowest expression (Kaplan & Meier, 1958). Patients with high *ALPP* expression have lower survival rate compared to lower ALPP expressing patients. For *ALPPL2*, by plotting the 25% lowest expressed and 25% highest expressed, it shows patients with high expression have lower survival rate compared to the lower expressing of colorectal cancer patients. That indicates the prognosis of colorectal cancer is decreased in relation to the elevated expression of both *ALPP* and *ALPPL2.* (Figure 3.1 A).

We used GMMchi to describe the *ALPP* and *ALPPL2* expression on 698 patients' samples of colorectal cancer obtained from the TCGA database (Figure 3.1.B). Both genes *ALPP* and *ALPPL2* have bimodal distributions among the patients' samples. Blue bars represent the positive expressed samples compared to the yellow and pink which represent samples with low or negative expression. The red dotted lines in the middle define thresholds delineating high versus low expression as analysed by the GMMchi algorithm Liu et al 2023 (T. C. Liu et al., 2022) The relation between the expressions of the two genes-*ALPP* and *ALPPL2* in the TCGA colorectal cancers patients' is shown in the 2x2 Table 3.1.

The 22 colorectal cancer patients co-expressed both genes and 593 patients are negative for both genes. The 8 patients are only *ALPP* positive, and 75 patients are only *ALPPL2* positive. That indicated a very strong correlation between *ALPP* and *ALPPL2* with more colorectal cancer patients expressing *ALPPL2* than *ALPP*.

A.

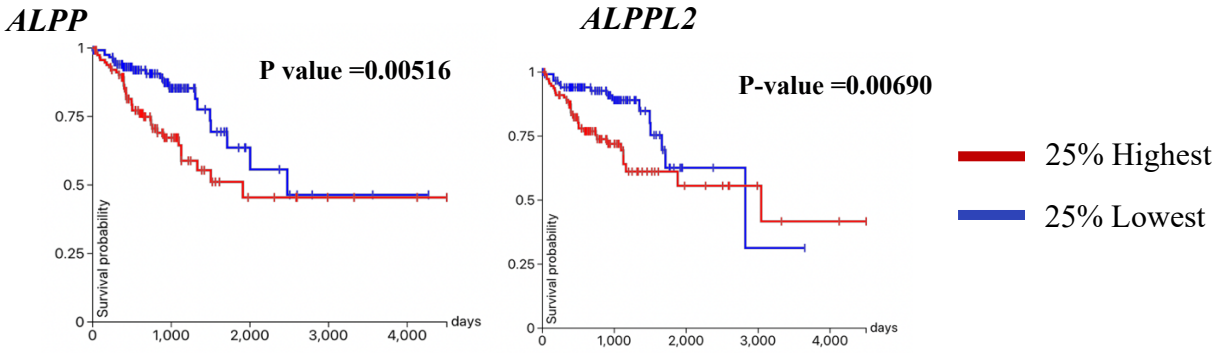

B.

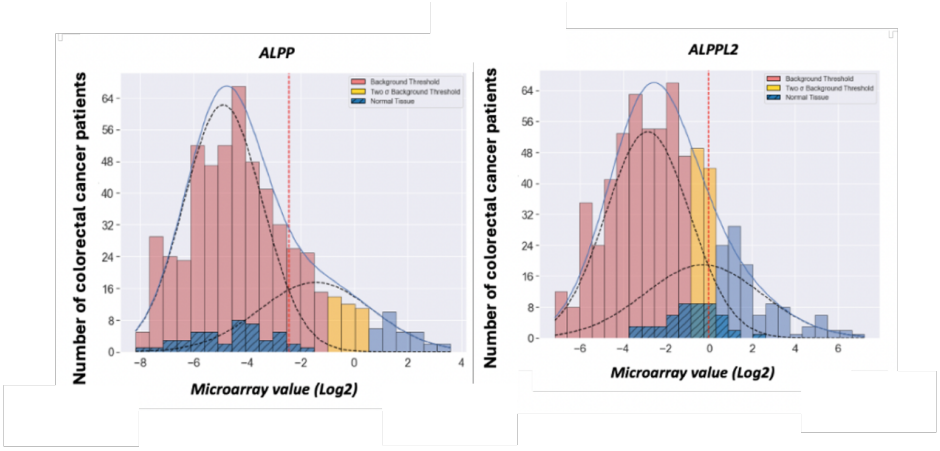

Figure 3.1: ALPP and ALPPL2 expression of colorectal cancer patients using TCGA RNA-seq data.

A. The Kaplan-Meier survival curve for 517 patients of colon and rectal primary tumours. The RNAseq data expression for ALPP and ALPPL2 expression. Both curves for both genes represent top high (red) 25% expressed and 25% low (blue) expressed for ALPP or ALPPL2. B. GMMchi analysis of ALPP and ALPPL2 expression on TCGA RNA-seq dataset. Both histograms of both genes show bimodal distributions, y-axis displays the number of samples and X- axis shows the gene expression calculated on log2 scale. Pink bars represent the background level which calculated from the estimation of independent analysis of the measurement of overall gene expression. The yellow represents the samples close to the background. Blue bars represent the positive expressed patients of each gene. Dashed blue bars are normal samples tissue obtained from a small subset of the TCG cancer samples. The red cut-off line defines the point of intersection of two fitted normal distribution of two groups of ALPP/ALPPL2 positive, and ALPP/ALPPL2 negative/ low.

Table 3.1 2x2 table obtained by GMMchi of 1 TCGA RNA-seq data for both genes ALPP and ALPPL2.

		ALPP	
		-	+
ALPPL2	-	593	8
	+	75	22
		P value< 0.0001	

3.2.2 The expression of *ALPP* and *ALPPL2* on colorectal cancer cell lines

ALPP and *ALPPL2* mRNA expression on a panel of over 100 colorectal cancer cell lines is shown in figure 3.2. The mRNA expression values for ALPP and ALPPL2 of the panel of colorectal cancer cell lines are listed in appendix 1. The expression of the two genes is very similar in that if *ALPPL2* high *ALPP* is also high. The majority of the CRC cell lines are low for both *ALPP* and *ALPPL2* expression. There are some exceptions where the cell lines have higher expression for *ALPP* compared to *ALPPL2* expression, for example CL14.

The GMMchi analysis of 78 of the cell lines for the expression of *ALPP* and *ALPPL2* is shown in Figure 3.3. It shows that both *ALPP* and *ALPPL2* have bimodal distributions. ALPP is expressed in 20.50% of the cell lines, and *ALPPL2* is expressed in 10% of our cell lines. Referring to 2x2 table (table 3.2), both genes are highly expressed in 7 cell lines and negative for 62 cell lines. There are no *ALPPL2* positive cell lines which are negative for *ALPP*. That depends on where you draw the cut7off between - and +. 9 cell lines out of 78 cell lines are positive for *ALPP* and negative for *ALPPL2*. In comparison to human colorectal cancer patients' samples, more ALPPL2 positive compared to patients' samples which are positive for ALPP.

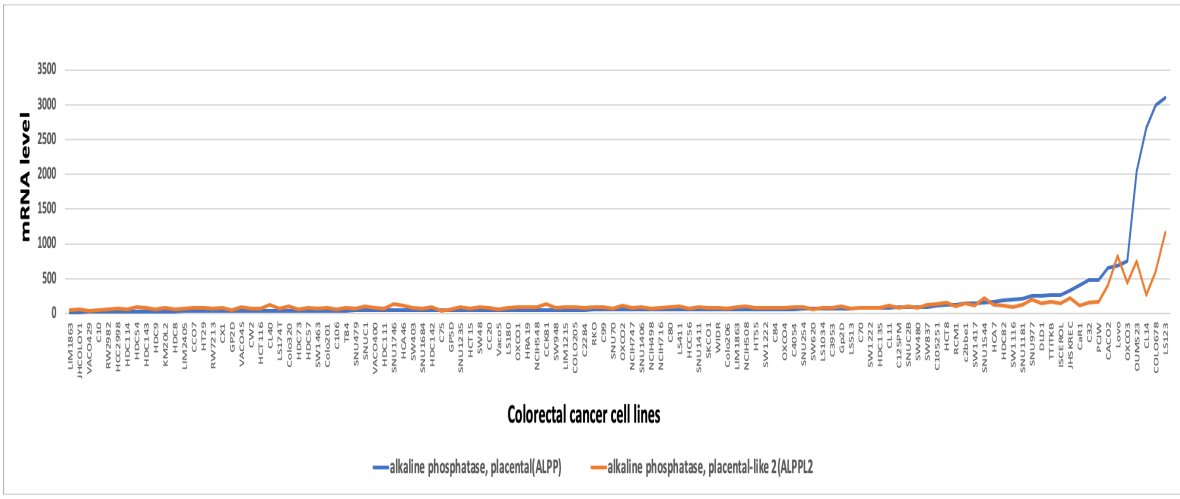

Figure 3.2: ALPP and ALPPL2 mRNA expression of panel of over 100 colorectal cancer cell lines.

A

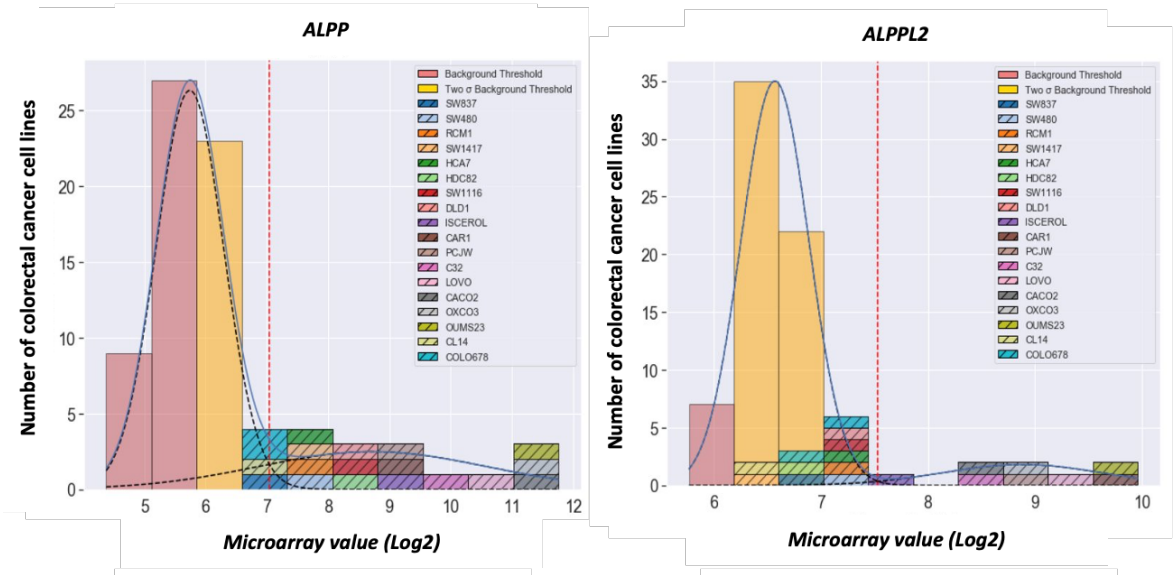

B

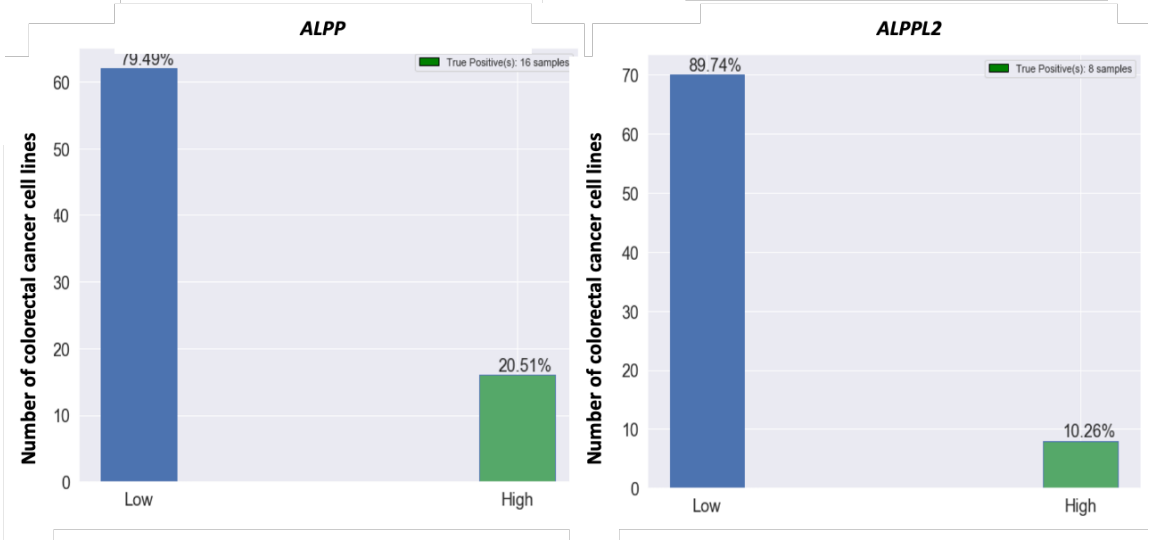

Figure 3.3: GMMchi analysis of ALPP, and ALPPL2 cell lines.
A. shows the GMMchi analysis for each of ALPP and ALPPL2 in 78 cell lines all representing different CRCs, giving a bimodal distribution for each expression. As before, in each case the x axis gives the log2 expression levels and the Y axis the number of lines with a given level of expression. The dotted black lines are the two fitted normal distributions, and the red vertical lines define the estimated thresholds between high and low expression. The ALPP+ cell lines are identified by the colored boxes. The similar positions of these cell lines in the ALPPL2 analysis confirms the strong association between the two expressions. B shows the estimation of the number of high and low expressing cell lines, 20.51% high for ALPP and 10.26% for ALPPL2.

Table 3.2: The 2x2 table obtained by GMMchi of CRC cell lines mRNA data for the association between ALPP and ALPPL2 expression.

		ALPP	
		-	+
ALPPL2	-	62	9
	+	0	7
		P value< 0.0001	

3.2.3 Cleavage and internalization of PLAP

PLAP is, as already discussed, a phospholipid attached membrane bound glycoprotein protein. COLO678 cells were treated with phosphatidylinositol-specific phospholipase c used at a concentration of 0.5 or 1 unit for 30 minutes or 1 hours at 37.2°C to cleave PLAP from the cell surface. PLAP was labelled with anti PLAP antibody and secondary antibody so that the cleavage was detected using immunofluorescences staining. The signal of PLAP on the surface was reduced by the treatment with 0.5-unit phospholipase c for 30 minutes and strong reduction of the signal after the treatment for 1 hour.

The PLAP cleavage were studied using FACS staining of PLAP. COLO678 and CC20 were treated with 1 unit phospholipase c for 1 hour, signal was reduced on COLO678. CC20 is PLAP negative see Figure 3.4.A.B

A.

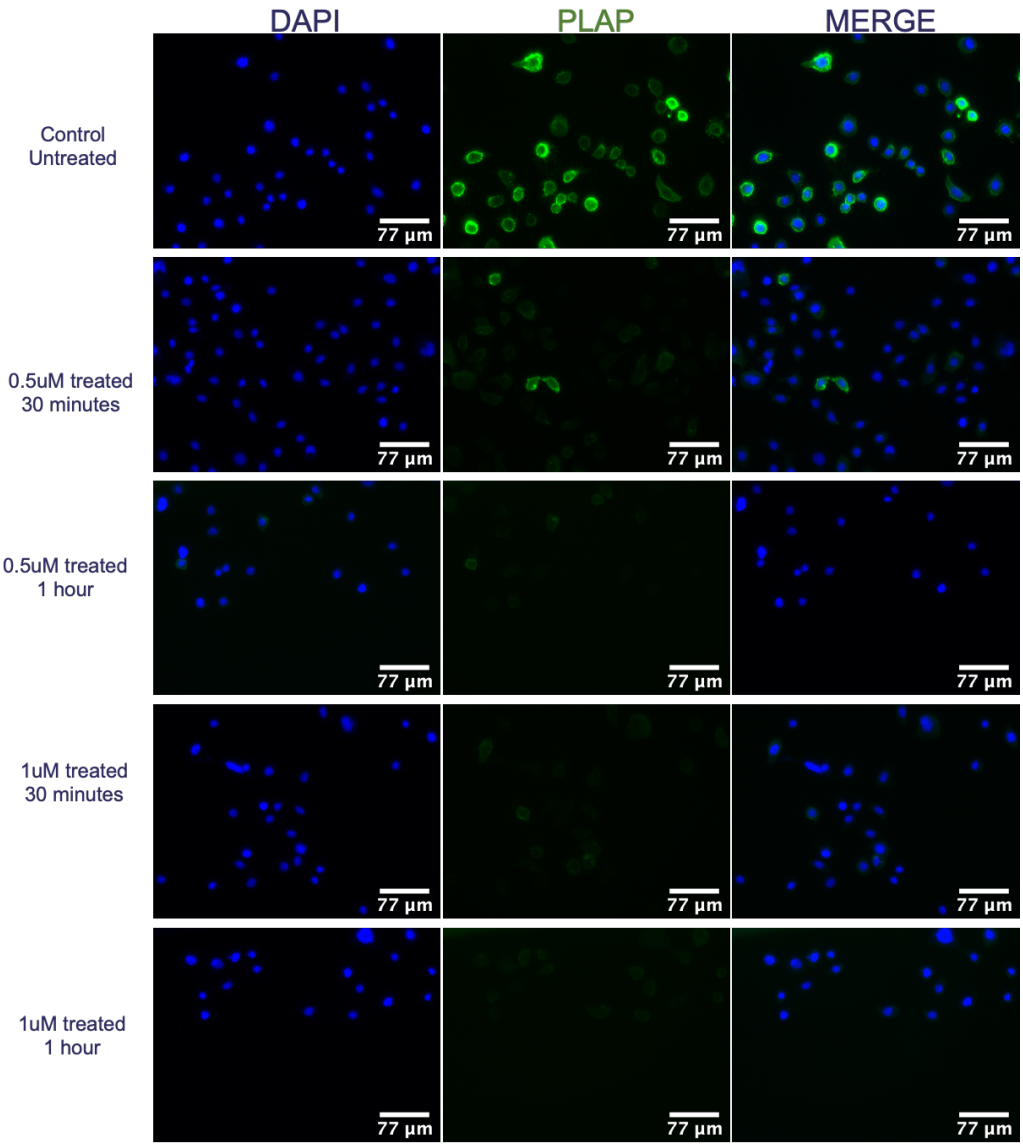

B.

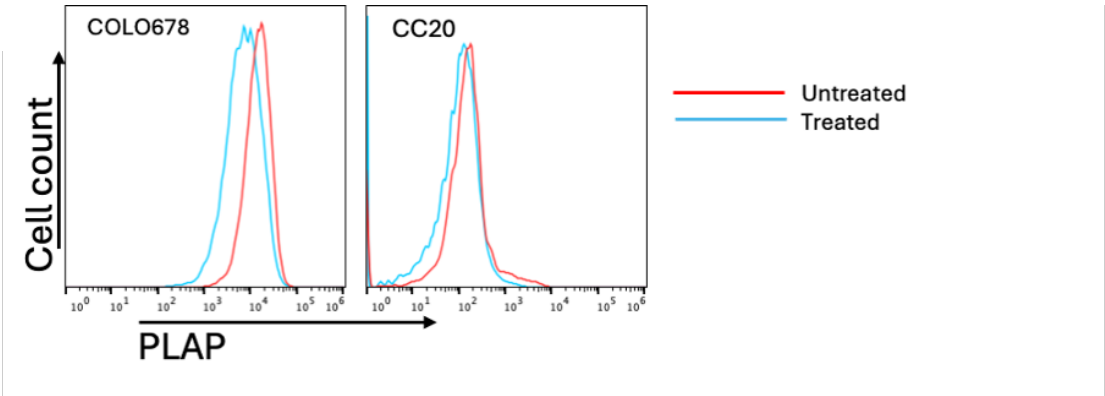

Figure 3.4: PLAP cleavage by phospholipase C.
Immunofluorescence staining of PLAP in COLO678 cells after treatment with phospholipase C for 30 minutes or 1 hour A. FACS staining of PLAP on COLO678 treated with phospholipase C 1uM for one hour B.

3.2.4 Internalization of anti PLAP antibody

The internalization of PLAP into COLO678 was traced by staining with anti-PLAP antibody (H17E2) by immunofluorescence. Cells were stained with anti PLAP (H17E2) and labelled with fluorescence secondary antibody and the internalization measured after 6 hours. There was antibody internalization and to localize the antibody inside the cells, cells were stained with LAMP1 (Lysosomal-associated membrane protein 1 antibody). In PLAP positive COLO678 show colocalization of anti-PLAP and LAMP1. The PLAP-negative cell line HT29 show staining for LAMP1 only figure 3.5.

To confirm PLAP expression, cells were incubated with H17E2 anti-PLAP for 6 hours then washed. Cells incubated with anti-mouse Alexa fluor 568 for 30 minutes and washed away. Cells then incubated with 5nM RPLP3 (humanized H17E2) for 4 hours. Next cells fixed and stained with anti-human Alexa fluor 488 then cells washed.

PLAP were expressed back on the cell's membrane. To confirm the location of antibody inside the lysosome in the cells. Cells were stained with LAMP1 (Lysosomal-associated membrane protein 1 antibody). In PLAP positive COLO678 show colocalization of anti PLAP and LAPM1. In PLAP negative HT29 show staining for LAMP1 only Figure 3.5.

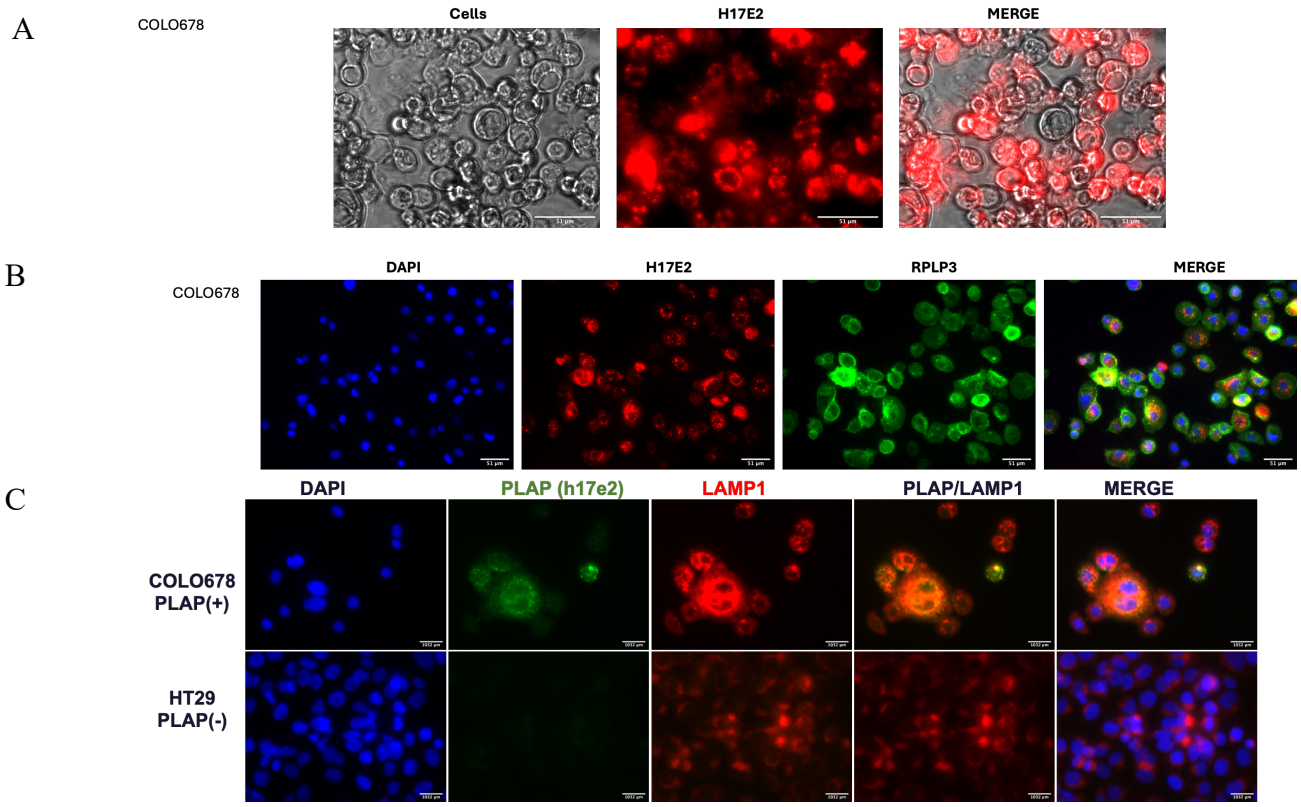

Figure 3.5: Internalization of anti PLAP antibody (H17E2).
A. Anti PLAP (H17E2) was labelled with secondary antibody and the internalization of the antibody after incubation for 6 hours on COLO678 shown by image of live cells in a fluorescence microscope. Fixed COLO678 stained with humanized H17E2 (RPLP3) B. C. Anti-PLAP (H17E2) internalization tested on COLO678 (PLAP+) and HT29 (PLAP -) by immunofluorescence staining and the localization detected by staining the cells with anti LAMP1, the green dots inside the cells could indicate the fragmentation of secondary antibody.

3.2.5 In-house antibodies cross react with ALPPL2 and PLAP

PLAP consists of 535 amino acid and ALPPL2 consists of 532 amino acids and their sequence alignment shows that the similarity is 96.99% (Bateman et al., 2023) (Figure 3.6).

```
PLAP      MQGPW---VLLLLGLRLQLSLGIIPVEEENPDFWNRQAAEALGAAKKLQPAQTAAKNLII  57
ALPPL2    MLGPCMLLLLLLLGLRLQLSLGIIPVEEENPDFWNREAAEALGAAKKLQPAQTAAKNLII  60
          * **    :**************************:**********************

PLAP      FLGDGMGVSTVTAARILKGQKKDKLGPETFLAMDRFPYVALSKTYSVDKHVPDSGATATA  117
ALPPL2    FLGDGMGVSTVTAARILKGQKKDKLGPEIPLAMDRFPYVALSKTYNVDKHVPDSGATATA  120
          ***************************  ***************.**************

PLAP      YLCGVKGNFQTIGLSAAARFNQCNTTRGNEVISVMNRAKKAGKSVGVVTTTRVQHASPAG  177
ALPPL2    YLCGVKGNFQTIGLSAAARFNQCNTTRGNEVISVMNRAKKAGKSVGVVTTTRVQHASPAG  180
          ************************************************************

PLAP      AYAHTVNRNWYSDADVPASARQEGCQDIATQLISNMDIDVILGGGRKYMFPMGTPDPEYP  237
ALPPL2    TYAHTVNRNWYSDADVPASARQEGCQDIATQLISNMDIDVILGGGRKYMFRMGTPDPEYP  240
          :********************************************** *********

PLAP      DDYSQGGTRLDGKNLVQEWLAKHQGARYVWNRTELLQASLDPSVTHLMGLFEPGDMKYEI  297
ALPPL2    DDYSQGGTRLDGKNLVQEWLAKRQGARYVWNRTELMQASLDPSVTHLMGLFEPGDMKYEI  300
          **********************:************:************************

PLAP      HRDSTLDPSLMEMTEAALLLLSRNPRGFFLFVEGGRIDHGHHESRAYRALTETIMFDDAI  357
ALPPL2    HRDSTLDPSLMEMTEAALRLLSRNPRGFFLFVEGGRIDHGHHESRAYRALTETIMFDDAI  360
          ****************** ****************************************

PLAP      ERAGQLTSEEDTLSLVTADHSHVFSFGGYPLRGSSIFGLAPGKARDRKAYTVLLYGNGPG  417
ALPPL2    ERAGQLTSEEDTLSLVTADHSHVFSFGGYPLRGSSIFGLAPGKARDRKAYTVLLYGNGPG  420
          ************************************************************

PLAP      YVLKDGARPDVTESESGSPEYRQQSAVPLDGETHAGEDVAVFARGPQAHLVHGVQEQTFI  477
ALPPL2    YVLKDGARPDVTESESGSPEYRQQSAVPLDEETHAGEDVAVFARGPQAHLVHGVQEQTFI  480
          ***************************** ****************************

PLAP      AHVMAFAACLEPYTACDLAPRAGTTDAAHPGPSVVPALLPLLAGTLLLLGTATAP       532
ALPPL2    AHVMAFAACLEPYTACDLAPPAGTTDAAHPGRSVVPALLPLLAGTLLLLETATAP       535
          ******************* ********** ***************** *****
```

Figure 3.6: The amino acid sequencing alignment of human ALPP and human ALPPL2 The sequences obtained from uniport and aligned using uniport alignment tool.

The stars indicate the similarity and gaps indicates the differences in the sequences in both genes. Overall, the sequence alignment is 96% similarity.

Due to their high similarity, it is likely that the in-house anti-PLAP antibodies (mouse anti- human antibodies H17E2 and HD8B6) will cross-react with both proteins. To test both antibodies reactivity, co-staining was done by using both HD8B6 and RPLP3 (the humanized form of H17E2). The co-staining of both antibodies shows the similar antigenic site on PLAP/ALPPL2 positive cell lines COLO678, CAR1 and LS123, and negative for the PLAP/ALPPL2 negative cell line HDC75 see Figure 3.7.

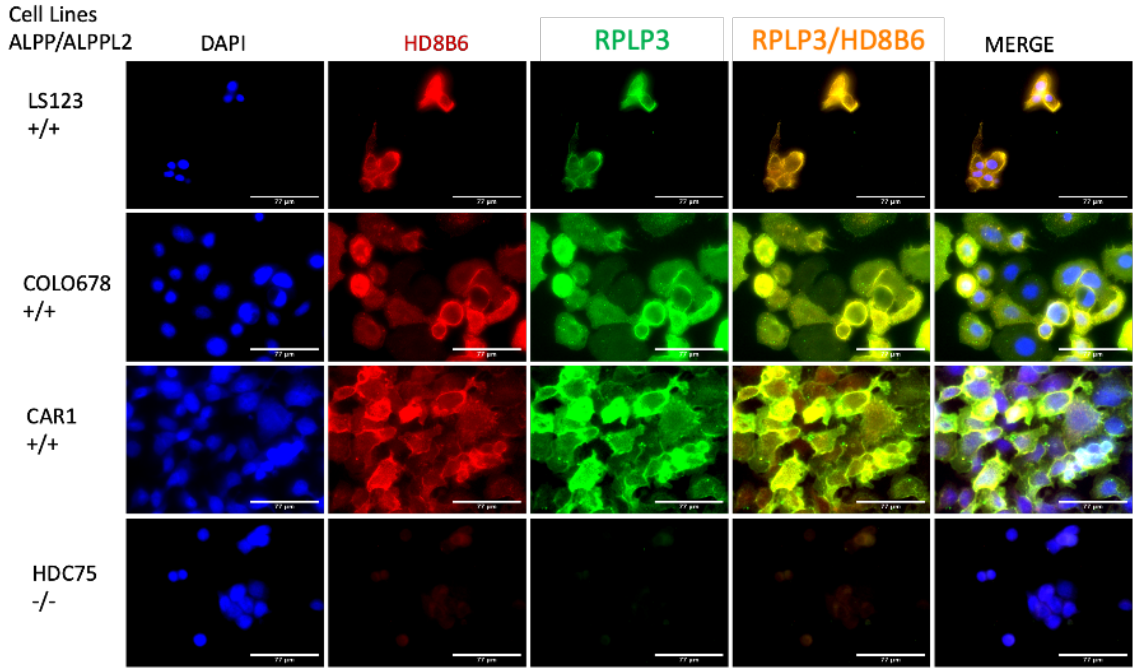

Figure 3.7: Immunofluorescence co-staining CRC cell lines with HD8B6 and RPLP3 (humanized form of H17E2). Co-staining of the ALPP/ ALPPL2 positive CRC cell lines LS123, COLO678 and CAR1 and the ALPP/ ALPPL2 negative HDC75. Co-staining with mouse anti-PLAP HD8B6 and human anti-PLAP PLAPh4. Co-staining shows the overlap of recognition of both antibodies.

To study the specificity or cross reactivity of the antibodies to PLAP and ALPPL2 we carried out transient transfection with siRNAs for PLAP and ALPPL2 on cell lines with positive expression. For example, COLO678 is a PLAP/ALPPL2-positive CRC cell line. After siALPP knockdown, we observed a reduction of protein expression by using H17E2 and HD8B6 antibodies compared to the protein expression of the control (siScramble). Also, siALPPL2 knockdown on COLO678 show reduction of the signal of protein expression by using both antibodies. However, performing siALPP and siALPPL2 knockdown together on COLO678 cells shows a more complete reduction of protein signal by using both anti-PLAP antibodies. By using siALPP and siALPPL2 it reduces the expression of both genes on COLO678. siRNA knockdown of one gene left some expression of the other genes. That suggests that, both antibodies recognize equally both PLAP and ALPPL2 see figures3. 8A and3. 8B.

The second method to study the recognition site of in-house antibodies (H17E2, HD8B6) is by the over expression of ALPP or ALPPL2 on ALPP/ALPPL2-negative cell lines (HT29 and LS180) for 72 hours. ALLP and ALPPL2 over-expression in both cell lines show an increase of protein expression and negative expression on control un-transfected cells. Protein expression was examined by using anti PLAP antibodies (H17E2 and HD8B6) by Immunofluorescence see Figure 3.9.A, B. GFP plasmid transfected on HT29 as control condition of transfection method see Figure 3.9.C.

Third method to study the reactivity of both antibodies is to stain normal human testis and normal human placenta by both antibodies using immunohistochemistry and immunofluorescence. ALPP is placental specific enzyme and ALPPL2 is testis specific enzyme. Both antibodies show reactivity on both human tissues type, placenta and testis. See figure 3.10).

A

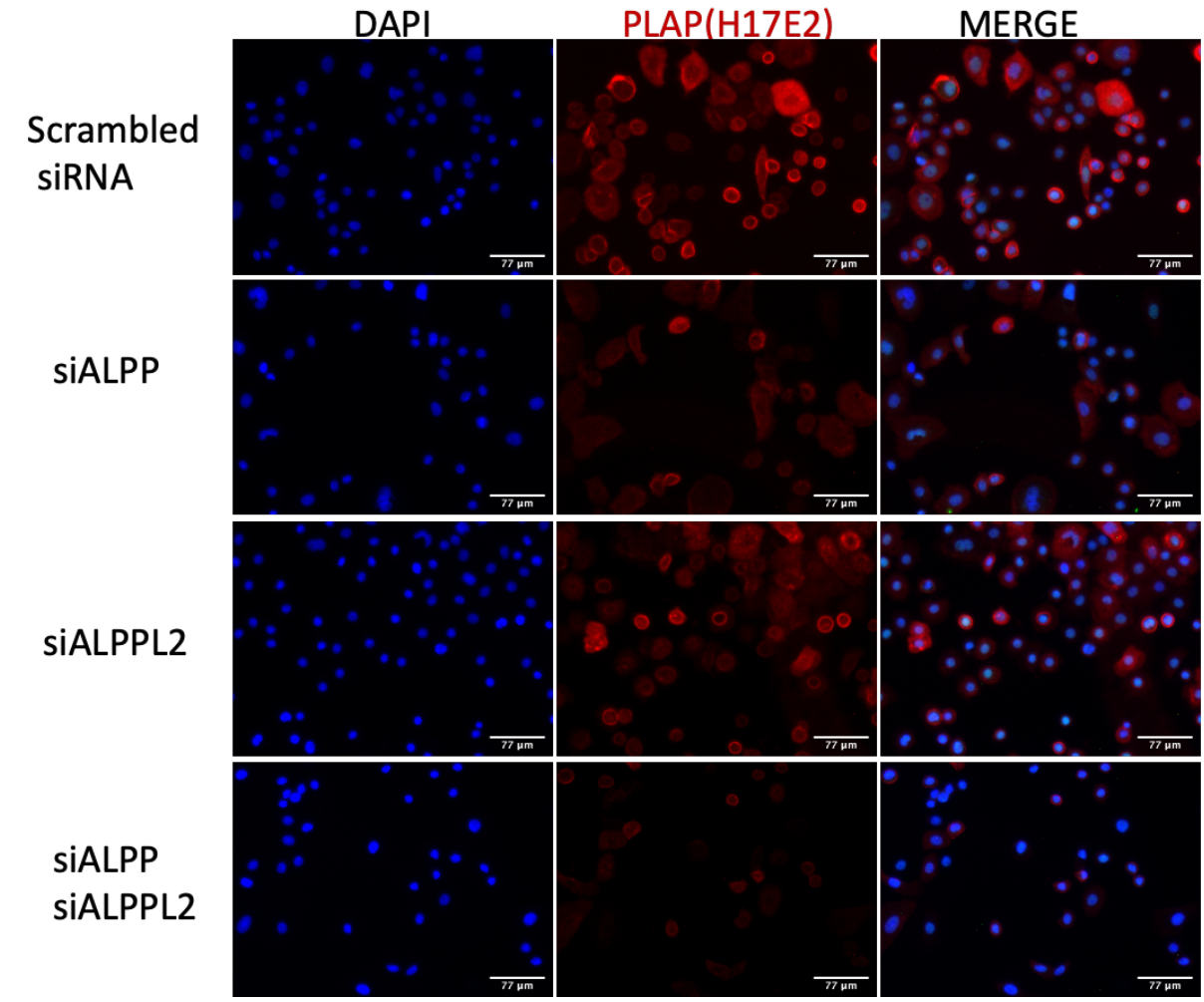

B

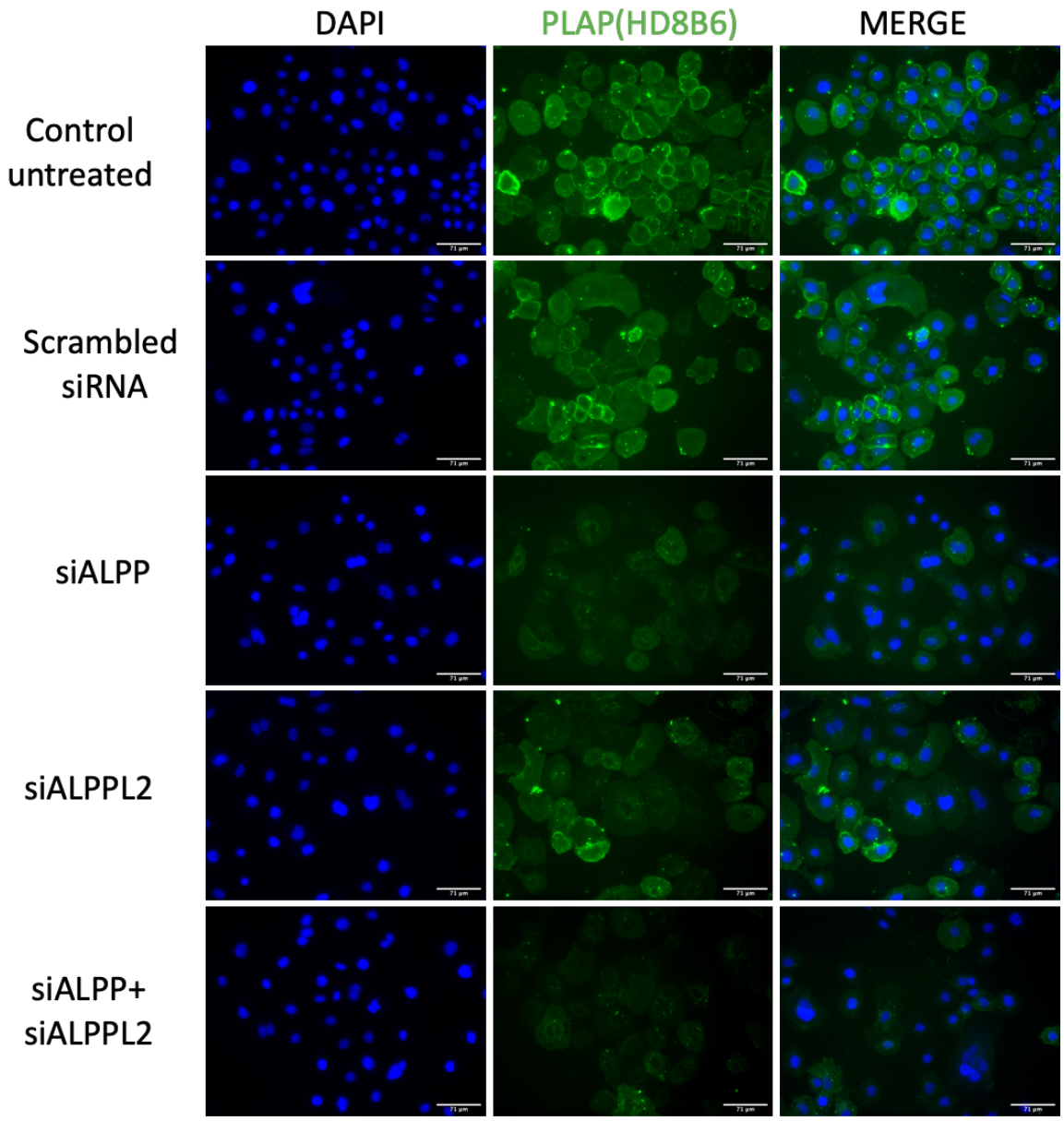

Figure 3.8: siALPP,and siALPPL2 Knockdown in PLAP positive cell line COLO678.siALPP and siALPPL2 Knockdown Experiment in COLO678.
(A) IF staining using in house H17E2 (anti PLAP). B. IF staining using in house HD8B6 (anti PLAP). siRNA used 20uM for 72 hours. siALPP or siALPPL2 knockdown alone each shows reduced the expression compared to the siRNA scramble. Knock down by both siALPP and siALPPL2 shows complete reduction of signal.

A.

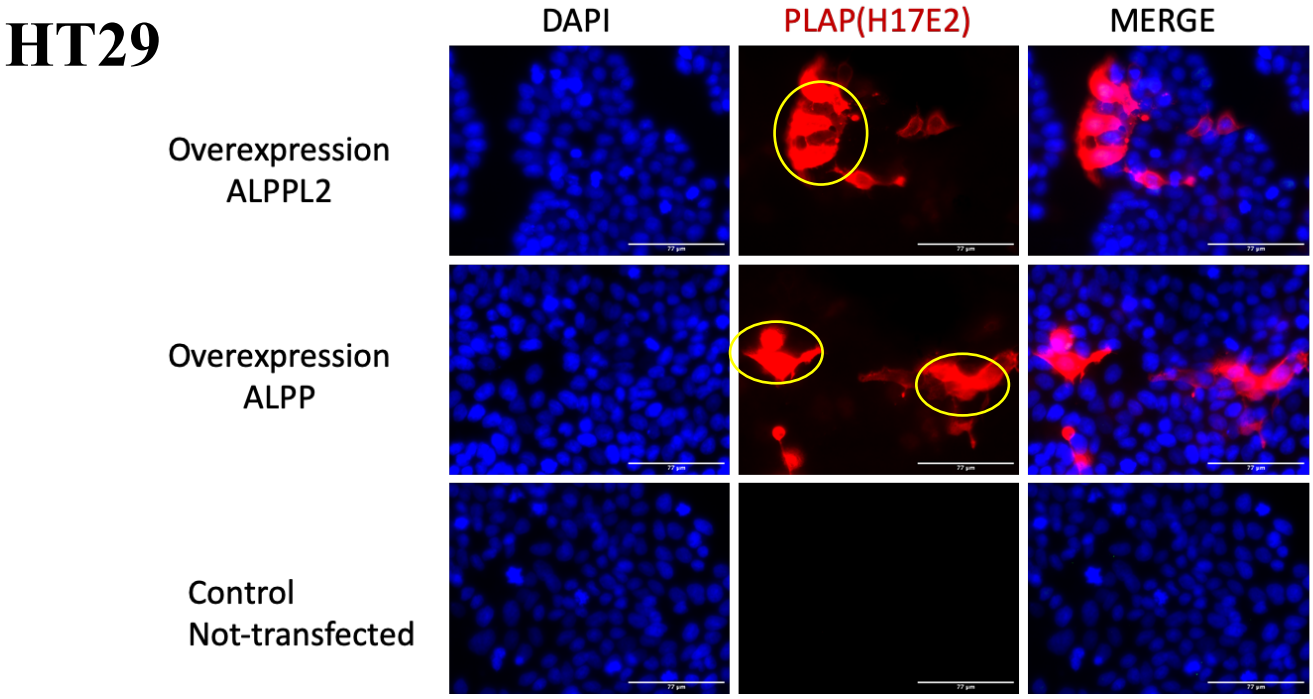
HT29
DAPI
PLAP(H17E2)
MERGE
Overexpression ALPPL2
Overexpression ALPP
Control Not-transfected

B.

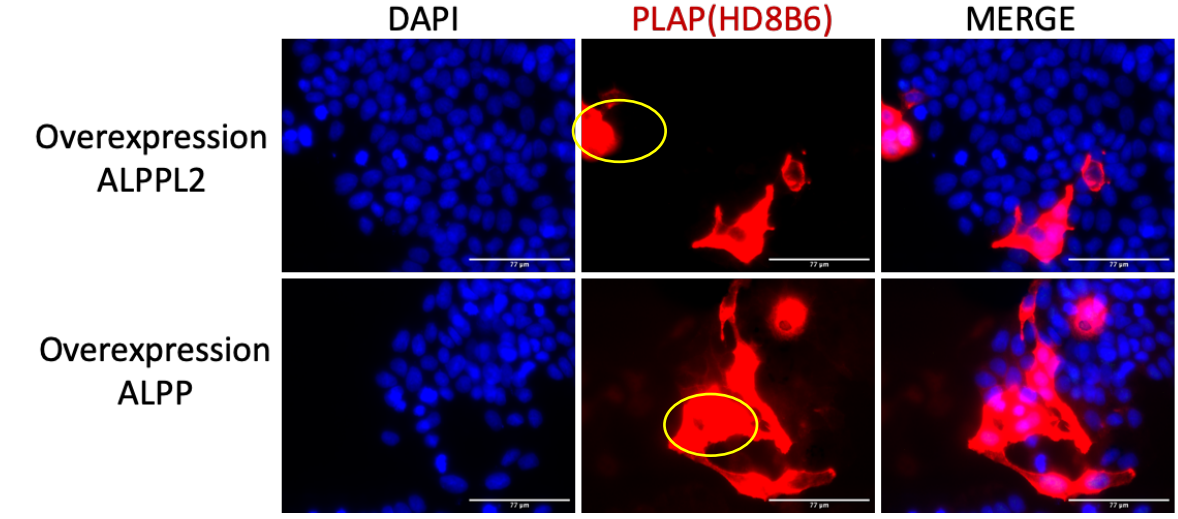
DAPI
PLAP(HD8B6)
MERGE
Overexpression ALPPL2
Overexpression ALPP

LS180

C.

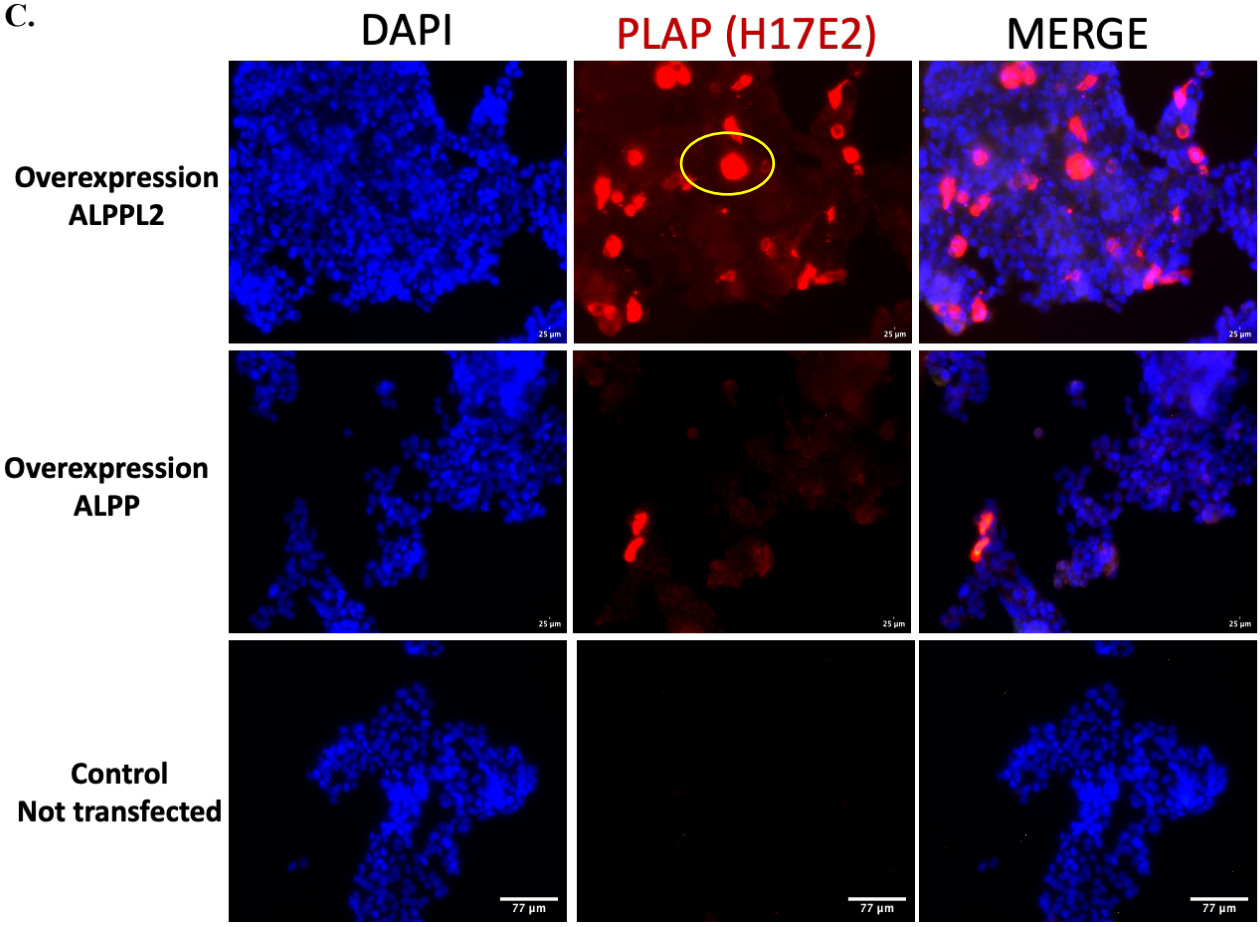
DAPI
PLAP (H17E2)
MERGE
Overexpression ALPPL2
Overexpression ALPP
Control Not transfected
77 µm

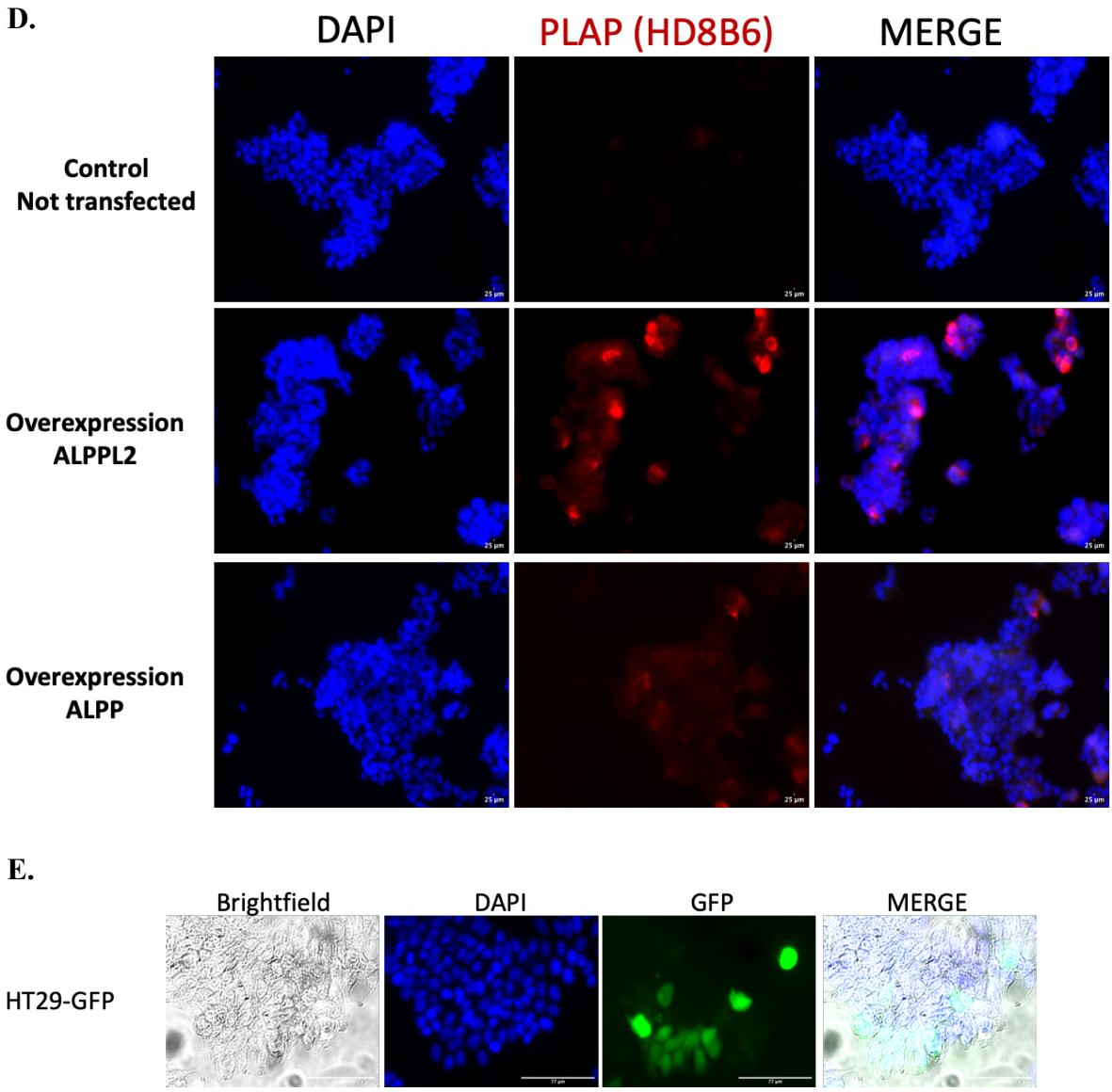

Figure 3.9: Over expression of ALPP and ALPPL2 on negative cell lines (LS180, HT29).
ALPP or ALPPL2 overexpression on HT29. A.C staining protein for both genes by anti PLAP H17E2 antibody and for both are showing positive staining. B D staining protein for both genes by anti PLAP HD8B6 antibody and for both are showing positive staining. E GFP overexpression on HT29 as control for the efficiency of transfection condition of the experiment. The immunofluorescent bulk not specific membrane staining indicated in yellow circle suggested an overexpression of PLAP/ALPPL2 due to might be aggregation of signal or overexpression and saturation of the protein or misfolding of the protein inside the cells.

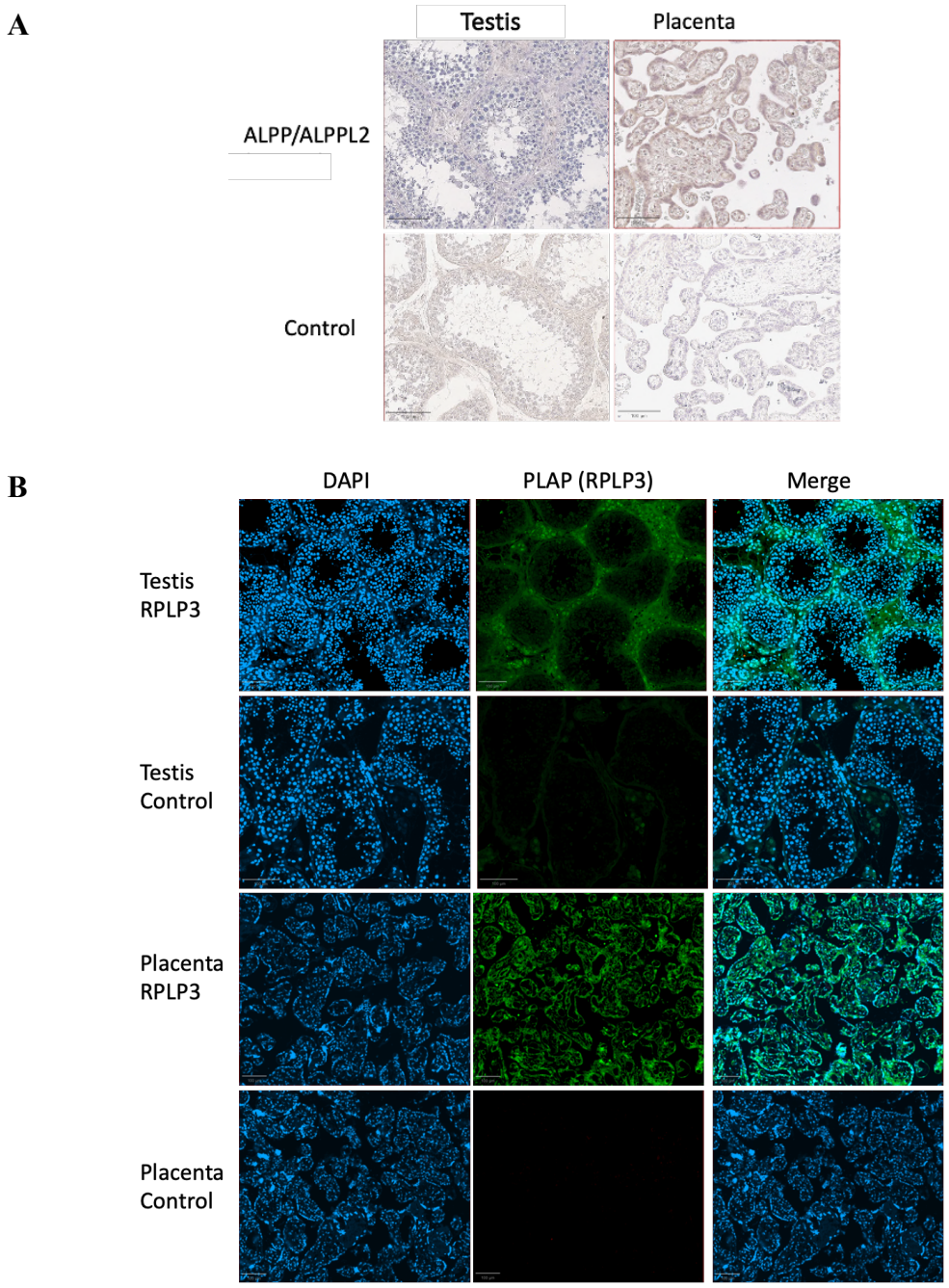

Figure 3.10: Human placenta and human testis tissues stained with HD8B6 and RPLP3 (humanized form of H17E2).

A. Immunohistochemistry staining with HD8B6 on human placenta and human testis, shows positive staining compared to negative control (secondary antibody) only B. Immunofluorescence staining of human placenta and human testis with RPLP3 (humanized H17E2), shows positive staining for both tissues compare to negative control placenta and control testis stained with secondary only (Rabbit anti-human). The tissues were blocked with serum to reduce nonspecific binding and placenta, and testis controls are secondary antibody only used as control to recognize nonspecific binding or any autofluorescence.

3.2.6 PLAP protein expression on panel of CRC cell lines

We next investigated the protein expression of PLAP and ALPPL2 on a panel of CRC cell lines and compared it the mRNA level. The expression of ALPP and ALPPL2 varies between cell lines based on their mRNA and protein level. The ALPP protein expression was tested by using FACS and immunofluorescence staining. The panel of CRC cell lines selected varies in their *ALPP* mRNA expression as seen in Table 3.3. The CRC cell lines selected are categorized according to three mRNA level (Figure 3.11, A. PLAP high, B. PLAP medium and C. PLAP low). PLAP high CRC cell lines based on mRNA level are CACO2, LS123, C14, in agreement with their protein expression by IF and FACS. The PLAP medium expressing CRC cell lines are DLD1, CCO7, OXCO1 and SW620, in agreement with their protein expression by IF and FACS. PLAP-low expressing CRC cell lines are VACO5, LS180, and HT29.

In comparison of ALPPPL2 with ALPP expression CACO2, LS123 and OXCO3 are both high mRNA expressing cell lines. CL14 has higher expression of ALPP than APPL2. CCO7 and OXCO1 and SW620 have low *ALPP* and *ALPPL2* mRNA expression but their protein staining on IF and FACS show a subset of positive staining. HT29 and LS180 and VACO5 are low expressing for both genes and have no positive staining by IF and FACS. PLAP expression distribution within the cell lines is varied. In PLAP positive expressing CRC cell lines, there is heterogeneity of PLAP expression within cell lines

That cannot be detected on mRNA expression as it is bulk mRNA analysis. In case of The LS123 cell line for example shows a unimodal high distribution of PLAP by FACS staining. For PLAP low CRC cell lines the distribution of PLAP staining and the isotype are generally overlapping.

Table 3.3: mRNA ALPP and ALPPL2 expression in a selected subset of CRC cell lines.

CRC cell lines	alkaline phosphatase, placental (ALPP)	alkaline phosphatase, placental-like 2 (ALPPL2)
CACO2	657	412
CL14	2664	266
LS123	3100	1163
OXCO3	749	439
DLD1	260	143
CCO7	34	79
SW620	69	65
OXCO1	51	89
HT29	35	82
LS180	51	85
Vaco5	51	58

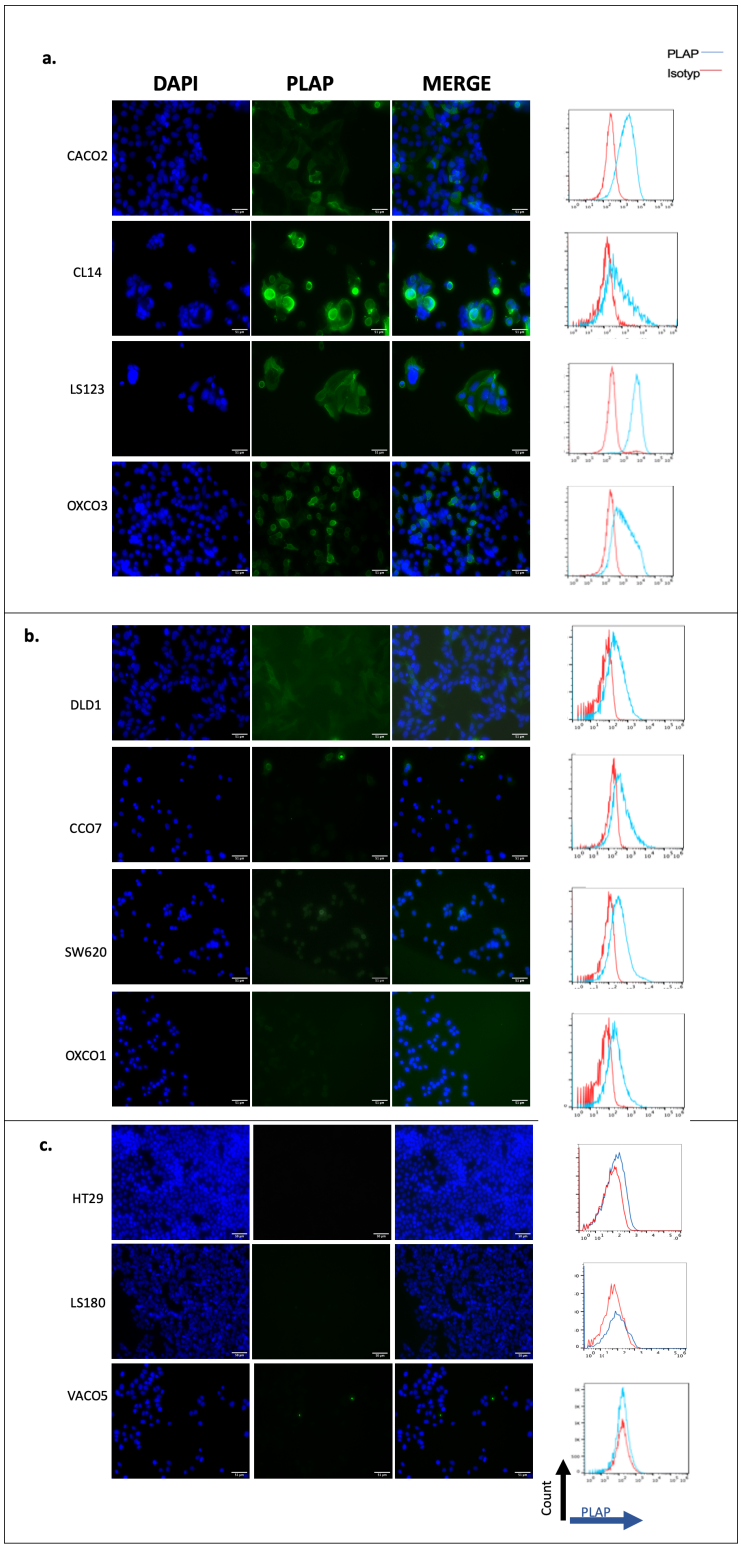

Figure 3.11: PLAP expression in CRC cell lines by immunofluorescence and FACS. PLAP expression was analysed by immunofluorescence and FACS on selected CRC cell lines. CACO2, CL14 LS123, and OXCO3 cells lines have high levels of PLAP expression (a), DLD1, CCO7, SW620 and OXCO1 have low levels (b). HT29, VACO5 and LS180 are PLAP-negative (c).

3.3 Discussion:

ALPP and *ALPPL2* are promising targets for cancer bispecific monoclonal antibody immunotherapy for colorectal cancer and other types of tumours(X. Li et al., 2020a). *ALPP* is express in placenta and *ALPPL2* expressed in testis but neither have been detected on other normal tissues, except for low expression on some lung tissues as will be discussed later, which make them a potent target for cancer immunotherapy (X. Li et al., 2020a; Su et al., 2020c). Both genes have been used as cancer specific antigens for immunotherapy (Su et al., 2020c).

Their high expression indicates the poor prognosis of cancer as is suggested from analysing *ALPP/ALPPL2* expression using the Kaplan-Meier survival curve on 517 patients of colon and rectal primary tumours. The top high 25% expressed compared to low expressed cancer for *ALPP* or *ALPPL2* had lower survival. The presented analysis shows almost 15% of colorectal cancer patients express *ALPP* or *ALPPL2* or both out of the 698 colorectal cancer patients.

Our panel of colorectal cancer cell lines shows that almost 20% of the CRC cell lines express ALPP or ALPPL2 or both. To compare both analyses, we found from cancer patients and cancer cell lines they are both agreed with the correlation between both genes expression making the panel of colorectal cancer cell lines good model to study colorectal cancer. The panel of CRC cancer cell lines is a good model to study the expression of cancer specific genes for immunotherapy for colorectal cancer.

PLAP is glycoprotein anchored to the plasma membrane and is cleaved by the phospholipase C enzyme (Berger et al., 1987). It is detected in the serum of cancer patients whose tumours express PLAP and so is a potent biomarker in the serum of the patients (Neumann et al., 2011). The internalization of anti-PLAP antibody shows the trafficking and degradation of anti-PLAP antibody by lysosomes. It suggests the PLAP/ ALPPL2 itself gets pulled inside the cells which could limit its availability on the cell surface to be targeted by therapy. As well as binding the bispecific antibody to PLAP/ ALPPL2 both get pulled inside the cells could limit the presence of bispecific antibody to attached to immune cells.

ALPP and ALPPL2 are members of the alkaline phosphatase family which have high similarity and many antibodies produced have cross reactivity to both genes (Su et al., 2020d). In this thesis the in-house mouse monoclonal antibodies H17E2 and HD8B6 have similar antibody recognition sites. Both antibodies were produced in our laboratory (Durbin, Milligan, et al., 1988; Travers & Bodmer, 1984a). From our earlier work, there is cross reactivity of ALPP and ALPPL2 using H17E2 however here more tests have been done to confirm the cross reactivity of both ALPP and ALPPL2. Also, from the previous work there is clearly no obvious cross reaction with ALPPI (Travers & Bodmer, 1984a). Here we show the cross reactivity of HD8B6 with both genes as well, however as it was made to recognize fixed conformation of protein, it cannot be used for the bispecific antibody therapy. Detecting ALPP from ALPPL2 is challenging, as any of the panel of

cell lines that don't express ALPP also does not express ALPPL2, which suggests both genes are regulated by the same expression control.

The study of the panel of colorectal cancer cell lines' mRNA expression patterns gives a starting point for testing targeted immunotherapy on any interesting genes. Here we screen *ALPP* and *ALPPL2* mRNA expression and mostly the protein expression staining agreed on mRNA expression. However, some CRC cell lines show heterogeneity of *ALPP* and *ALPPL2* protein expression, which cannot be observed on mRNA bulk analysis. Understanding the cause of expression cancer specific antigens on solid tumour and understanding the expression pattern and the heterogeneity are key to optimizing bispecific antibodies for therapy as will be discussed further in chapter 8.

Chapter 4: Testing PLAP-CD3 bispecific monoclonal antibody (RPLPh3) and EpCAM-CD3 bispecific monoclonal antibody as immunotherapy treatments for colorectal cancer.

4.1 Introduction

Bispecific T cell engaging monoclonal antibodies (BiMAb) are targeted immunotherapies based on antibodies that bind specifically a cancer target antigen and CD3 on T cells, through this, an artificial synapses are created between two cells; T cells and cancer cells, bypassing HLA recognition leading to T cell activation and killing the cancer cells (Herrera et al., 2024) (Klinger et al., 2016b). Engineering and developing the structure of antibodies can be done using different ways (Hosseini et al., 2021c). This is then engineered to include an anti-human CD3ε antibody and mutations in the Fc portion of the overall structure to prevent unwanted Fc mediated activity (Bacac et al., 2016c). The simultaneous binding of BiMAbs to a tumour associated antigen on cancer cells and to CD3ε on T cells results in redirection and activation of T cells and subsequent tumour cell cytotoxicity (Bacac et al., 2016b) (Klinger et al., 2016b). T cells induce cancer cell apoptosis by two mechanisms: through granule exocytosis releasing perforin and granzymes, and by releasing death ligands, such as FAS ligand (FASL) or TNF related apoptosis inducing ligand (TRAIL) (Martínez-Lostao et al., 2015).

In this work three bispecific T cell attracting antibodies were tested on a panel of colorectal cancer cell lines: PLAP-CD3 BiMAb HIN FC, EpCAM-CD3 BiMAb KIN FC, and EPCAM-CD3 BiMAb (BITE). These antibodies were also delivered as mRNA -lipid nanoparticles (LNPs). EpCAM-CD3 hFc mRNA-LNPs, EpCAM-CD3 bite mRNA-LNPs, and PLAP-CD3 mRNA LNPs were tested on a panel of colorectal cancer cell lines. PLAP is an antigen which has been detected on colon cancer (Harmenberg et al., 1991b). EpCAM is often over expressed in epithelial cell cancers and has been used as target for targeted therapy (Macdonald et al., 2018).

4.1.1 The Anti-PLAP-CD3 BiMAb (PLAPh3) and mRNA LNP delivered Anti-PLAP-CD3 BiMAb

A T cell attracting anti-PLAP bispecific monoclonal antibody (RPLP3) has been developed and received from our collaborators ProMab and Roche. The bispecific antibody against the PLAP target was developed from our in-house mouse anti- human PLAP (H17E2) (Travers & Bodmer, 1984, see chapter 3) (X. Li et al., 2020b) . The mouse anti-PLAP (H17E2) was humanized and engineered to be human T cell attracting antibody by Roche similarly to the approach used for our in-house anti CEA mAb (Bacac et al., 2016c). The anti-PLAP bispecific monoclonal antibody (RPLP3) is IgG1 and has two binding sites to PLAP bivalently on the membrane of cancer cell to increase the avidity to PLAP, and univalent to the CD3 epsilon chain on T cells. This is a key feature to avoid excess binding to T cells which might cause unwanted reactions and releasing excess of cytokines (Bacac et al., 2016c). The presence of an inactive Fc region on RPLP3, due to the introduced mutations, prevents unwanted effects of having a functionally active Fc region, while preventing rapid degradation by proteolytic enzymes in the blood giving the antibody a much longer half-life once it is delivered to a patient. (Bacac et al., 2016c) .The PLAP-CD3 BiMAb mRNA /LNP was received from ProMAb.

4.1.2 The Anti-EpCAM-CD3 BiMAbs / mRNA LNP delivered Anti-EpCAM-CD3 BiMAb

The T cell attracting anti EpCAM bispecific monoclonal antibodies have been developed by our commercial collaborator ProMab. The development of the bispecific antibody against EpCAM was based on our in-house mouse anti human EpCAM (AUA1) (Ntouroupi et al., 2008). (Durbin et al., 1990b). EPCAM is used as a target for the in vitro killing studies alongside PLAP because it is expressed on essentially all epithelial cells and so in most epithelial based cancers (adenocarcinomas) it is expressed by all the cells in the cancer. The mouse anti EpCAM antibody, AUA1, was humanized and engineered to be a human T cell attracting BiMAb by ProMab (Durbin et al., 1990b). Anti-EPCAM X CD3 BiMAb used in this work are used in two formats with same specificity: BiMAbs EpCAM-CD3 (BITE) and EpCAM-CD3 hFC. They have different formats as shown in Figure 4.1. The EpCAM-CD3 BiMAb mRNA /LNP was received from ProMAb.

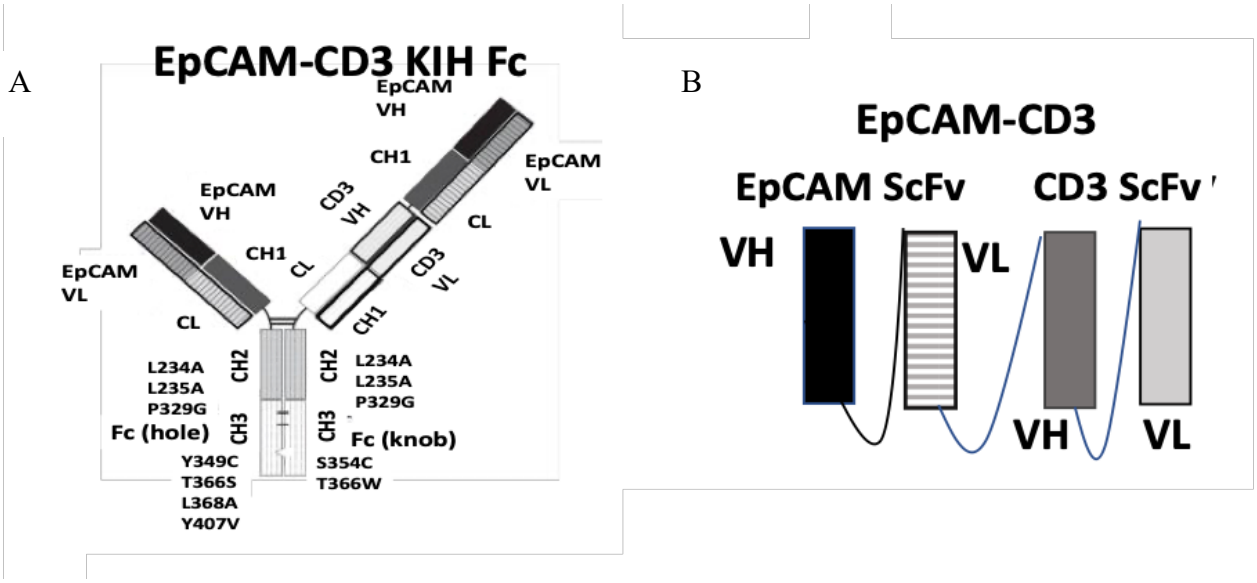

Figure 4.1: Diagram of CD3 X EPCAM bispecific monoclonal antibody formats. A. CD3-EPCAM hFC BiMAb has one CD3-, two EPCAM-binding sites, and an engineered silent Fc region. It consists of four peptides; two black and grey heavy chains, labelled (As I have already emphasized both the heavy and the light chains that contribute to binding the antigen, in this case EpCAM.); its specificity comes from AUA1 mouse anti-EpCAM. The white part of the heavy chain on one arm binds to CD3 epsilon and its specificity comes from the anti CD3 antibody. Light chains from the anti EpCAM and anti CD3 antibodies are labelled L. B. EpCAM-CD3 (BITE) BiMAb has monovalent binding site to EpCAM and monovalent binding to CD3(Golubovskaya et al., 2023b).

The effector cells from peripheral blood mononuclear cells (PBMC) from blood buffy coat cones of healthy donors were received from the blood bank at the John Radcliff hospital, Oxford, UK. PBMCs were purified using density-based centrifugation (refer to chapter 2 materials and methods for details). The percentage of T cells in PBMCs was between 45-70% of total PBMC (Lozano-Ojalvo et al., 2015). The T cell mediated killing of the CRC cell lines was measured in this thesis using the methods described in chapter 2 Materials and methods.

4.2 Results

4.2.1 The specificity of mouse anti-PLAP antibody was used to design PLAP-CD3 BiMAb (RPLP3)

The PLAP-CD3 BiMAb was designed using the specificity of the mouse anti-PLAP (H17E2). The staining of individual antibodies or co-staining of both antibodies using RPLP3 and H17E2 was tested on PLAP positive and PLAP negative colorectal cancer cell lines. The aim was to test the overlap of staining of both antibodies to prove the similarity of the epitope antigen recognition of both antibodies. COLO678, a PLAP positive colorectal cancer cell line, was tested for both antibodies' against PLAP. COLO678 cells were stained with H17E2 alone and stained with RPLP3 alone, or co-stained with both antibodies or isotype and analysed using FACS. Cells were stained with H17E2 and secondary anti mouse antibody Alexa fluor 568. Cells were stained with RPLP3 and secondary anti-human Alexa fluor 488 84.5% of the COLO678 cells were labelled with H17E2 and 85.6% of the cells with RPLP3. Overlap of staining by the two antibodies was clearly seen 84.6% of the cells (Figure 4.2).

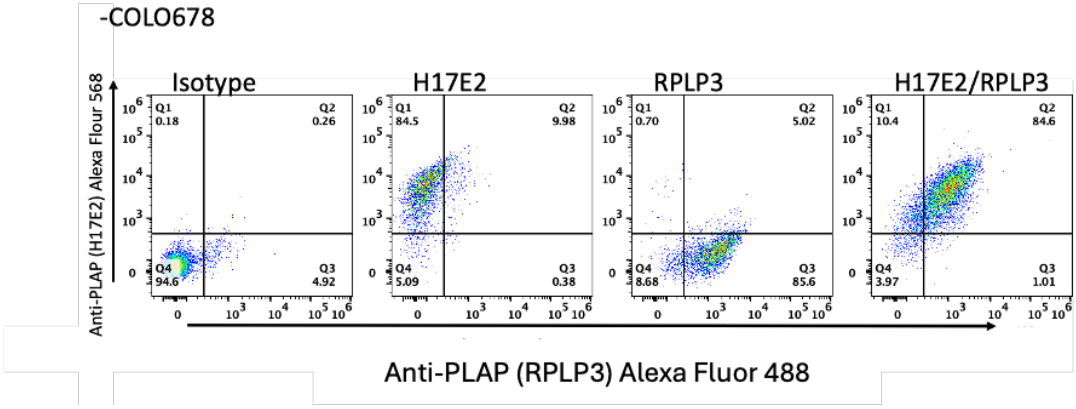

Figure 4.2: H17E2 and RPLP3 staining specificity for PLAP positive COLO678 cells by FACS analysis.
Flow cytometry analysis of staining of COLO678 with Isotype IgG and anti-PLAP (H17E2), and RPLP3 separately. As well co-staining COLO678 with both anti-PLAP antibodies (H17E2 and RPLP3) and both secondary antibodies (anti-Alexa fluor 488 and anti-human Alexa fluor 568).

4.2.2 Human anti-PLAP (PLAP-CD3 BiMAb (RPLP3) binds competitively to same epitope site as Mouse anti PLAP (H17E2)

We next aimed to test whether the engineered bispecific antibody still reacted with the H17E2 target on which it was based. We used two procedures: to stain the cells first with H17E2, then with RPLP3, or to stain the cells with RPLP3 first and then with H17E2. First, COLO678 incubated with H17E2 in different concentrations (1:1000), (1:500), (1:200), (1:100), and (1:10) for one hour. The cells were washed and then incubated with 5nM RPLP3 for 1 hour. The cells were fixed and stained with secondary antibodies. There was saturation of PLAP binding by H17E2 at a 1:10 concentration as shown by the lack of RPL3 binding at that concentration of H17E2. (Figure 4.3 A).

Secondly, COLO678 were stained with 5nM of RPLP3 for 1 hour, then the cells were washed and stained with different concentrations of H17E2 (1:1000), (1:500), (1:200), (1:100), and (1:10). The cells were fixed and stained with secondary anti-human Alexa fluor 568 and anti-mouse Alexa fluor 488. While there was evidence for some blocking of H17E2 by RPL3 it was not as clear cut as the other way round, suggesting that the effective concentration of RPLP3 was higher or that it was binding more strongly. (Figure 4.3.B)

A.

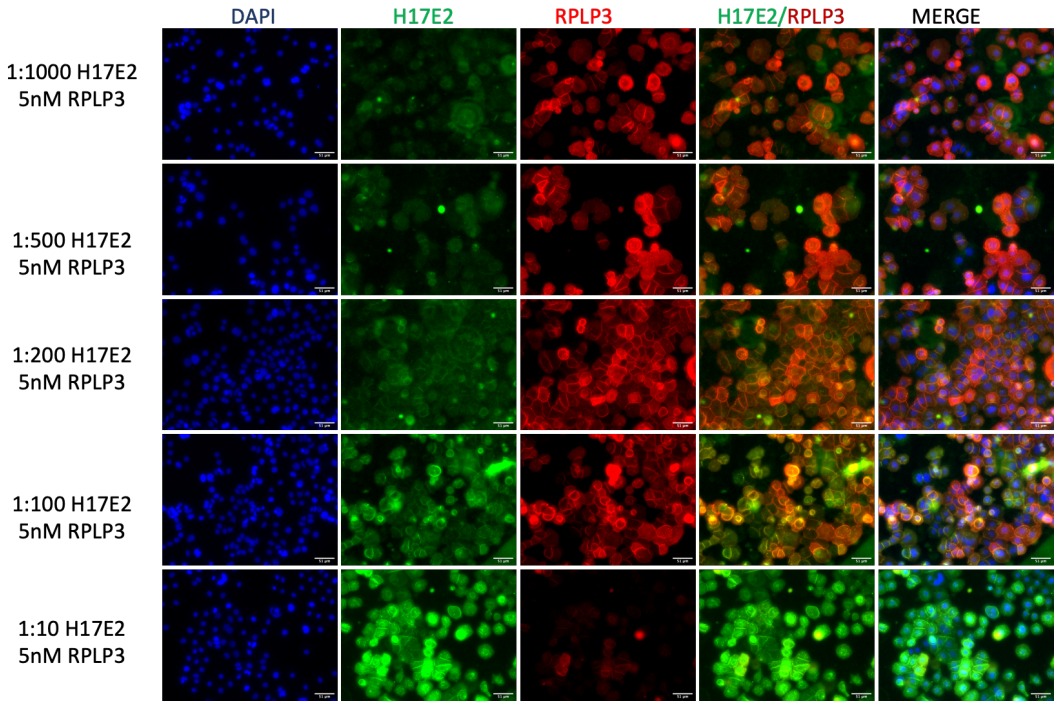

B.

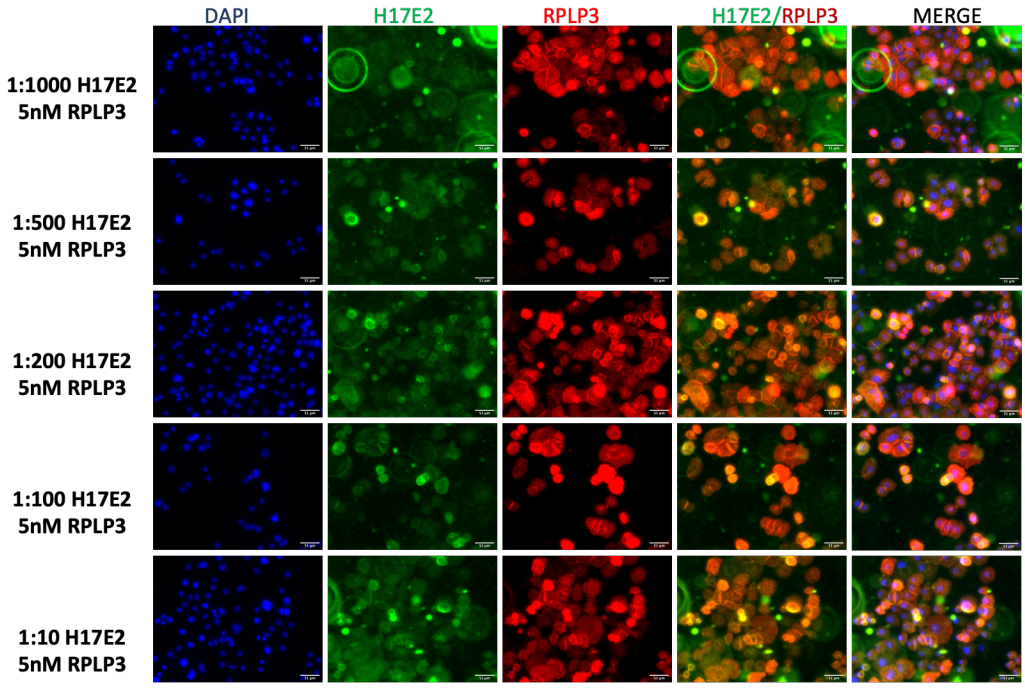

Figure 4.3: Binding of H17E2 and RPLP3 on the same antigenic site.
COLO678 were seeded in 96 well plates and stained using different conditions as labeled. A. COLO678 were incubated with H17E2 for 1 hour and washed, then stained with RPLP3 for 1 hour. The cells were washed and then fixed and stained with secondary anti-human Alexa fluor 568 and anti- mouse Alexa fluor 488. B. The cells were incubated with 5nM RPLP3 then washed and incubated with H17E2 with a different antibody dilution then fixed and stained with secondary antibodies anti-human Alexa fluor 568 and anti-mouse Alexa fluor 488.

4.2.3. RPLP3 and H17E2 staining on colorectal cancer cell lines.

We next validated the binding of anti-PLAP antibodies (H17E2 and RPLP3) to PLAP positive colorectal cancer cell lines and PLAP negative colorectal cancer cell lines. Immunofluorescence and flow cytometry staining of PLAP-positive and PLAP negative colorectal cancer cell lines with anti-PLAP antibodies H17E2 and RPLP3 was carried out. The PLAP-positive cell lines used were COLO678, DLD1 and LOVO. PLAP expression on these cell lines was recognized by immunofluorescence staining with RPLP3 as well as H17E2. The PLAP negative cell lines used were HT29, SKCO1, and LS180. No PLAP expression was detected using either anti-PLAP antibodies (H17E2 and RPLP3) (Figure 4.4.A).

We used flow cytometry analysis to test the specificity of RPLP3 on PLAP-positive CRC cell lines and PLAP-negative cell lines. The PLAP positive cell lines used were CACO2, LOVO, and HCA7 and PLAP-negative CRC cell lines used were HCC56, CX1, and C99 RPLP3 staining was positive on PLAP positive cell lines and negative for PLAP negative cell lines (Figure 4.4.B).

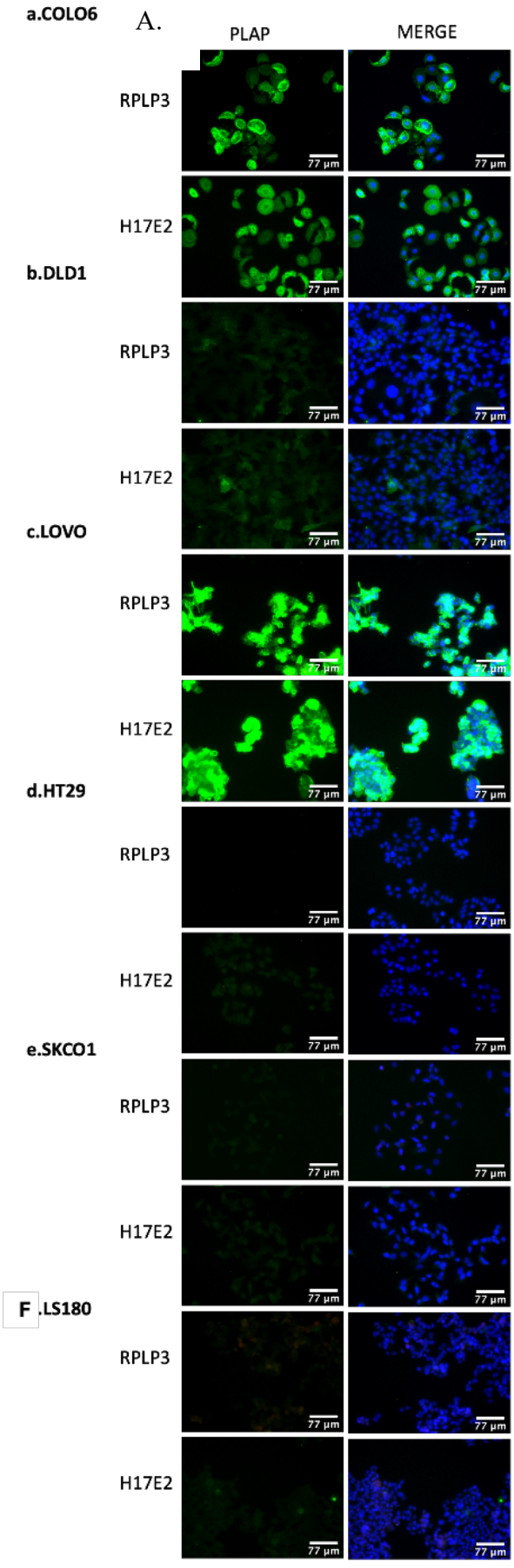
A.
PLAP
MERGE
a.COLO6
RPLP3
H17E2
b.DLD1
RPLP3
H17E2
c.LOVO
RPLP3
H17E2
d.HT29
RPLP3
H17E2
e.SKCO1
RPLP3
H17E2
F .LS180
RPLP3
H17E2
77 µm

B.

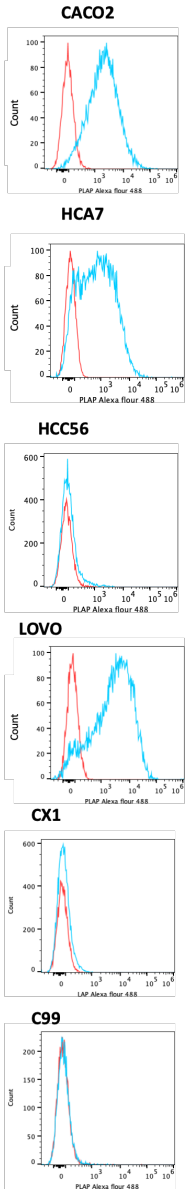

Figure 4.4: 5 Colorectal cancer cell lines PLAP staining with RPLP3.
A. Immunofluorescence staining of PLAP using RPLP3 and H17E2 on PLAP positive (COLO678, DLD1, LOVO) and PLAP negative CRC cell lines (SKCO1, HT29, and LS180). B. Flow cytometry staining of PLAP using RPLP3 on PLAP-positive (CACO2, HCA7 and LOVO), and negative on PLAP-negative CRC cell lines (HCC56, C99, and CX1), CACO2 staining shows positively unimodal continuous distribution for most population are positive except some of the population overlap with isotype could indicate negative or low expressed cells which are indistinguishable by the staining but no obvious shoulder presented, LOVO and HCA7 staining is continuous distribution with shoulder overlap with isotype control suggest subpopulation with low or negative population and there is heterogeneity of PLAP expression on these cell lines.

4.2.4 PLAP positive but not PLAP negative colorectal cancer cells lines were killed by T cells in the presence of RPLP3

We selected CRC cell lines with different PLAP expression levels to test the efficacy of RPLP3 immune mediated cell killing: COLO678, LOVO, and DLD1 are PLAP high expressed cell lines, and SKCO1 is low in PLAP. HT29, HDC75 and LS180 are negative CRC cell lines for PLAP expression. The cells were treated with 5nM RPLP3 and PBMCs were used as source of T cells. A ratio of cancer to PBMC cells of 1:10 was used and cell death was analysed by Apoptosense® ELISA M30 assay (PEVIVA).

PBMCs used in this work were obtained from healthy donors and the PBMC isolation was carried as method described in chapter 2 (material and methods). The percentage of CD3+ T cells within the PBMC population from healthy donors varies slightly, for example between 45.3% and 55.8% out of total PBMC population were CD3 positive (Figure 4.5 A).

As shown in Figure 4.5 B, RPLP3-mediated cell killing occurred in the PLAP positive cells, but not in PLAP negative cells, in agreement with their PLAP expression levels. There was a correlation between PLAP expression and RPLP3 mediated killing. Refer to table 4.1 for the level of mRNA expression of selected cell lines. There was no toxicity induced by the co culture CRC cell lines and PBMC or CRC cell lines and RPLP3.

Despite the sensitivity of using ELISA M30 as method to measure apoptosis there are some points need to be considerered. This method measures the amount of ccK18 which is released from cells undergoing apoptosis so if the positive cell line divides and increases the number of cells the amount of ccK18 will increase reflecting ~~to~~ the number of cells being killed. This does quantitatively compare the amount of killing between cell lines as this varies depending on their rate of division. Here, DLD1 divides rapidly as compared to LOVO. This shown by the difference in the amount killing measured by ELISA M30 of DLD1 being higher than for LOVO. The results show that this method of measuring killing is quite sensitive and so may often give overall killing of the cells even when some cells only express low levels of PLAP. If the cell line is heterogeneous in its level of PLAP expression, the variation of killing within the cell line will not be shown in this method.

Cell death was also measured by staining with the early apoptosis marker cleaved caspase 3 using immunofluorescence (Figure 4.6). The cleaved caspase 3 staining is positive on PLAP-positive cells COLO678, LOVO, and DLD1 but negative on PLAP negative cell lines HT29, LS180. Even the low expressed DLD1 cells show killing indicating the sensitivity of RPLP3 detection of PLAP with respect to killing.

The limitation of using this approach is that when cells undergo apoptosis, they lose their attachment to the bottom of the well. This makes it challenged to quantify the killing using IF staining of death markers. Cells also lose their morphology when undergoing apoptosis so staining the cells with cell membrane marker PLAP could be challenging as well. Nevertheless, this method can show the killing of heterogeneous populations within the cell lines.

A.

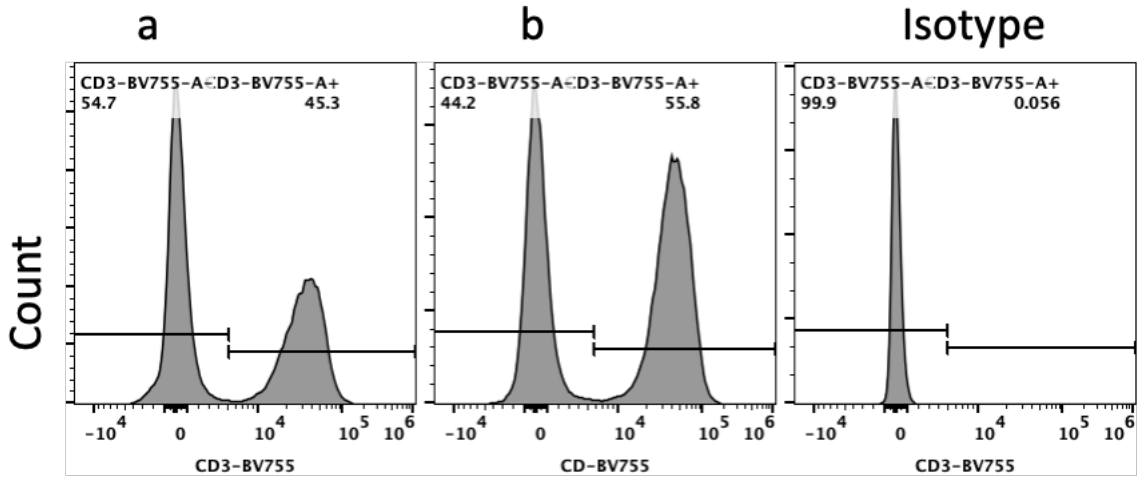

B.

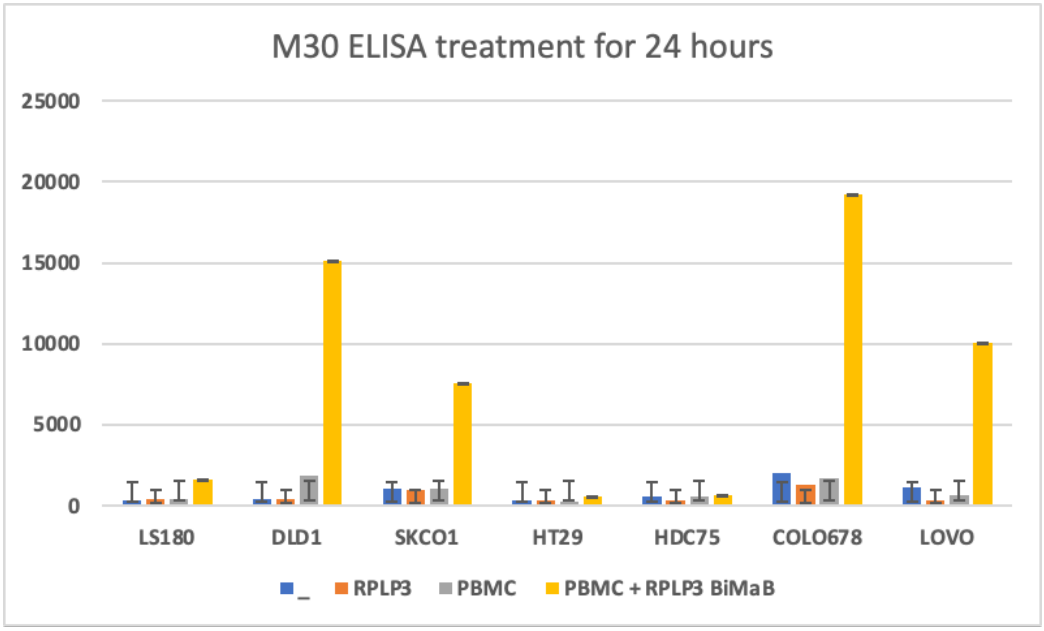

Figure 4.5: PLAP-positive and not PLAP-negative colorectal cancer cell lines are killed by T cells in the presence of RPLP3.
A. CD3-positive T cell percentage in the PBMC population from 3 different donors. PBMCs were stained by FACS with anti-CD3 antibody and BV755 isotype a. 45.3% of CD3+ cells and b. 55.8% CD3+ cells within the PBMC population. B. CRC cell lines were treated with 5nM RPLP3 and co culture with PBMC in ratio effector cells to cancer cells (1:10). Killing was measured after 24 hours as indicated in the graph, using a M30 ELISA kit. Blue nothing; Orange only RPLP3; Gray only PBMC added; Yellow PBMC + RPLP3.

Table 4.1 mRNA expression of ALPP, ALPPL2 on selected CRC cell lines.

CRC cell lines	***ALPP***	***ALPPL2***
COLO678	2998	601
DLD1	260	143
SKCO1	63	85
HCA46	46	112
HCC56	30	90
LS180	51	85
CC20	50	77
LOVO	693	831
HT29	35	82

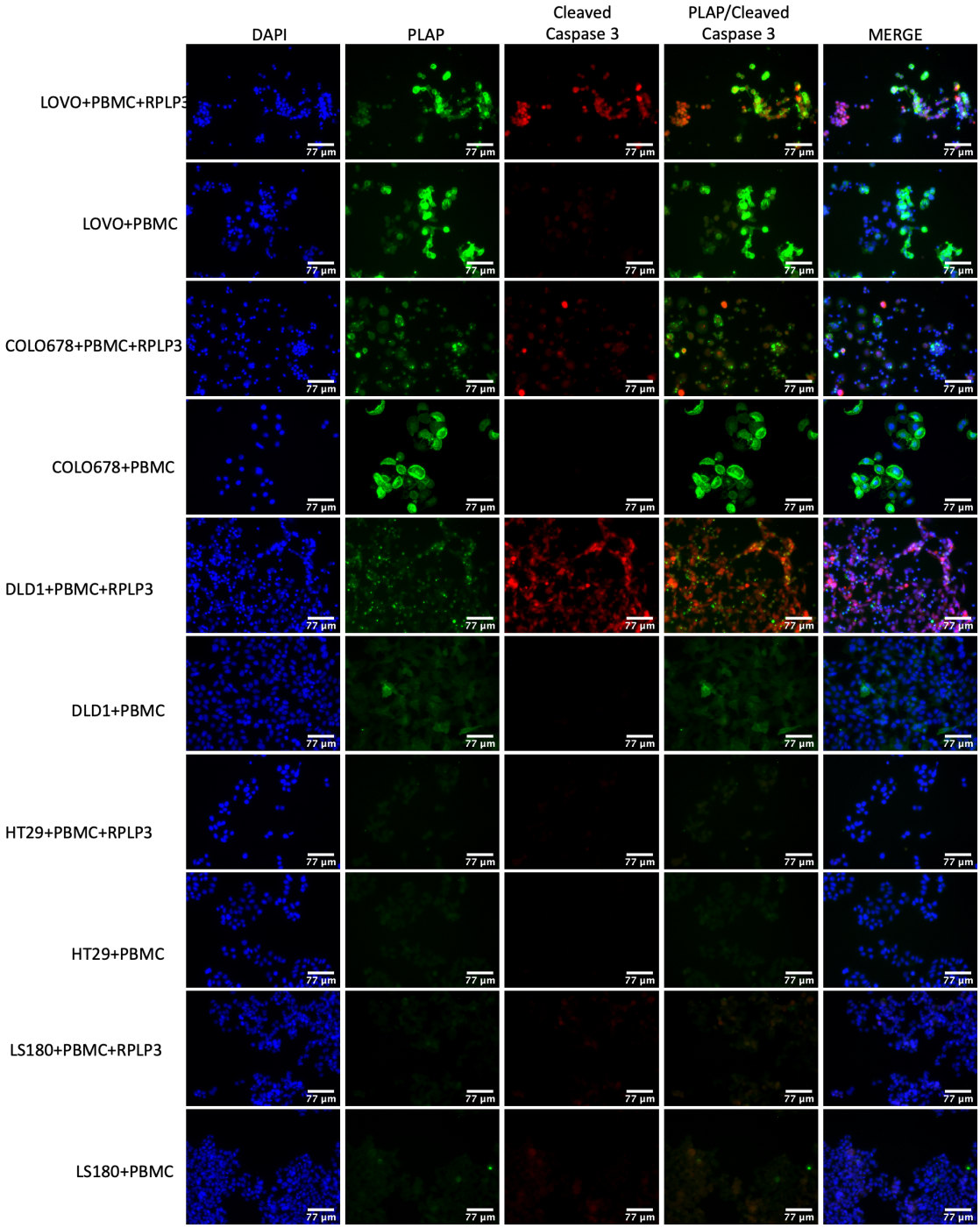

Figure 4.6: PLAP-positive (Lovo, COLO678, DLD1) and not PLAP-negative colorectal cancer cell lines (HT29, LS180) are killed by T cells in the presence of RPLP3.

CRC cell lines were treated with 5nM RPLP3 and co-culture with PBMC in a ratio of effector cells to cancer cells (10:1). Killing was measured after 24 hours, analyzed using immunofluorescence staining of cleaved caspase 3. The proportion of killing stained by cleaved caspase 3 is not a reliable quantitively measurement as when cells go under apoptosis they detached get washed off.

4.2.5 PLAP positive but not PLAP negative colorectal cancer cells lines were killed by T cells in the presence of RPLP3 for 24 hours and 48 hours.

We selected CRC cell lines with different PLAP expression levels to test the efficacy of RPLP3 immune mediated cell killing: COLO678, and DLD1 were used as PLAP high cell lines, and SKCO1 is low in PLAP. CC20, and LS180 are negative CRC cell lines for PLAP expression. The cells were treated with 5nM RPLP3 and PBMCs were used as source of T cells for 24 hours and 48 hours. A ratio of cancer to PBMC cells of 1:10 was used and cell death was analysed by Apoptosis ® ELISA M30 assay (PEVIVA). As shown in Figure 4.7, RPLP3-mediated cell killing occurred in the PLAP positive cells even with low expressed cells, but not in PLAP negative cells, in agreement with their PLAP expression levels. There was a correlation between PLAP expression and RPLP3 mediated killing. As mentioned earlier the killing induced by RPLP3 on low expressed cells as high expressed cells indicate the sensitivity of RPLP3. The effect of RPLP3 induced killing increased with the time of the treatment and the killing increased almost double for the treatment of 48 hours.

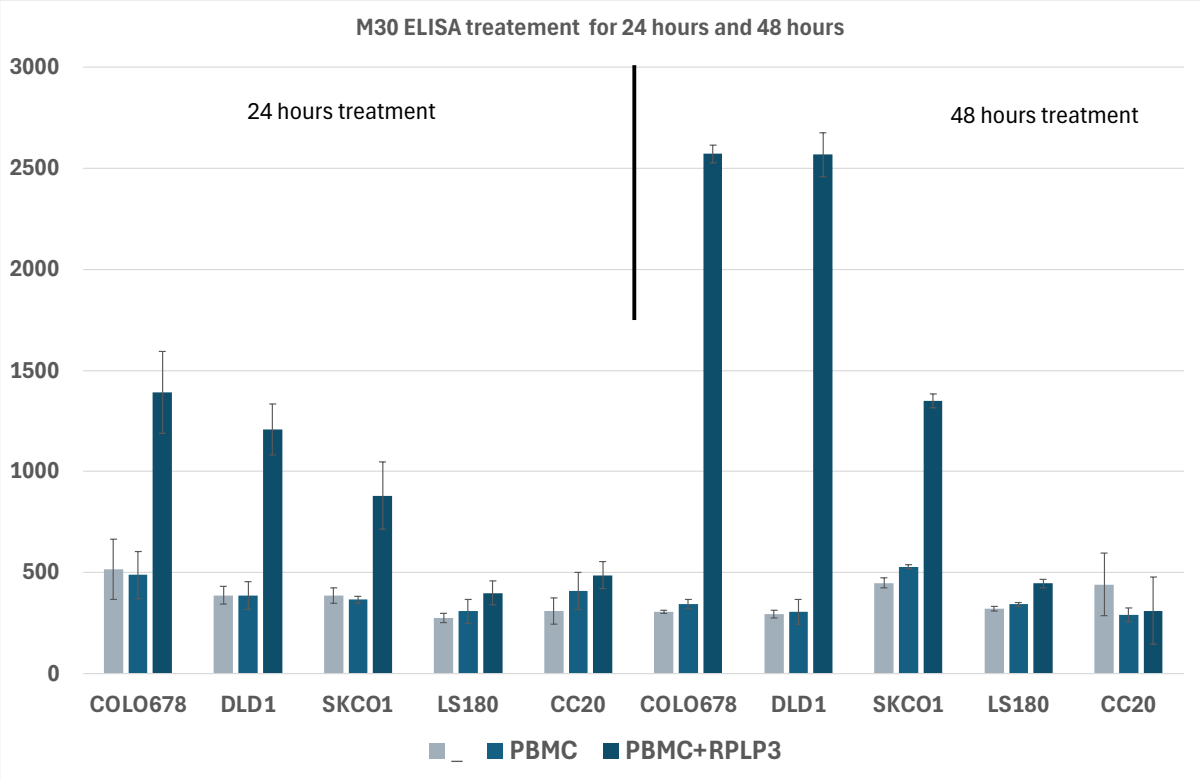

Figure 4.7: PLAP-positive and not PLAP-negative colorectal cancer cell lines are killed by T cells in the presence of RPLP3 CRC cell lines were treated with 5nM RPLP3 and co culture with PBMC in ratio effector cells to cancer cells (1:10). Killing was measured after 24 hours and 48 hours as indicated in the graph, using a M30 ELISA kit. There were differences between samples treated with RPLP3 and control cells (PBMC only), the differences were statistically significance ($P < 0.05$ T-test).

4.2.6 The Colorectal cancer cells lines that have ALPPL2 higher expression than ALPP were killed by T cells in the presence of RPLP3 for 24 hours and 48 hours.

We selected CRC cell lines with different *ALPP* and *ALPPL2* expression levels to test the efficacy of RPLP3 immune mediated cell killing: COLO678, and DLD1 were used as *ALPP* and *ALPPL2* high cell lines, their mRNA expression is above the threshold, and HCC56 and HCA46 expressed *ALPPL2* higher than *ALPP* (below the threshold for ALL and above the threshold, indicated by GMM refer to chapter 3*)*. CC20 is negative CRC cell lines for *ALPP* and *ALPPL2*. SKCO1 is low for both genes but has heterogeneity in its expression as seen in IF staining. The mRNA level of the selected cell lines is given Table 4.1.

The cells were treated with 5nM RPLP3 and PBMCs were used as source of T cells for 24 hours and 48 hours. A ratio of cancer to PBMC cells of 1:10 was used and cell death was analysed by Apoptosense® ELISA M30 assay (PEVIVA). As shown in Figure 4.8, RPLP3-mediated cell killing occurred in the *ALPP* and *ALPPL2* positive cells (COLO678 and DLD1), but not in PLAP negative cells (CC20), in agreement with their *ALPP*, *ALPPL2* expression levels. In the *ALPPL2* expressing cell lines, HCA46 and HCC56, with *ALPPL2* expression higher than *ALPP,* there was some killing at 24 hours treatment which was significantly increased after 48 hours treatment. This clearly shows that the RPLP3 antibody will kill low expressing ALPPL2 cell lines even in the absence of ALPP expression.

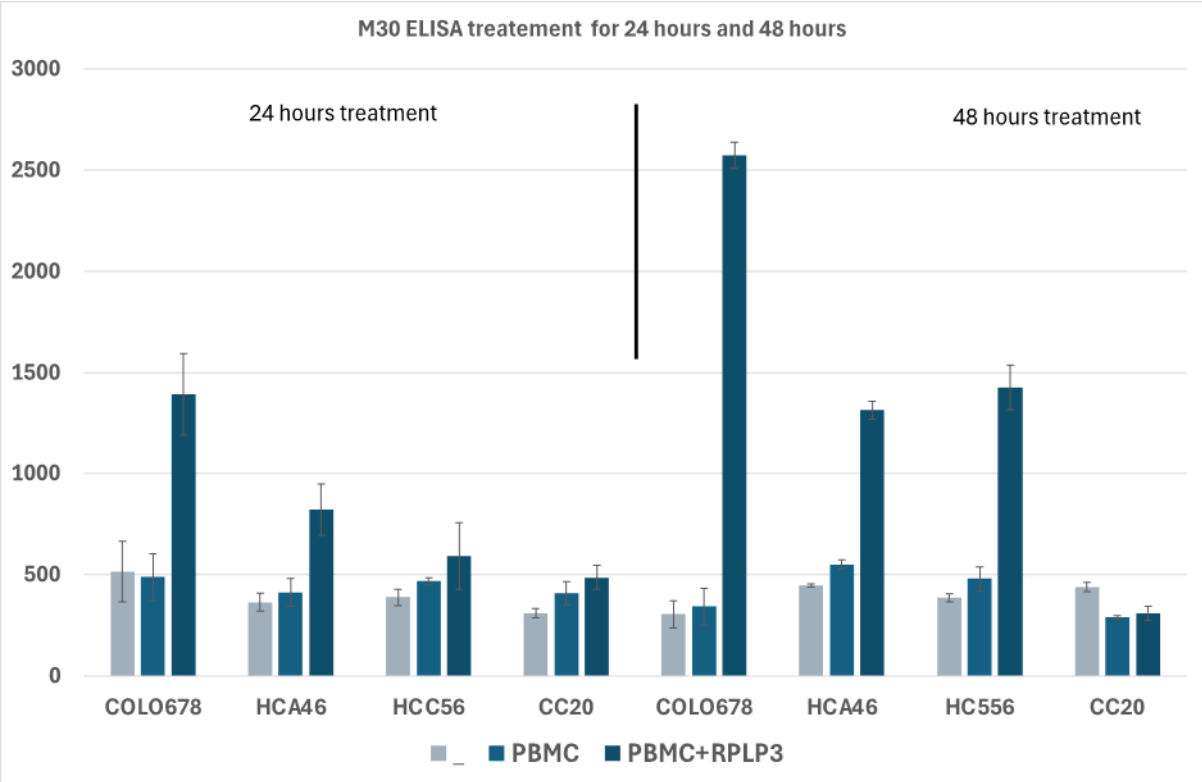

Figure 4.8. ALPP, ALPPL2 - positive and and not ALPP, ALPPL2-negative colorectal cancer cell lines are killed by T cells in the presence of RPLP3.
ALPP, ALPPL2 - positive and not ALPP, ALPPL2-negative colorectal cancer cell lines are killed by T cells in the presence of RPLP3 CRC cell lines were treated with 5nM RPLP3 and co culture with PBMC in ratio effector cells to cancer cells (1:10). Killing was measured after 24 hours and 48 hours as indicated in the graph, using a M30 ELISA kit.

4.2.7 The expression of EpCAM in colorectal cancer cell lines

EpCAM mRNA expression on a panel of 78 of colorectal cancer cell lines is shown in Figure 4.9. Nearly all of the CRC cell lines express EpCAM. The GMMchi algorithm on 78 of the cell lines was used to show the expression of EpCAM (Figure 4.10) It shows that EpCAM has a unimodal distribution and that all but one (CC20) of the cell lines express EpCAM, with a few with low EpCAM expression (e.g. CCO7, OXCO1).

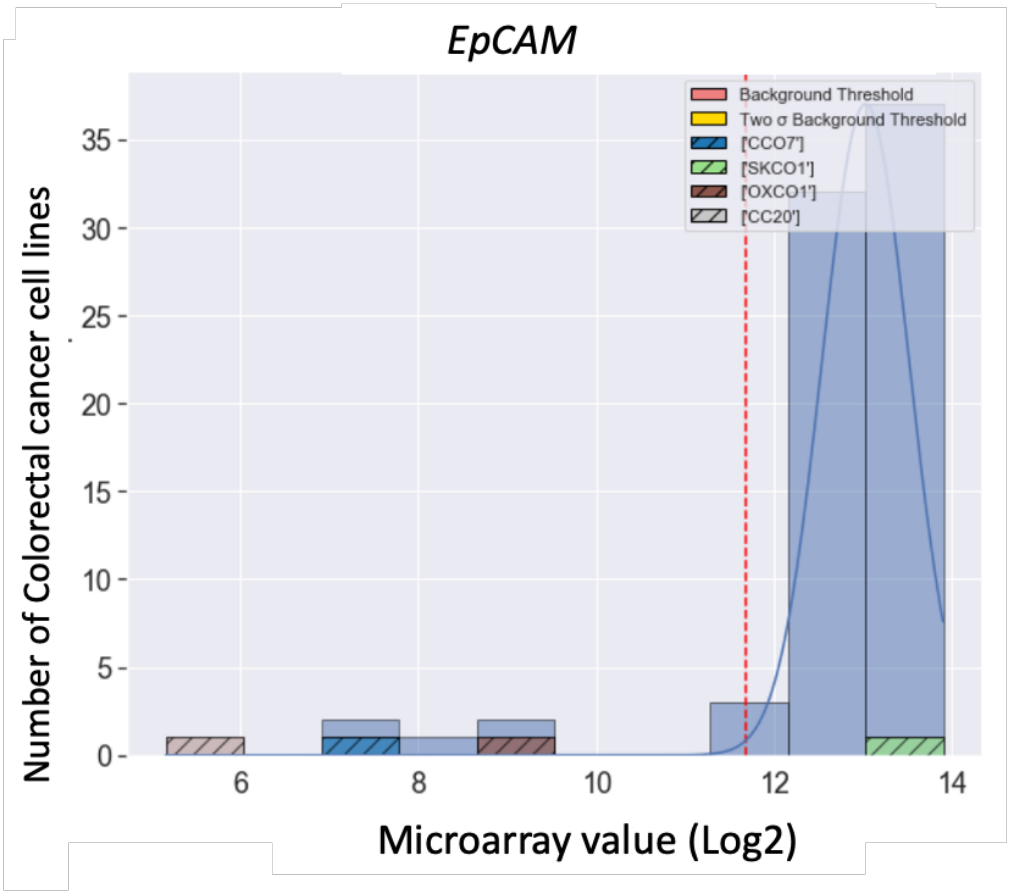

Figure 4.9: The analysis by using Gaussian Mixture Modeling (GMM) to draw the distribution of expression and the identification of EpCAM negative or weakly positive cell lines.
The GMM analysis shows the microarray expression of 78 CRC cells lines for EpCAM. The GMM distribution shows the number of cell lines positive as well negative or low expression for EpCAM. The GMMchi algorithm was created by Dr. Ta-Chun Liu (description in chapter 2 the materials and methods). The GMM histogram description explained in chapter 1.

4.2.8 EpCAM positive, but not the EpCAM negative colorectal cancer cell lines were killed by T cells in the presence of EpCAM antibody

CRC cell lines with high EpCAM expression levels (COLO678, DLD1, HCA46, HCC56, and LS180) were selected to test the efficacy of EpCAM CD3 BiMAB in immune mediated cell killing. CC20 was used as the example of an EpCAM negative cell line. The cells were treated with 8 nM EpCAM-CD3 BiMAb and PBMCs as source of T cells in a ratio of effector to cancer cells of 10:1. Cell death was analysed by Apoptosense® ELISA M30 (PEVIVA). As shown in Figure 4.10, the EpCAM-CD3 BiMAb mediated cell killing of EpCAM positive cells, but not the EpCAM negative cell line, in agreement with their EpCAM expression levels.

Cell death was also measured by staining for the early apoptosis marker cleaved caspase 3 by immunofluorescence (Figure 4.11). DLD1 cells were transfected to stably express GFP and CC20 were transfected to stably express mCherry. DLD1cells are EpCAM positive and CC20 cells EpCAM negative. Both cell lines were treated with 8 nM of EpCAM-CD3 BiMAb and PBMC for 24 hours.

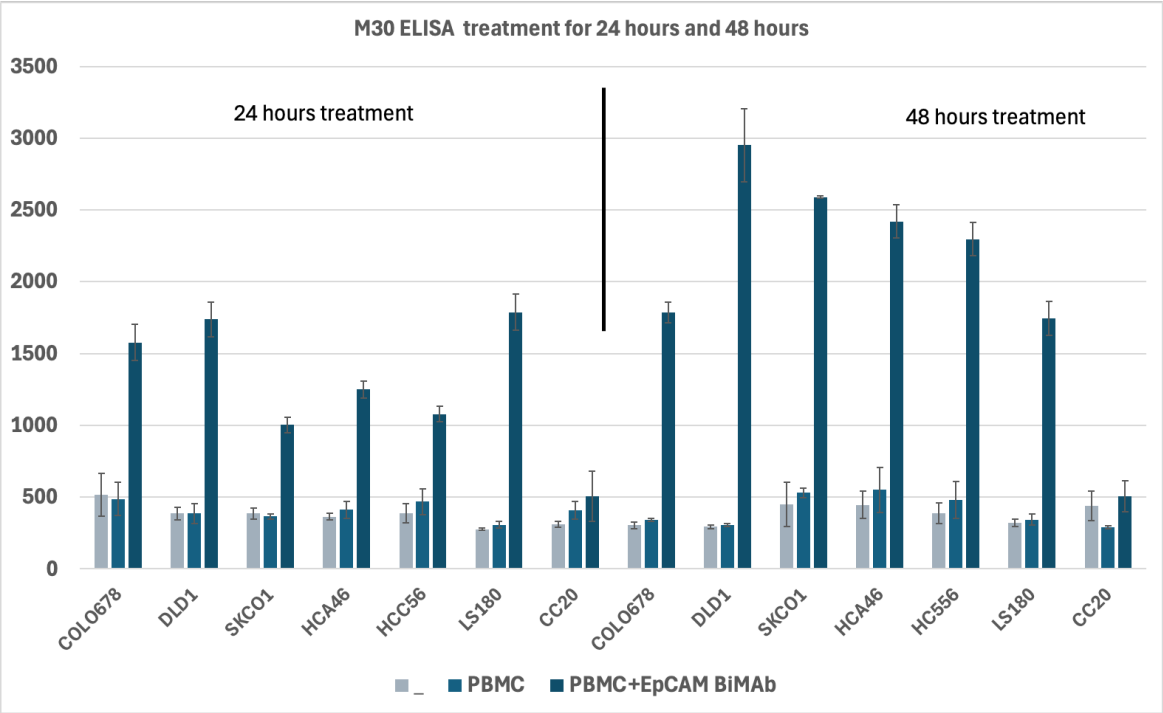

Figure 4.10: EpCAM-positive and not EpCAM -negative colorectal cancer cell lines are killed by T cells in the presence of EpCAM CD3 BiMAb.
CRC cell lines were treated with 8 nM BiMAb and co culture with PBMC in ratio effector cells to cancer cells (1:10). Killing measured after 24 hours and 48 hours, then were analyzed using a M30 ELISA.

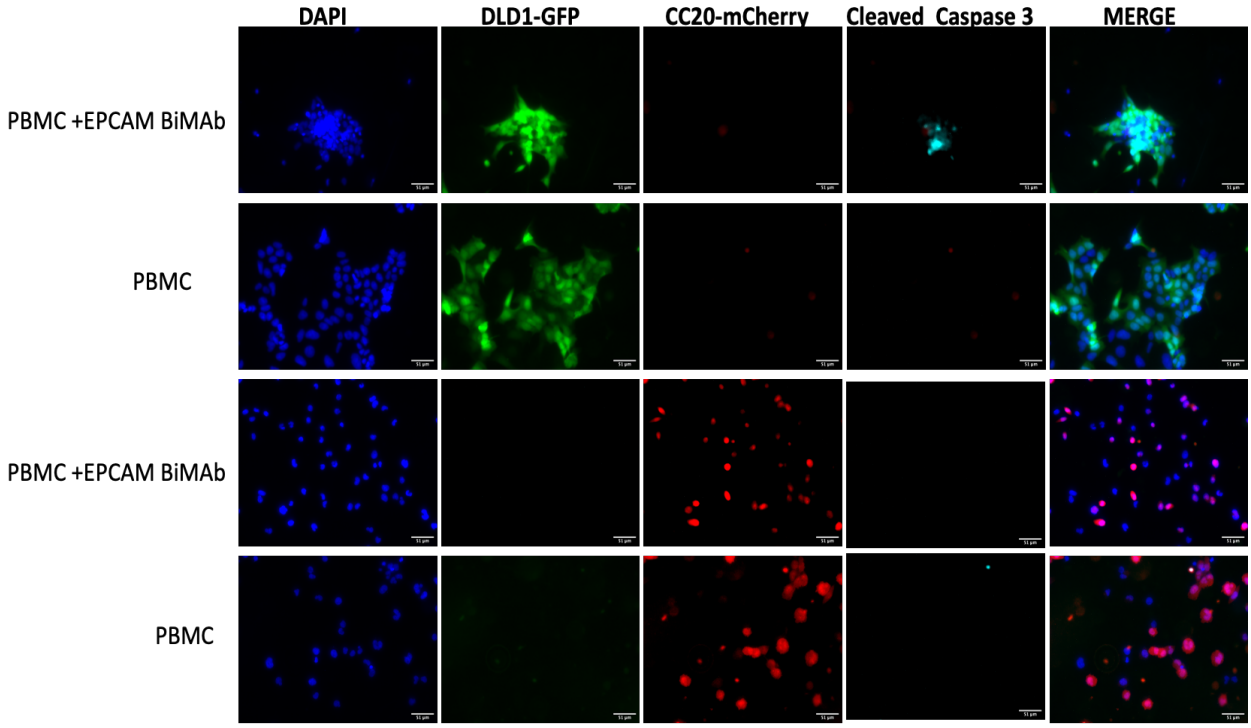

Figure 4.11: EpCAM-positive DLD1 but not EpCAM-negative CC20 colorectal cancer cells are killed by T cells in the presence of EpCAM CD3 BiMAb.
CRC cell lines were treated with 8 nM BiMAb and co culture with PBMC in ratio effector cells to cancer cells (10:1). Killing measured in 24 hours, then were analyzed using immunofluorescence staining of cleaved caspase 3.

4.2.9 PLAP CD3 BiMAb mRNA delivered to cells in a CRC cell line by LNPs shows antibody produced by the cells binds to PLAP on the cell's membrane.

We next tested the effectiveness of LNP based delivery of mRNA coding for the antibody to CRC cell lines for production by the targeted cells of the antibody. mRNA/LNPs were incubated with PLAP positive cell lines and stained with secondary anti human antibody to test the binding of BiMAb secreted from the cells due to LNPs treatment.

LOVO is a PLAP positive cell line and CC20 is a PLAP negative cell line. Both were incubated with PLAP-CD3 BiMAb /LNP (1:100) for 24 hours, then stained with anti-human alexa fluor 488. The binding was tested by immunofluorescence. LOVO shows positive binding by PLAP CD3 BiMAb, but not CC20 (figure 4.12).

To test the secreted PLAP-CD3 BiMAb from the treatment of LNP on CC20, after incubation for 24 hours, the supernatants were added to fresh LOVO cells for 1 hour. Afterwards, the cells were stained using immunofluorescence and show positive binding to LOVO (Figure 4.12). Cells were stained with H17E2 as well to confirm the specificity of PLAP-CD3 BiMABb released.

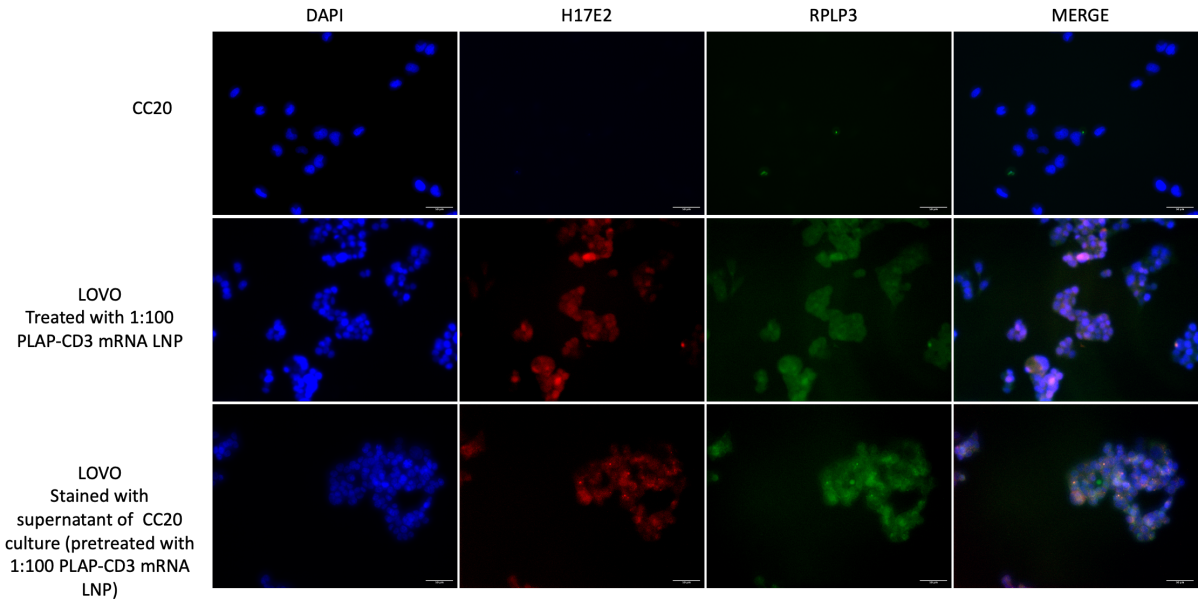

Figure 4.12: Colorectal cancer cell lines PLAP staining with PLAP-CD3 mRNA LNPs.

Immunofluorescence staining using mRNA LNPS delivered PLAP-CD3 BiMAb on PLAP positive LOVO and PLAP negative CC20 cells. Cells were seeded in a 96 well plate and treated with mRNA LNPs for 24 hours. Cells washed and incubated with 1:100 H17E2. The cells were fixed and stained with secondary antibodies (anti mouse Alexa fluor 568 and anti-human Alexa fluor 488. LOVO cells were stained with PLAP-CD3 collected from the supernatant of CC20 prior treatment with mRNA LNPs for 1 hour and H17E2 for 1 hour. The cells were then washed and stained with secondary antibodies.

4.2.10 EpCAM CD3 BiMAb mRNA delivered to cells in a CRC cell line by LNPs shows antibody produced by the cells binds to EpCAM on the cells in the cell line.

We next tested the effectiveness of LNP based delivery of mRNA coding for the antibody to CRC cell lines for production by the targeted cells of the antibody. mRNA/LNPs were incubated with EpCAM positive cell lines and stained with secondary anti human antibody to test the binding of BiMAb secreted from the cells due to LNPs treatment.

HT29 is an EpCAM positive cell line and CC20 is an EpCAM negative cell line. Both were incubated with EpCAM-CD3 BiMAb LNP (1:100) for 24 hours, 48 hours and 96 hours then stained with anti-human alexa fluor 488. The binding was tested by immunofluorescence. HT29 show positive binding to EpCAM CD3 BiMAb, but not CC20 figure 4.13. The longer time incubation shows stronger staining.

To test the secreted PLAP-CD3 BiMAb from the treatment of LNP on CC20, after incubation for 24 hours, the supernatants were added to fresh HT29 cells for 1 hour. Afterwards, the cells were stained using immunofluorescence and show positive binding to HT29 Figure 4.13. Cells were stained with anti EpCAM mouse antibody (AUA1) as well to confirm the specificity and as positive control. of PLAP-CD3 BiMABb released (Figure 4.13).

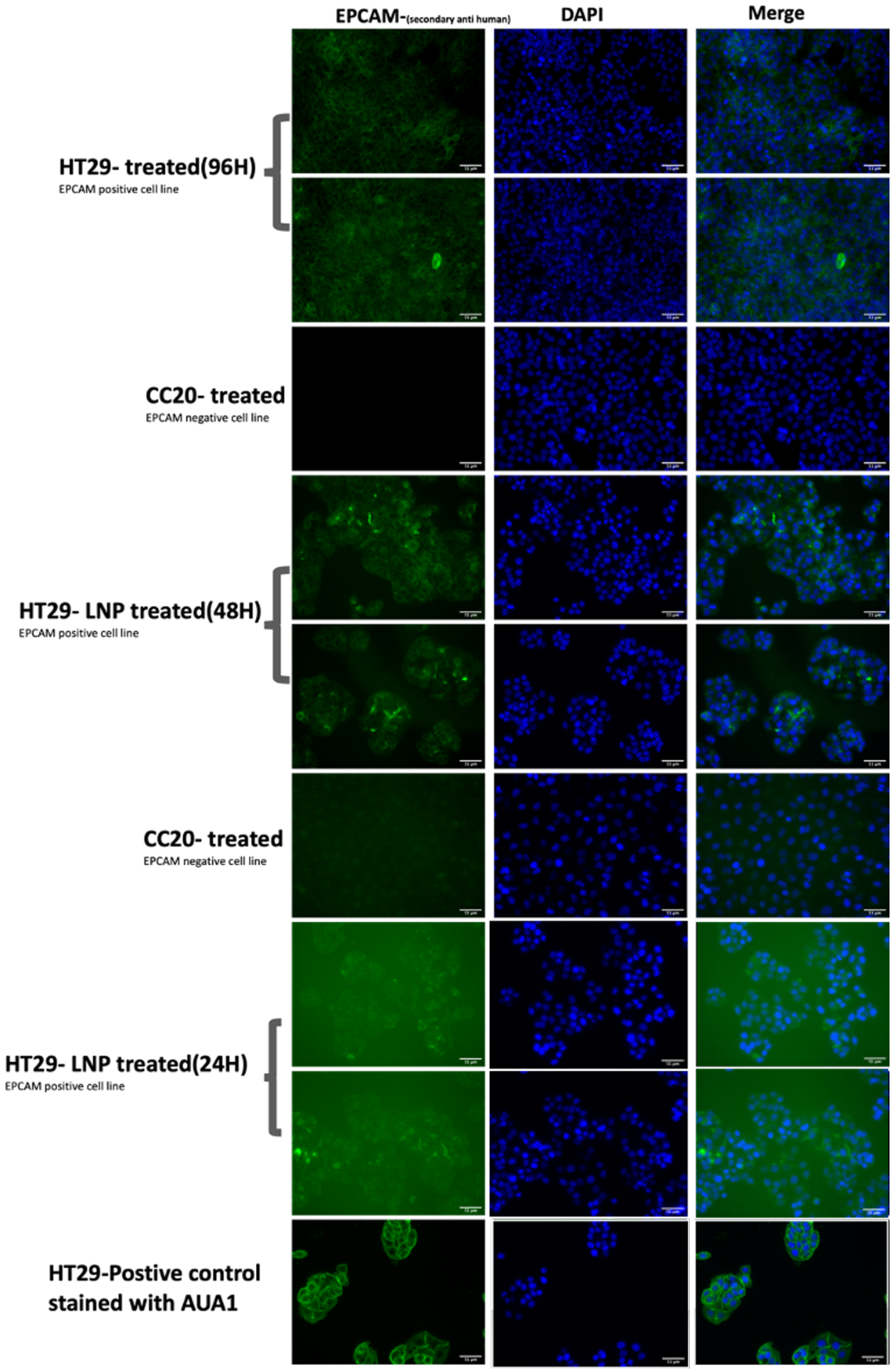

Figure 4. 13: Colorectal cancer cell lines EpCAM staining with EpCAM-CD3 mRNA LNPs. Immunofluorescence staining using mRNA LNPS delivered EpCAM-CD3 BiMAb on EpCAM positive HT29 and EpCAM negative CC20.

4.2.11 EpCAM positive, but not the EpCAM negative colorectal cancer cell lines were killed by T cells in the presence of LNP based delivery of mRNA coding for the antibody EpCAM BiMaB

We next tested the effectiveness of LNP based delivery of mRNA coding for the EpCAM CD3 BiMaB antibody to CRC cell lines killing. LNPs were incubated with EpCAM positive cell line CCO7 and CC20 EpCAM negative. The cells were treated with 8 nM EpCAM-CD3 BiMAb and PBMCs as source of T cells in a ratio of effector to cancer cells of 10:1 and incubated with EpCAM- CD3 BiMAb LNP (1:100). Cell death was analysed by Apoptosense® ELISA M30 (PEVIVA) after the treatment for 24 hours and 48 hours. As shown in Figure 4.14 A, the EpCAM-CD3 BiMAb mediated cell killing of EpCAM positive cells, but not the EpCAM negative cell line, in agreement with their EpCAM expression levels. The killing by EpCAM CD3 BiMab on EpCAM positive cells was higher compared to the killing by EpCAM CD3 BiMaB LNP. With longer time treatment at 48 hours treatment the killing by both EpCAM CD3 BiMab and EpCAM CD3 BiMaB LNP was similar. EpCAM negative cell line CC20 did not get killed by either EpCAM CD3 BiMab or EpCAM CD3 BiMaB LNP.

Killing was measured by xCELLigence Real-Time Cell Analysis on EpCAM positive CCO7 Figure 4.14 B. The cells were not affected with LNP incubation with cells.

A.

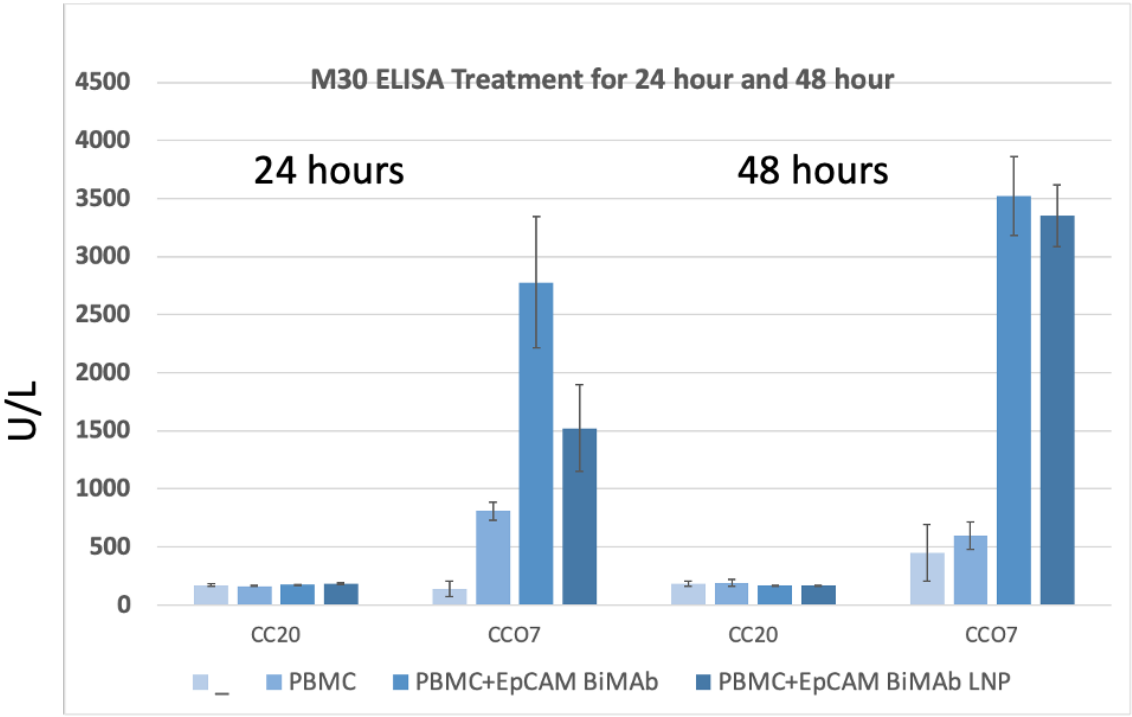

B.

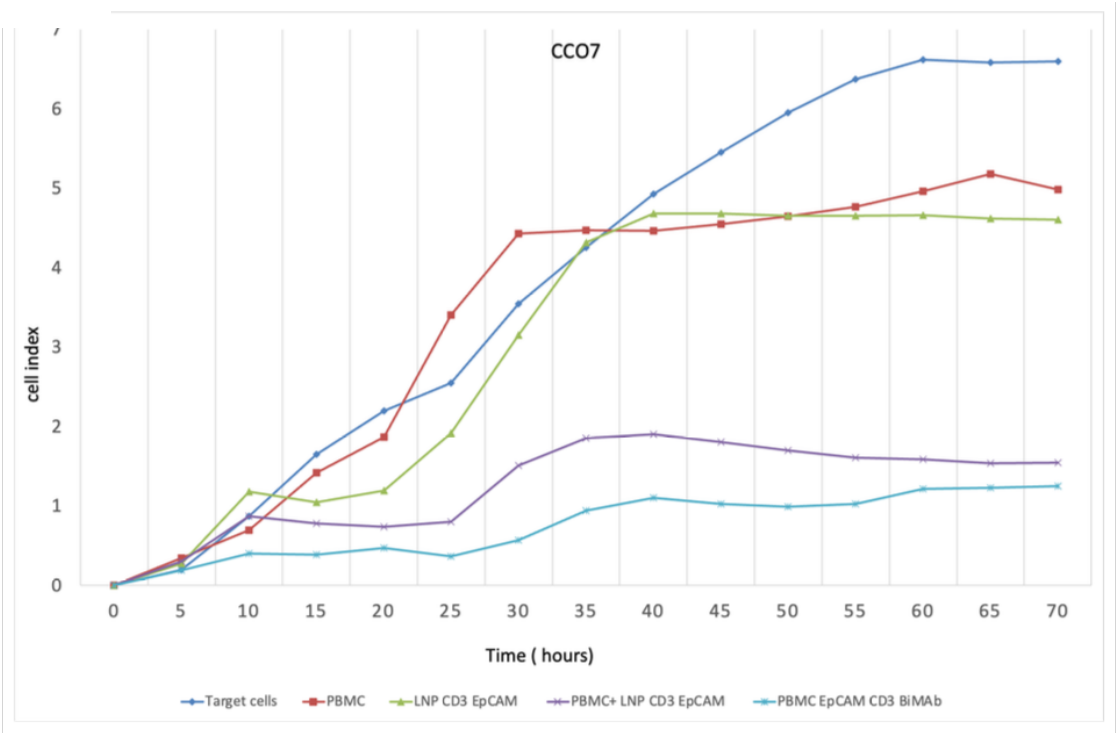

Figure 4.14: A. EpCAM CD3 biMAB mRNA LNP induced killing in the EpCAM positive colorectal cancer cell line (CCO7), but not in EpCAM negative CRC cell line (CC20).

Killing was measured by M30 ELISA A. B. EpCAM CD3 biMAB mRNA LNP delivered induced killing in the EpCAM positive colorectal cancer cell line (CCO7) killing measured by xCelligence Real-Time Cell Analysis.

4.3 Discussion

The current study shows the effectiveness of testing targeted bispecific monoclonal antibody therapy for colorectal cancer in vitro. Despite the challenges faced by bispecific monoclonal antibody therapy on solid tumours, this study could be a promising solution for solid tumour treatment in refined parameters.

The choice of cancer antigen is a critical aspect of bispecific monoclonal antibody therapy, so selecting a compatible target is key for the therapy's success. Here we used PLAP and EpCAM as cancer antigens for bispecific antibody therapy. PLAP is ectopically expressed in CRC and not in normal tissues, therefore, it is a good target for bispecific monoclonal antibody immunotherapy to treat colon cancer (X. Li et al., 2020a). The present data shows specific binding of RPLP3 on PLAP positive CRC cell lines and not PLAP negative CRC cell lines. There was good immune mediated killing of PLAP expressing CRC lines by RPLP3, a T cell engaging bispecific monoclonal antibody produced by commercial collaborators, Roche and ProMab based on the mouse mAb anti PLAP, H17E2. The extent of killing was dependent on the level of PLAP protein expression, which varies both within and between cell lines. The level of cancer antigens presented on cancer cells affects the response of bispecific antibody therapy.

The presented data found that CRC cancer cells lines are different in their PLAP expression. The sensitivity of different cancer cell lines to RPLP3 is varies due to the cell line differences such as resistance mechanism and anti-apoptotic signally, but overall, there were effective T cell mediated cytotoxicity induced by RPLP3 on the PLAP expressed cell lines within 24 hours or 48 hours.

Some cell lines were not killed completely with RPLP3 treatment, suggesting heterogenous PLAP expression or resistance that could be a limitation for BiMaB therapy. Studying precisely the antigen density at the protein level and threshold of triggering T cells activation for bispecific antibodies will be effective for predicting the response of the therapy.

There are some methodological limitations that need further optimisation such as quantifiable measurement of antigen density on cancer cells. Measurement of killing by biological methods can be limited. Using death marker staining can be challenging as the cells lose their attachment when they die. The measurement of cell death marker by using Elisa M30 is not reflect the level of individual cell killing in the cell line. Further optimizations are needed to evaluate the killing taking into account intra cell line heterogeneity of expression and development of resistance to the killing.

The other cancer target antigen used is EpCAM which is expressed on most of our CRC cell lines. EpCAM has been studied widely as target for targeted immunotherapy such as CAR T cells (D. Li et al., 2023). EpCAM CD3 BiMAb shows a specific binding to EpCAM positive CRC cell lines. EpCAM CD3 BiMAb induces specific killing in EpCAM positive CRC cell lines and not EpCAM negative CRC cell lines.

The mRNA of BiMAb encapsulation in lipid nanoparticles (LNPs) is a novel approach for delivering antibody to tumours may overcome some of the obstacles faced by BiMAb therapy such as extending the BiMAb in circulation with lower production costs compare to direct BiMAb delivery (L. Wu et al., 2021). The approach of using mRNA LNP delivered BiMAb may bypass the microenvironment restriction on BiMAb susceptibility to solid tumours (Thakur et al., 2018). The mRNA /LNP delivered EpCAM CD3 BiMAB

produced by commercial ProMab added to the cells showed good antibody production and release of EpCAM CD3 BiMAb binding to EpCAM positive cells as well as inducing killing to EpCAM positive cells. Using mRNA /LNP delivered PLAP CD3 BiMAb added to cells PLAP positive and PLAP negative cells release PLAP CD3 RPLP which show good specific binding to PLAP positive cells.

Chapter 5: Heterogeneity of PLAP expression on CRC cell lines

5.1 Introduction

Cancer specific antigens on solid tumour are heterogeneous both intertumoural and intratumorally which causes a challenge for targeted immunotherapy (Dagogo-Jack & Shaw, 2018). Intertumoral heterogeneity refers the heterogeneity or variation of cancer cells of deferent patients of the same tumors type, the differences influenced due to the personalize either genetic or epigenetic or environmental factors. Intratumoural heterogeneity is the heterogeneity of cancer cells in the same cancer of the patient (Dagogo-Jack & Shaw, 2017). Genetic or epigenetic alternation can cause cancer heterogeneity (Jamal-Hanjani et al., 2017). Cancer evolution and development are not yet fully understood (Graham & Sottoriva, 2017) . Cancers escape immune attack of target antigens by evasion due to selection for loss of the target antigen by mutation or stable epigenetic changes (O'Donnell et al., 2018)

PLAP expression patterns between colorectal cancer cell lines and within colorectal cancer cell lines as cancer specific antigen expression are an interesting observation and discussed in chapter 3 and are discussed further in this chapter. In this chapter, we study further the heterogeneity of PLAP expression on CRC cell lines, what controls the PLAP expression and what causes the heterogeneity of PLAP expression within cell lines. As well we investigate the killing induced by RPLP3 of heterogenous PLAP expressed cell lines.

5.2 Results

5.2.1 Analysis of heterogeneity of PLAP expression within cell lines over time.

The pattern of PLAP expression on CRC cell lines, what triggers the PLAP expression and what causes the heterogeneity of PLAP expression within cell lines over time was investigated using a small panel of lines with different patterns of expression.

CACO2 and OXCO3, are PLAP high expressing colorectal cancer cell lines at the mRNA level. Looking to their protein expression by IF and FACS in chapter 3, they are heterogeneous cell lines with high to negative PLAP expression within their population. CACO2 and OXCO3 were stained with anti-PLAP antibody (H17E2) and sorted by FACS sorting according to their PLAP expression. The sort was in three levels, the 10% highest, 10% medium, and 10% lowest expressing cells Figure 5.1A. The sorted cells were cultured for one and three weeks to follow their PLAP expression changes and see whether they kept the same expression levels over time or returned to their original heterogenous expression pattern. The PLAP expression in each category of the sorted population after one week in culture studied by immunofluorescence showed that cells kept their PLAP levels of expression for the first week (Figure 5.1 B).

The other timing point was 3 weeks culture to follow further the PLAP expression changes of the sorted cells. The cell sorted populations after three weeks were stained with anti-PLAP antibody (H17E2) by FACS then analysed to see whether they kept the same expression levels over time or returned to their original heterogenous expression pattern (Figure 5.1 C).

The results show that high and medium selected PLAP-expressing populations of OXCO3 were similar to the original population for their PLAP expression while for CACO2 they were somewhat lower. However, the low 10% PLAP-expressing cells remained different and very low for the OXCO3 cell line. For CACO2, while the majority of the 10% low population kept their low PLAP level, there was a significant subset distributed towards the higher level. These rather unexpected results raise the question of what is maintaining the persistence of low-level expression, and for how long this remains. One possible explanation is that the low PLAP expression level population of cells was more differentiated and did not contain the cancer stem cells of the cell line.

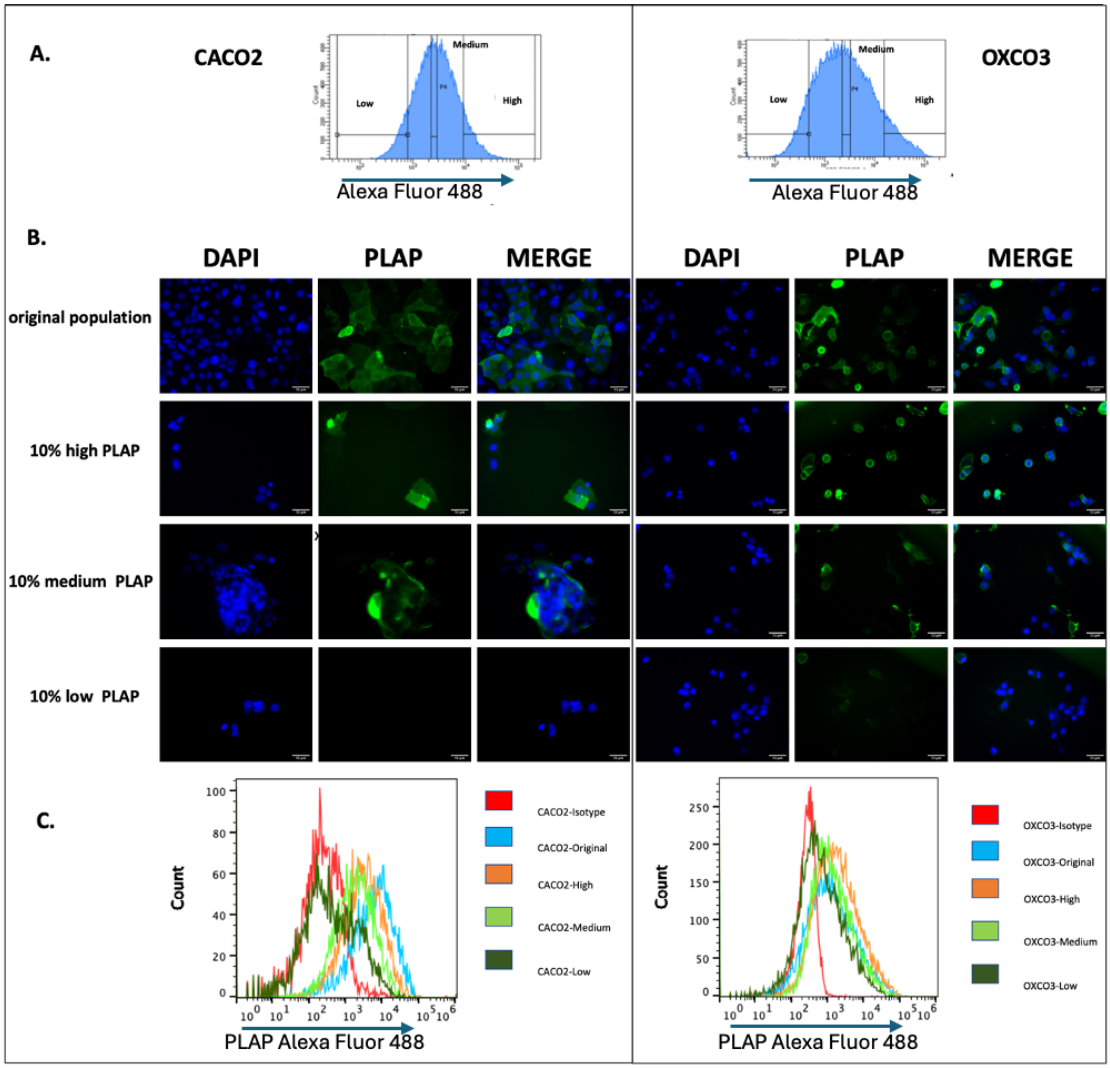

Figure 5.1: Analysis of heterogeneity of PLAP expression in CACO2 and OXCO3 cell lines over time.
(A). CACO2 and OXCO3 cell lines were sorted into 10% high, 10% medium- and 10% low- PLAP groups. (B) Sorted populations are analysed by Immunofluorescence after one week's culture. (C) FACS analysis of PLAP expression three weeks after sorting. 10% PLAP high ,10% medium and 10% Low sorted. The cells are analysed for their PLAP expression and compared to PLAP expression in the original population. The 10% high and 10% medium sorted cells returned to their original expression profiles for OXCO3 but not completely for CACO2. The majority of 10% sorted, however, cells kept their PLAP low expression levels for both cell lines.

5.2.2 Analysis of PLAP expression on single cells sorted from heterogeneous CACO2.

As discussed earlier, CACO2 is a PLAP high expressed cell line and has heterogeneous PLAP expression ranging from high expressed to low express cells within the population. Staining of CACO2 with anti PLAP (H17E2) by IF shows the heterogeneity in figure 5.2.A. CACO2 original population stained with anti PLAP (H17E2) and by comparing to the isotype control the gates of PLAP high, low expressed are created: Figure 5.2B. Cells were single cell sorted from these three PLAP expression categories.

Single cells were sorted onto 96 wells plate each well seeded with one cell. The single cells were sorted from the 10% highest PLAP expressed, 10% low PLAP expressed population and single cells from the original population. The single cell colonies for these sorted cells were then checked to see whether the single cell sorted colonies keep their expression or return to their original population in single cell level. Single cell colonies were stained with anti PLAP (H17E2) after two weeks culture. The colonies growing from the 10% highest PLAP expressed kept their expression as high. The size of the colonies was smaller compared to the colonies generated from the single cells from original population. Low PLAP expressed single cell colonies kept their expression as PLAP low. The size of the colonies is small. Figure 5.2C shows images of PLAP IF staining of representative fields of single cell colonies from triplicate experiments.

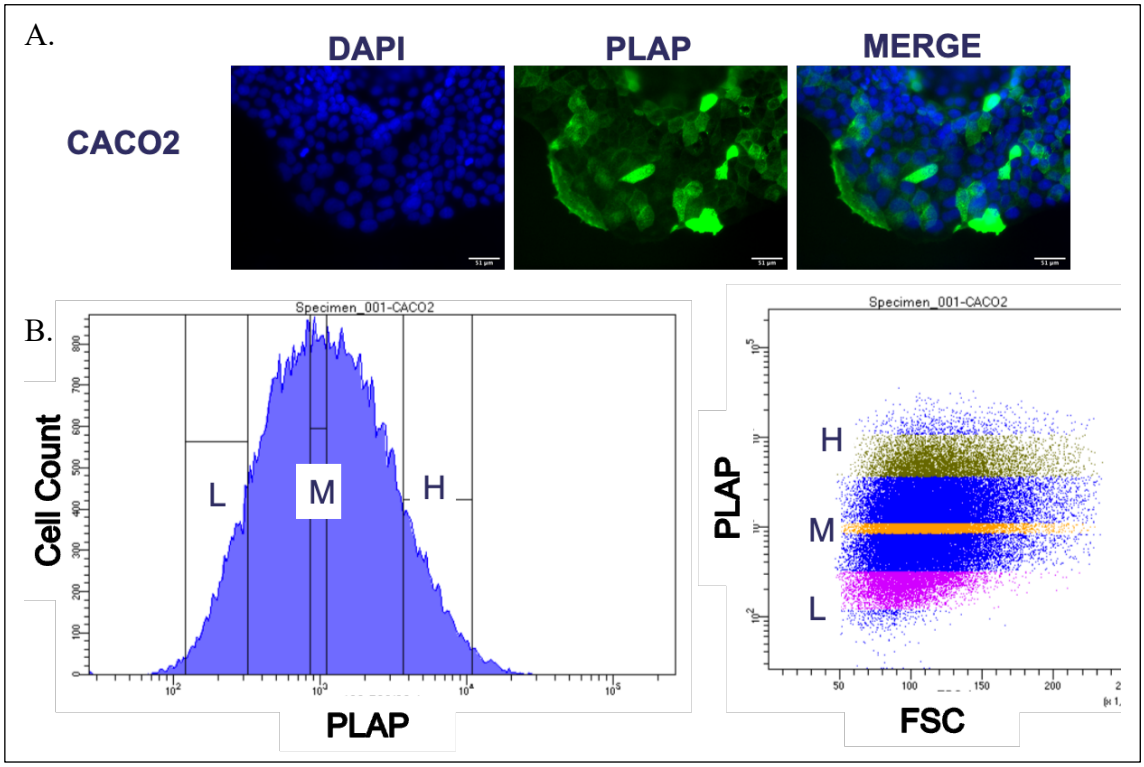
A.
DAPI
PLAP
MERGE
CACO2
B.
Specimen_001-CACO2
Cell Count
L
M
H
PLAP
Specimen_001-CACO2
PLAP
H
M
L
FSC

C.

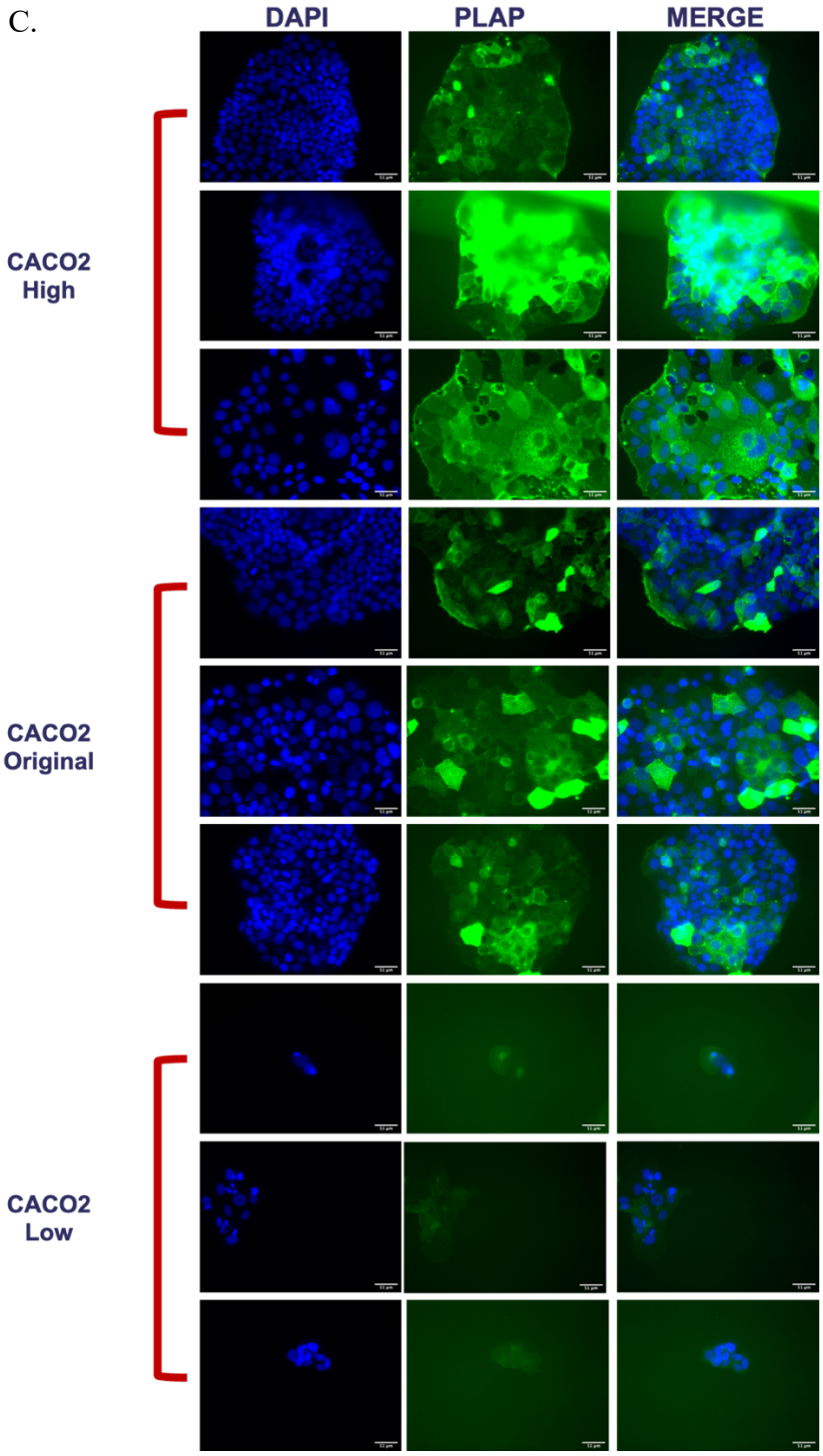

Figure 5.2: Analysis of PLAP expression on single cell colonies from the heterogeneity of PLAP expressing CACO2.

A. IF staining of CACO2 with anti-PLAP. B FACS sorting histogram of CACO2 with anti-PLAP and highlights showing the sorting gate's location on the histogram of sorted high and sorted low PLAP expressed on the level of PLAP signal distribution. C. IF staining of single cell colonies from CACO2, sorted high, low, and original population stained with anti- PLAP.

5.2.3 Colony formation of sorted cells from heterogeneously PLAP expressing cell lines.

To investigate the ability of single cells sorted from high or low PLAP expressed cells within PLAP expressed CRC cell lines to form colonies. CACO2, CCO7 and DLD1 are PLAP positive cell lines, and they have heterogeneous expression of PLAP. The single cells sorted by FACS according to their PLAP expression are marked on the histogram distribution as H (high) 10% highest and L (Low) as 10% of the lowest PLAP of each cell lines separately (Figure 5.3).

CACO2, a high expressing cell line, was sorted by the method described on Figure 5.3. CACO2 high and Low sorted, and in bulk, for immunofluorescence staining confirmed the level of PLAP expression after sorting compared to the original population and shows that the cells kept their original level of expression Figure 5.4A.

Single cells sorted from CACO2 High, and Low population seeded in 96 wells plate after one- week single cells colonies were counted with the results shown in Figure 5.4 B. The number of single cell colonies formed from CACO2 Low is less compared to those from the high and original population (Figure 5.4B).

DLD1 is a medium expressing cell line with a more homogeneous PLAP expression. DLD1 single cells were sorted by the method described on Figure 5.3. The DLD1 high and Low sorted populations stained in bulk by immunofluorescence agreed with the level of PLAP expression after sorting compared to the original population. (Figure 5.5A). The numbers of colonies formed from the single cells sorted from DLD1 High, and Low population seeded in 96 wells plates, after one-week's growth, are given in Figure 5.5 B. The number of colonies formed from DLD1 high has higher number of colonies sorted from single cells, the number colonies from low DLD1 is clearly less.

CCO7 is a low PLAP expressing cell line but with a subset of PLAP high expressing cells. CCO7 single cells were sorted by the same method described in Figure 5.3. As for the previous two cases, CCO7 sorted populations stained in bulk kept their original level of expression (Figure 5.6A). As for CACO2, the number of colonies from the low PLAP sorted group of sorted single sorted cells of gave significantly fewer colonies than those sorted from the high population (Figure 5.6 B).

The number of single cells colonies of PLAP - low were significantly less compared to the number of single cells colonies generated from PLAP – high sorted cells for all the three cell lines (CACO2, DLD1, CCO7).

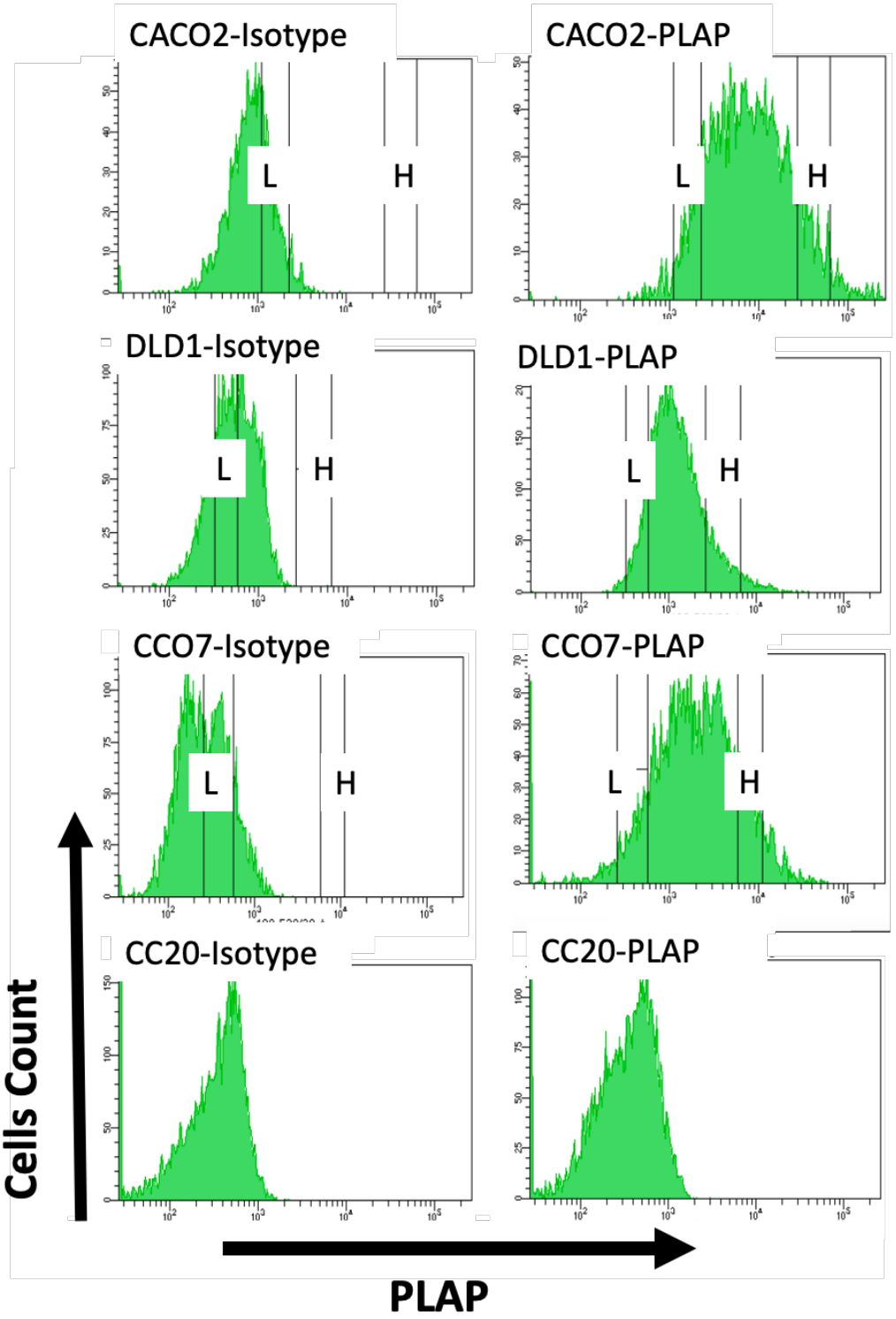

Figure 5.3: Method of cell sorting by FACS on CACO2, DLD1 and CCO7.
CRC cell lines CACO2, DLD1, CCO7 and CC20 stained with anti-PLAP and secondary antibody goat anti-mouse Alexa flour 488. Cells were sorted from the 10% highest and 10% lowest PLAP expressed cells indicated in the histogram of each cell.

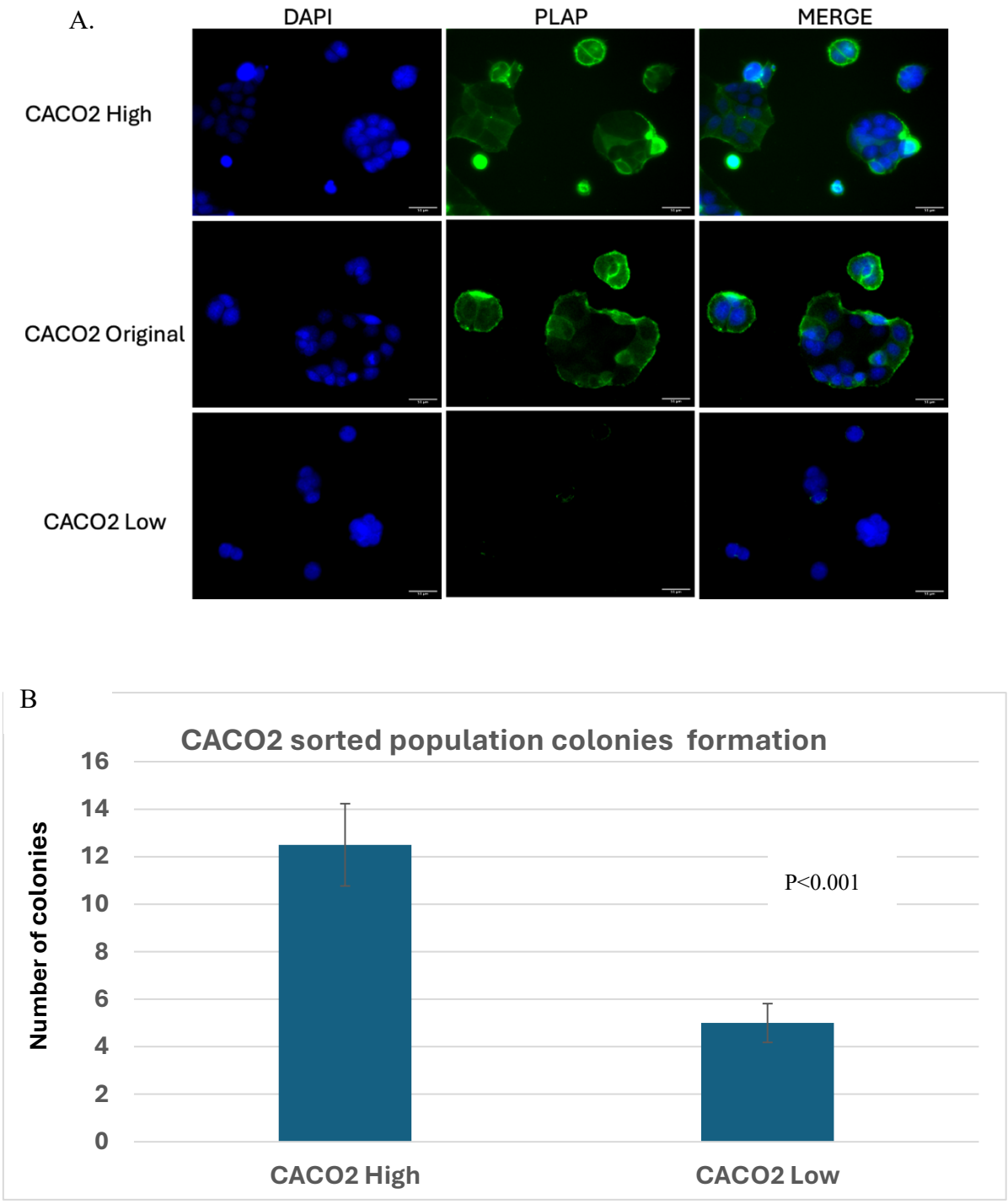

Figure 5.4 The colonies formation of sorted sorted CACO2.
. IF of cells sorted from high, low and original CACO2 A. The number of colonies from single cells sorted of CACO2 by FACS based on their PLAP expression, high, and low B. The experiment is done three times.

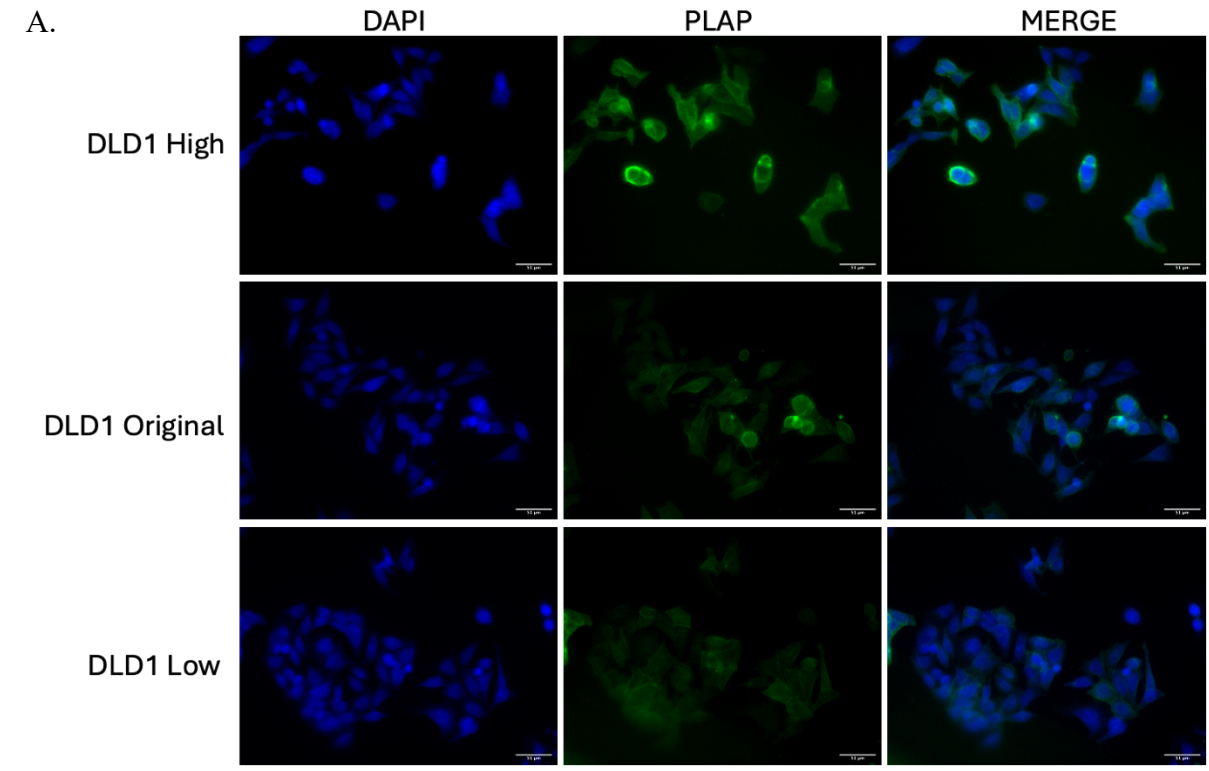

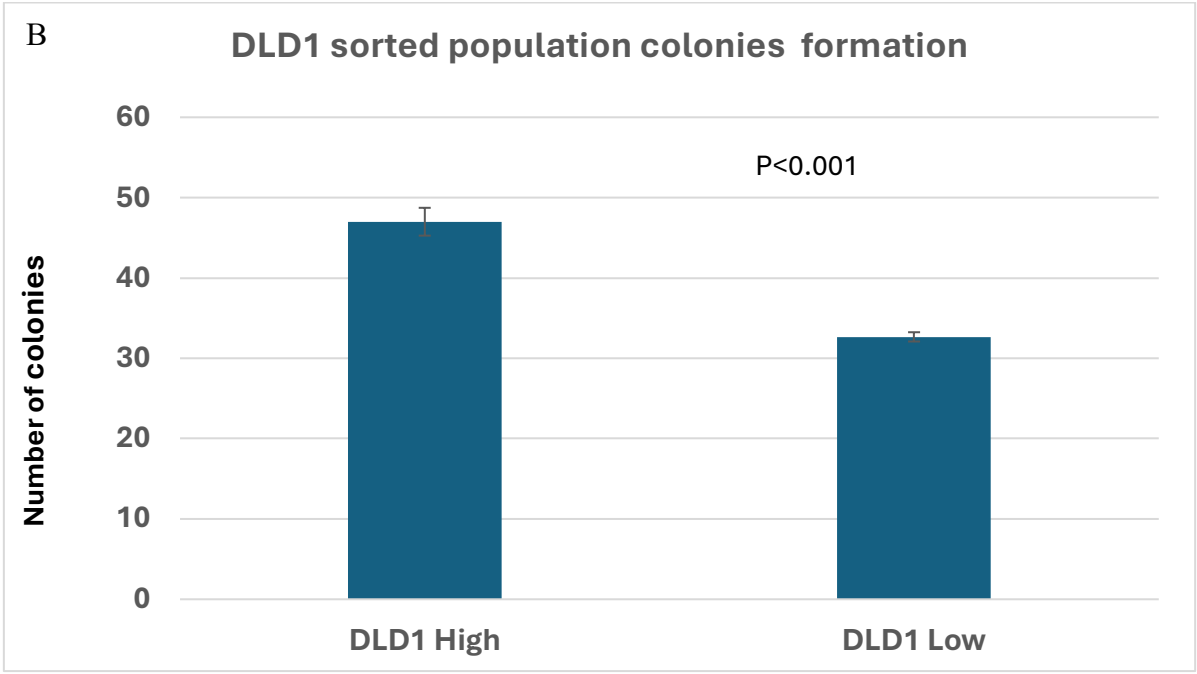

Figure 5.5: The colonies formation of sorted CACO2 .
IF of cells sorted from high, low and original CACO2 A. The number of colonies from single cells sorted of CACO2 by FACS based on their PLAP expression, high, and low B. The experiment is done three times.

A.

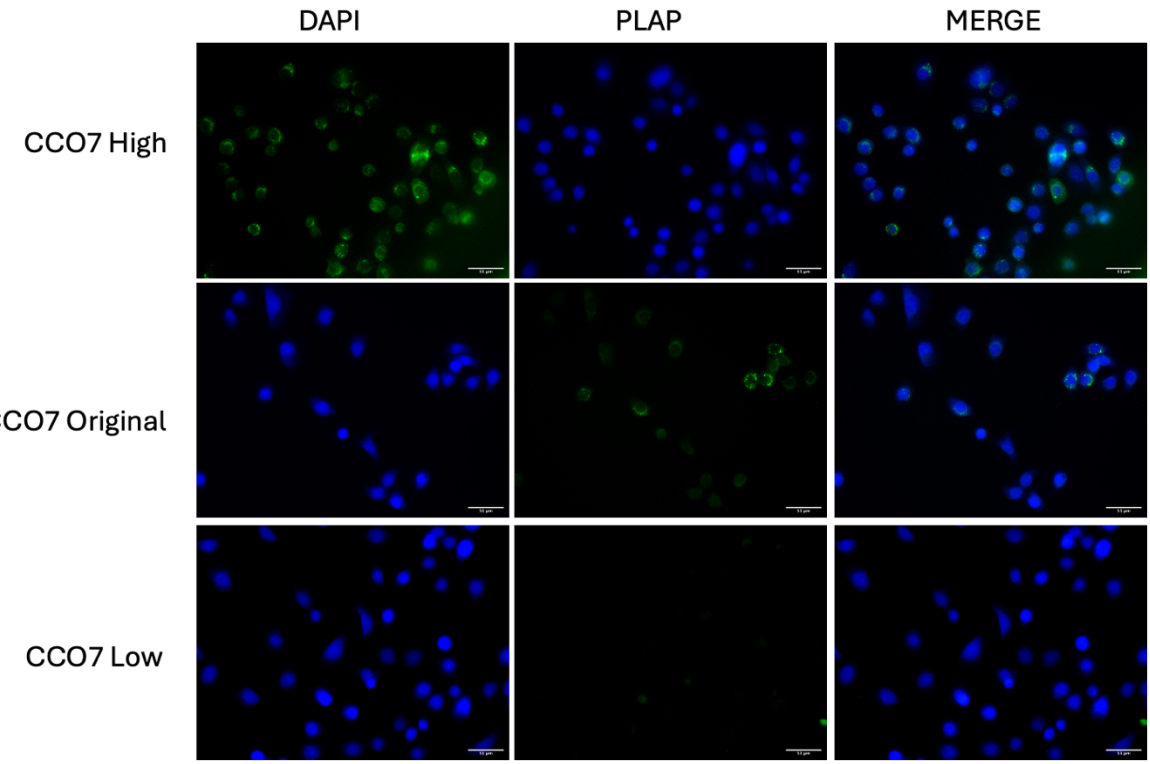

B

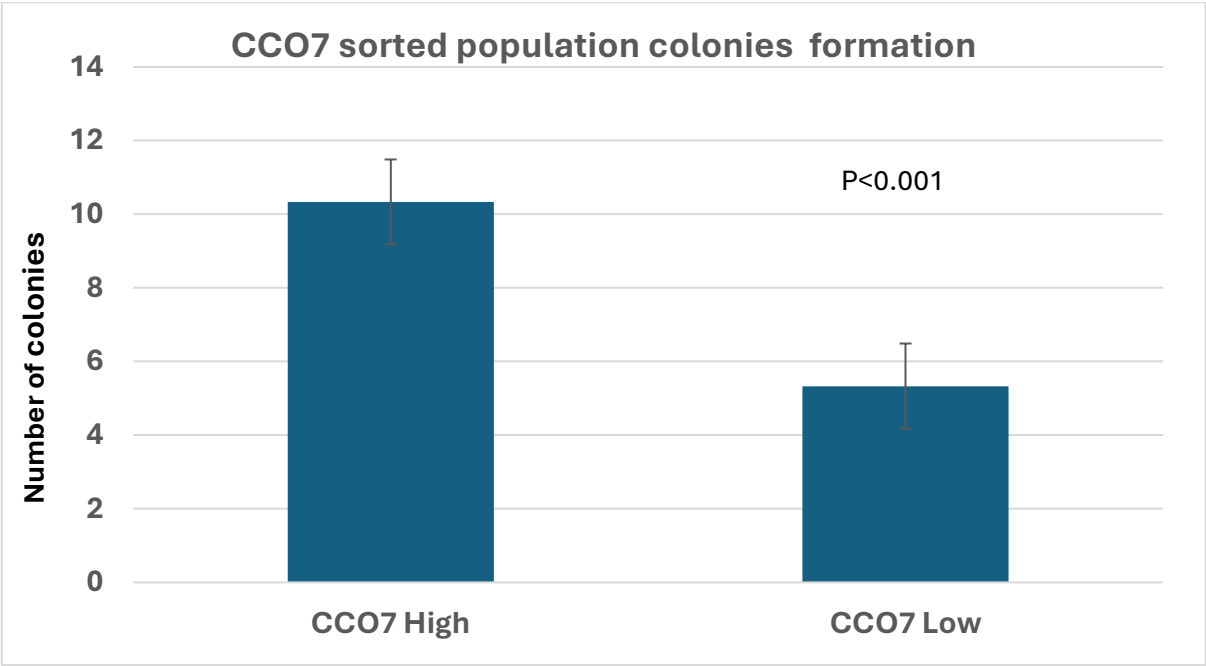

Figure 5.6: Colony formation of sorted CCO7 cells.
IF of cells sorted from high, low and original CCO7 A. The number of colonies from single cells sorted of CCo7 by FACS on their PLAP expression, high, and low B. The experiment is done three times.

5.2.4 RPLP3 induces killing of low PLAP expressing cells in a CRC cell line with heterogeneous PLAP expression

The effect of variations in the patterns of PLAP expression on RPLP3 killing was studied by sorting from FACS into three groups: the highest 10% PLAP expressing cells, the 10% lowest and the original population. Selected cell lines were CACO2 for high PLAP expressing cell line, DLD1 for medium PLAP expressing cell line and CCO7 for low PLAP expressing cell line. All three cell lines are EpCAM positive and to compare the complete killing of the cells in each group, the cells were treated with both BiMABs (RPLP3 and EpCAM-CD3 BiMAb). The sorting of cells according to their PLAP expression are discussed earlier in this chapter.

Cells from each sorted population were seeded at a density of 3000 cells per well in a 96 well plate. The cells were co-cultured with PBMC (1:10 ratio) and treated with RPLP3 or EpCAM CD3 BiMAb separately. Killing was measured by M30 ELISA. As seen in Figure 5.7, cells from each cell line the high and original population are killed as is expected. Even the sorted low population was killed by both biMABs with longer time of incubation. The amount of killing on low populations is less than on high or original. That could be due to the lower growth rate of low population compared to the other populations. ELISA M30 measurement of cell killing reflects the number of cells killed.

- For high PLAP expressed cell line CACO2, the selected populations were treated with RPLP3 and EpCAM BiMAb. The killing induced by RPLP3 on 10% high PLAP sorted was higher than the killing on the original population after 24 hours treatment and 48 hours. That is due to the high level of expression of PLAP leading to the stronger binding or effect of RPLP3 induce killing. On the other hand, PLAP low expressed cells had less killing after 24 hours and the killing increased after 48 hours treatment.

To compare the killing of RPLP3 to the killing induced by EpCAM BiMaB, on high PLAP expressed cells the amount of killing measured by RPLP3 was less compared to EpCAM BiMAb for 24 hours treatment but increased after 48 hours treatment. For the original population the killing induced by RPLP3 was less than killing induced by EpCAM BiMAb. Lastly, the low PLAP expressed cells were killed by RPLP3 BiMab less than the killing by EpCAM BiMaB on 24 hours treatment but increased on the treatment for 48 hours.

The killing of all the subsets of sorted cells was dependent on PLAP expression by RPLP3 for 24 hours treatment and 48 hours treatment and killing increased with longer time treatment. As the whole subset of cells expresses EpCAM the killing might be expected to be similar in all subsets however on PLAP low there was less amount of killing induced by EpCAM BiMAb suggested due to the growth rate of PLAP low as shown in this chapter Figure 5.7.

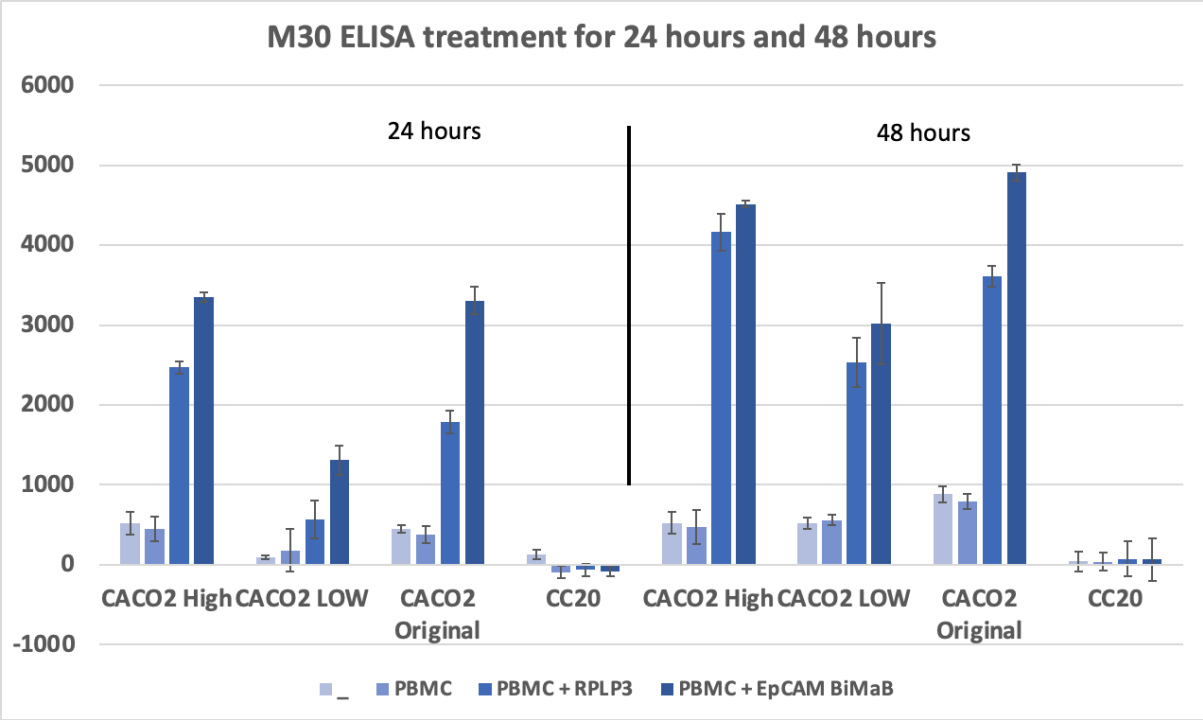

Figure 5.7: RPLP3 induced killing on low PLAP expressing or heterogeneous PLAP expressing cell lines, CACO2.
Cells were sorted by FACS according to their PLAP expression 10% high, 10% low and original population. Cells seeded in a 96 well plate each well with 3000 cells. Cells were co-cultured with PBMC and treated with 5nM RPLP3 and 8nM EpCAM CD3 BiMAb for 24 hours and 48 hours. Killing was analysed using M30 ELISA.

- For medium expressed cell line DLD1, were sorted into 10% high, 10% low PLAP and original and treated with RPLP3 and EpCAM BiMAb. The killing induced by RPLP3 on 10% high PLAP sorted was the same as the killing measured on the original population after 24 hours treatment and 48 hours. That is due to PLAP expression on DLD1 being nearly homogenous. Still the high-level expression of PLAP lead to a stronger binding or effect of RPLP3 induced killing. The low PLAP expressed cells had less killing after 24 hours but the killing increased after 48 hours treatment.

To compare the killing of RPLP3 to the killing induced by EpCAM BiMaB, on high PLAP expressed cells the amount of killing measured by RPLP3 was less compared to EpCAM BiMAb for 24 hours treatment but increased after 48 hours treatment. For the original population the killing induced by RPLP3 was less than killing induced by EpCAM BiMAb. Lastly, the low PLAP expressed cells were killed by EpCAM BiMab less than the killing by EpCAM BiMaB on 24 hours treatment but increased on the treatment for 48 hours.

The killing by RPLP3 for 24 hours treatment and 48 hours of all the subset of sorted cells were dependent on level of PLAP expression, and the time of treatment. The killing increased with longer time treatment. As all the cells are EpCAM positive the killing was expected to be similar in all subsets; however, on PLAP cells there was less killing induced by EpCAM BiMAb suggested due to the growth rate of PLAP low as shown in this chapter Figure 5.8.

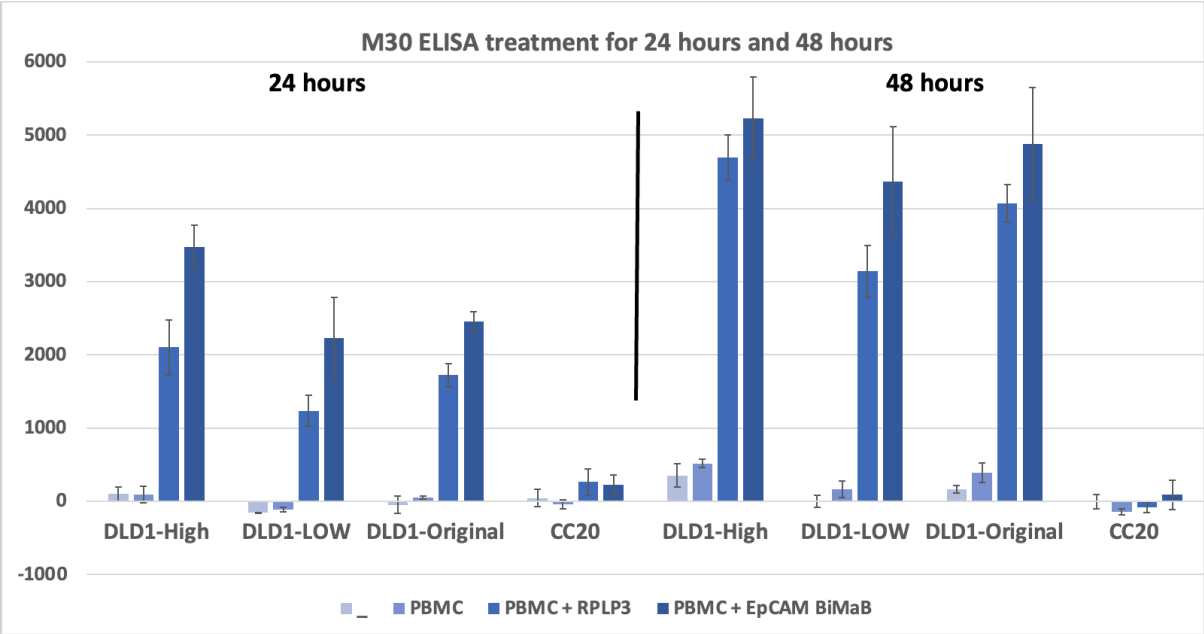

Figure 5.8: PLP3 induced killing on low PLAP expressing or heterogeneous PLAP expressing cell lines, DLD1.

Cells were sorted by FACS according to their PLAP expression 10% high, 10% low and original population. Cells seeded in a 96 well plate each well with 3000 cells. Cells were co-cultured with PBMC and treated with 5nM RPLP3 and 8nM EpCAM CD3 BiMAb for 24 hours and 48 hours. Killing was analysed using M30 ELISA.

For low expressed cell line CCO7, cells were sorted into 10% high, 10% low PLAP and original and treated with RPLP3 and EpCAM BiMAb. The killing induced by RPLP3 on 10% high PLAP sorted was higher than the killing measured on the original population after 24 hours treatment and 48 hours. The low PLAP expressed cells showed little or no killing at 24 hours presumably due to low PLAP expression on CCO7, but the killing increased markedly after 48 hours treatment.

To compare the killing of RPLP3 to the killing induced by EpCAM BiMaB, on high PLAP expressing cells the amount of killing measured by RPLP3 was less compared to EpCAM BiMAb for 24 hours treatment but increased after 48 hours treatment. For the original population the killing induced by RPLP3 was less than killing induced by EpCAM BiMAb.

Lastly, the low PLAP expressed cells were not killed by EpCAM BiMab after 24 hours treatment. 48 hours treatment increased killing by both BiMaBs. For both time points there were significant differences between the killing induced by EpCAM and RPLP3 ($P < 0.01$).

The killings of all the subsets of sorted cells were dependent on PLAP expression by RPLP3 for 24 hours treatment while at 48 hours treatment killing increased substantially with longer treatment. As all the subsets of cells express EpCAM the killing might be expected to be similar for all subsets. However, on PLAP low expressing cells there was less killing induced by EpCAM BiMAb which could be due to the lower growth rate of PLAP low expressing cells as shown earlier in this chapter. The PLAP low express cells grow less compared to other populations and the underlying mechanism is not clear.

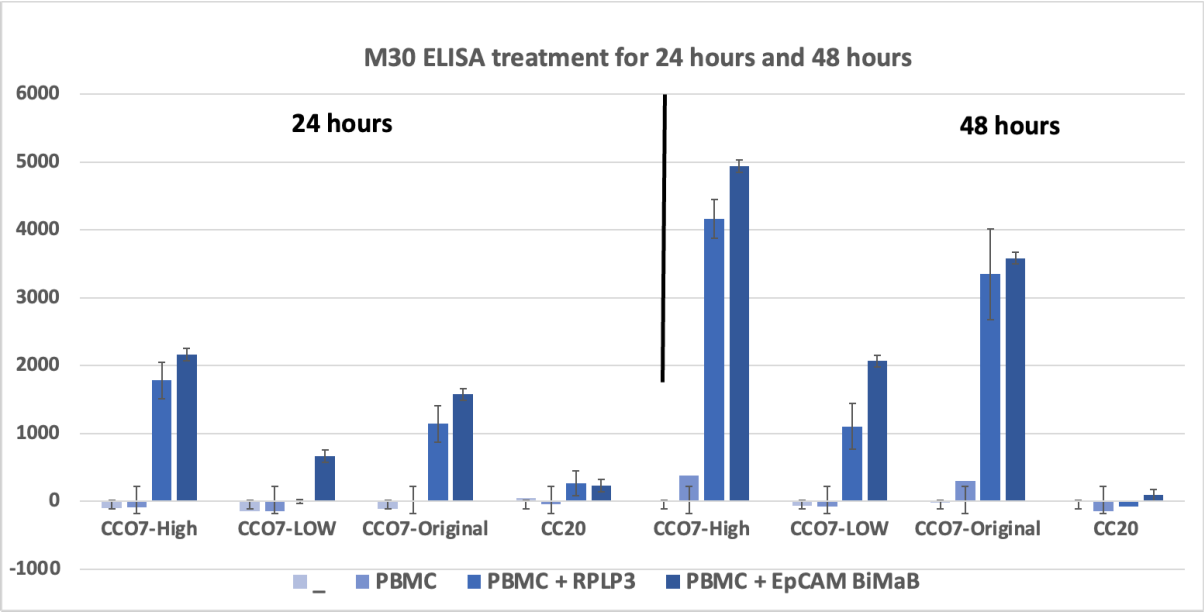

Figure 5.9: RPLP3 induced killing on low PLAP expressing or heterogeneous PLAP expressing cell line CCO7.
Cells were sorted by FACS according to their PLAP expression 10% high, 10% low and original population. Cells seeded in a 96 well plate each well with 3000 cells. Cells were co- cultured with PBMC and treated with 5nM RPLP3 and 8nM EpCAM CD3 BiMAb for 24 hours and 48 hours. Killing was analysed using M30 ELISA.

5.3 Discussion:

As shown, PLAP is heterogeneous within CRC cell lines and between CRC cell lines. What induces PLAP expression on cancer is yet unknown (X. Li et al., 2020a). From the results presented in chapter 3, the mRNA expression of PLAP does not necessarily correspond to what is seen in protein expression. For example, SKCO1 is PLAP low expressed cell line but after staining it with anti PLAP antibody we can see detectable staining. As well as applying RPLP3 treatment on SKCO1 shows good killing. That shows that mRNA expression levels are not enough for studying the homogeneity of the protein expression of a gene of interest.

It is shown here that CCO7 has more heterogeneity of PLAP expression than DLD1, just like some cancers are more heterogeneous than others. This reveal the advantage of our panel of colorectal cancer cell lines is a good model for studying cancer heterogeneity (Haffner et al., 2020).

As shown PLAP has heterogeneous expression from high to low expressed cells within the cell lines, nevertheless applying RPLP3 can mediate killing of low expressing cells. This shows the sensitivity of RPLPR3 killing on low PLAP expressed cells. The killing observed on low expressed cells which were sorted from the lower end of PLAP expression happened after longer incubation. That brings up the issue of whether the cells have completely negative or low expressed, or whether they induce PLAP expression over time. The expression of low expressed cells after a period of time goes back to the heterogeneity of original population.

The low PLAP expressed cells have slower growth rates as well low colony forming ability compared to the original population. That could suggest they have less stemness and are more differentiated. Scanning limited cancer samples for cancer antigens sometimes may not be adequate because the samples isolated from patients may not represent the entire pattern of a tumour's antigen expression. What controls the PLAP expression alterations in the cell lines, and so in the cancers from which they are derived is investigated further in chapter 8.

Chapter 6: RPLP3 (PLAP-CD3) and EpCAM CD3 BiMAb induce bystander killing on PLAP and EpCAM negative cell lines.

6.1 Introduction:

The previous chapter showed the efficacy and specificity of RPLP3 and EpCAM CD3 BiMAb killing of PLAP or EpCAM positive cells. BiMAbs bind to T cells and the positive tumour cell at the tumour site, so the binding will make them close enough to trigger the immune reaction, then it binds to T cells through CD3 which contributes to the activation of T cells, upon T cell binding and activation T cells release cytokines which induce apoptosis in antigen positive cancer cells(Z. Wu & Cheung, 2017) . The results show that RPLP3 or EpCAM CD3 BiMaB induces immune based killing even on low PLAP expressing cells. However, since cancer is heterogeneous in its expression of targeted protein by BiMaB therapy, some cells might lack expression of the targeted antigen and so limit the complete eradiation of a tumour (Kailayangiri et al., 2020) .

The effect of activated T cells on surrounding negative cancer cells of the targeted antigen was therefore investigated by studying the killing by BiMaBs with PBMCs of mixtures of cultures of cancer antigen positive with cancer antigen negative cells in different ratios. This killing of neighbouring target negative cells by target positive activated T cells is called "bystander killing". The bystander killing was also investigated using purified CD8+, CD4+ and gamma delta T cells rather than just PBMCs.

Activated T cells, as already mentioned, release cytokines such as interferon gamma and TNF alpha which, in addition to their role in killing target positive cells, induce the expression of FAS and ICAM1 on the cancer cells, which are thought to be the targets of the activated T cells on cancer cells that do not express the original targets of the BiMaB, such as PLAP and EPCAM . Here the aim of this chapter is to study the effect of bystander killing induced by BiMaB and the mechanism of bystander killing and what induces the activation of T cells to effect bystander killing (see Figure 6.1).

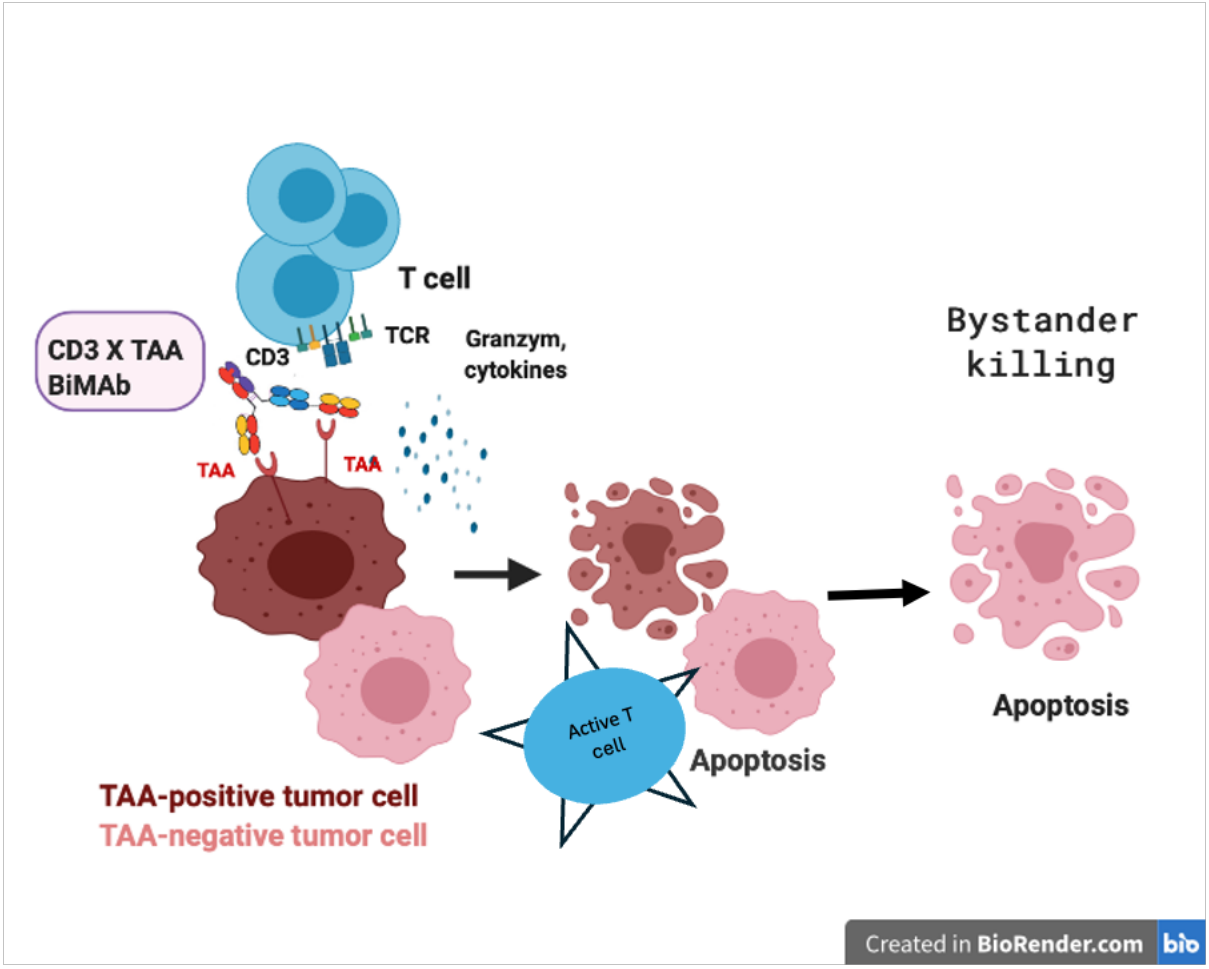

Figure 6.1: Diagram of bispecific monoclonal monoclonal antibody induces killing of TAA positive tumour cell and later induced bystander killing on TAA negative tumour cells.
TAA X CD3 BiMAb has one CD3-, two TAA-binding sites, it recruits T cells to TAA-positive cancer cells resulting in T cell activation, release of cytolytic granules and subsequent apoptosis of TAA-positive cancer cells. Activated T cells induce killing on TAA-negative cancer cell (bystander killing) independent of BiMaB binding.

6.2 Results

6.2.1 Bystander killing of PLAP negative by RPLP3

To investigate bystander cell killing induced by PLAP CD3 BiMAb PLPh3, we co-cultured PLAP-positive (LOVO) and PLAP negative (HT29) cells in different ratios and treated them with RPLP3 and PBMCs for 24 hours and 48 hours. The cell death was measured by Apoptosense® ELISA M30 (PEVIVA®) (see Figure 6.2), and by cleaved caspase-3 immunofluorescence (see Figure 6.3). As shown in Figure 6.2 and Figure 6.3. The RPLP3 mediated cell killing of the PLAP positive (LOVO) cells, and not the PLAP negative cells (HT29) was clear especially after 48 hours and 48 hours of treatment.

Bystander killing seen after 48 hours treatment is shown in (Figure 6.2) by killing of the co-culture of 50% LOVO with 50% HT29 by nearly as much as total killing for 100% LOVO, and the killing was higher than the killing on 50% LOVO alone. Similarly, the killing of co-culture 25% LOVO with 75% HT29 was higher than killing of 25% of LOVO alone. These data clear suggest bystander killing of PLAP negative HT29. Immunofluorescence staining of cleaved caspase 3 also clearly shows the bystander killing of HT29 PLAP negative cells in Figure 6.3. These are identified by cells that stain red for the caspase 3 cleaved but not green for PLAP, as indicated by the yellow arrows.

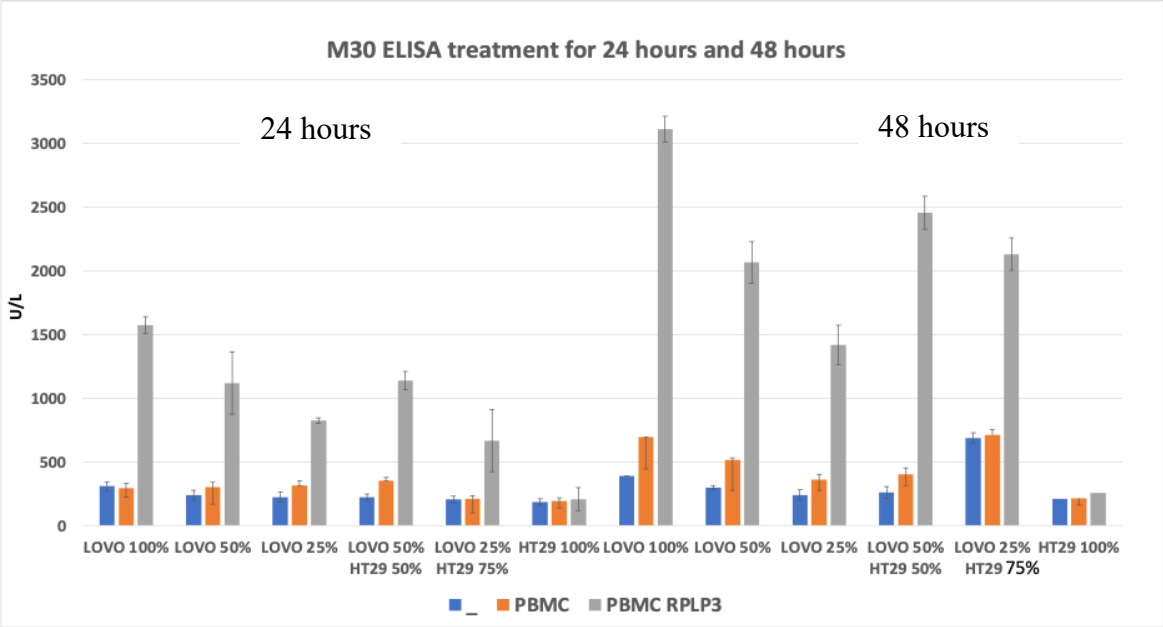

Figure 6.2: Bystander killing mediated by RPLP3 measured by ELISA M30. PLAP- positive (LOVO) and PLAP negative (HT29) cells were seeded in 96 well plate and co-cultured with PBMCs in a ratio of 1:10 and treated with RPLP3 for 24 hours and 48 hours. The conditions are target cells alone and, target cells with PBMC and target cells with PBMC and RPLP3. PLAP- positive LOVO and not PLAP-negative HT29 colorectal cancer cell lines are killed by T cells in the presence of RPLP3. After 24 hours the amount of PLAP positive (LOVO) cell killing is correlated with the number of PLAP positive percentage. 100% LOVO treatment released higher amount of M30 than 50% LOVO treated, and the treatment on LOVO 25% and 5% LOVO. However, at 48 hours treatment RPLP3 induces killing of PLAP-negative (HT29) bystander cells when PLAP-positive and PLAP-negative cells were co-cultured at various ratios as shown by the higher level of killing when 50% HT29 are added to 50% LOVO and similarly for 25% added HT29 to 25% LOVO. After 48 hours treatment the killing difference on 50% LOVO + 50% HT29 is significantly higher than the 50% LOVO alone killing, as well as 25% LOVO + 75% HT29 killing is significantly higher than the 25% LOVO killing ($p < 0.05$).

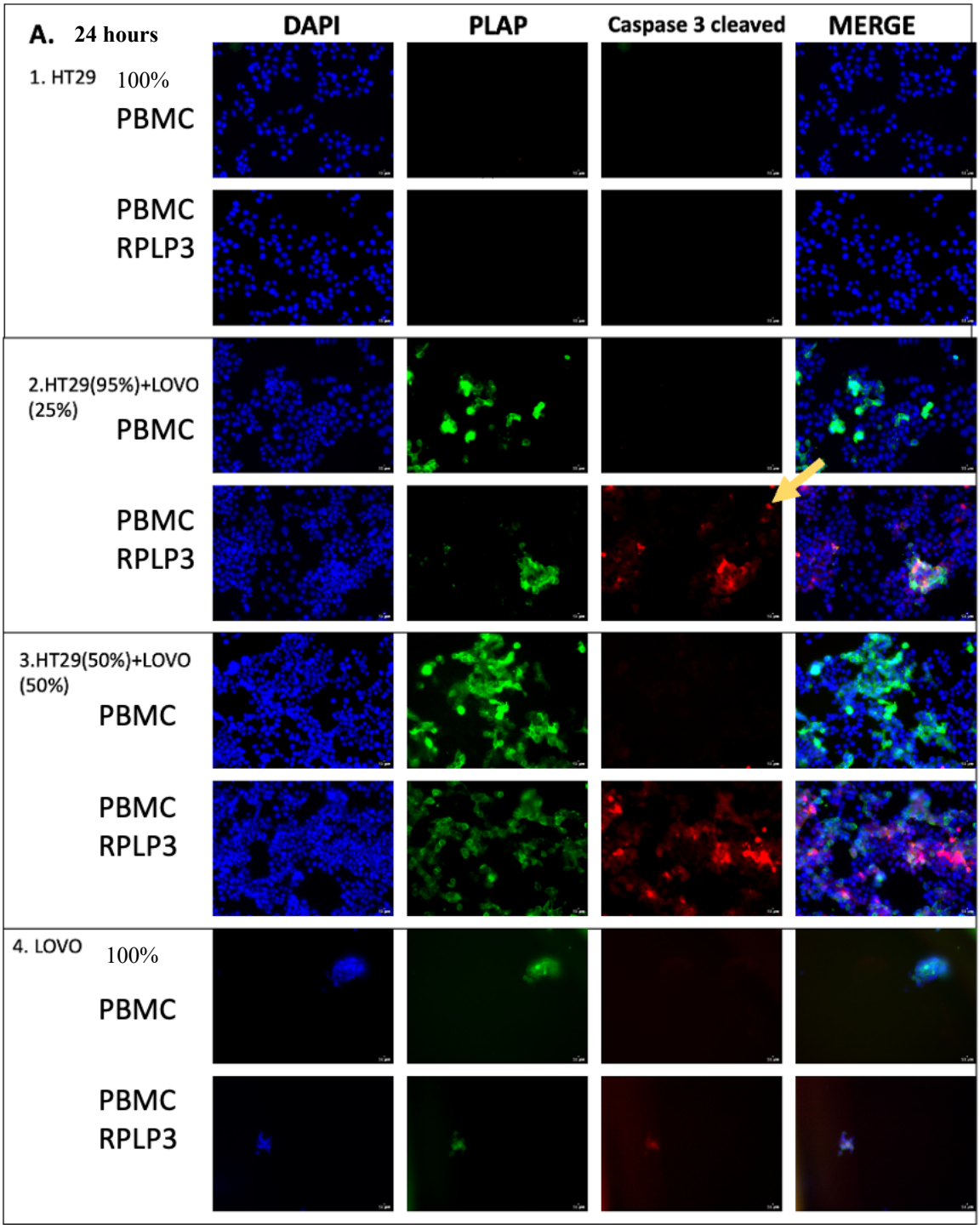
A. 24 hours
DAPI
PLAP
Caspase 3 cleaved
MERGE
1. HT29 100%
PBMC
PBMC
RPLP3
2.HT29(95%)+LOVO (25%)
PBMC
PBMC
RPLP3
3.HT29(50%)+LOVO (50%)
PBMC
PBMC
RPLP3
4. LOVO 100%
PBMC
PBMC
RPLP3

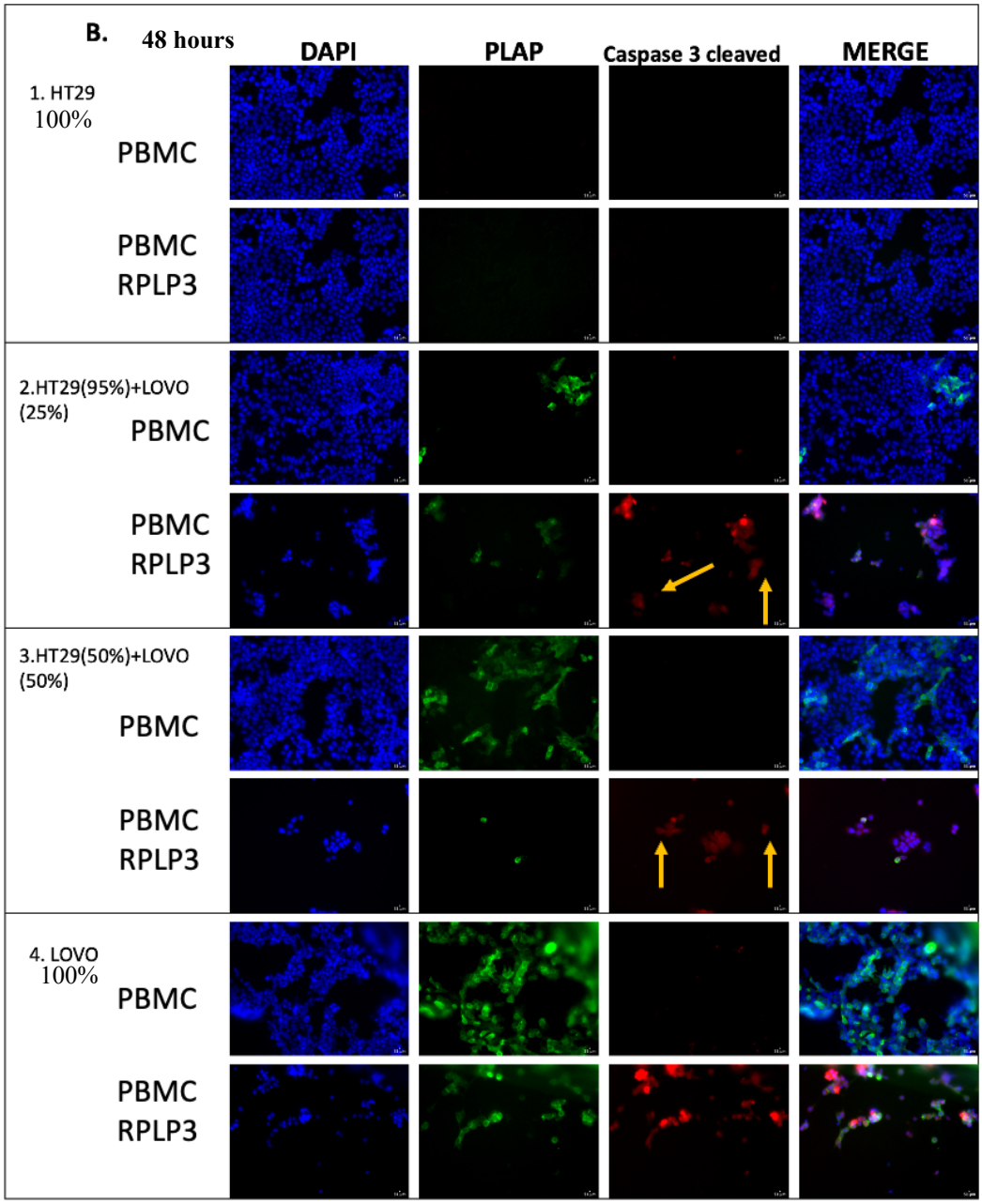

Figure 6.3. Bystander cell killing mediated by RPLP3 measured by immunofluorescence.
For both (A) 24 hours RPLP3 treatment and (B) 48 hours RPLP3 treatment. In each case the first row is control (target cells and PBMC with no RPLP3) and the second row is targeting cells and PBMC with RPLP3. Cell death was analysed by staining for cleaved Caspase 3 as an apoptosis marker using immunofluorescence. The bystander killing is shown by red stained cleaved caspase3 killed cells that are not green, and so PLAP-ve cells, as shown by the yellow arrows. The bystander killing is clearly stronger after 48 hours than after 24 hours treatment. At 24 hours treatment PLAP-positive (LOVO) and a few PLAP-negative (HT29) colorectal cancer cell lines are killed by T cells in the presence of RPLP3. The bystander killing in (B), with 48 hours treatment by RFLP3, is clearly shown by the killing of PLAP-negative cells.

6.2.2 Bystander killing combining RPLP3 and EpCAM CD3 BiMaB

To investigate bystander cell killing induced by PLPh3 on different PLAP negative CRC cell lines, we co-cultured PLAP-positive and PLAP negative CRC cell lines in different ratios and treated them with RPLP3 and PBMCs for 24 hours and 48 hours, with control treatment by the anti- EpCAM antibody, EpCAM CD3 BiMaB. As nearly all of our cell lines express EpCAM, killing by EpCAM CD3 BiMaB should serve as a positive control of complete killing of cells in CRC EpCAM positive cell lines.

The cell death was measured by Apoptosense® ELISA M30 (PEVIVA®), Immunofluorescence and xCELLigence Real-Time Cell Analysis.

The cell lines used in this analysis are listed in table 6.1 with their mRNA levels of PLAP and EpCAM.

Table 6.1: mRNA expression (log2) of ALPP 1 *EpCAM* in CRC cell lines used to study bystander killing.

Cell lines	*ALPP*	*EpCAM*
LOVO	693	9016
DLD1	260	10532
HCT116	50	5432
HT29	46	10379
CC20	50	38
LS180	51	6902

The expression of PLAP and EpCAM on cell lines DLD1 and CC20 is shown in Figure 6.4. The PLAP and EpCAM killing of different ratios of cell lines DLD1 and CC20, as measured by the M30 assay, following 24 hour or 48 treatments with antibodies RPLP3 and EpCAM CD3 BiMAb is shown in Figure 6.5. At both times DLD1 shows almost equal killing by the two antibodies suggesting that the anti PLAP, RPLF3, is killing all, or at least nearly all cells. as expected, CC20 alone is not killed at all. As expected from the previous results shown in Figure 6.2, bystander killing is shown for both antibodies for 50:50 and 25:75 mixtures of DLD1 and CC20 at 24- and 48-hours treatment, but with a much stronger effect after 48 hours treatment, especially with the anti EpCAM antibody. This is probably due to the bystander killing requiring at least 48 hours for a clearly significant effect and possibly also the substantially higher level of EpCAM than PLAP expression in DLD1. The overall higher level of killing at 48 hours treatment is due to the larger number of cells after 48 hours of growth. The bystander killing induced by EpCAM BiMAb is higher than the killing induced by RPLP3. As well when the percentage of positive cells are in higher percentage in the mixture with negative cells there are more bystander killing seen. The bystander killing on mixture of positive 50% and negative 50% is higher than the mixture of 25% positive and 75% negative, the mechanism is not clear.

A

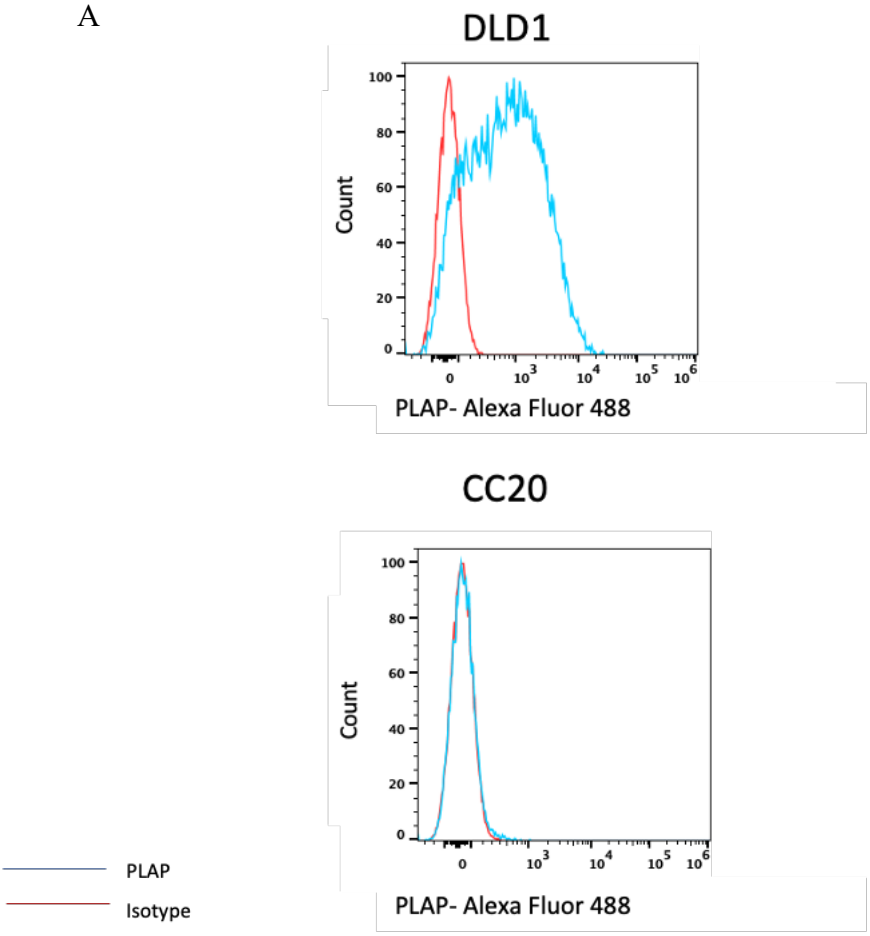
DLD1
Count
PLAP- Alexa Fluor 488
CC20
Count
PLAP- Alexa Fluor 488
PLAP
Isotype

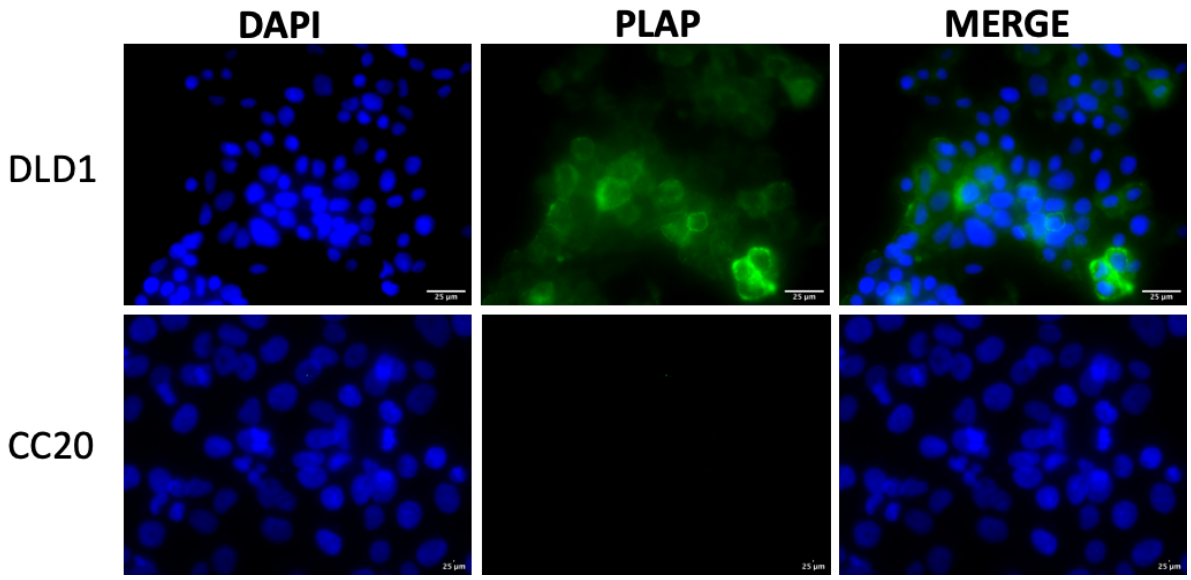
DAPI
PLAP
MERGE
DLD1
CC20

B.

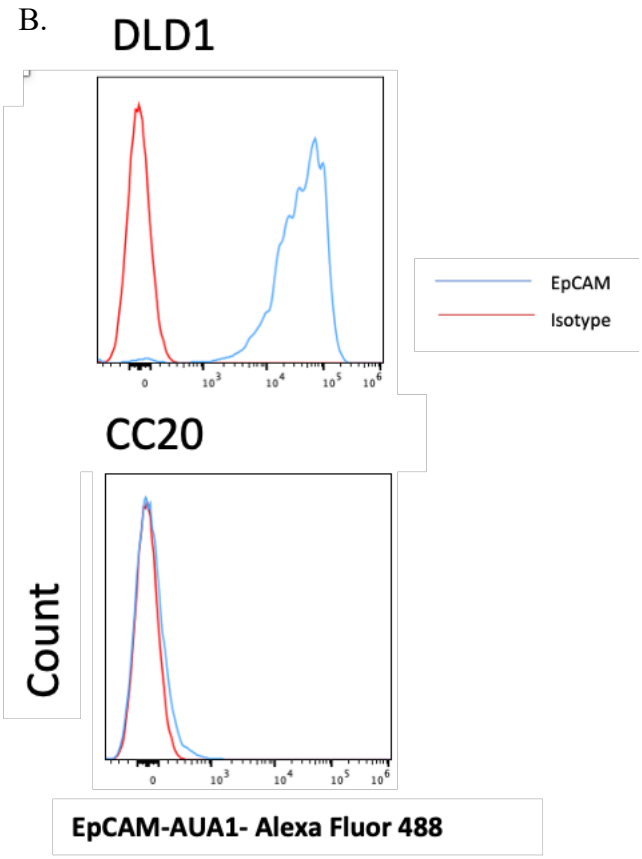

Figure 6.4 PLAP and EpCAM staining on DLD1 and CC20 .
A. Cells were stained with H17E2 anti-PLAP and secondary anti-mouse Alexa fluor 488 secondary antibodies. PLAP expressions were analysed by immunofluorescence and flow cytometry. B Cells were stained with AUA1 anti-EpCAM and secondary anti-mouse Alexa fluor 488 secondary antibodies EpCAM expression were studied by flow cytometry.

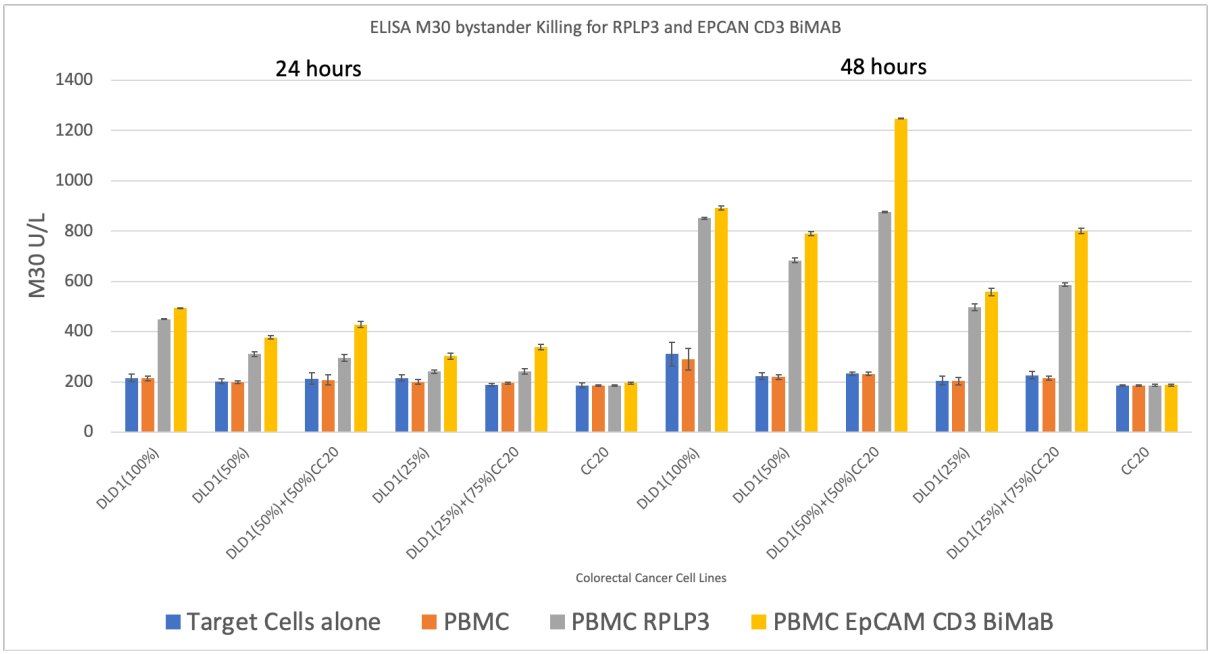

Figure 6.5: Bystander cell killing mediated by RPLP3 measured by ELISA M30 . PLAP-positive, EpCAM-positive (DLD1) and not PLAP-negative, EpCAM-negative (CC20) colorectal cancer cell lines are killed by T cells in the presence of RPLP3 and EpCAM CD3 BiMaB. Both BiMaBs induce killing of PLAP-negative, EpCAM-negative bystander cells at 48 hours of treatment when both cells are co-cultured at various ratios. Cell death was analysed by ELISA M30. After the 48 hours treatment with both BiMabs the killing on 50% DLD1+50% CC20 is significantly higher from the 50% DLD1 killing, and 25% DLD1+ 75% CC20 killing is significantly higher from the 25% DLD1 killing ($p < 0.05$).

In a different experiment, mixtures of DLD1 cells labelled with GFP and CC20 cells labelled with mCherry were used for treatment by RPLP3 and EpCAM CD3 for 48 hours and stained for cleaved caspase3 as a measure of killing (see Figure6.6). As expected, DLD1 stained for cleaved caspase 3 while CC20 did not. In the mixed culture however both DLD1 and CC20 showed cleaved caspase 3, clearly demonstrating bystander killing of CC20.

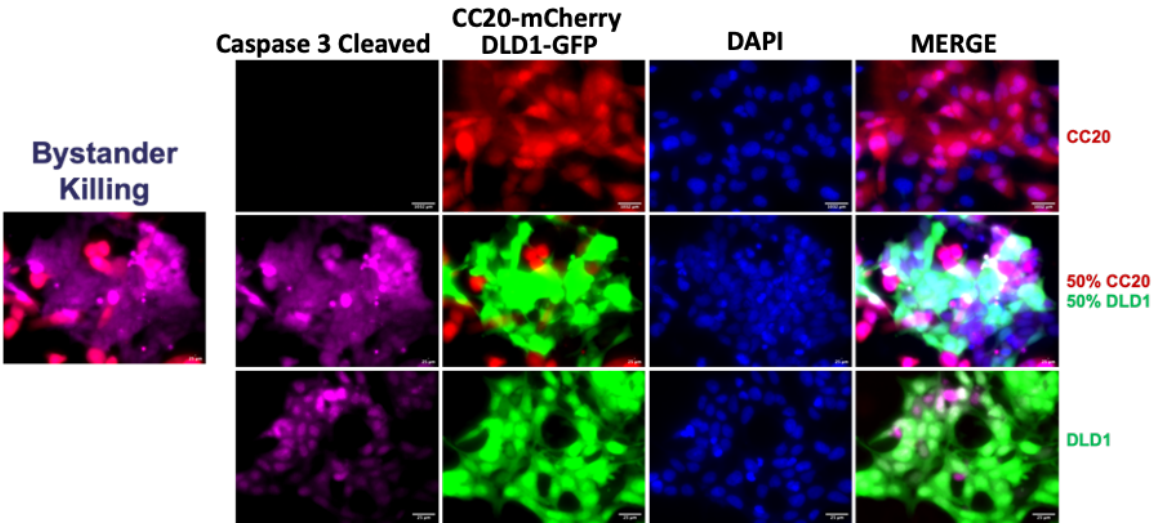

Figure 6.6 Bystander killing mediated by RPLP3 BiMaB measured by Immunofluorescence staining.
CC20 -mCherry alone treated with RPLP3 in the presence of PBMC for 48 hours showed no purple staining of cleaved caspase 3 while DLD1 clearly stained positive for cleaved caspase 3. Co-culture 50% DLD1 and 50% CC20 mCherry showed positive staining of Cleaved caspase 3 on red cells, CC20 mCherry, and on green cells DLD1 GFP.

A final experiment using mixed cultures was carried out using killing measured by xCELLigence Real-Time Cell Analysis, see Figure 6.7. The DLD1 PLAP, EpCAM positive cell line DLD1 was mixed with the double negative line CC20, seeded in different proportions and treated with RPLP3 and EpCAM CD3 BiMAB in the presence of PBMC. Killing was measured over the time of incubation. As shown clearly in Figures 6.7A, C, and D, for DLD1, alone all cells were killed by both antibodies, while for CC20 (figure 6.7B) no cells were killed by either antibody. Figures 6.7 E, F and G show the results for different ratios of DLD1 to CC20, ranging from 50:50 through 25:75 to 5:95. In all cases it appears, that even for a 5% DLD1 to 95% CC20 ratio both antibodies killed all the cells. Similar experiments were carried out using COLO678, a strongly PLAP positive and EpCAM positive cell line and LS180, a PLAP negative but EpCAM positive cell line, with CC20 as a totally negative control (Figure 6.8). The 50:50 mixture of COLO678 and LS180 (Figure 6.8 D) showed complete killing by the anti PLAP antibody, as also shown by both antibodies in the combinations of COLO678 and CC20. These results support very clear bystander killing of LS180 by the anti PLAP antibody and also, again, by anti EpCAM in the killing of CC20 cells by both antibodies.

A.

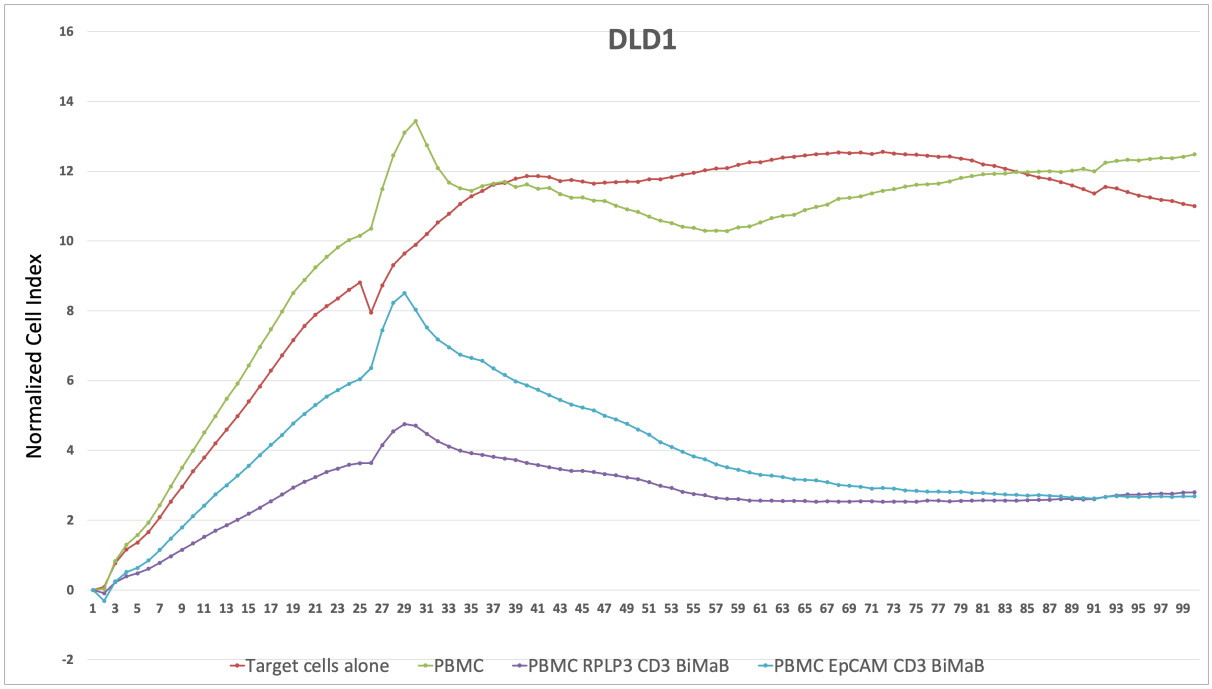
DLD1
Normalized Cell Index
16
14
12
10
8
6
4
2
0
-2
1 3 5 7 9 11 13 15 17 19 21 23 25 27 29 31 33 35 37 39 41 43 45 47 49 51 53 55 57 59 61 63 65 67 69 71 73 75 77 79 81 83 85 87 89 91 93 95 97 99
Target cells alone
PBMC
PBMC RPLP3 CD3 BiMaB
PBMC EpCAM CD3 BiMaB

B.

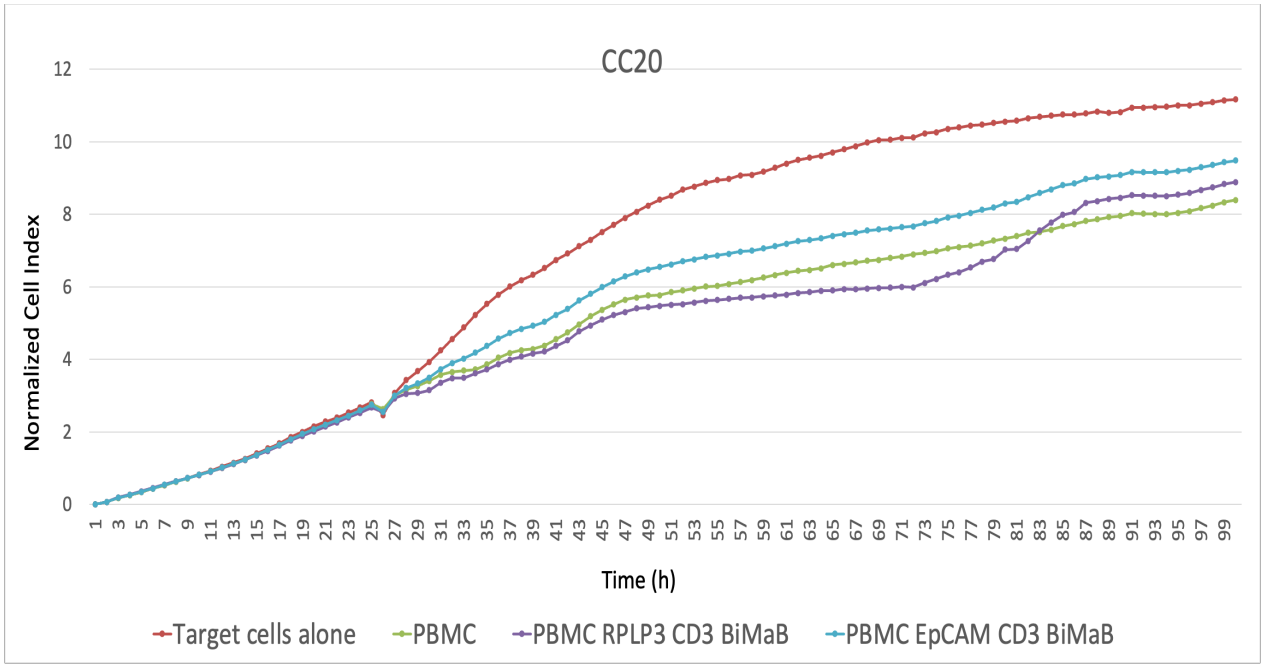
CC20
Normalized Cell Index
12
10
8
6
4
2
0
1 3 5 7 9 11 13 15 17 19 21 23 25 27 29 31 33 35 37 39 41 43 45 47 49 51 53 55 57 59 61 63 65 67 69 71 73 75 77 79 81 83 85 87 89 91 93 95 97 99
Time (h)
Target cells alone
PBMC
PBMC RPLP3 CD3 BiMaB
PBMC EpCAM CD3 BiMaB

C.

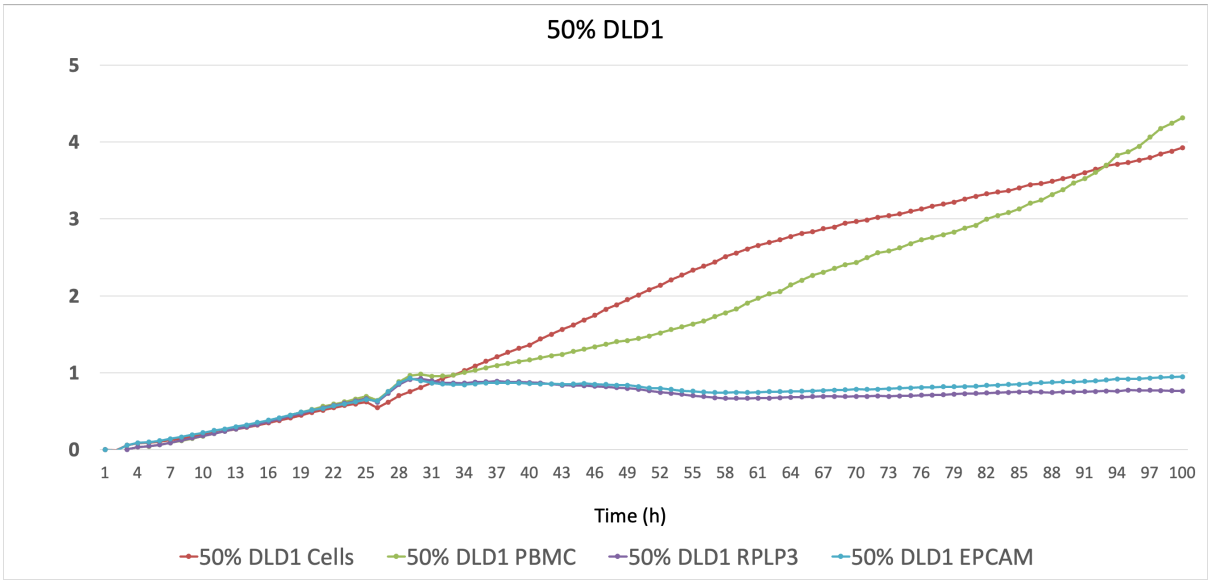
50% DLD1
5
4
3
2
1
0
1 4 7 10 13 16 19 22 25 28 31 34 37 40 43 46 49 52 55 58 61 64 67 70 73 76 79 82 85 88 91 94 97 100
Time (h)
50% DLD1 Cells
50% DLD1 PBMC
50% DLD1 RPLP3
50% DLD1 EPCAM

D.

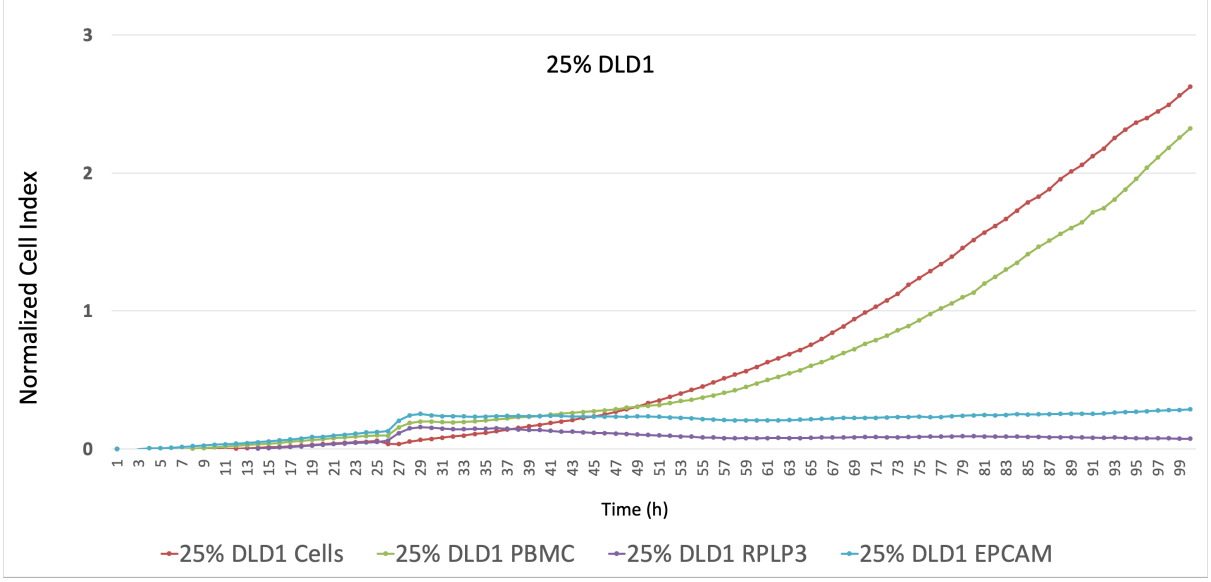
25% DLD1
Normalized Cell Index
3
2
1
0
1 3 5 7 9 11 13 15 17 19 21 23 25 27 29 31 33 35 37 39 41 43 45 47 49 51 53 55 57 59 61 63 65 67 69 71 73 75 77 79 81 83 85 87 89 91 93 95 97 99
Time (h)
25% DLD1 Cells
25% DLD1 PBMC
25% DLD1 RPLP3
25% DLD1 EPCAM

E.

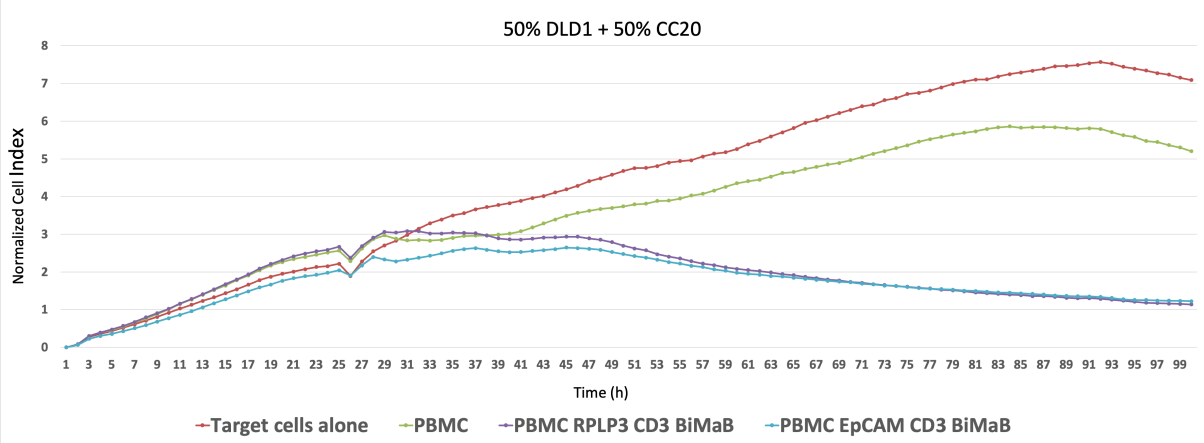
50% DLD1 + 50% CC20
Normalized Cell Index
Time (h)
Target cells alone
PBMC
PBMC RPLP3 CD3 BiMaB
PBMC EpCAM CD3 BiMaB

F.

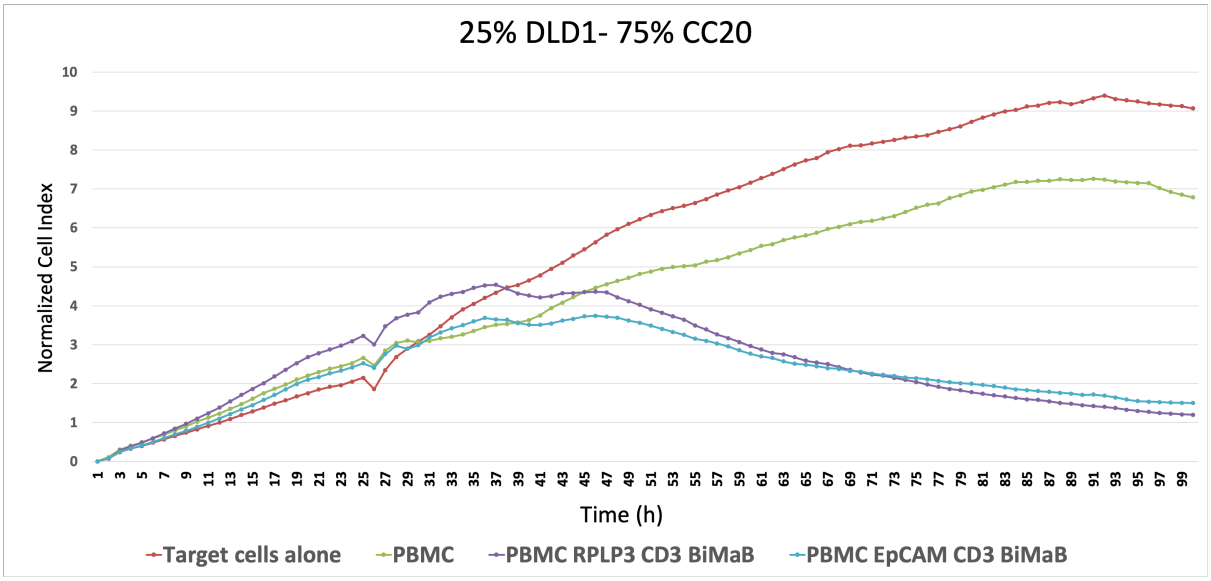
25% DLD1- 75% CC20
Normalized Cell Index
Time (h)
Target cells alone
PBMC
PBMC RPLP3 CD3 BiMaB
PBMC EpCAM CD3 BiMaB

G.

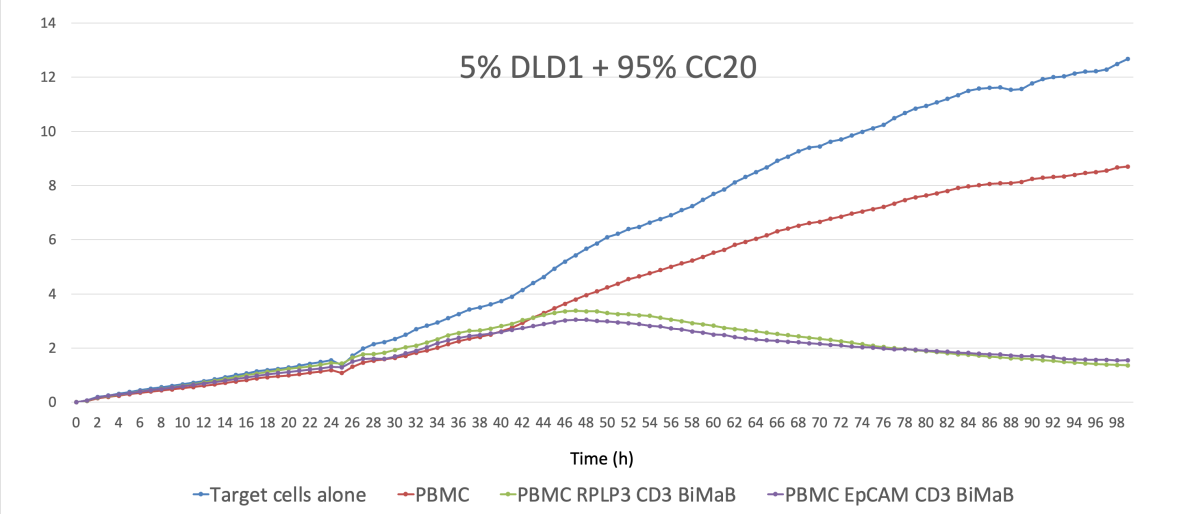

Figure 6.7 Bystander cell killing mediated by RPLP3, EpCAM CD3 BiMAB measured by xCELLigence Real-Time Cell Analysis.
Cell lines DLD1 and CC20, both alone and together, were seeded in 96 well E-plates and after 24 hours, PBMCs and 5nM RPLP3 or 8 ng EpCAM CD3 BiMAb was added to the cells. A. PLAP-positive, EpCAM-positive (DLD1) were killed with both BiMAbs over time. B. PLAP-negative, EpCAM-negative (CC20) was not killed by either BiMAb. C, D. 50% DLD1 and 25% DLD1 alone were killed by both BiMABs. E, F, G the co-culture of DLD1 and CC20 in different ratios show the bystander killing of CC20 starting after 24 hours treatment by both BiMabs.

A.

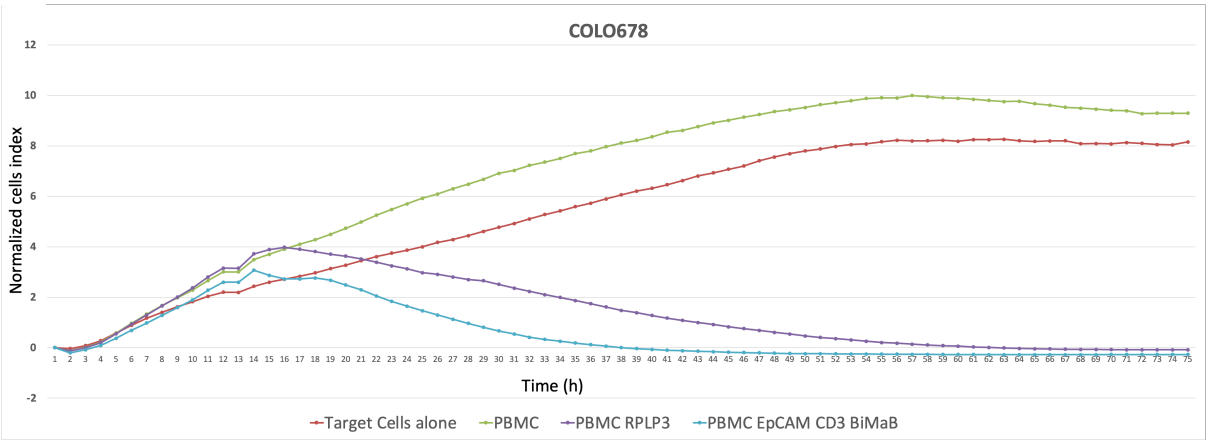
COLO678
Normalized cells index
Time (h)
Target Cells alone
PBMC
PBMC RPLP3
PBMC EpCAM CD3 BiMaB

B.

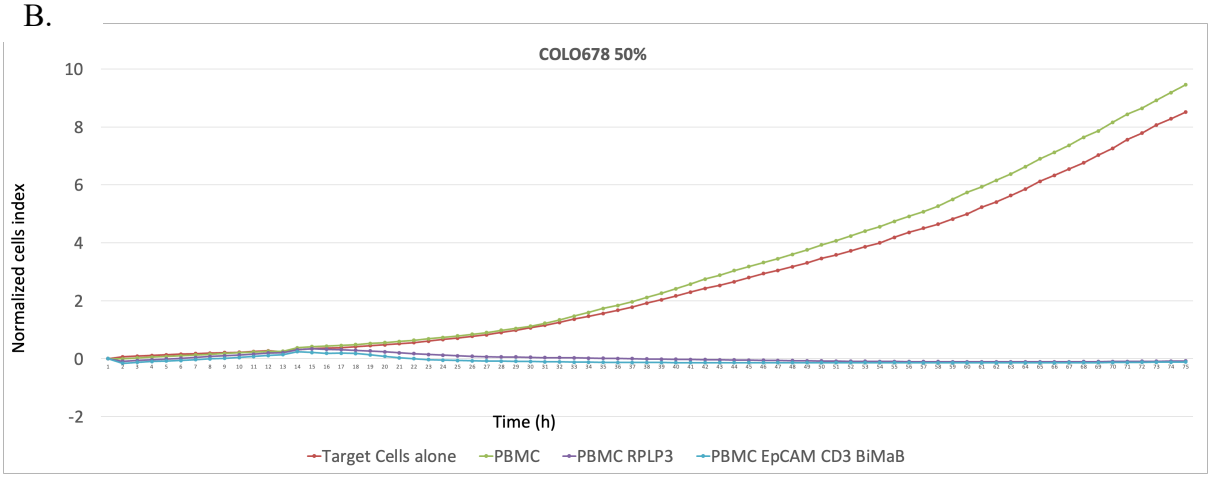
COLO678 50%
Normalized cells index
Time (h)
Target Cells alone
PBMC
PBMC RPLP3
PBMC EpCAM CD3 BiMaB

C.

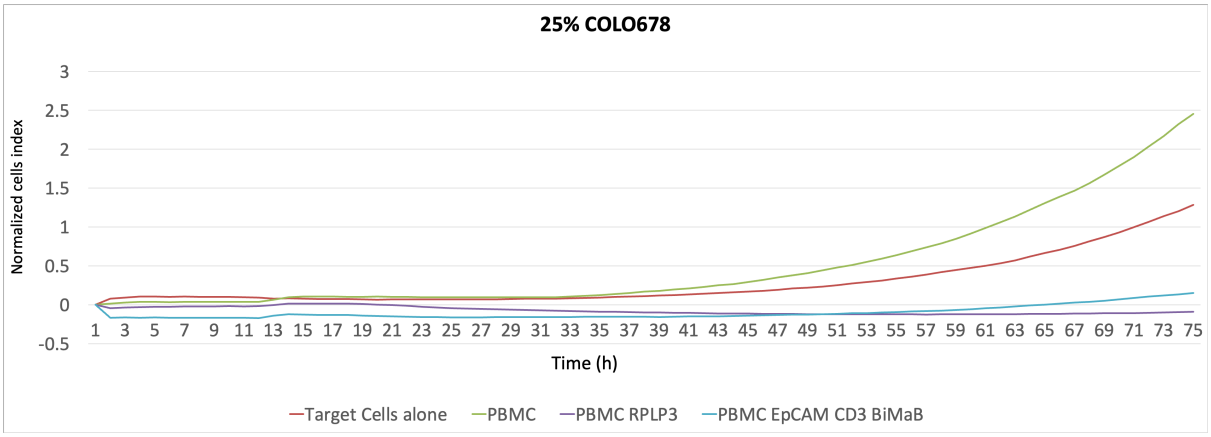
25% COLO678
Normalized cells index
Time (h)
Target Cells alone
PBMC
PBMC RPLP3
PBMC EpCAM CD3 BiMaB

D.

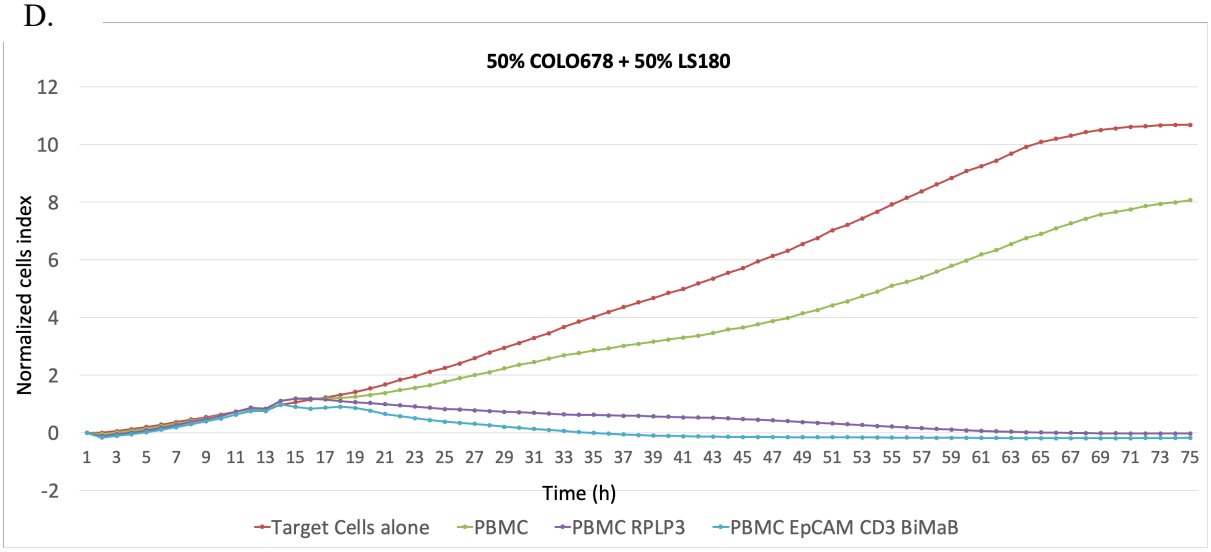
50% COLO678 + 50% LS180
Normalized cells index
Time (h)
Target Cells alone
PBMC
PBMC RPLP3
PBMC EpCAM CD3 BiMaB

E.

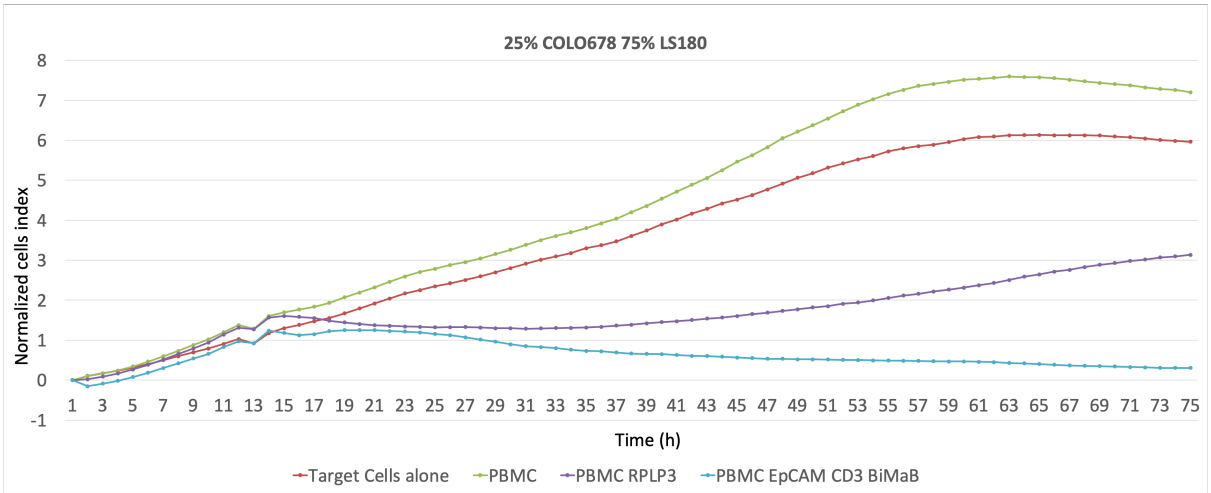
25% COLO678 75% LS180
Normalized cells index
Time (h)
Target Cells alone
PBMC
PBMC RPLP3
PBMC EpCAM CD3 BiMaB

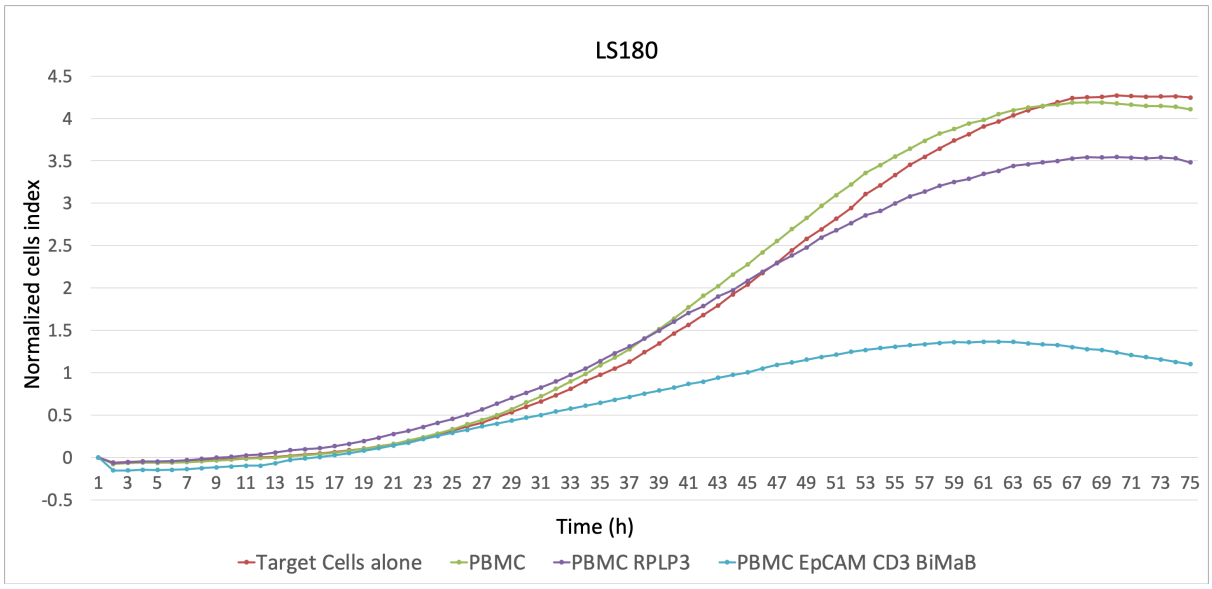
LS180
Normalized cells index
4.5
4
3.5
3
2.5
2
1.5
1
0.5
0
-0.5
1 3 5 7 9 11 13 15 17 19 21 23 25 27 29 31 33 35 37 39 41 43 45 47 49 51 53 55 57 59 61 63 65 67 69 71 73 75
Time (h)
Target Cells alone
PBMC
PBMC RPLP3
PBMC EpCAM CD3 BiMaB

G.

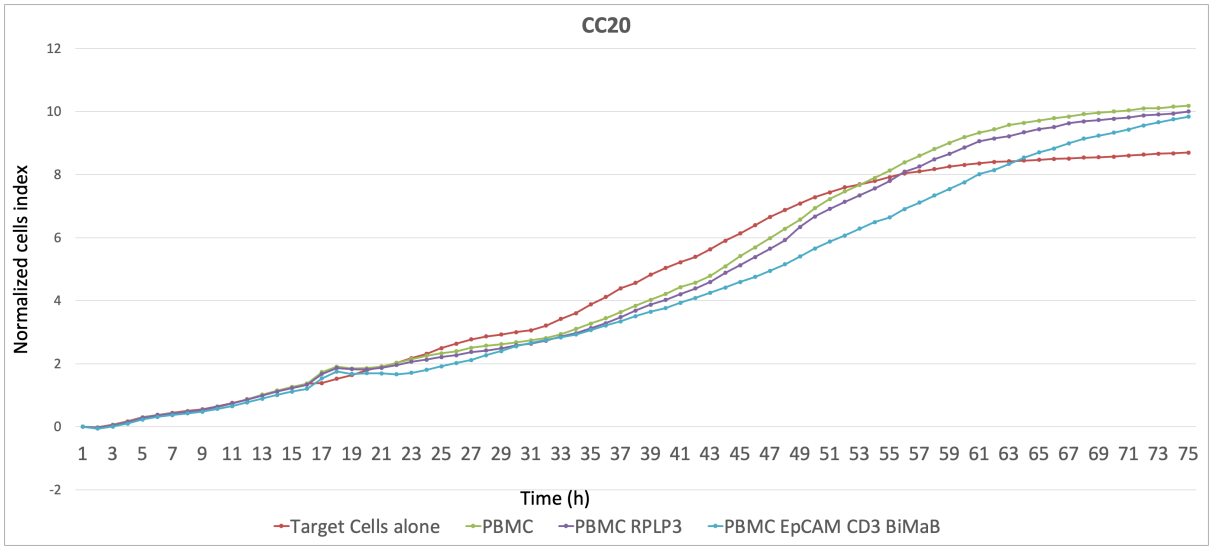
CC20
Normalized cells index
12
10
8
6
4
2
0
-2
1 3 5 7 9 11 13 15 17 19 21 23 25 27 29 31 33 35 37 39 41 43 45 47 49 51 53 55 57 59 61 63 65 67 69 71 73 75
Time (h)
Target Cells alone
PBMC
PBMC RPLP3
PBMC EpCAM CD3 BiMaB

H.

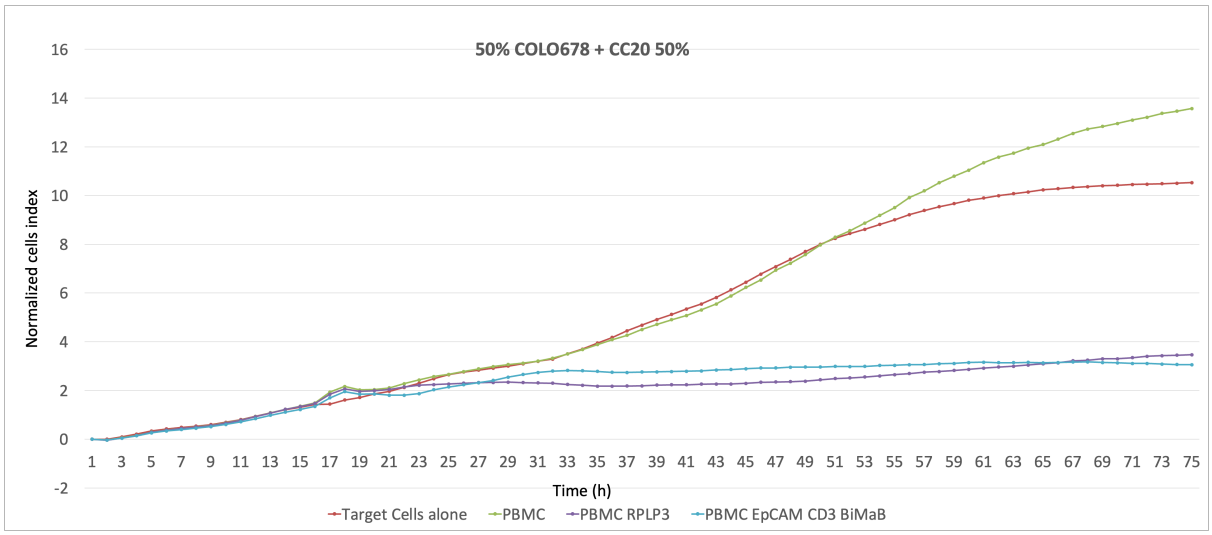

I

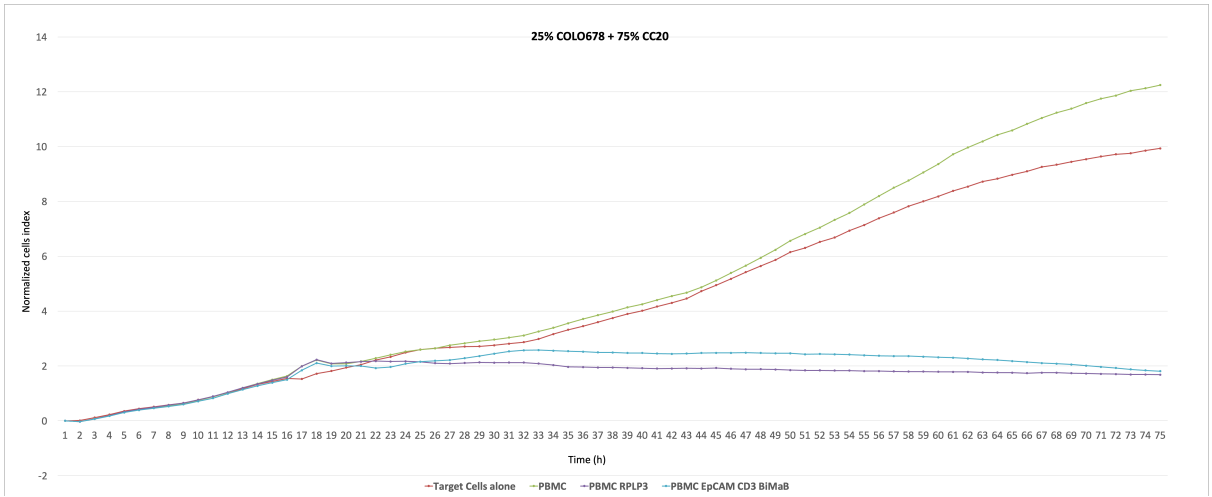

Figure 6.8 Bystander cell killing mediated by RPLP3, EpCAM CD3 BiMAB measured by xCELLigence Real-Time Cell Analysis.
Cell lines COLO678, PALP and EpCAM positive, CC20, PLAP and EpCAM both negative, and LS180, PLAP negative and EpCAM positive, were cultured separately or co-cultured pairwise, either COLO678 with LS180, or Colo678 with CC20. Cells were seeded in 96 well E-plates and after 24 hours, PBMCs and 5nM RPLP3 or 8 ng EpCAM CD3 BiMAb added to the cells. A, B, and C: PLAP-positive, EpCAM-positive COLO678 cells alone were eventually killed with both BiMAbs. F: LS180 cells alone were only killed by the anti EpCAM antibody and not the anti PLAP antibody. G: CC20 cells alone were not killed by either antibody. D and E: PLAP-negative, and EpCAM-positive LS180 cells co-cultured with COLO678 in different ratios - there was killing by RPLP3 compared to LS180 treated with RPLP3 alone showing no killing, especially at 50:50 ratio. H and I: killing of all cells by both antibodies at COLO678:CC20 ratios of 50:50 and 25:75.

6.2.3 Killing assay using supernatant transfer of activated T cells or cell free medium

To study the cause of bystander killing by either activated PBMC or cell free supernatant, DLD1 cells were treated with RPLP3 or EpCAM CD3 BiMAb for 48 hours. The supernatants were divided in two: 0.2μM filtered medium or PBMC cells collected by centrifugation. Each was then added to PLAP negative CRC cell lines and killing measured after 24 and 48 hours by ELISA M30 (see Figure 6.9).

CC20, which is negative for both PLAP and EpCAM, was not killed initially after 24 hours. However, after 48 hours treatment CC20 cells were killed by the PBMC activated transferred cells but not by the cell free supernatant (Figure 6.9A). HCT116 (PLAP negative but EpCAM positive) cells were killed by treatment with EpCAM CD3 BiMAb in the control, as expected but not by the anti PLAP antibody, RPLP3. The HCT116 cells were, however, killed after 48 hours treatment by the transferred activated PBMCs cells that were pre-treated with DLD1 cells and PLAP antibody, Figure 6.9B. A similar result was obtained using LS180 cells as PLAP negative targets, Figure 6.9C. There was no effect of treatment of the three sets of cells with the cell free filtered supernatants.

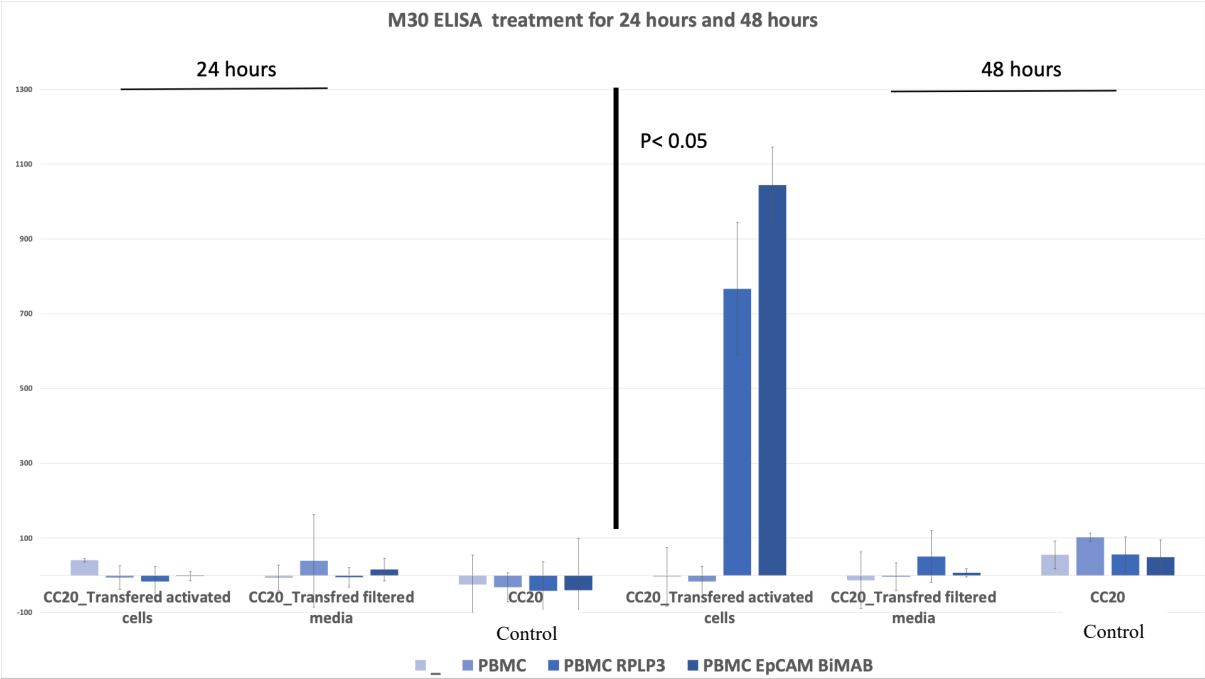
M30 ELISA treatment for 24 hours and 48 hours
24 hours
48 hours
P< 0.05
1300
1100
900
700
500
300
100
-100
CC20_Transfered activated cells
CC20_Transfred filtered media
CC20
Control
CC20_Transfered activated cells
CC20_Transfred filtered media
CC20
Control
_
PBMC
PBMC RPLP3
PBMC EpCAM BiMAB

B.

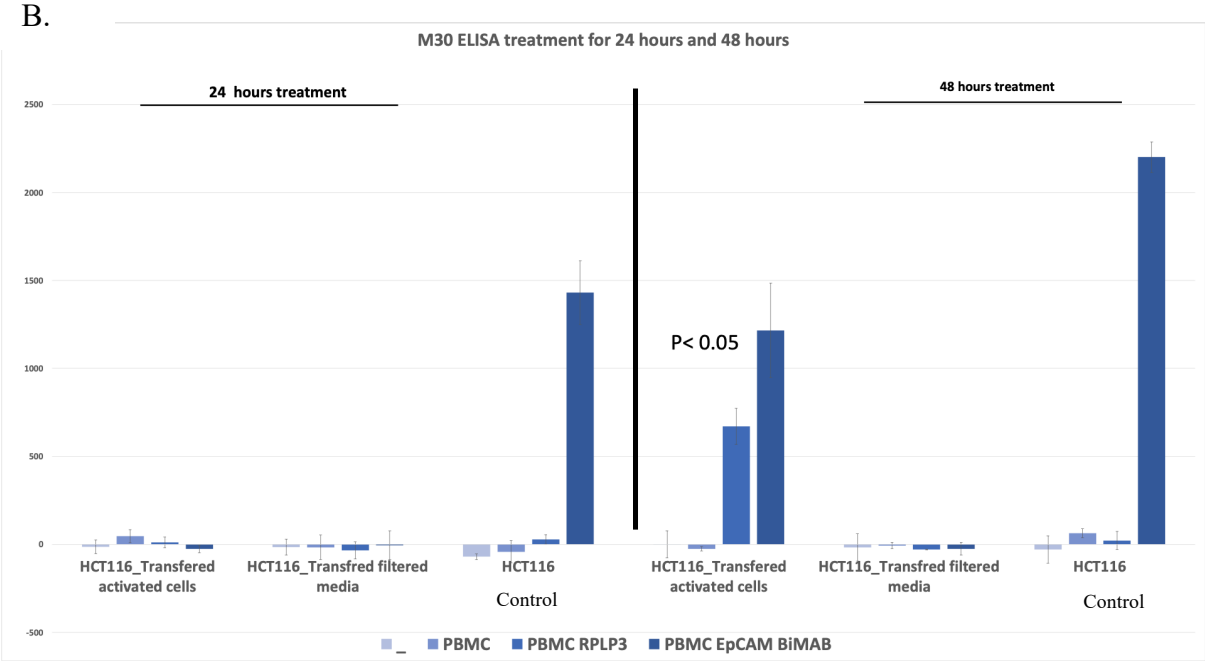
M30 ELISA treatment for 24 hours and 48 hours
24 hours treatment
48 hours treatment
P< 0.05
2500
2000
1500
1000
500
0
-500
HCT116_Transfered activated cells
HCT116_Transfred filtered media
HCT116
Control
HCT116_Transfered activated cells
HCT116_Transfred filtered media
HCT116
Control
_
PBMC
PBMC RPLP3
PBMC EpCAM BiMAB

C.

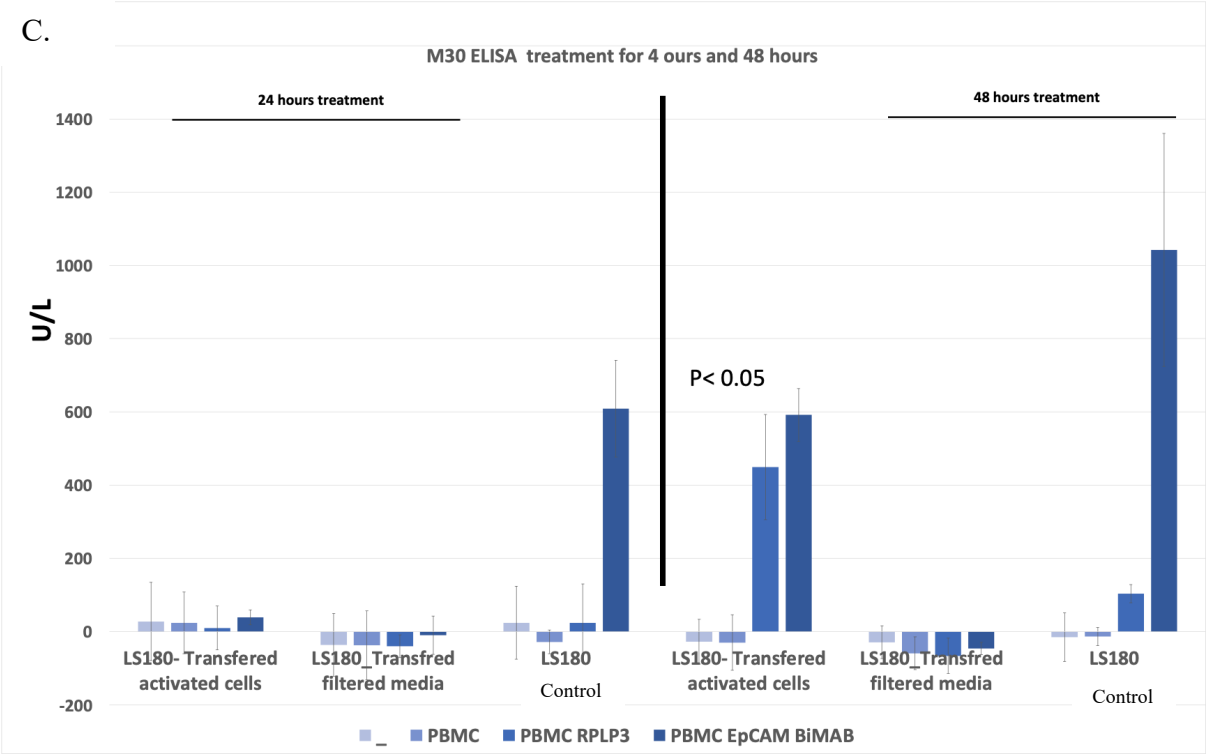

Figure 6.9 Activated T cells and filtered medium treatment of negative cells for 24 hours and 48 hours.
DLD1 cells were treated with PBMC and RPLP3 or EpCAM CD3 BiMAb for 48 hours. The resulting supernatants filtered by 0.2µM filters, and activated PBMCs, were added to cell lines as follows. A. CC20, PLAP and EpCAM negative B. HCT116, PLAP negative and EpCAM positive. D. LS180, PLAP negative, EpCAM positive. Killing was measured by the ELISA M30 assay. Control killing is given in each case in the third set of columns.

In another experiment, cells from DLD1 and COLO678, which are both PLAP positive cell lines, were treated with RPLP3 and PBMC for 48 hours. The resulting activated PBMC cells were collected and added to CC20-mCherry (negative for PLAP) cells for 48 hours followed by immunofluorescence staining for cleaved caspase 3. The control was treating CC20 mCherry cells with RPLP3 and not activated PBMC, where no killing was detected (Figure 6.10). The co staining for mCherry and caspase 3 with either COLO678 or DLD1 activated PBMCs is, again, direct evidence for bystander killing of the CC20 PLAP negative cells.

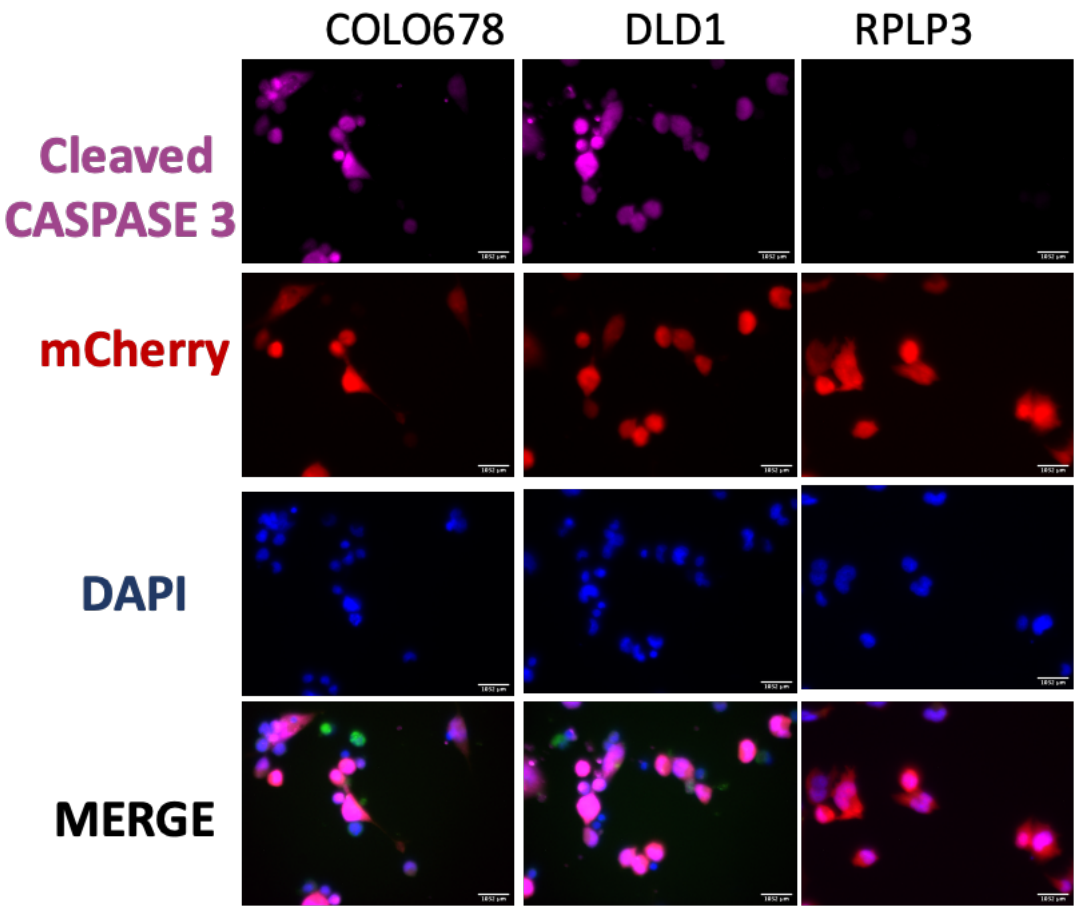

Figure 6.10 Killing by activated T cell treatment of negative cells for 48 hours assessed by cleaved caspase 3 staining.
DLD1, and COLO678 were treated with PBMC and RPLP3 for 48 hours. The activated cells were collected and added to negative mCherry-CC20 cells and killing assessed by immunofluorescence staining with cleaved caspase 3. Negative control is the third row mCherry-CC20 treated with RPLP3 and not activated PBMC for 48 hours.

6.2.4 Bystander killing by activated subtypes of T cells (CD4, CD8, Gamma delta (γδ) T cells)

The aim was to explore the efficacy of isolated subtypes of T cells (CD3, CD4, CD8, Gamma delta (γδ) T cells) in bystander killing rather than the PBMC mixture of different immune cell types. Each subtype of T cells was isolated from PBMC using appropriately targeted magnetic beads the selection was positive selection for CD8 T cells were using antibody against CD8, and for CD4 T cells used antibodies against CD4, and for Gamma delta (γδ) T cells) we used antibody for Gamma delta receptor (γδR)), and added to cells from the PLAP and EpCAM positive line DLD1 or the PLAP and EpCAM negative CC20 cell line in 1:5 ratios of cell line cells to T cells. This mixture was then treated with RPLP3 or EpCAM CD3 BiMaB for 48 hours. The isolated T cell subtypes were stained with anti-CD3, anti CD4, anti-CD8, and anti-Gamma delta T cell antibodies for flow cytometry analysis to confirm they had been effectively purified. The purified T cell subtypes were then used instead of a PBMC mixture to show their bystander killing effectiveness. The overall results for the three T cell subtypes are shown in Figure 6.11. The FACS analyses show that each subtype purification was quite effective, with only small numbers of cells not fitting under the main peak distribution given by the relevant antibody. The clear cut killing of DLD1 alone by both antibodies for each of the three T cell subsets shows that each T cell subset is an effective mediator of BiMab based killing of target positive cells. The modest difference between the anti EpCAM and anti PLAP killing again suggests that a high proportion of all DLD1 cells are killed by the RPLP3 antibody after 48 hours treatment and that perhaps a longer treatment might kill nearly all the cells. Lastly all three T cell subsets show the excess killing with the 50:50 DLD1:CC20 cells compared to the 50% DLD1 only cells, indeed a level of killing that almost matches the 100% DLD1 killing. This shows the efficacy of all three T cell subsets also for bystander killing. For

CD8+ or Gamma delta (γδ) T cells, the 48 hours treatments with both BiMabs, shows the killing difference on 50% DLD1:50% CC20 is significantly greater that the killing of 50% DLD1 alone ($p < 0.05$). For the CD4+ T cells treatment with EpCAM on DLD1 50% DLD1 alone or in combination, the killing was not significantly different compared to the killing with RPLP3 on DLD1 50% alone compared to the combination of both cell lines $P<0.05$ (Figure 6.11 A,B,C).

A CD8+ T cells

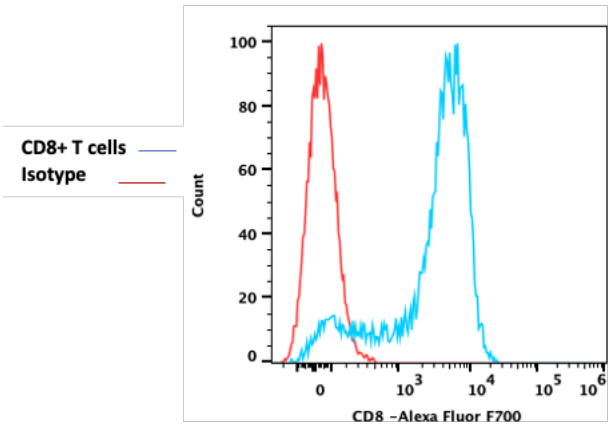

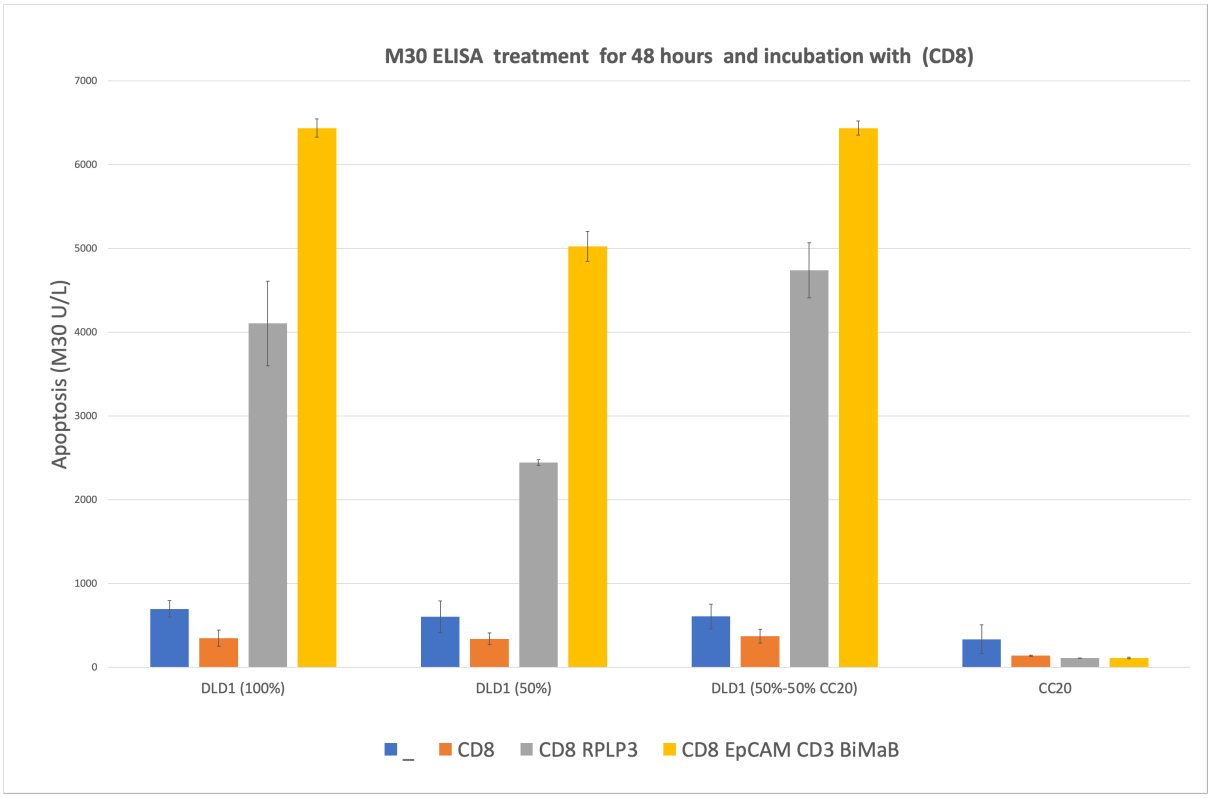

B. CD4+ T cells

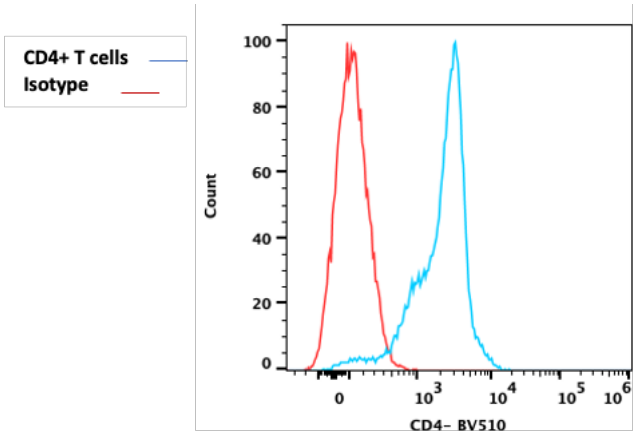
CD4+ T cells
Isotype
Count
100
80
60
40
20
0
0
10^3
10^4
10^5
10^6
CD4- BV510

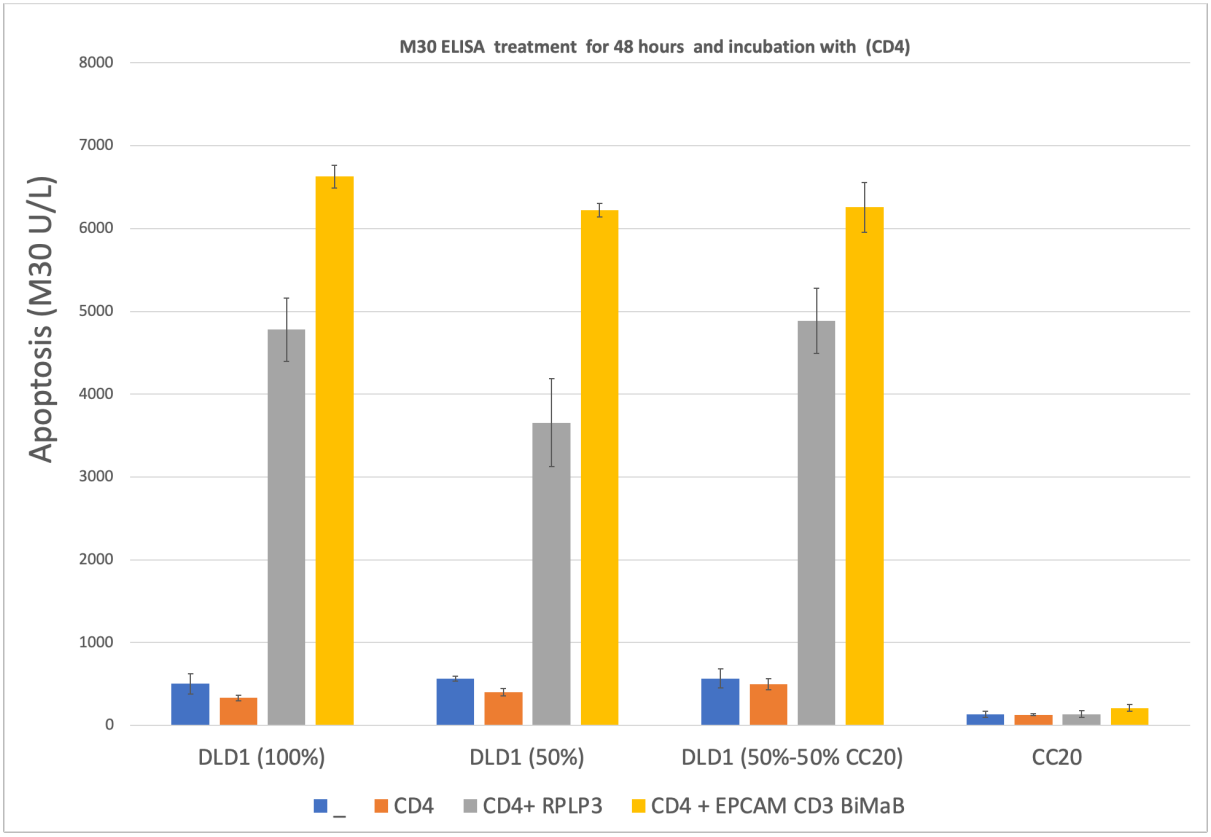
M30 ELISA treatment for 48 hours and incubation with (CD4)
Apoptosis (M30 U/L)
8000
7000
6000
5000
4000
3000
2000
1000
0
DLD1 (100%)
DLD1 (50%)
DLD1 (50%-50% CC20)
CC20
_
CD4
CD4+ RPLP3
CD4 + EPCAM CD3 BiMaB

C. γδ T cells

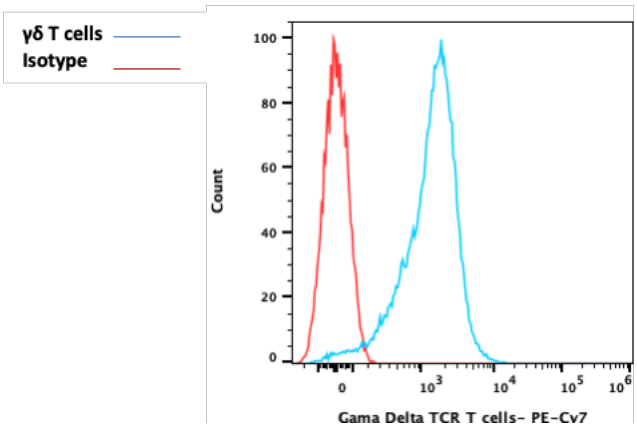

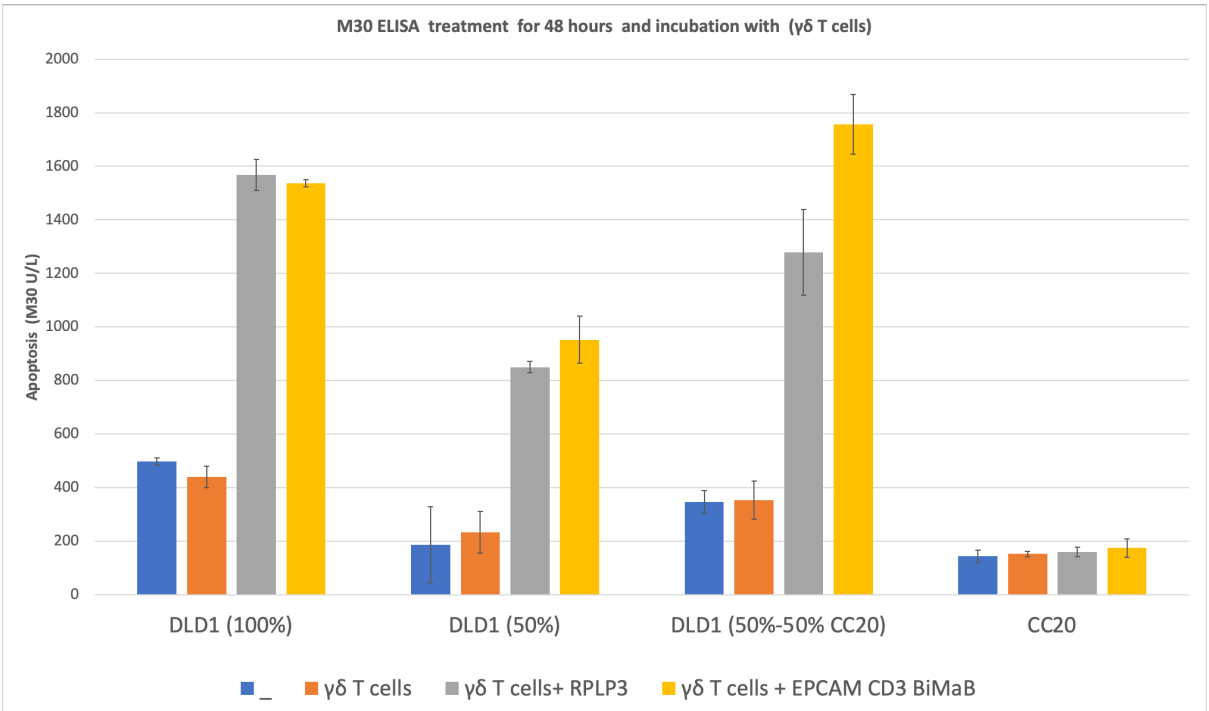

Figure 6.11 Suggested bystander killing measured by the ELISA M30 assay using T cell subsets. DLD1 is PLAP, EpCAM positive and CC20 is PLAP and EpCAM negative.

Isolated T cell subtypes were used in a 5:1 ratio for treatment of DLD1 and CC20 cells alone or in 1:1 mixture for 48 hours with RPLP3 and EpCAM BiMAB. Bystander killing was assessed, as before, by comparison of the killing of DLD1 alone and with that in mixtures of DLD1 and CC20. The figures for each T cell subtype give their verification by FACs and then their bystander killing efficacy A.CD4 T cells, B. CD8 T cells C.γδ T cells.

6.2.5 IFNγ and TNFα induce the expression of ICAM and FAS on bystander cells.

It has been suggested that bystander killing might be affected by T cell recognition of expression or increased expression of ICAM1 and FAS on the cancer cells induced by cytokines such as IFNγ and TNFα released by activated T cells (Ross et al., 2017a). To pursue this possibility the direct effect of added IFNγ and TNFα on cancer cell expression of ICAM1 and FAS and the effect of this on bystander killing was investigated. Thus, IFNγ and TNFα recombinant proteins were added to cells of various different cell lines and ICAM1 and FAS expression measured by flow cytometer antibody-based staining. HCT116 and CC20 are cell lines that both have low expressions of FAS and ICAM (table 6.2). In each case ICAM1 expression increased after the treatment with 10ng of IFNγ and increase of FAS expression after the treatment of 10 ng IFNγ and 10 ng TNFα. (Figures 6. 12 and 6.13).

Table 6.2: mRNA expression of ICAM1 and FAS on selected CRC cell lines.

ICAM1 (intercellular adhesion molecule 1)	Fas(TNF receptor superfamily, member 6)	Cell lines
103	173	CC20
486	1060	COLO678
398	89	DLD1
169	85	HCT116
123	31	HT29
170	281	Lovo
182	104	LS180

A.

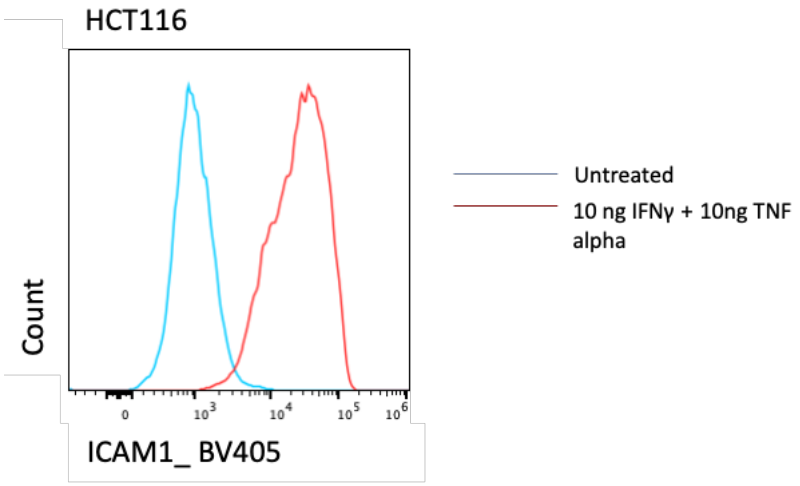

B.

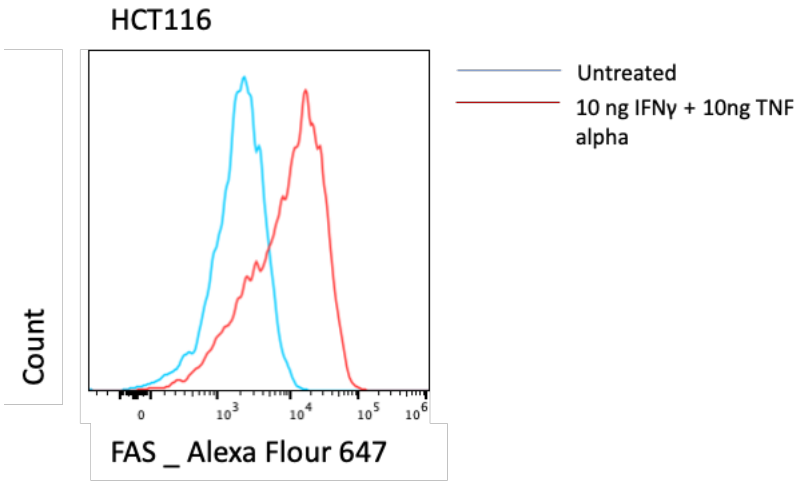

Figure 6.12 Upregulation of FAS and ICAM1 on CRC cell line on response to incubation with IFNγ and TNFα.
Recombinant 10ng IFNγ and 10 ng TNFα were added to HCT116 for 24 hours and FAS and ICAM1 expression were analysed by flowcytometry. A ICAM1 expression. B. FAS expression.

A.

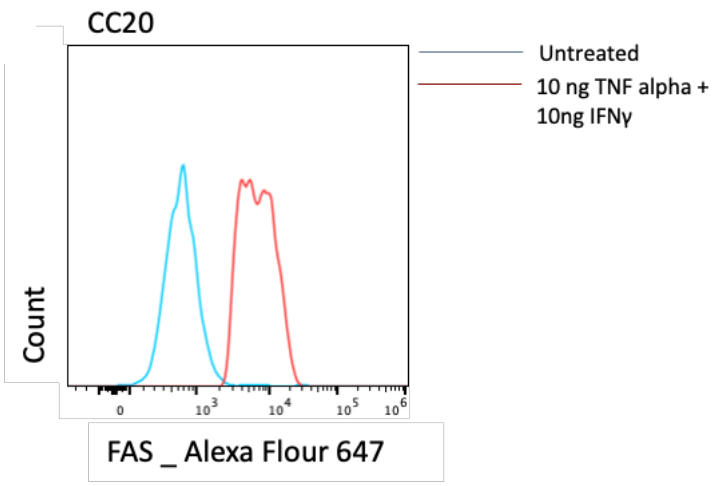

B.

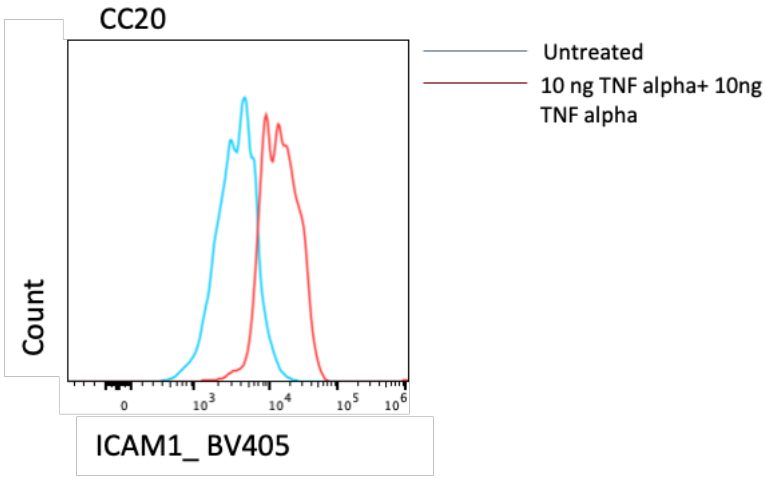

Figure 6.13 Upregulation of FAS and ICAM on CRC CC20 cell line on response to incubation of IFNγ and TNFα incubation.
Recombinant 10ng IFNγ and 10 ng TNFα were added to CC20 for 24 hours and FAS and ICAM1 expression were analysed by flowcytometry. A ICAM1 expression. B. FAS expression

6.2.6 IFNγ and TNFα released from activated T cells in the presence RPLP3 or EpCAM CD3 BiMaB induces the expression of ICAM and FAS on bystander non-target cells.

To investigate the effect of IFNγ and TNFα released from activated T cells on bystander cells and their effect on bystander killing, DLD1(EpCAM +) cell line (positive) was co-cultured with CC20 (EpCAM-) in a ratio of 50% DLD1 and 50% CC20 and the mixture treated with RPLP3 or EpCAM CD3 BiMaB together with PBMC. The control was targeting cells with only PBMC. After 48 hours treatment, cells were harvested and stained with anti-ICAM and anti FAS antibodies and analyzed using Flow cytometer staining (Figure 6.14). When the anti EpCAM antibody was added with PBMC there was clear increase in both ICAM1 and FAS expression on the double negative cell line CC20. This was presumably due to cytokines released by the T cells activated by interaction with the cell line DLD1 and the antibody to a positive target on DLD1. The effect of the anti PLAP antibody was small for ICAM1 and hardly noticeable for FAS. This could be due to the low level of PLAP on DLD1 and a not sufficient time for activation and subsequent cytokine production.

A.

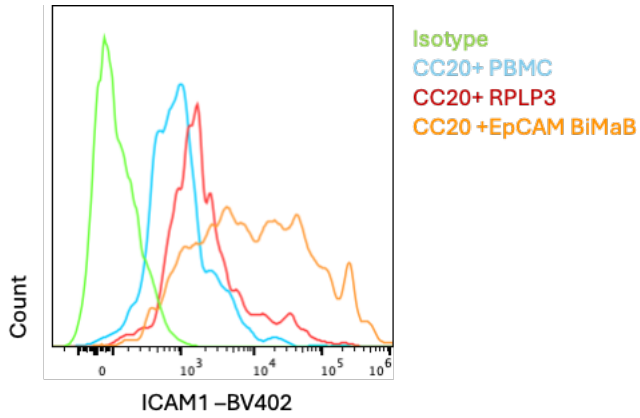

B.

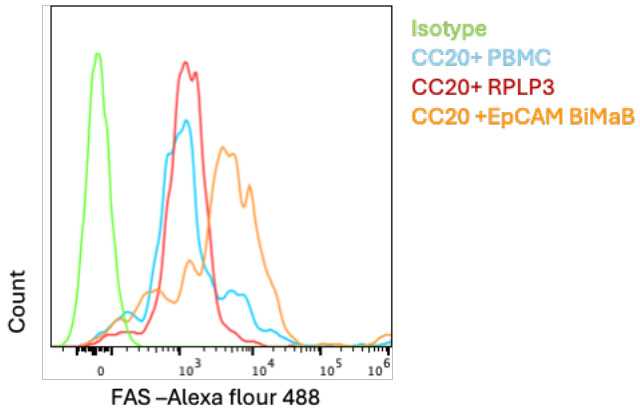

Figure 6.14: Upregulation of FAS and ICAM1 on CC20 when it was co-cultured with DLD1 50% CC20 and 50% DLD1 and antibodies and PBMCs.
A co -culture of 50% DLD1 and 50% CC20 was incubated with PBMC as a control or treated with RPLP3 or EpCAM CD3 BiMAb and PBMCs for 48 hours. A. Flow cytometry staining of ICAM1 expression on CC20. B. Flow cytometry staining of FAS expression on CC20. In each case + PBMCs means only treatment with PBMC, +RPLP3 the only treatment and EpCM BiMab the only treatment. The results show that both antibodies in the mixture induce expression of both FAS and ICAM1 in CC20 through the production of cytokines by T cells activated by the combination of antibodies and T cells with EpCAM and PLAP positive DLD1.

6.2.7 Blocking bystander killing by blocking IFNγ or TNF alpha receptor and so blocking increased expression ICAM1 and FAS.

As shown above, IFNγ and TNF alpha can increase the cellular expression of FAS and ICAM1. The effect of IFNγ and TNF alpha alone did not induce killing on cells.

To investigate the role of FAS and ICAM1 on bystander killing on the presence of activities T cells, DLD1 was treated with RPLP3 or EpCAM CD3 BiMAb and PBMC for 48 hours and the activated cells were added to CC20 which had been pre- incubated with either anti-IFNγ receptor antibody or anti-TNF alpha antibody or both. CC20 cells were also pre incubated with either anti-ICAM1 or Anti FAS neutralizing antibodies or both. In all cases the killing of CC20 was measured by ELISA M30 (see figure 6.15). The killings by activated transferred cells were higher than killing after blocking IFNγ receptor and TNF alpha as well FAS and ICAM1 neutralizing antibodies. In each case one or more of the blocking antibodies has what seems to be a significant effect on the bystander killing of CC20 by the activated T cells. This suggests that activated T cell bystander killing most probably does involved killing through FAS and other TNF receptors as originally suggested by (Ross et al., 2017a) .

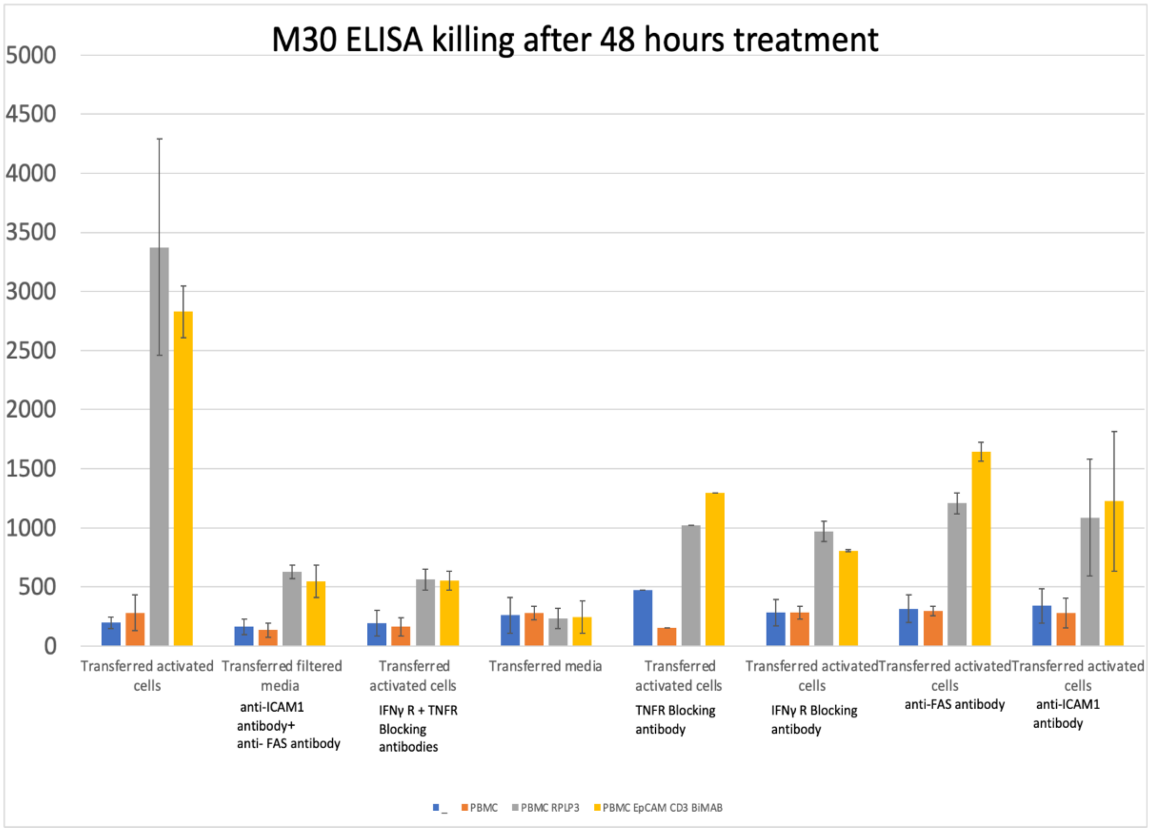

Figure 6.15: The effect of blocking ICAM1 , FAS, IFNγ or TNFR on suggested bystander killing of CC20.
DLD1 was treated with RPLP3 and EpCAM CD3 BiMAB in the presence of PBMC for 48 hours. The supernatant media and activated cells were collected and added to CC20 for assessment of killing as measured by the Elisa M30 assay. Each triplicate was pre-treated by one of the blocking antibodies, as indicated, for 24 hours before adding the activated cells. Killing of CC20 was assessed after 48 hours treatment. There is significance of reduction of killing in the presence of antibody blocking compared the killing by the activated cells alone ***P< 0.05.

6.3 Discussion:

The earlier data showed that the RPLP3 antibody is capable of inducing killing on low PLAP expressed cells in a mixture of heterogeneous population. Here in this chapter this bystander killing has been investigated. To study bystander cell killing we co-cultured PLAP positive and PLAP negative CRC cell lines and found presumptive killing of the PLAP negative cells. The anti EpCAM antiboy EpCAM CD3 BiMaB also showed strong bystander killing on EpCAM negative cells when they are co cultured with EpCAM positive cells. It was also shown that the T cells subtypes, defined as CD4, CD8 and gamma delta T cells, were, on their own probably effective, in inducing direct BiMab mediated killing and bystander killing of target negative. T cells activated by the anti PLAP antibody, RPLP3 were slightly less effective for bystander killing possibly due to lower cell surface antigen concentration of PLAP than EpCAM.

The bystander killing of TAA negative cells, induced by Bi-specific T-cell engagers (BiTEs) has been detected earlier when negative cells were cocultured with TAA positive cells and T cells, suggesting the production of cytokines, which induce the expression of ICAM and FAS on TAA negative cells, making them sensitive to T cells contact-dependent killing (Ross et al., 2017b). It has also been shown that IFNγ secreted by antigen-specific T cells can act on bystander tumour and stromal cells, resulting in contact-independent cell killing (Harjes, 2020).

IFNγ and TNF alpha proteins induced the expression of ICAM1 and FAS expression on some tested cell lines. This suggests that such cytokine secretion by activated cells may enable bystander killing on target negative cancer cells through targeting ICAM1-leukocyte function associated antigen-1 (LFA-1), and FAS to its FAS ligand (FASL) (Bui et al., 2020) (Volpe et al., 2016). Preliminary experiments showed that the bystander killing by activated T cells was inhibited at least to some extent by blocking IFNγ or TNF receptors in agreement with these earlier reports. However, blocking only ICAM1 and FAS was not enough to completely block bystander killing so that there is still a need for further research to properly understand bystander killing. Exploring the effect of CD8+, CD4+ or gamma delta T cells separately using blocking antibodies could give further knowledge of controlling the bystander killing. As well studying other molecules in T cells cancer cells synapse and their function on bystander killing. Understanding bystander killing is very important for achieving ultimately successful cancer immunotherapy.

Chapter 7: Expression of PLAP and EPCAM on Human FFPE tissue samples

7.1 Introduction:

Placenta alkaline phosphatase (PLAP) is highly expressed in the syncytiotrophoblasts of the placenta, and been shown by other researchers that PLAP is expressed in many cancers including colon, testis and ovarian cancer (see (X. Li et al., 2020c) . Another study showed the expression of PLAP on metastatic melanoma (Frieling et al., 2014) A study on 16,000 cancer samples shows a correlation between PLAP high expressed colorectal cancer samples and advancement of disease (Reiswich et al., 2021) .Bispecific monoclonal antibody immunotherapy is targeted therapy, so it is necessary to examine a patient's sample for the cancer specific antigen of interest prior administrating the therapy to the patient. Studying the expression of PLAP on normal tissue is important to avoid side effects of cytotoxicity on normal non-cancerous tissues.

Epithelial cell adhesion molecule (EpCAM) is highly expressed in the membrane of all epithelial cells and so essentially on all epithelial cancer cells (Keller et al., 2019). In cancer PLAP is expressed on the cell membrane of cells as it is normally in the placenta (Reiswich et al., 2021). EpCAM is used in this chapter as a reference marker for localization of epithelium cell membrane to study the expression of PLAP on colorectal cancer samples and normal tissue. As discussed in chapter 3, PLAP is expressed in around 20% of human colorectal cancer derived cell lines and the pattern of the expression within cell lines varies between high, low and negative and so is heterogenous within the cell lines. The focus of this chapter is to study the pattern of PLAP expression in human colorectal cancer tissue samples, and human normal lung tissues by using two PLAP antibodies (HD8B6 and RPLP3 BiMaB) and to localize epithelium cells by staining for EpCAM using the in house (AUA1) antibody.

7.2 Results:

7.2.1 PLAP is expressed in primary human colorectal cancer samples.

Human colorectal cancer patients' samples, and normal colon slides were kindly provided by Prof. David Church. Human placenta tissue was received from Prof. Manu Vatish. Tissue slides were immunofluorescence stained with anti-EpCAM (AUA1) and anti-PLAP (RPLP3 BiMaB) antibodies. EpCAM was used as reference marker for epithelial cells in the staining. Human placenta tissue samples were used as positive control for PLAP expression. Negative control for staining was normal colon Formalin-fixed Paraffin-embedded (FFPE) tissues slides stained with both secondary antibodies (goat anti-mouse Alexa fluor 568 and rabbit anti-human 488 Alexa fluor). 5 out of 20 human colorectal cancer samples were positive for PLAP. The expression of PLAP on the cell membrane of epithelium cells of colorectal cancer FFPE slides is shown in Figure 7.1 for PLAP positive cancers and Figure 7.2 for PLAP negative cancers. Corresponding tissue slides were also stained using immunohistochemistry (Figure 7.3). The staining patterns for colorectal cancer FFPE slides using immunofluorescence and immunohistochemistry agreed.

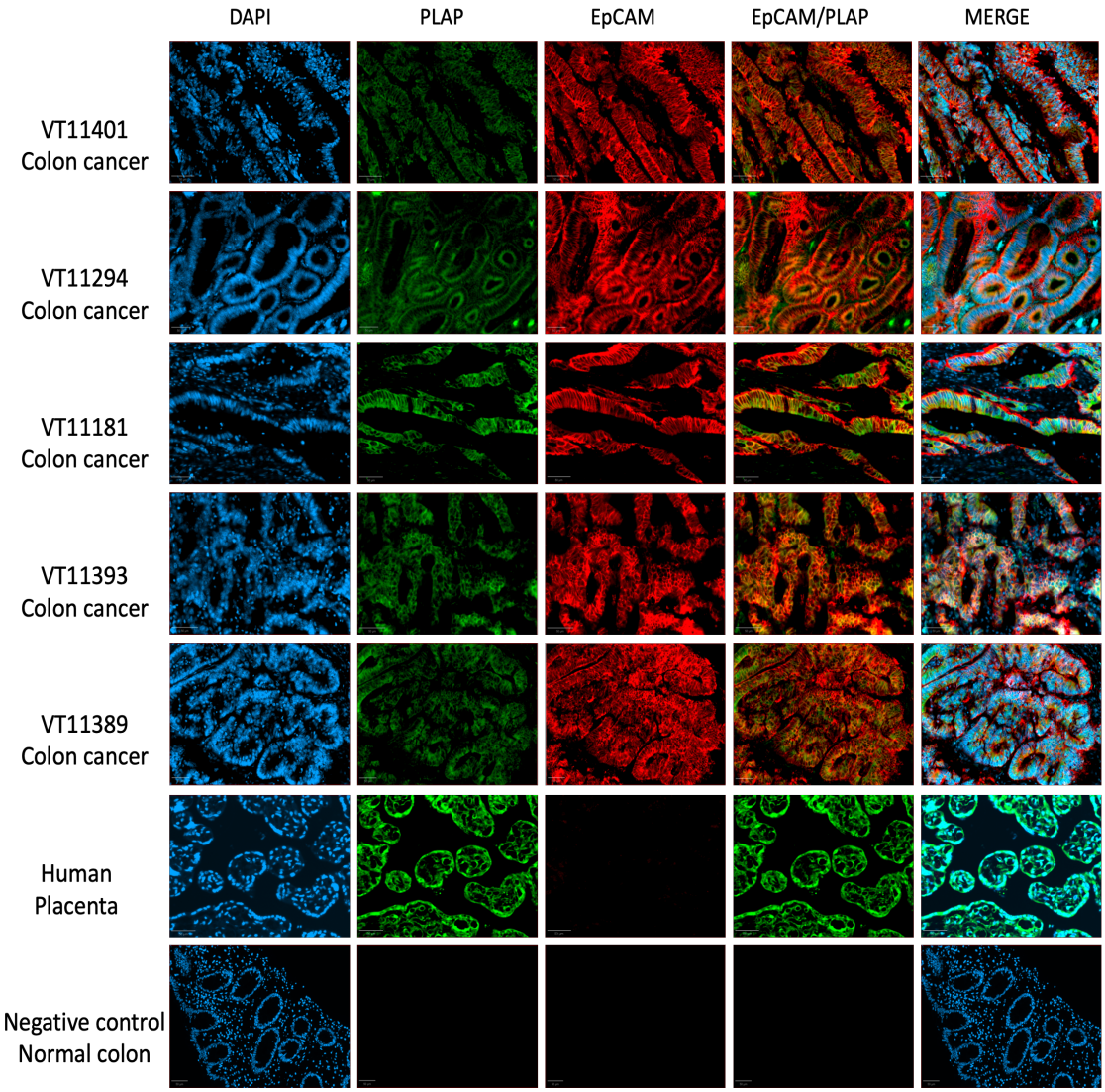

Figure 7.1: Subset of human colorectal cancer FFPE slides which are positive for PLAP.
FFPE slides were stained with anti-PLAP (RPLP3) and anti-EpCAM (AUA1) antibodies. Human placenta is a positive control for PLAP expression. Negative control for staining is human normal colon stained with secondary antibodies goat anti-mouse Alexa fluor 568 and rabbit anti human 488 Alexa fluor.

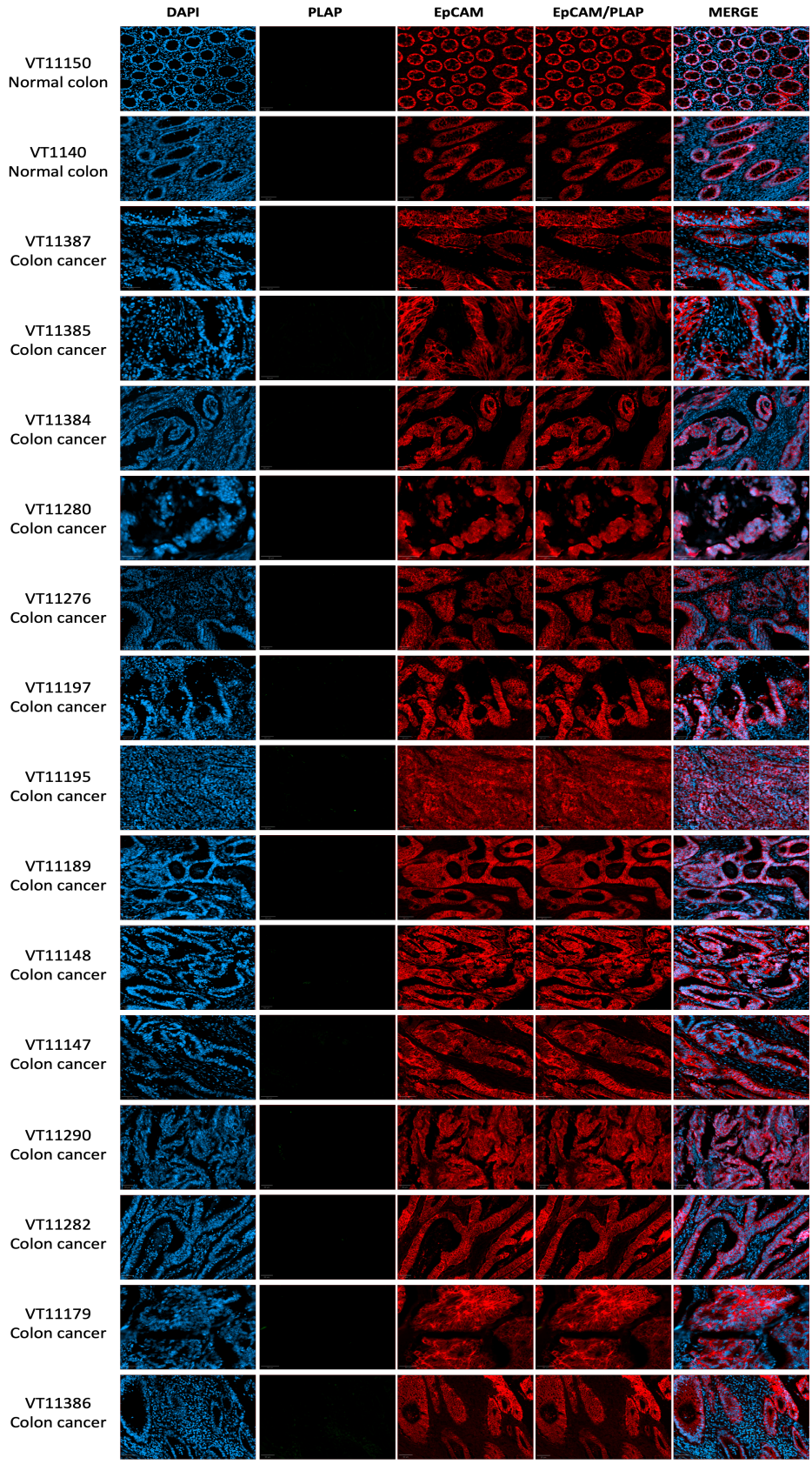

Figure 7.2: Subset of human colorectal cancer FFPE samples which are PLAP negative. Human normal colon is PLAP negative.

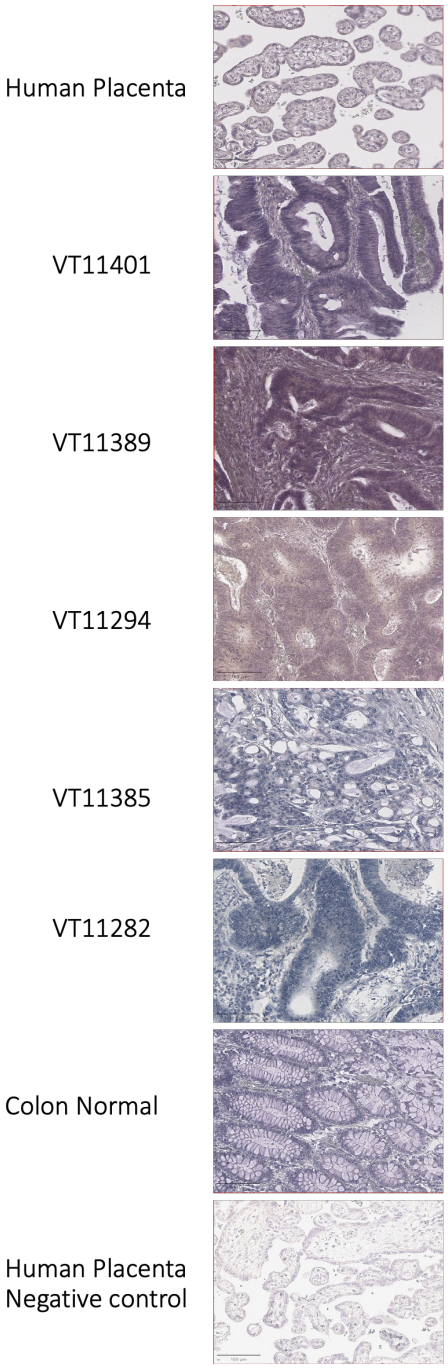

Figure 7.3: IHC staining for PLAP by HD8B6 on human placenta and on Human colorectal cancer samples.
The samples which are PLAP positive are VT11401, VT11389, VT11294. PLAP-negative samples are VT11385, VT11282 and normal colon.

7.2.2 Quantification of PLAP expression on PLAP positive cancer patient tissue slides.

PLAP expression on the 5 colorectal cancer patients varies from high to low. Also, there is heterogeneity of PLAP expression within colon cancer patient sample. The degree of heterogeneous expression varies between samples (Table 7.1).
The areas measured by QuPath (including Tissue Area μm^2, EPCAM Positive area μm^2,
EPCAM negative area μm^2, PLAP Positive area μm^2, PLAP Negative area μm^2) et al., 2017).
The calculation of the heterogeneity of PLAP was as follows:
- EPCAM Positive % = EPCAM Positive area μm^2 / Tissue Area μm^2 *100 - EPCAM Negative % = EPCAM Negative area μm^2 / Tissue Area μm^2 *100
(Bankhead

- - % of PLAP positive = PLAP Positive area μm^2/ Tissue Area μm^2 *100
- - % of PLAP negative = PLAP Negative area μm^2 / Tissue Area μm^2 *100
- - % of PLAP on EPCAM positive (Heterogeneity %) = % of PLAP positive / EPCAM Positive % *100

Table 7.1: table shows the quantification of of EpCAM and PLAP expression on colorectal cancer patients' samples. It shows the percentage of PLAP expression out of EpCAM positive staining.

Tissue slide number	presence of normal area	Tissue Area µm^2	EPCAM Positive area µm^2	EPCAM Negative area µm^2	EPCAM Positive %	EPCAM Negative %	PLAP Positive area µm^2	PLAP Negative area µm^2	PLAP Positive %	PLAP Negative %	% of PLAP on EPCAM positive	
VT11389	yes	1.E+08	86885360	16426043	85	15	86885360	15922883	85	15	100	moderate differentiated adenocarcinoma
VT11401	no	31350192	14526321	16837050	47	53	14293128	17070244	45	54	97	moderate differentiated adenocarcinoma
VT11189	no	1.E+08	61437044	43385572	59	41	19640558	85182056	18	81	31	moderate differentiated adenocarcinoma
VT11891	yes	1.E+08	89096152	15425347	86	14	10091761	94429736	10	90	11	moderate differentiated adenocarcinoma
VT11181	no	93044330	30421946	62618584	33	67	5643356	87397176	6	94	18	moderate differentiated adenocarcinoma
VT11393	yes	12189717	9376174	2808699	77	23	0	12184873	0	100	0	moderate differentiated adenocarcinoma

VT11386	yes	3314612	2621365.75	688762.875	80	20	0	3310128.75	0	100	0	moderate differentiated adenocarcinoma
VT11387	no	20393352	11670464	8722888	58	42	0	20393352	0	100	0	moderate differentiated adenocarcinoma
VT11385	yes	2E+08	75496976	131004256	37	63	0	206501232	0	100	0	moderate differentiated adenocarcinoma
VT11384	yes	1E+08	46009968	79855824	37	63	0	125865792	0	100	0	moderate differentiated adenocarcinoma
VT11294	no	1.E+08	96653104	82718568	54	46	94241232	85130432	52	48	96	moderate differentiated adenocarcinoma
VT11290	yes	9284205	6193674	3092078	67	33	0	9285752	0	100	0	moderate differentiated adenocarcinoma
VT11282	no	1.1E+08	82546416	27094946	76	24	0	109641360	0	100	0	moderate differentiated adenocarcinoma
VT11280	no	14562267	3535534	11027994	25	75	0	14563528	0	100	0	mucinous moderate differentiated adenocarcinoma(mostly necrotic)
VT11276	yes	1E+08	124957680	10751969	93	7	0	135709648	0	100	0	moderate differentiated adenocarcinoma

VT11197	no	5639401	3751421.5	1885012.5	67	33	0	5636434	0	100	0	mucinous moderate differentiated adenocarcinoma
VT11195	no	1E+08	122698000	41672752	75	25	0	164370752	0	100	0	lymph node with poorly differentiated adenoc
VT11179	yes	74396536	53055940	21352082	72	28	0	74408024	0	100	0	moderate differentiated adenocarcinoma
VT11148	no	75254771	62512152	12748170	84	16	0	75260320	0	100	0	moderate differentiated adenocarcinoma
VT11147	no	2.6E+08	106405216	153679360	40.91	59.09	0	260084560	0	100	0	moderate differentiated adenocarcinoma
vt1140-norm	yes	6554064	6324764	229299.203	97	3	0	6554063.5	0	100	0	normal colon
VT11150	yes	1.E+08	56437024	50169368	53	47	0	106606392	0	100	0	normal colon

7.2.3 Clinical outcome:

There was no correlation between PLAP expression in patients' samples and clinical outcomes. There was no correlation with sex, age and grade or stage of cancer and no relation between the presence of mutations in kras, braf, etc and PLAP expression on colorectal cancer patients (Table 7.2).

Table7.2 Clinical data tumour sample donors 1

sample_tumour	trial_no	sex	age	grade	kras	braf	nras	pik3ca	pt53	PLAP expression
VT11389	12090	F	69.2	1	0	0	0	1	0	Yes/high
VT11393	11781	M	83	1	0	1	0	0	0	No
VT11401	10815	F	67.8	1	1	0	0	1	0	Yes /high
VT11181	10548	M	58.4	1	1	0	0	1		yes/low
VT11294	11729	F	78.4	1	0	0	0	0	1	No
VT11386	11876	F	39.2	1	0	0	0	0	0	No
VT11387	11061	F	65.8	1	0	0	0	0	1	No
VT11385	50021	M	24.6	1	1	0	0	0	0	No
VT11290	50007	F	73.5	1	0	0	0	0	0	No
VT11282	11290	M	55.9	1	1	0	0	1	0	No
VT11280	11388	F	83.9	1	0	1	0	0	0	No
VT11276	10820	F	75	1	0	0	0	1	1	No
VT11197	10265	F	60.2	1	0	0	0	0	1	No
VT11195	10919	F	44.6	2	0	0	0	0	1	No
VT11179	10444	F	62.7	1	1	0	0	0	1	No
VT11148	10983	F	74.3	1	0	0	0	0	1	No
VT11189	10443	M	62.1	2	1	0	0	0	0	Yes/low

7.2.3 Expression of PLAP in Human normal lung tissues

PLAP expression was studied in human normal lung tissue samples. Data from Human protein atlas shows PLAP mRNA expression detected on alveolar cell type 1 (Pontén et al., 2008) (Figure 7.4) but there is substantial disagreement about whether PLAP is expressed in the normal lung. To examine this question at the protein level, PLAP was stained on human lung tissues. The staining was done by using RPLP3 and HD8B6 to study PLAP expression and AUA1 to study the expression of EpCAM. Human lung staining showed some limited positive staining for PLAP, which was located on some small bronchioles (Figure 7.5). The cells were positive for EpCAM as well. Staining was carried out by using IHC on corresponding tissue slides and the finding was in agreement with the fluorescence staining (figure 7.6). The area of PLAP/EpCAM expression of the slides is highlighted in Figure 7.7.

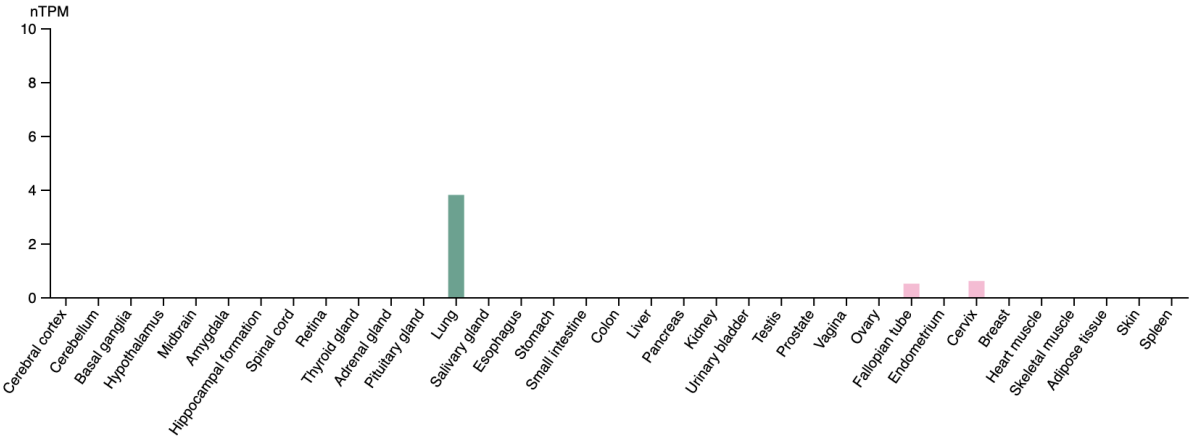

Figure 7.4: Single cells expression data for PLAP on human tissues. It shows PLAP mRNA expression on alveolar cell type 1 in lung (Pontén et al., 2008). The data is obtained from Human Protein Atlas (https://www.proteinatlas.org). Image credit: Human Protein Atlas.ALPP gene page:
(https://www.proteinatlas.org/ENSG00000163283-ALPP/tissue#rna_expression)

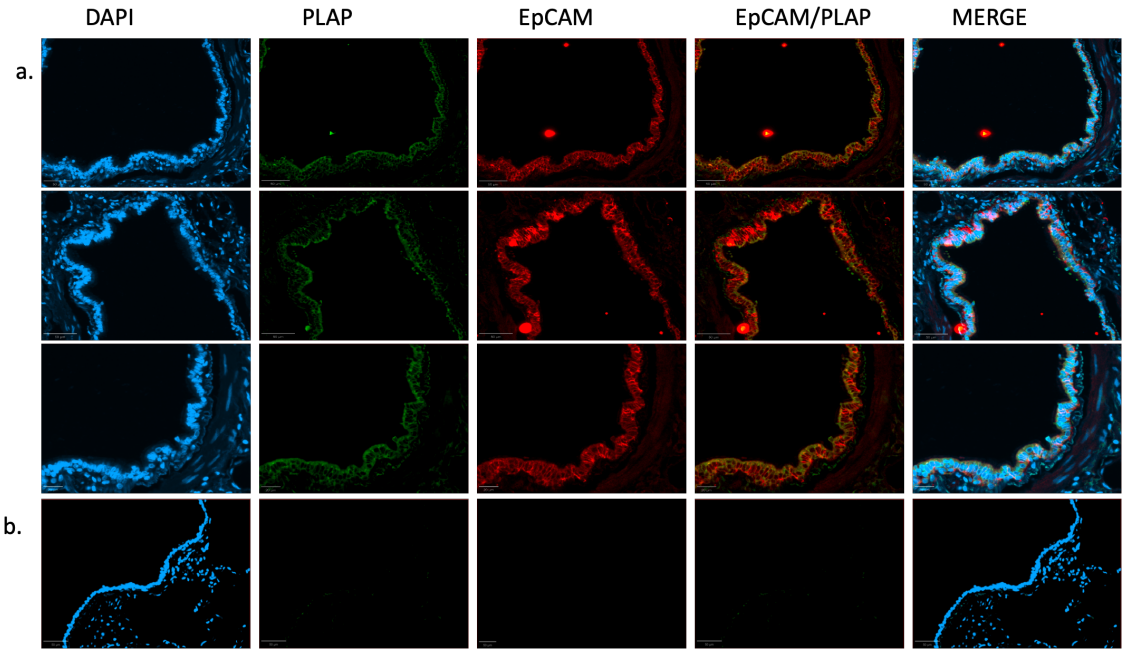

Figure 7.5: Human lung staining with RPLP3 and AUA1 in different positive areas (a). (b) is negative control for staining on human lung tissue slides stained with secondary antibodies only (goat anti mouse Alexa fluor 568 and rabbit anti human 488 Alexa fluor).

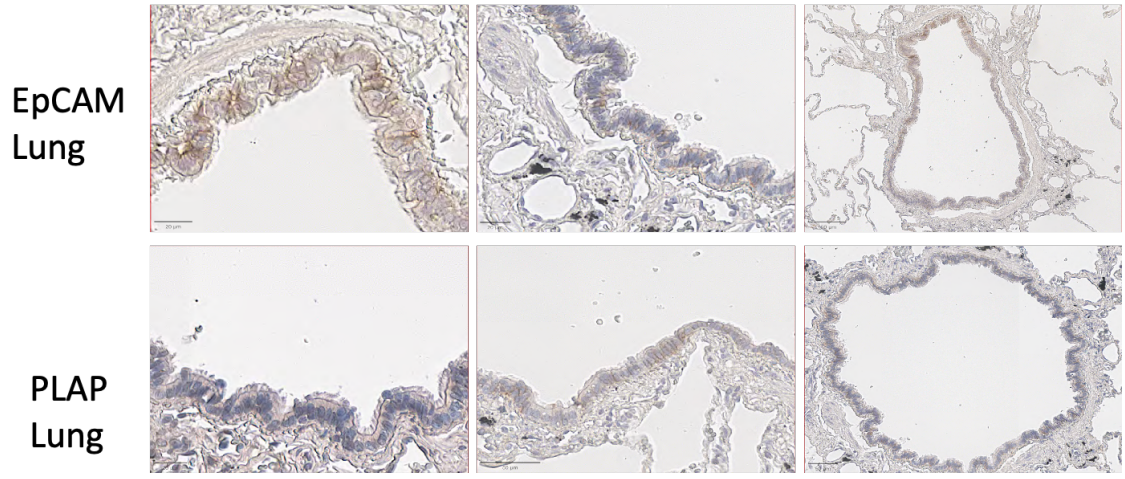

Figure 7.6. IHC staining for PLAP using anti-PLAP HD8B6 and anti-EpCAM AUA1 on human lung tissue.

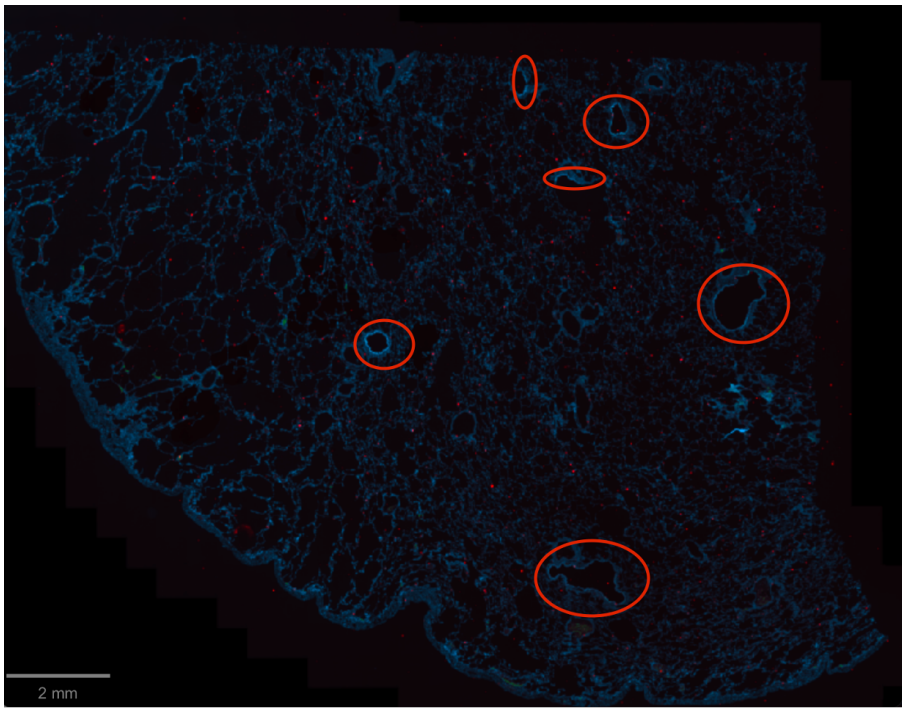

Figure 7.7: FFPE sample of human normal lung. The red circles indicate the area of PLAP/ EpCAM expression. PLAP is green and stained with anti-PLAP mouse anti PLAP (HD8B6) and secondary anti mouse alexa fluor 488.

7.2.4 PLAP expression in lung of cigarette smokers and non-smokers.

It has been known for a long time that smokers can have PLAP in their serum but the reason for this is not known (See e,g. Vengerov et al., 1988). It was therefore decided to see whether the PLAP expression seen in some normal human lung tissue could be connected with smoking. A panel of FFPE tissue slides from normal lungs from smokers or nonsmokers was therefore used to study PLAP expression in relation to smoking. Tissues were received from a company (refer to chapter 2 materials and methods) with data about the donors, including their smoking habits. (Table 7.3)

Immunofluorescence staining of PLAP/ EpCAM on normal lung using AUA1 and RPLP3 is shown in figure 7.8 . The staining shows 5 out of 9 samples of smoker FFPE were positive for PLAP and 2 out of 7 of non-smoker samples were positive, but clearly less so. There was no correlation between PLAP expression and age or gender (table 7.3).

Table 7.3: Clinical and smoking data from normal lung donors of FFPE slides used for PLAP staining

Sample ID	Smoking Status	Age	Gender	PLAP expression
198729	Smoker	60	Female	yes
198730	Smoker	80	Male	yes
198731	Smoker	62	Male	Yes
198732	Smoker	64	Male	No
198733	Smoker	60	Female	No
198734	Smoker	62	Male	yes
198735	Smoker	61	Male	yes
198736	Smoker	53	Female	No
198737	Smoker	62	Male	No
198738	Non Smoker	66	Male	yes
198757	Non Smoker	45	Male	No
198759	Non Smoker	59	Male	No
198760	Non Smoker	53	Female	No
198763	Non Smoker	45	Male	No
198764	Non Smoker	63	Male	No

A.

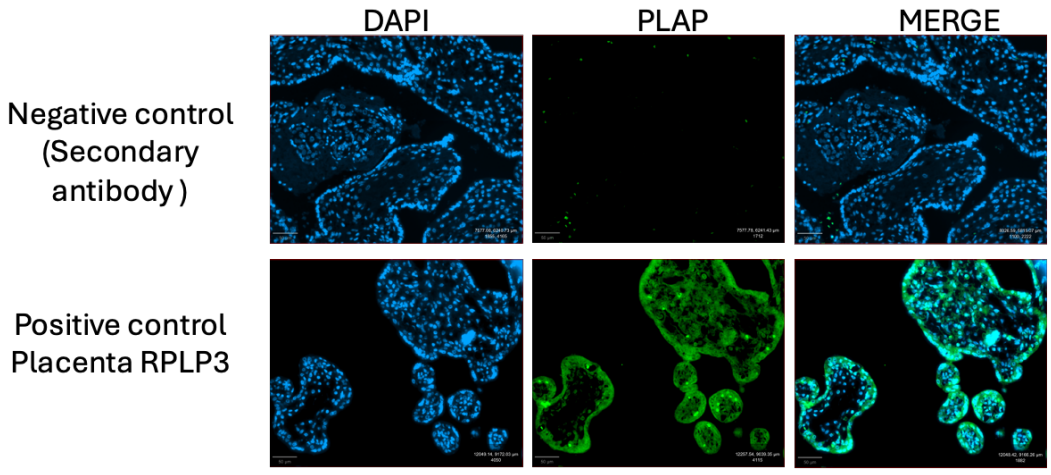

B.

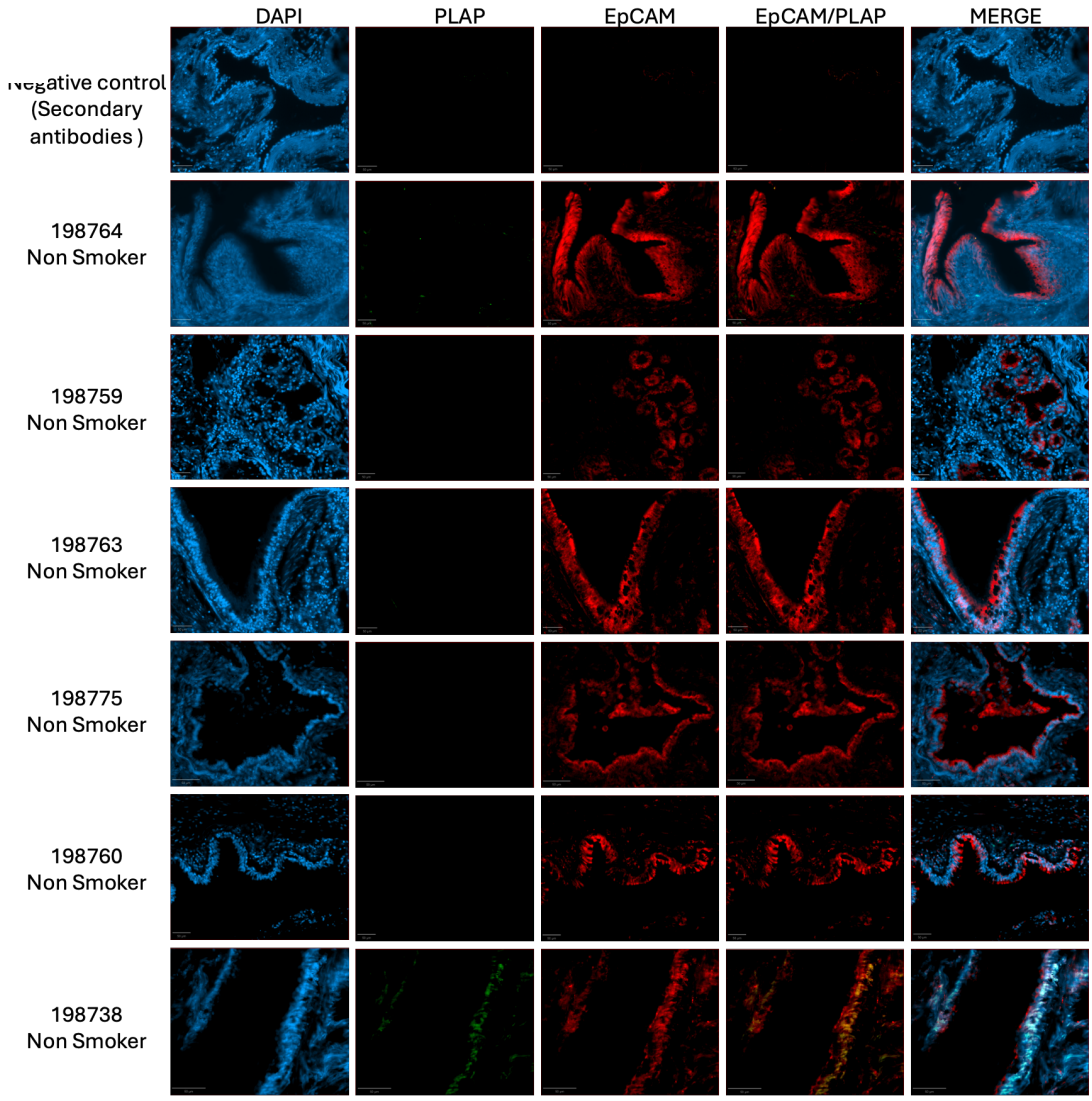
DAPI
PLAP
EpCAM
EpCAM/PLAP
MERGE
Negative control (Secondary antibodies)
198764 Non Smoker
198759 Non Smoker
198763 Non Smoker
198775 Non Smoker
198760 Non Smoker
198738 Non Smoker

C.

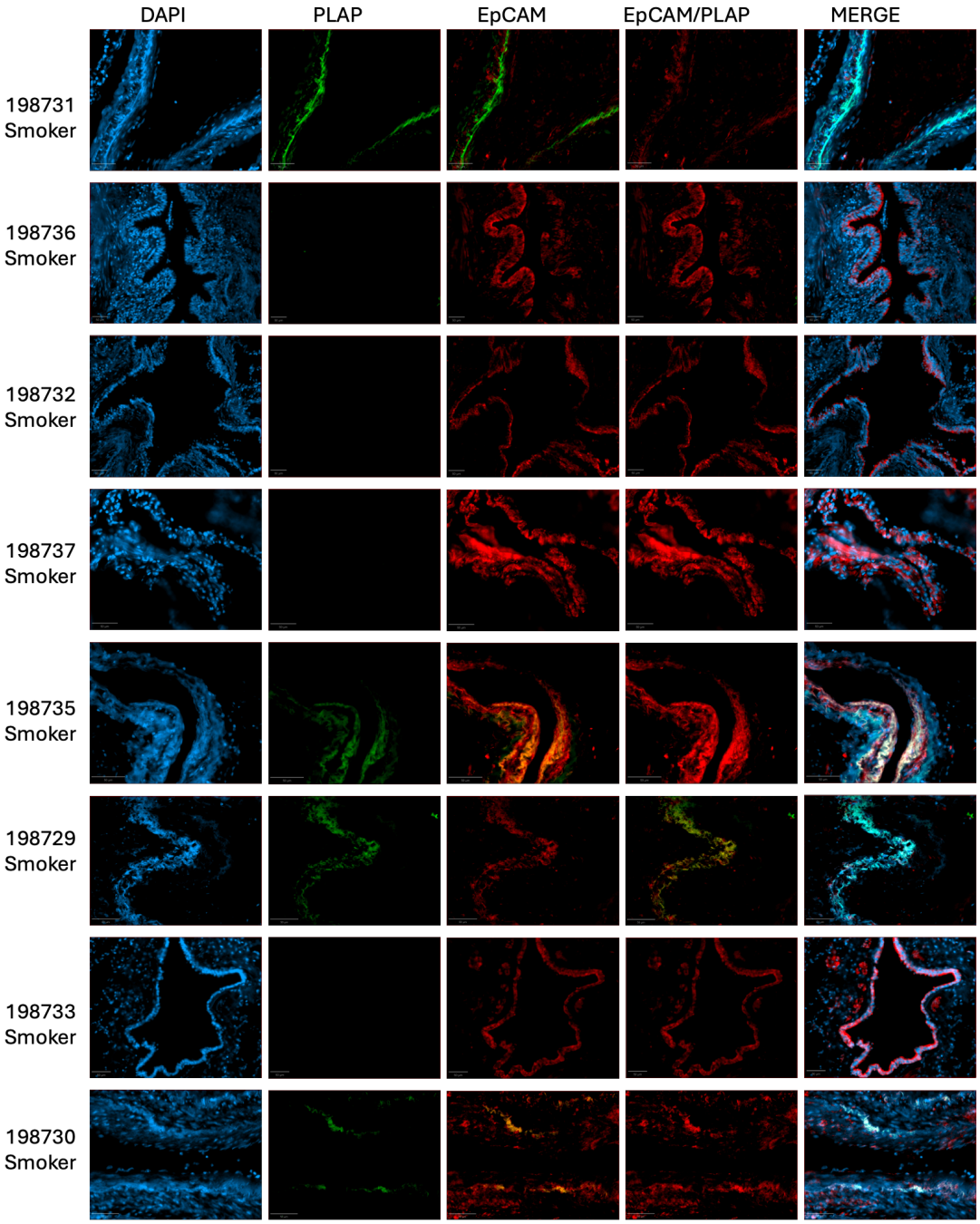

Figure 7.8 Immunofluorescence staining of PLAP/EPCAM on Human normal lung of smoker or nonsmoker samples.

A. positive control staining of RPLP3 using human placenta including secondary alone control. Staining of FFPE of non-smoker samples of PLAP/EpCAM. C. Staining of FFPE of smoker samples of PLAP/EpCAM.

7.3 Discussion:

It been studied that PLAP expressed in almost 20% of colorectal cancer. Our finding demonstrates the expression of PLAP on some of colorectal cancer samples. As well clearly showing heterogeneity of PLAP expression on patients' samples. The staining of FFPE slides from colorectal cancer patients matched what was seen in the cell lines. The efficient staining and the sensitivity of anti PLAP antibodies used, the data is showing clearly that this could be used for screening patients' biopsies to see whether they are eligible for anti PLAP BiMab treatment. Some of the samples expressed very low amount of PLAP but were detected. The heterogeneity of PALP expression on cancer patients can be challenges for the histological staining efficiency.

Cancer antigens for targeted immunotherapy such as bispecific antibody ideally to be highly expressed in cancer not on other normal tissues. From our findings earlier in chapter 3, our antibodies including RPLP3 are cross react with ALPPL2, meaning applying the therapy to male patients could do toxicity. From our staining on normal colon there were no cross reactivity with ALPI. Other normal tissues could be tested especially female tissues such as cervix. As been studied before PLAP was detected in serum of smoker and testicular patients. Our interest is in the presence of PLAP expression in normal lung. The presence of PLAP expression in normal lung seems clearly to be largely associated with smoking. The pattern of PLAP expression in the two non-smokers was much less, and less clear cut, than that in the smokers. To be super cautious against possible side effects of PLAP BiMab therapy for CRC patients one could exclude smoker patients.

However, it seems unlikely that such a low expression even in the lungs of smokers would be likely to give rise to serious side effects. In any case, a carefully managed Phase 1 escalation trial would soon pick up any side serious effects on the lungs of PLAP CD3 RPLP3 BiMab treated patients. Further studies would be needed on larger samples of normal lung tissue from smokers and non- smokers, ideally with data on how long it is since former smokers stopped smoking and relate this to the extent of PLAP expression in the lung alveolar cells. Molecular analysis of the expression profile of PLAP expressing cells in smokers would also be of interest.

Chapter 8: What controls the ectopic expression of PLAP?

8.1 Introduction

Successful bispecific antibody therapy depends highly on the target antigens and cancer antigens can be over expressed or mutated but cannot be expressed in high amount in normal tissues (Huehls et al., 2014b). Finding appropriate genes and studying their regulation in cancer is crucial for the successful outcome of bispecific antibody therapy (Sonar et al., 2024). Gene expression can be controlled genetically or epigenetically (Dhatchinamoorthy et al., 2021). Epigenetic regulation can affect the expression of a specific gene without altering its DNA sequence, for example by DNA methylation (Kulis & Esteller, 2010). DNA methylation is a process of adding methyl (-CH3) group to cytosine bases at CpG islands that can lead to suppression of gene expression (Sonar et al., 2024).

PLAP has valid properties of specificity as a cancer antigen, but nevertheless it is heterogeneous within tumours and between different tumours. There have also been some claims that PLAP may sometimes be expressed in lung tissue as discussed in the previous chapter. Understanding the reason for its mainly ectopic expression and finding out why it may sometimes be expressed in the lung, may help improve the use of PLAP for targeted bispecific antibody immunotherapy of a significant subset of many common cancers.

In this chapter, we studied the possibility of epigenetic control of PLAP in colorectal cancer cell lines. We also searched for genes whose expression is associated with PLAP expression in colorectal cancer cell lines.

8.2 Result:

8.2.1 5-azacytidine treatment effect on PLAP expression

Blocking DNA methylation by 5-azacytidine treatment is a common approach to seeing whether the stable control of altered expression of a gene might be due to stable methylation, as is the basis for important aspects of the control of differentiation, rather than mutation. To study if PLAP expression on colorectal cancer cell lines is controlled by methylation mechanism or if the methylation mechanism has control of the PLAP expression heterogeneity within cell lines, negative PLAP expressing CRC cell line CC20 was treated with 5-azacytidine treatment for 24 hours, 48 hours and 72 hours. PLAP expression was measured at each time point by the anti- PLAP antibody H17E2 using FACS analysis (see Figure 8.1). There is a small effect of on PLAP expression after 24 hours treatment relative to the control and this increases with time from 48 to 72 hours.

The effect of 5-Aza treatment on PLAP expression in CRC cell lines with different PLAP levels of expression was next studied (Figure 8.2)

In the low PLAP expressing CRC cell lines LS10, HT29 and CCO7, there is upregulation of PLAP expression from more or less zero to a clearly detectable level after treatment with 5- azacytidine.

To study the effect of methylation mechanism on PLAP expression within cell lines, the top 10% high and 10% low were sorted in the cell lines CACO2, CCO7 and DLD1 by the method described in Figure 6.3. Each subset of cells was treated with 5-azacytidine for 72 hours and then stained with anti-PLAP. The results are shown in Figure 8.3.

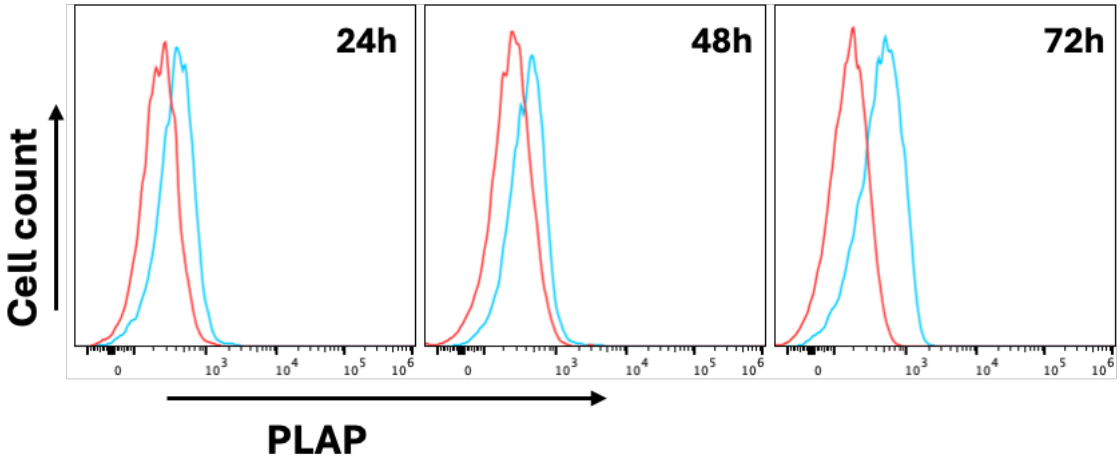

Figure 8.1:5-AZA treatment of CC20 for different times. FACS staining of PLAP of CC20 PLAP- negative cell line treated with 10uM of 5-Aza and an untreated control with anti-PLAP (H17E2). Red is control and blue is 5- Aza treated.

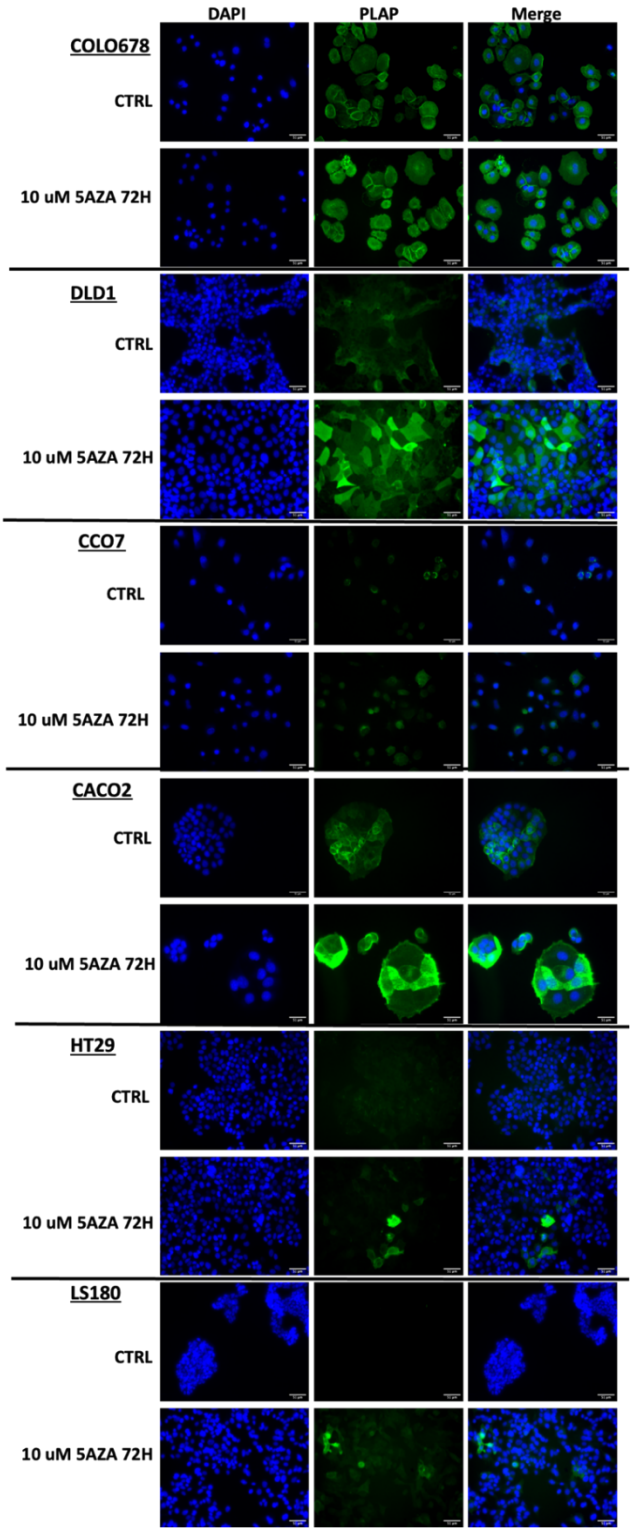

Figure 8.2: 5-azacytidine treatment of CRC cell lines. IF staining of PLAP on CRC cell lines after treatment with 10uM 5aza for 72 hours.

A DLD1

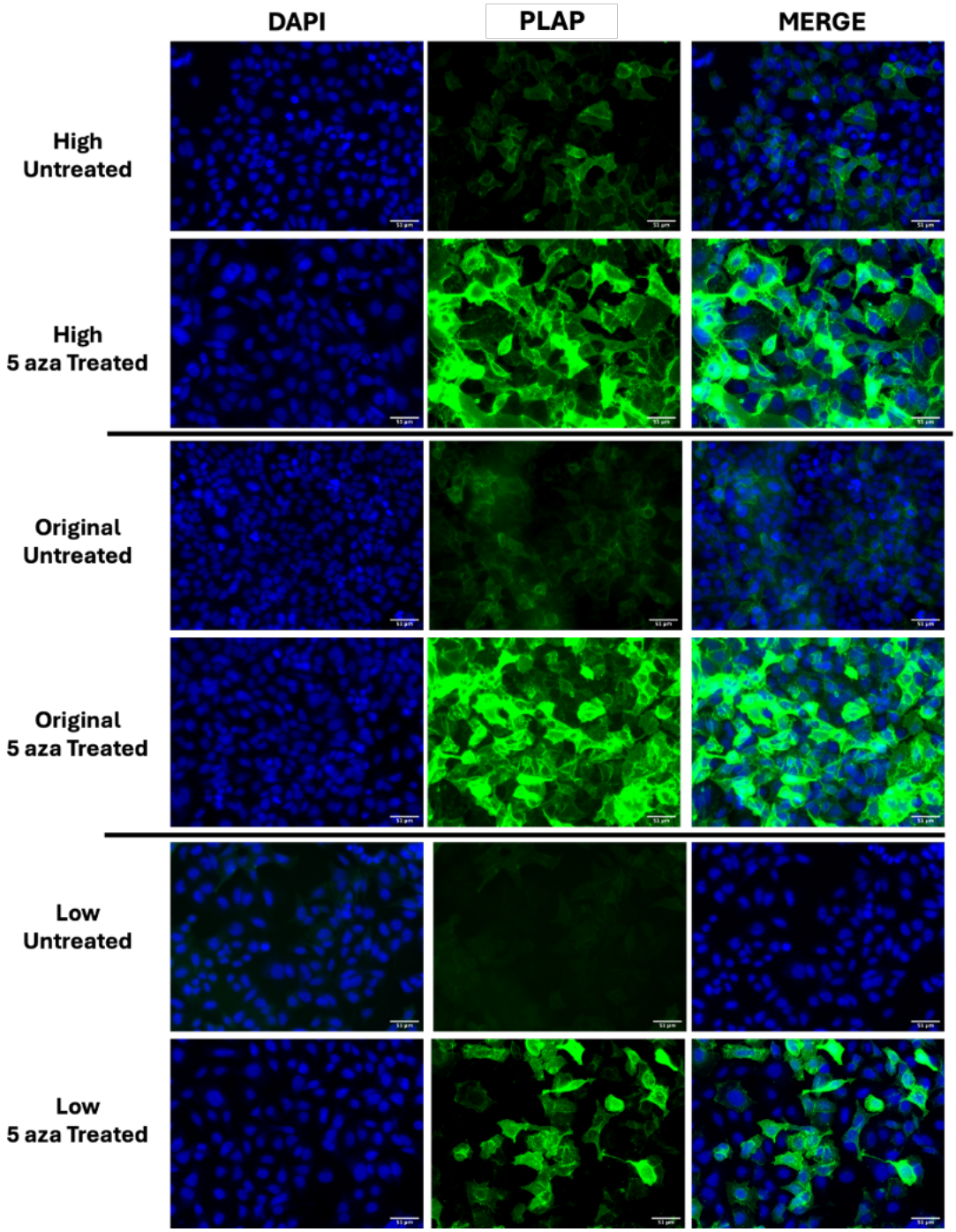
DAPI
PLAP
MERGE
High
Untreated
High
5 aza Treated
Original
Untreated
Original
5 aza Treated
Low
Untreated
Low
5 aza Treated

B CACO2

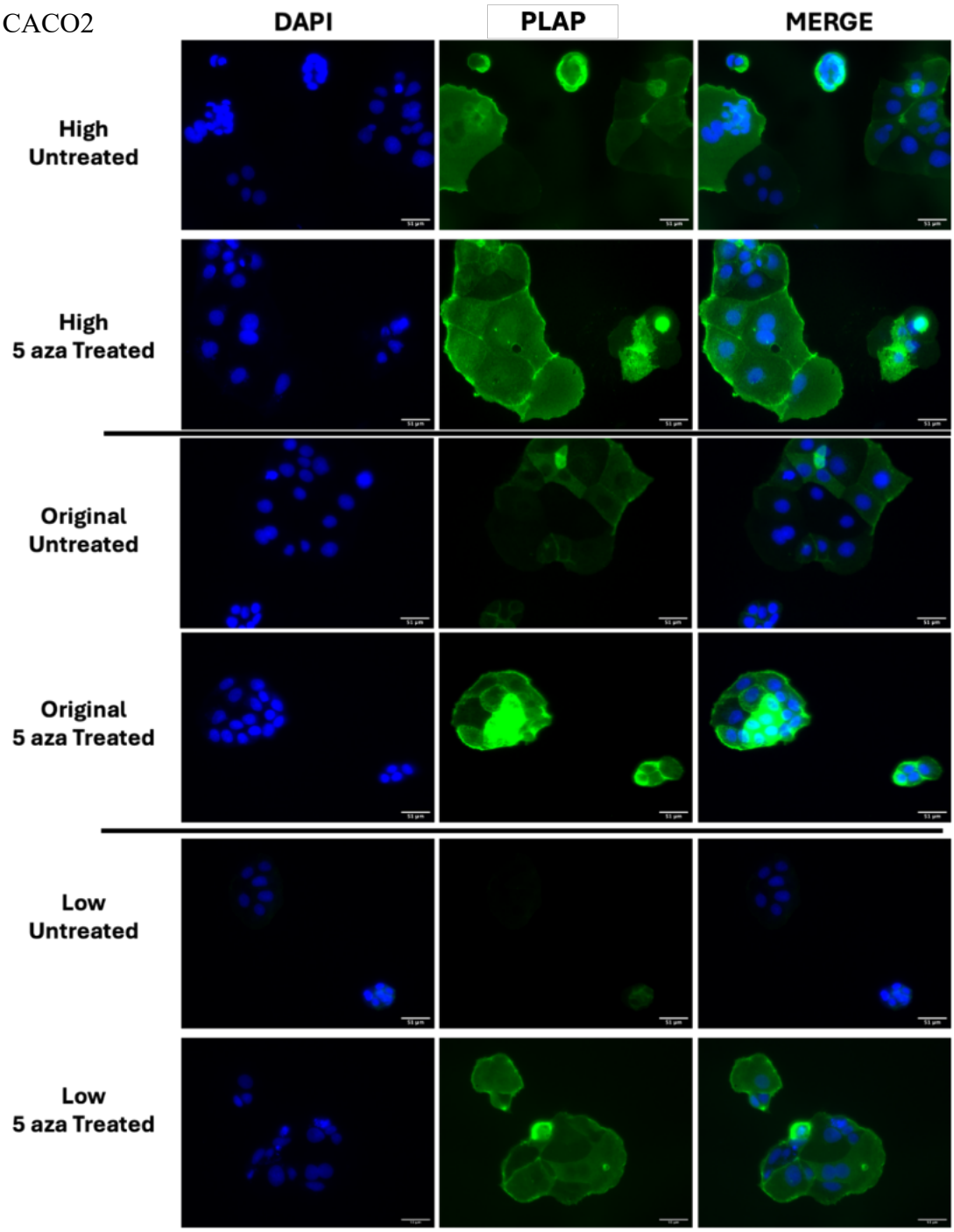
DAPI
PLAP
MERGE
High
Untreated
High
5 aza Treated
Original
Untreated
Original
5 aza Treated
Low
Untreated
Low
5 aza Treated

C. CCO7

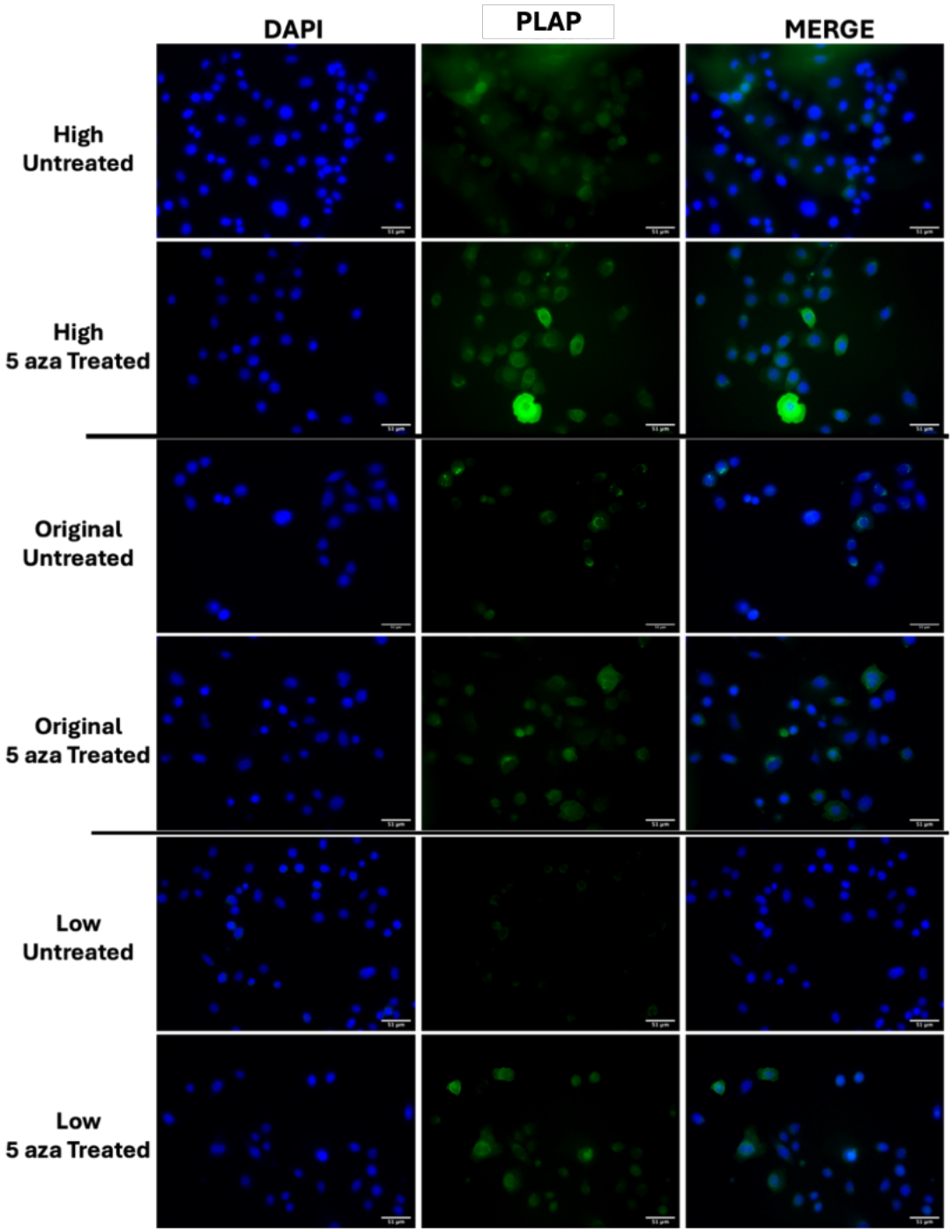

Figure 8.3: 5-azacytidine treatment to subsets of sorted cells from high, low, and original population of CRC cell lines.
IF staining of PLAP on high, low, and original population of DLD1 after treatment with 5-azacytidine for 72 hours. B. IF staining of PLAP on high, low, and original population of CACO2 after treatment with 5-azacytidine for 72 hours. C.IF staining of PLAP on high, low, and original population of CCO7 after treatment with 5-azacytidine for 72 hours. For DLD1 each subset shows a very striking high increase of PLAP expression. CC07 shows a clear increase at a lower level but less at other PLAP levels.

For DLD1 all three groups show clear increase in PLAP expression. For CACO2 the low and original are increased, but the high is not further increased. For CCO7 the high selected show the largest increase with much lesser increase for the original and low selected groups.

Thus, in all three cell lines there is a clear effect of 5Aza treatment leading to increased PLAP expression, though it seems that there are subsets of cells within cell lines for which 5Aza treatment has a greater effect. Overall, these 5Aza cell line treatment data strongly suggest that at least part of the drive of PLAP ectopic expression is due to changes in methylation of DNA sequences controlling PLAP expression rather than mutations in protein coding genes.

8.2.2 Identifying candidate genes closely related to PLAP expression in CRC cell lines.

To search for genes whose expressions are closely associated with PLAP expression in CRC cell lines a volcano plot was obtained comparing the overall differences in gene expression between PLAP positive and PLAP negative cell lines. A volcano plot of gene expression differences between high and low PLAP expressing cell lines is shown in Figure 8.4. The volcano plot is derived from the expression data of the two sets of lines given in table 8.1. Genes with expression differences of interest are encircled in the plot. These data were obtained by Dr Jeff Liu using the GMMchi algorithm.

The GMMchi analysis of the cell lines for selected genes of interest chosen from the volcano plot are shown in Figure 8.5: 8.5A for positively associated genes and 8.5B for those negatively associated. The position of high PLAP expressed cell lines, identified by GMMchi analysis for PLAP, is shown by hashed blue bars.

Table 8.1 CRC cell line lists of PLAP positiv and low/negative PLAP CRC cell lines used to generate the volcano plot.

PLAP positive CRC cell lines	PLAP negative CRC cell lines
DLD1	VACO429
ISCEROL	JHCOLOY1
CAR1	C10
PCJW	HCC2998
C32	HDC114
LOVO	CCO7
CACO2	HDC8
OXCO3	RW2982
OUMS23	HDC143
CL14	COLO320DM
COLO678	HDC9
LS123	VACO4A

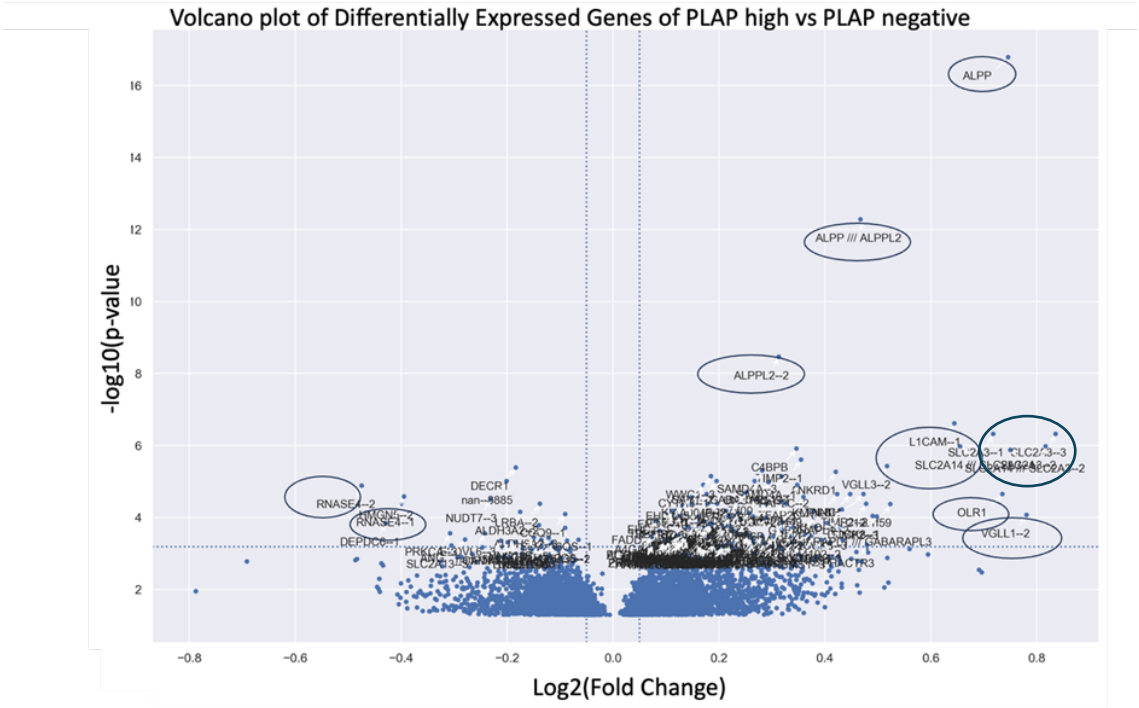

Figure 8.4: Volcano plot of genes associates with ALPP and ALPPL2 positive mRNA expression (right hand) versus negative expression (left hand). Genes with strongly associated expression difference are encircled.

Table 8.2 Genes are 1 are associated with *ALPP positively or negatively*. The genes positively associated are SLC2A3 and VGLL1 and genes negatively associated are RNASE4, LRRC31, METTL7A, AGR3 and OLFM4.

Genes	P-V
SLC2A3+	4.71E-07
VGLL1+	8.40E-05
RNASE4-	1.30E-05
LRRC31-	1.41E-03
METTL7A-	1.52E-03
AGR3-	1.66E-03
OLFM4-	1.10E-02

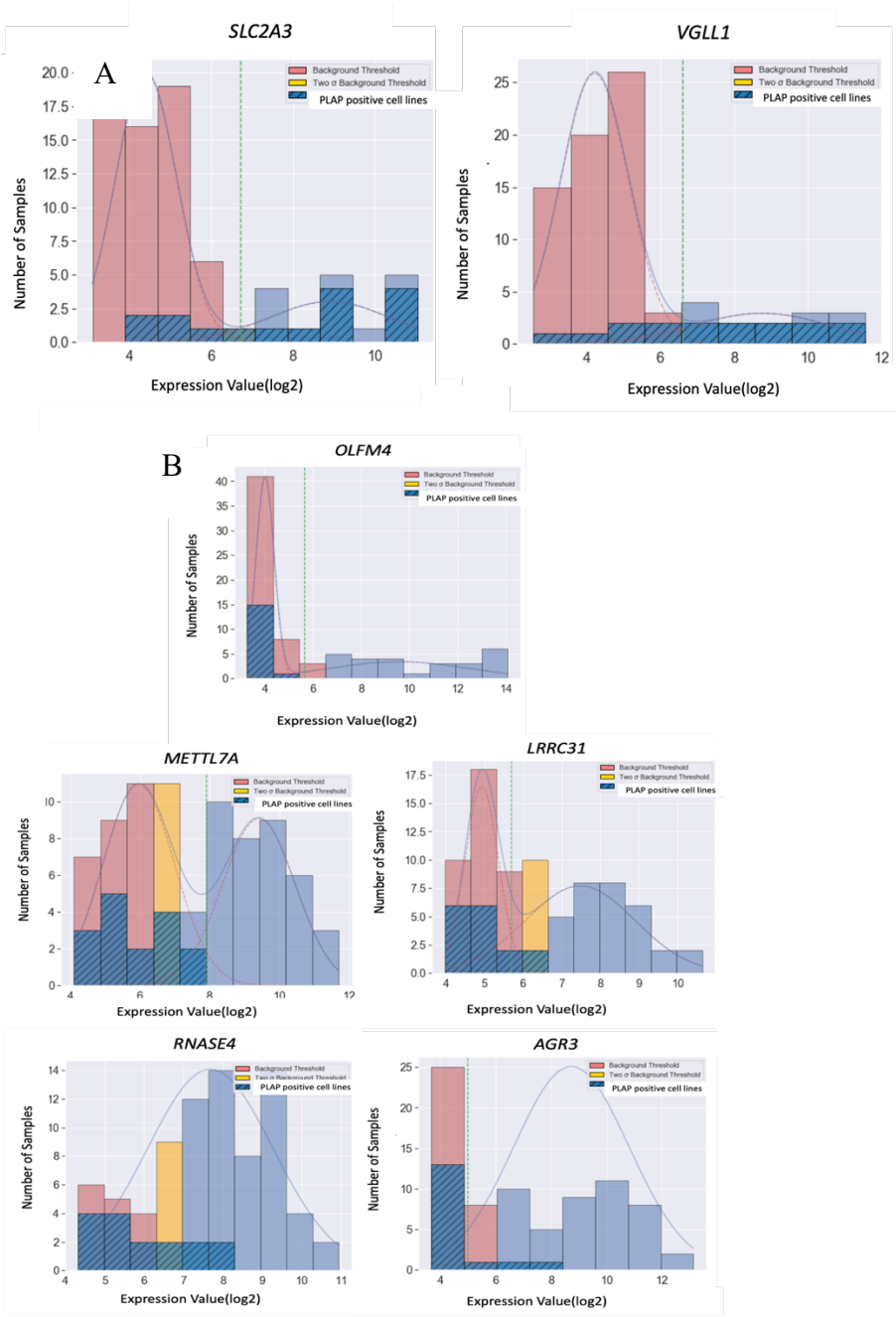

Figure 8.5: GMMchi of genes that are correlated with PLAP.
Blue bars are cell lines positive for the indicated gene expression and blue hashed are PLAP positive cell lines. Pink is negative and yellow bars are low PLAP expressed cell lines. GMMchi analysis was carried out as described before see Liu et al 2022. The vertical green dotted line indicates the threshold estimated by GMMchi for the distinction between high and low expression of the relevant gene. The 4 genes METTL7A, LRRC31, RNASE4 and AGR3 are predominantly expressed in low PLAP expressing cell lines while the cell lines expressing SLC2A3, SLC2A14 and VGLL1 are all skewed to high PLAP expression. Genes are associated with *ALPP positively or negatively*. The genes positively associated are SLC2A3 and VGLL1 and genes negatively associated are RNASE4, LRRC31, METTL7A, AGR3 and OLFM4.

8.2.3 The VGLL1 association with ALPP expression in CRC cell lines.

VGLL1 is highly positively associated with *ALPP* expression in the CRC cell lines. 60 of CRC cell lines are negative for both genes and 6 CRC cell lines are positive for both genes. 2 CRC cell lines are positive for *VGLL1* and negative for *ALPP*, and 10 CRC cell lines are positive for *ALPP* and negative for *VGLL1,* see table 8.3. For the ALPPL2 association with VGLL1 on CRC cell lines 65 of CRC cell lines are negative for both genes and 5 CRC cell lines are positive for both genes. 6 CRC cell lines are positive for VGLL1 and negative for ALPPL2, and 2 CRC cell lines are positive for ALPPL2 and negative for VGLL1: see table 8.3.and 2 CRC cell lines are positive for *ALPPL2* and negative for *VGLL1*: see table 8.3.

We compared our findings of 2X2 tables of gene association in our cell lines to colorectal cancer patient data obtained from The Cancer Genome Atlas (TCGA). For *ALPPL2* association with *VGLL1* on CRC patients, 590 of CRC patients are negative for both genes and 11 CRC patients are positive for both genes. 11 CRC patients are positive for VGLL1 and negative for ALPPL2, and 86 CRC patients are positive for *ALPPL2* and negative for *VGLL1* - see table 8.4.

For ALPP association with VGLL1 on CRC patients, 652 of CRC patients are negative for both genes and 6 CRC patients are positive for both genes. 16 CRC patients are positive for VGLL1 and negative for ALPP, and 24 CRC patients are positive for ALPP and negative for VGLL1 -see table 8.4.

Having shown upregulation of PLAP by 5-Aza it seemed worth testing to see what the effect of 5-Aza treatment was on VGLL1 expression. VGLL1 negative CRC cell lines were treated with 10uM 5-azacytidine for 72 hours then stained with anti-VGLL1 and the VGLL1 expression tested by FACS (Figure 8.6). There is very slight upregulation of VGLL1 on COLO678 and CC20, and somewhat more on DLD1 and HT29, which have lower normal levels of PLAP expression than COLO678.

To study the direct effect of VGLL1 on PLAP expression on CRC cell lines, Si VGLL1 was used to knock down VGLL1 expression on COLO678 but with no obvious effect (Figure 8.7).

Table 8.3 2x2 table associations of VGLL1 to ALPP, ALPPL2 on CRC cell lines

Gene 1	Gene 2	-/-	-/+	+/-	+/+	p-value
ALPP	VGLL1	60	2	10	6	0.0001
ALPPL2	VGLL1	65	6	2	5	0.0004

Table 8.4 2X2 1 table association of VGLL1 to ALPP, and ALPPL2 on Colorectal cancer patients' data obtained from TCGA data.

gene1	**gene2**	**-/-**	**-/+**	**+/-**	**+/+**	**P-value**
ALPP	VGLL1	652	16	24	6	0.0001735 2
ALPPL2	VGLL1	590	11	86	11	4.13E-05

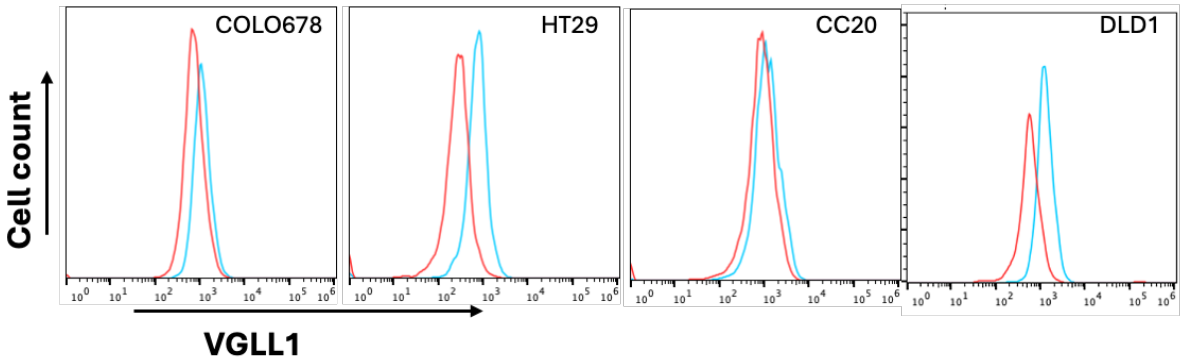

Figure 8.6 5-Aza treatment of CRC cell lines for 72hours. FACS staining of VGLL1 in CRC cell lines treated with 10uM of 5-Aza (blue) compared with untreated control (red).

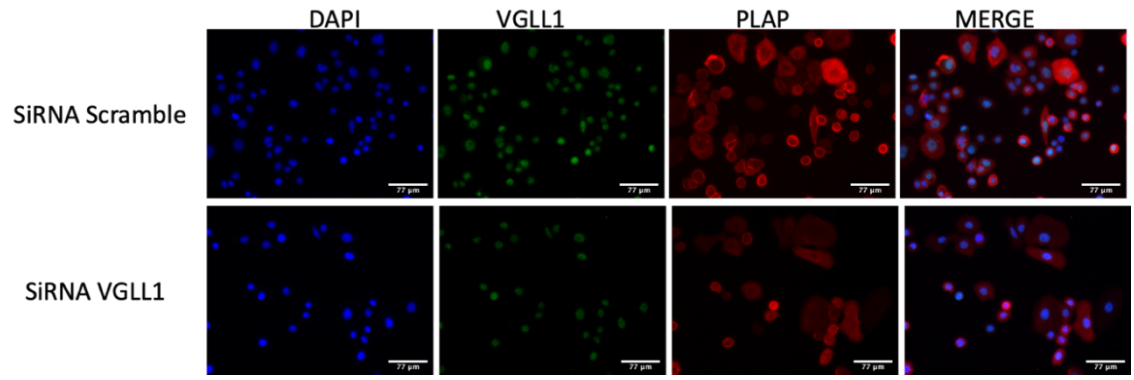

Figure 8.7 VGLL1 siRNA knock down on PLAP 1positive COLO678. IF staining of PLAP and VGLL1 with siScramble as control.

8.2.4 The SLC2A3 association with ALPP expression in CRC cell lines.

SLC2A14 is very similar to *SLC2A3* in terms of sequence and the two genes are not distinguished by the microarray mRNA detection system used on our cell lines**.** 52 CRC cell lines are negative for both genes and 12 CRC cell lines are positive for both genes. 10 CRC cell lines are positive for *SLC2A3* and negative for *ALPP*, and 4 CRC cell lines are positive for *ALPP* and negative for *SLC2A3* see table 8.5.

For ALPPL2 association with SLC2A3 on CRC cell lines 61 of CRC cell lines are negative for both genes and 6 CRC cell lines are positive for both genes.10 CRC cell lines are positive for SLC2A3 and negative for ALPPL2, and 1 CRC cell line is positive for ALPPL2 and negative for SLC2A3 see table 8.5. Both these associations are highly significant.

Table 8.5 1 *SLC2A3* association with *ALPP* and *ALPPL2* expression in CRC cell lines

Gene 1	**Gene 2**	**-/-**	**-/+**	**+/-**	**+/+**	**p-value**
ALPP	*SLC2A3*	52	10	4	12	2.34E-05
ALPPL2	*SLC2A3*	61	10	1	6	0.0002

8.3 Discussions

The cancer antigen alterations of in a cancer can be a challenge for cancer targeted immune therapy. Studying the expression pattern of cancer antigens can help the understanding of immune therapy responses to cancer. It helps predicting the outcome of therapy as well helping personalized treatment. As discussed, earlier cancer antigen expression can be heterogeneous and therefore understanding the control of heterogeneous expression can help for managing and improving the therapy and overcoming treatment resistance.

It is not clear what controls ectopic PLAP expression in the CRC lines and in other cancers. The effects of 5-Aza treatment on PLAP expression in many of the cell lines clearly suggests a role for methylation control of expression in some form. The results show the effect on the sorted population suggesting the role of methylation on the heterogeneity of PLAP within cell lines. Gene methylation can be dynamic and can be affected by many factors. Further work is needed to study the methylation effect on upregulation of PLAP expression. Methylation can be directly or indirectly affected if only assessed by 5-Aza treatment.

The 2X2 table study showing the highly associated genes can help predicting which genes may be involved in the control of PLAP expression in the cell lines. The finding of the mainly testis expressed transcription factor VGLL1 showing an association with PLAP expression is intriguing and may be a contributing factor to the PLAP ectopic expression, but that possibility needs further investigation. *VGLL1* is a transcription factor that seems to control aspects of placental gene expression and so when switch on might contribute to PLAP expression (Sonnemann et al., 2023). Such control of tissue specific gene expression is mostly by stable methylation.

Also of interest is the strong association between the SLC2A3,14 expression and ectopic PLAP expression. Both SLC2A3 and SLCA14 are very similar and their sequences similarity is 95%, and so their difference is hard to pick up by our microarray probe-based assay (Mueckler & Thorens, 2013). As solute carriers for glucose and other sugars the expression of SLC2A3/14 could be a driver of cancer growth selected for as a byproduct of switching on ectopic placental and testis expression patterns in cancers (Gao et al., 2021). The variation in colony forming ability relating to some extent to PLAP expression levels could be a function of variation in differentiation patterns in different cancers, the less the differentiation, the greater the proportion of stem cells and so the greater the rate of cell division.

9. General discussion

9.1 Discussion

9.1.1 Placental alkaline phosphatase (PLAP) expression on colorectal cancer and other normal tissues.

This thesis work illustrates the promising results of in vitro studies of using RPLP3 or EpCAM CD3 BiMab on colorectal cancer cell lines suggesting its effectiveness as an immunotherapy for colorectal cancer. PLAP is ectopically expressed in almost 20% of our panel of colorectal cancer cell lines and this agrees with what been found in studies of PLAP expression in around of colorectal cancers (X. Li et al., 2020c). PLAP is not expressed in most normal tissues other than placenta, and through on spermatocytes, and so is a good target for bispecific monoclonal antibody immunotherapy to treat colon cancer (X. Li et al., 2020a). Our data showed the expression of PLAP on some alveolar cells on lung tissue samples. Further studies suggested the expression of PLAP was mainly, if not only, on lung from smokers. This is consistent with the idea that expression of PLAP in the lung could be induced because of smoking and so explain the presence of PLAP in the blood of smokers(Williams et al., 1986). Additional studies should focus on PLAP expression in alveolar lung tissues and its associated expression in blood using a larger number of donors than studied in this thesis.

The expression of PLAP on lung could lead to toxicity which might limit the clinical application of RPLP3, but this as at a very low level. One solution that could be used for antigens with expression on normal tissue is to use a new technology for delivering bispecific antibody to the tumour site avoiding its presence in blood circulation, namely injecting the tumour with Lipid nano particles (LNP) delivering mRNAs coding for bispecific monoclonal antibodies (Wang et al., 2021).

RPLP3 might induce toxicity to male patients as it recognizes ALPPL2 which expressed on the testis, but this could mostly be acceptable for an effective anti -cancer therapy. Cross reactivity of the antibody with the testis ALPPL2 has the advantage of covering a wider range of ectopic expression on cancers (X. Li et al., 2020a)(Su et al., 2020e).

IgG designed bispecific antibodies have been used and approved by FDA especially for the treatment of blood cancers (Suurs et al., 2019b). However, effective development for treating solid tumors will depend on the selection of appropriate cancer antigen targets for immune therapy that are not highly expressed on normal tissues (Gu et al., 2024). Sometimes detecting low expression of a promising target cancer antigen on either the cancers or normal tissues could be a problem. Also, it is difficult to positively diagnose cancer patients if their tumor has low PLAP expression. The major problem is if the expression is heterogeneous in the cancer, and perhaps even not expressed on the cancer stem cells. Any proposed cancer target antigen will need to be extensively tested on all normal tissue types. The level of bispecific monoclonal antibody sensitivity needed to induce killing in relation to the level of antigen expression will also need to be established. Studying the threshold of bispecific monoclonal antibody therapy sensitivity and specificity to its antigens should enable prediction of efficiency of the therapy

A suggested method for diagnosing PLAP cancer patients who can receive the therapy could be by detecting the presence of PLAP in serum of cancer patients as a biomarker, as well labeling PLAP with radiolabel particles indium-111 for cancer imaging (Epenetos et al., 1985) (X. Li et al., 2020a).

9.1.2 Overcome Cancer antigen heterogeneity

Cancer antigen heterogeneity of expression can cause difficulties for diagnosis or treatment of cancer. It can cause treatment resistance or preventing the therapy from reaching to cancer.

Variation of cancer cell expression within a tumour result in non-uniform treatment of the whole tumour by BiMAB targeted therapy. The development of cancer treatment resistance is a dynamic response can result from selection of genetic or epigenetic changes. Within cell line variation in PLAP expression was subcategorize according the PLAP expression level. These categories tended to return to their original expression levels after period of time in culture. There was no distinct genetic variation but there is some evidence that methylation-based control of PLAP expression within cell lines may be a cause of heterogeneity of expression, since demethylation treatment of some PLAP negative cell lines by 5aza increases expression of PLAP mRNA. Stable DNA methylation could be a mechanism for cancer immune resistance. Further exploration of these mechanisms should give answers as to how the genes giving rise to resistance to treatment are switched on and off.

Further studies are also needed to understand the control of PLAP expression, for example, by methylation DNA sequencing of the ALPP promoter region in PLAP negative cell lines to explore if the PLAP expression is controlled by methylation of the ALPP promoter region DNA sequence. Single cell mRNA analysis may also help to find whether changes in the expression of other genes are involved in the control of PLAP expression. These studies may open up the possibility of short-term treatments of patients to increase the levels of PLAP before antibody treatment.

9.1.3 Implication of BiMabs therapy

The data presented in this thesis shows promising result of using BiMAb-mediated immune killing of PLAP expressing CRC lines by PLAP x CD3 BiMAb (RPLP3) as well as EpCAM CD3 BiMAb. The barriers to biMAbs therapy are due to the heterogeneity of cancers as well as the immune suppressive microenvironment, which can reduce the level of immune attack on the cancer. For effective cancer treatment it is important to kill all the cancer cells within the tumour whether they are positive or negative. Killing the stromal cells might also help. The results of this thesis show clear and convincing evidence of killing of bystander PLAP/EpCAM negative cells in co-cultures of PLAP/EpCAM positive and negative cell lines. Bystander killing was clearly seen in the killing of the mixture of 5% positive cells with 95% negative cells. Bystander killing of PLAP/EpCAM negative cells was induced by T cells activated by prior incubation of PBMCs and BiMAbs for treatment of PLAP/EpCAM positive cell lines. It was shown that the activated T cells produced cytokines which induce the expression of ICAM and FAS on PLAP negative cells, making them sensitive to activated T cell killing. There was no killing induced by the secreted cytokines by the

activated T cells. The three major subsets of T cells (CD4, CD8, gamma delta T cells), when purified, were equally effective in direct and bystander killing.
However more work with advanced methodologies, for example by studying the activation of each T cell subtype or exploring differences in their roles for inducing bystander killing.

There are various laboratory methodologies for detection or measuring the killing induced by BiMAbs. Here we used ELISA M30, Immunofluorescence staining and xCELLigence real time assay technology. Each provided evidence of bystander killing yet cannot easily provide quantitative measurements of levels of bystander killing. We developed a method to quantify bystander killing by flow cytometry staining. We distinguished different cell types by making stable transfected cells with difference colours (GFP-DLD1, mCherry CC20), while PBMC were stained with CD45 and then killing was measured by levels of cleaved caspase 3.
We also did preliminary cloning studies showing at most 1% colony formation after applying RPLP3 or EpCAM on PLAP or EpCAM positive cells compared to almost 50% colony formation of PLAP or EpCAM negative CRC cell lines. That suggested more or less complete killing by using RPLP3 or EpCAM CD3 BiMAb.
Following up these results will need to include studying the effects of stromal, cells such as myofibroblasts, on bystander killing. The experiments described for understanding EpCAM CD3 BiMAb or RPLP3 -mediated cancer cell killing will all be relevant to the preclinical development of T cell engaging bispecific antibodies to new targets. Although bystander killing is a positive aspect for solid tumor treatment by BiMAB, it might induce immune medicate toxicity so understanding the mechanism behind bystander killing for clinical application is important.

9.1.4 Future of Bispecific monoclonal antibody therapy

Combination therapies are a way to maximize the effect of BiMAb therapy. There is increasing evidence in animal models for increased killing when check point inhibitors, such as anti PDL-1 antibodies, are combined with the T cell engaging bispecific antibodies (Cui et al., 2021). The reason for this is presumed to be the induction of PD-1 and PDL-1 expression in both the effector T cells and the target cancer cells (Ray et al., 2015). Further study of the mRNA profiles of INFy treated cell lines and the relationship of this to induced levels of PD-1, PDL-1 and other relevant receptors will help to develop reliable in vitro cell culture models for studying such combination therapies. The role of expression of check point receptors, such as PDL-1, in myofibroblasts which are major cells in the tumour microenvironment, will be explored by, for example, exploring the effect on cell killing of simply adding the myofibroblasts to the antibody/cancer cell/effector cell mixture (Z. Zhao et al., 2023).

T cell receptor mimic antibody therapy (TCRm mAb) is designed to mimic the recognition by T cell receptors of peptides attached to -HLA on target cells (D. Li et al., 2017a). The proposed development and characterization of TCRm to the HLA-A2b2m/MAGE3A peptide will provide experience for the general potential for developing TCRm-based BiMAbs for the treatment of CRC and other cancers.

The candidate cancer specific testis antigen, MAGEA3, will be further investigated in our cell lines as the basis for our TCRm project. Cancer testis antigens, such as MAGE3A are expressed in some CRCs and so in some of our CRC lines (see Figure 9.1). They are a potentially important source of new targets for bispecific monoclonal antibody

immunotherapy development (Zajac et al., 2017). Through collaboration with the McMichael laboratory, we now have access to an HLA-A2/b2m/MAGE3A peptide construct which can be used to produce a TCRm specific for MAGE3A peptides attached to HLA-A2.

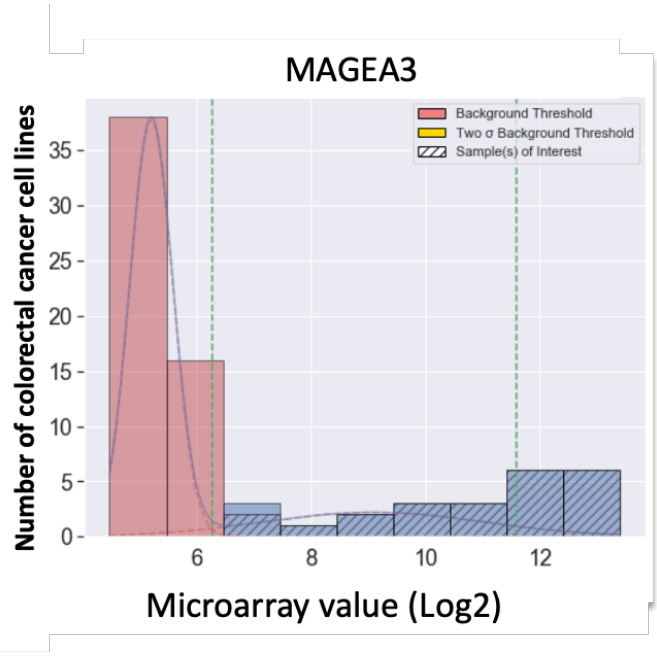

Figure 9 1: GMMchi of MAGEA3. Blue hashed bars are MAGEA3 positive cell lines.
Pink are MAGEA3 negative. GMMchi analysis was carried out as described before, see (T. C. Liu et al., 2022). The vertical green dotted line indicates the threshold estimated by GMMchi for the distinction between high and low expression of the relevant gene. The second green line indicates a third subset of more highly MAGEA3 expressing cell lines.

9.1.5 Concluding remarks:

In summary, the in vitro studies presented in this thesis show promise for BiMAb-mediated immune killing of PLAP and EpCAM expressing CRC lines by RPLP3 or EpCAM CD3 BiMAbs. Here we show strong evidence of bystander killing of PLAP/EpCAM negative cells in co-cultures of PLAP/EpCAM positive and negative cell lines. The bystander killing increases with the increasing the proportion of positive cells to negative cells. The bystander killing of PLAP negative cells was induced by T cells activated by prior incubation of PBMCs and RPLP3/ EpCAM CD3 BiMAbs for treatment of PLAP positive cell lines. It was shown that the activated T cells produced cytokines which induce the expression of ICAM and FAS on PLAP negative cells, making them sensitive to activated T cell killing. There are other factors behind bystander killing that need to be explored to optimize the therapeutic effect of BiMAb treatment.

Appendix

Supplementary S1 ALPP and ALPPL2 mRNA expression values for a panel of 114 colorectal cancer cell lines ordering the cell lines according to the mRNA expression of ALPP from low to high.

CRC cell lines	alkaline phosphatase, placental (*ALPP*)	alkaline phosphatase, placental-like 2 (*ALPPL2*)
LIM1863	12	50
JHCOLOY1	23	55
VACO429	23	43
C10	25	55
RW2982	26	58
HCC2998	28	71
HDC114	28	56
HDC54	30	90
HDC143	32	86
HDC9	33	61
KM20L2	33	81
HDC8	33	57
LIM2405	34	70
CCO7	34	79
HT29	35	82
RW7213	36	74
CX1	37	81
GP2D	37	45
VACO4S	38	94
CW2	38	68
HCT116	38	74
CL40	40	127
LS174T	41	70

Colo320	41	101
HDC73	41	60
HDC57	42	82
SW1463	42	68
Colo201	42	77
C106	42	63
T84	44	83
SNU479	44	69
SNUC1	46	103
VACO400	46	82
HDC111	46	73
SNU1746	46	135
HCA46	46	112
SW403	47	84
SNU1684	47	74
HDC142	48	95
C75	48	38
GP5D	49	63
SNU1235	50	95
HCT15	50	74
SW48	50	88
CC20	50	77
Vaco5	51	58
LS180	51	85
OXCO1	51	89
HRA19	52	94
NCIH548	52	91
CCK81	53	132

SW948	53	84
LIM1215	54	97
COLO205	54	96
C2284	55	79
RKO	57	96
C99	57	93
SNU70	57	73
OXCO2	57	118
NCIH747	57	78
SNU1406	60	94
NCIH498	60	76
NCIH716	60	81
C80	61	89
LS411	61	99
HCC56	61	70
SNU1411	63	95
SKCO1	63	85
WIDR	63	81
Colo206	63	69
LIM1863	64	90
NCIH508	64	102
HT55	64	79
SW1222	64	85
C84	64	83
OXCO4	65	80
C4054	65	98
SNU254	69	91
SW620	69	65

LS1034	71	79
C3953	74	80
Gp2D	75	99
LS513	76	74
C70	77	87
SW1222	80	81
HDC135	85	79
CL11	86	115
C125PM	88	83
SNUC2B	90	104
SW480	92	85
SW837	96	125
C105251	109	142
HCT8	124	157
RCM1	128	99
c2bbe1	144	147
SW1417	146	111
SNU1544	161	219
HCA7	170	125
HDC82	188	111
SW1116	196	97
SNU1181	214	124
SNU977	253	196
DLD1	260	143
TTITKB	262	167
ISCEROL	271	145
JHSKREC	332	223
CaR1	402	119

C32	482	158
PCJW	484	170
CACO2	657	412
Lovo	693	831
OXCO3	749	439
OUMS23	2040	757
CL14	2664	266
COLO678	2998	601
LS123	3100	1163

References:

Abbas, A. K., Murphy, K. M., & Sher, A. (1996). Functional diversity of helper T lymphocytes. *Nature 1996 383:6603*, *383*(6603), 787–793. https://doi.org/10.1038/383787a0

Aiman Mohtar, M., Syafruddin, S. E., Nasir, S. N., & Yew, L. T. (2020). Revisiting the Roles of Pro-Metastatic EpCAM in Cancer. *Biomolecules*, *10*(2), 255. https://doi.org/10.3390/BIOM10020255

Anatomical Pathology Equipment & Workflow Solutions: Leica Biosystems. (n.d.). Retrieved March 28, 2025, from https://www.leicabiosystems.com/

André, T., Boni, C., Mounedji-Boudiaf, L., Navarro, M., Tabernero, J., Hickish, T., Topham, C., Zaninelli, M., Clingan, P., Bridgewater, J., Tabah-Fisch, I., & de Gramont, A. (2004). Oxaliplatin, Fluorouracil, and Leucovorin as Adjuvant Treatment for Colon Cancer. *New England Journal of Medicine*, *350*(23), 2343–2351. https://doi.org/10.1056/NEJMOA032709/ASSET/6C1F77C2-DE3C-4FBC-BAC6-09898169CEC1/ASSETS/IMAGES/LARGE/NEJMOA032709_F3.JPG

Aperio pathology slide scanners - Leica Biosystems. (n.d.). Retrieved June 13, 2024, from https://www2.leicabiosystems.com/PPC-PI-UK-EN-Aperio-Scanners-GT450-DX-MAY-2022?utm_source=google&utm_term=slide%20scanner&matchtype=p&utm_medium=PPC&utm_campaign=PPC-PI-UK-EN-Aperio_Scanners&utm_content=&accountregion=UK&gad_source=1&gclid=EAIaIQobChMI09egq9vYhgMV6pBQBh0emw02EAAYASAAEgKHwPD_BwE

Araghi, M., Soerjomataram, I., Jenkins, M., Brierley, J., Morris, E., Bray, F., & Arnold, M. (2019a). Global trends in colorectal cancer mortality: projections to the year 2035. *International Journal of Cancer*, *144*(12), 2992–3000. https://doi.org/10.1002/IJC.32055

Araghi, M., Soerjomataram, I., Jenkins, M., Brierley, J., Morris, E., Bray, F., & Arnold, M. (2019b). Global trends in colorectal cancer mortality: projections to the year 2035. *International Journal of Cancer*, *144*(12), 2992–3000. https://doi.org/10.1002/IJC.32055

Armaghany, T., Wilson, J. D., Chu, Q., & Mills, G. (2012). Genetic Alterations in Colorectal Cancer. *Gastrointestinal Cancer Research : GCR*, *5*(1), 19. /pmc/articles/PMC3348713/

Ashby, K. M., & Hogquist, K. A. (2023). A guide to thymic selection of T cells. *Nature Reviews Immunology 2023 24:2*, *24*(2), 103–117. https://doi.org/10.1038/s41577-023-00911-8

Azzouz, L. L., & Sharma, S. (2023). Physiology, Large Intestine. *StatPearls*. https://www.ncbi.nlm.nih.gov/books/NBK507857/

Bacac, M., Fauti, T., Sam, J., Colombetti, S., Weinzierl, T., Ouaret, D., Bodmer, W., Lehmann, S., Hofer, T., Hosse, R. J., Moessner, E., Ast, O., Bruenker, P., Grau-Richards, S., Schaller, T., Seidl, A., Gerdes, C., Perro, M., Nicolini, V., … Umaña, P. (2016a). A Novel Carcinoembryonic Antigen T-Cell Bispecific Antibody (CEA TCB) for the Treatment of Solid Tumors. *Clinical Cancer Research : An Official Journal of the American Association for Cancer Research*, *22*(13), 3286–3297. https://doi.org/10.1158/1078-0432.CCR-15-1696

Bacac, M., Fauti, T., Sam, J., Colombetti, S., Weinzierl, T., Ouaret, D., Bodmer, W., Lehmann, S., Hofer, T., Hosse, R. J., Moessner, E., Ast, O., Bruenker, P., Grau-Richards, S., Schaller, T., Seidl, A., Gerdes, C., Perro, M., Nicolini, V., … Umaña, P. (2016b). A novel carcinoembryonic antigen T-cell bispecific antibody (CEA TCB) for the treatment of solid tumors. *Clinical Cancer Research*, *22*(13), 3286–3297. https://doi.org/10.1158/1078-0432.CCR-15-1696/268428/AM/A-NOVEL-CARCINOEMBRYONIC-ANTIGEN-T-CELL-BISPECIFIC

Bacac, M., Fauti, T., Sam, J., Colombetti, S., Weinzierl, T., Ouaret, D., Bodmer, W., Lehmann, S., Hofer, T., Hosse, R. J., Moessner, E., Ast, O., Bruenker, P., Grau-Richards, S., Schaller, T., Seidl, A., Gerdes, C., Perro, M., Nicolini, V., … Umaña, P. (2016c). A Novel Carcinoembryonic Antigen T-Cell Bispecific Antibody (CEA TCB) for the Treatment of Solid Tumors. *Clinical Cancer Research : An Official Journal of the American Association for Cancer Research*, *22*(13), 3286–3297. https://doi.org/10.1158/1078-0432.CCR-15-1696

Bankhead, P., Loughrey, M. B., Fernández, J. A., Dombrowski, Y., McArt, D. G., Dunne, P. D., McQuaid, S., Gray, R. T., Murray, L. J., Coleman, H. G., James, J. A., Salto-Tellez, M., & Hamilton, P. W. (2017). QuPath: Open source software for digital pathology image analysis. *Scientific Reports 2017 7:1*, *7*(1), 1–7. https://doi.org/10.1038/s41598-017-17204-5

Bassi, G., Favalli, N., Pellegrino, C., Onda, Y., Scheuermann, J., Cazzamalli, S., Manz, M. G., & Neri, D. (2021). Specific Inhibitor of Placental Alkaline Phosphatase Isolated from a DNA-Encoded Chemical Library Targets Tumor of the Female Reproductive Tract. *Journal of Medicinal Chemistry*, *64*(21), 15799–15809. https://doi.org/10.1021/ACS.JMEDCHEM.1C01103/SUPPL_FILE/JM1C01103_SI_002.CSV

Bateman, A., Martin, M. J., Orchard, S., Magrane, M., Ahmad, S., Alpi, E., Bowler-Barnett, E. H., Britto, R., Bye-A-Jee, H., Cukura, A., Denny, P., Dogan, T., Ebenezer, T. G., Fan, J., Garmiri, P., da Costa Gonzales, L. J., Hatton-Ellis, E., Hussein, A., Ignatchenko, A., … Zhang, J. (2023). UniProt: the Universal Protein Knowledgebase in 2023. *Nucleic Acids Research*, *51*(D1), D523–D531. https://doi.org/10.1093/NAR/GKAC1052

Benson, A. B., Venook, A. P., Al-Hawary, M. M., Azad, N., Chen, Y. J., Ciombor, K. K., Cohen, S., Cooper, H. S., Deming, D., Garrido-Laguna, I., Grem, J. L., Gunn, A., Hecht, J. R., Hoffe, S., Hubbard, J., Hunt, S., Jeck, W., Johung, K. L., Kirilcuk, N., … Gurski, L. (2022). Rectal Cancer, Version 2.2022, NCCN Clinical Practice Guidelines in Oncology. *Journal of the National Comprehensive Cancer Network*, *20*(10), 1139–1167. https://doi.org/10.6004/JNCCN.2022.0051

Berger, J., Howard, A. D., Gerber, L., Cullen, B. R., & Udenfriend, S. (1987). Expression of active, membrane-bound human placental alkaline phosphatase by transfected simian cells. *Proceedings of the National Academy of Sciences of the United States of America*, *84*(14), 4885. https://doi.org/10.1073/PNAS.84.14.4885

Biller, L. H., & Schrag, D. (2021). Diagnosis and Treatment of Metastatic Colorectal Cancer: A Review. *JAMA*, *325*(7), 669–685. https://doi.org/10.1001/JAMA.2021.0106

Bissell, M. J., & Hines, W. C. (2011). Why don't we get more cancer? A proposed role of the microenvironment in restraining cancer progression. *Nature Medicine*, *17*(3), 320–329. https://doi.org/10.1038/NM.2328

Bodmer, W., & Bodmer, W. (1999). Familial adenomatous polyposis (FAP) and its gene, APC. *Cytogenetics and Cell Genetics*, *86*(2), 99–104. https://doi.org/10.1159/000015360

Bodmer, W. F. (2006). Cancer genetics: colorectal cancer as a model. *Journal of Human Genetics*, *51*(5), 391. https://doi.org/10.1007/S10038-006-0373-X

Bodmer, W., & Golubovskaya, V. (2023a). Cancer Immunotherapy: Where Next? *Cancers*, *15*(8). https://doi.org/10.3390/CANCERS15082358

Bodmer, W., & Golubovskaya, V. (2023b). Cancer Immunotherapy: Where Next? *Cancers*, *15*(8). https://doi.org/10.3390/CANCERS15082358

Bodmer, W., & Golubovskaya, V. (2023c). Cancer Immunotherapy: Where Next? *Cancers*, *15*(8), 2358. https://doi.org/10.3390/CANCERS15082358

Bray, F., Ferlay, J., Soerjomataram, I., Siegel, R. L., Torre, L. A., & Jemal, A. (2018). Global cancer statistics 2018: GLOBOCAN estimates of incidence and mortality worldwide for 36 cancers in 185 countries. *CA: A Cancer Journal for Clinicians*, *68*(6), 394–424. https://doi.org/10.3322/CAAC.21492

Bui, T. M., Wiesolek, H. L., & Sumagin, R. (2020). ICAM-1: A master regulator of cellular responses in inflammation, injury resolution, and tumorigenesis. *Journal of Leukocyte Biology*, *108*(3), 787. https://doi.org/10.1002/JLB.2MR0220-549R

Cappell, M. S. (2008a). Pathophysiology, Clinical Presentation, and Management of Colon Cancer. *Gastroenterology Clinics of North America*, *37*(1), 1–24. https://doi.org/10.1016/J.GTC.2007.12.002

Cappell, M. S. (2008b). Pathophysiology, Clinical Presentation, and Management of Colon Cancer. *Gastroenterology Clinics of North America*, *37*(1), 1–24. https://doi.org/10.1016/J.GTC.2007.12.002

Carpenter, A. C., & Bosselut, R. (2010). Decision checkpoints in the thymus. *Nature Immunology 2010 11:8*, *11*(8), 666–673. https://doi.org/10.1038/ni.1887

Caulín, C., Salvesen, G. S., & Oshima, R. G. (1997). Caspase Cleavage of Keratin 18 and Reorganization of Intermediate Filaments during Epithelial Cell Apoptosis. *The Journal of Cell Biology*, *138*(6), 1379. https://doi.org/10.1083/JCB.138.6.1379

Chang, A. Y., Gejman, R. S., Brea, E. J., Oh, C. Y., Mathias, M. D., Pankov, D., Casey, E., Dao, T., & Scheinberg, D. A. (2016). Opportunities and challenges for TCR mimic antibodies in cancer therapy. *Expert Opinion on Biological Therapy*, *16*(8), 979. https://doi.org/10.1080/14712598.2016.1176138

Chen, Y., Yu, D., Qian, H., Shi, Y., & Tao, Z. (2024). CD8+ T cell-based cancer immunotherapy. *Journal of Translational Medicine 2024 22:1*, *22*(1), 1–17. https://doi.org/10.1186/S12967-024-05134-6

Cioffi, M., Dorado, J., Baeuerle, P. A., & Heeschen, C. (2012). EpCAM/CD3-bispecific T-cell engaging antibody MT110 eliminates primary human pancreatic cancer stem cells. *Clinical Cancer Research*, *18*(2), 465–474. https://doi.org/10.1158/1078-0432.CCR-11-1270/84542/AM/EPCAM-CD3-BISPECIFIC-T-CELL-ENGAGING-ANTIBODY-M110

COLEY, W. B. (1891). II. Contribution to the Knowledge of Sarcoma. *Annals of Surgery*, *14*(3), 199–220. https://doi.org/10.1097/00000658-189112000-00015

Conaghan, P. J., Ashraf, S. Q., Tytherleigh, M. G., Wilding, J. L., Tchilian, E., Bicknell, D., Mortensen, N. J. M. C., & Bodmer, W. F. (2008). Targeted killing of colorectal cancer cell lines by a humanised IgG1 monoclonal antibody that binds to membrane-bound carcinoembryonic antigen. *British Journal of Cancer*, *98*(7), 1217–1225. https://doi.org/10.1038/SJ.BJC.6604289

Crofton, P. M. (1982). Biochemistry of alkaline phosphatase isoenzymes. *Critical Reviews in Clinical Laboratory Sciences*, *16*(3), 161–194. https://doi.org/10.3109/10408368209107027

Cui, X., Jia, H., Xin, H., Zhang, L., Chen, S., Xia, S., Li, X., Xu, W., Chen, X., Feng, Y., Wei, X., Yu, H., Wang, Y., Zhan, Y., Zhu, X., & Zhang, X. (2021). A Novel Bispecific Antibody Targeting PD-L1 and VEGF With Combined Anti-Tumor Activities. *Frontiers in Immunology*, *12*. https://doi.org/10.3389/FIMMU.2021.778978

Dagogo-Jack, I., & Shaw, A. T. (2017). Tumour heterogeneity and resistance to cancer therapies. *Nature Reviews Clinical Oncology 2017 15:2*, *15*(2), 81–94. https://doi.org/10.1038/nrclinonc.2017.166

Danial, N. N., & Korsmeyer, S. J. (2004). Cell Death: Critical Control Points. *Cell*, *116*(2), 205–219. https://doi.org/10.1016/S0092-8674(04)00046-7

De Haas, E. C., Di Pietro, A., Simpson, K. L., Meijer, C., Suurmeijer, A. J. H., Lancashire, L. J., Cummings, J., De Jong, S., De Vries, E. G. E., Dive, C., & Gietema, J. A. (2008). Clinical evaluation of M30 and M65 ELISA cell death assays as circulating biomarkers in a drug-sensitive tumor, testicular cancer. *Neoplasia (New York, N.Y.)*, *10*(10), 1041–1048. https://doi.org/10.1593/NEO.08620

Dekker, E., Tanis, P. J., Vleugels, J. L. A., Kasi, P. M., & Wallace, M. B. (2019). Colorectal cancer. *The Lancet*, *394*(10207), 1467–1480. https://doi.org/10.1016/S0140-6736(19)32319-0

Dhatchinamoorthy, K., Colbert, J. D., & Rock, K. L. (2021). Cancer Immune Evasion Through Loss of MHC Class I Antigen Presentation. *Frontiers in Immunology*, *12*, 636568. https://doi.org/10.3389/FIMMU.2021.636568

Dubrovsky, L., Dao, T., Gejman, R. S., Brea, E. J., Chang, A. Y., Oh, C. Y., Casey, E., Pankov, D., & Scheinberg, D. A. (2015). T cell receptor mimic antibodies for cancer therapy. *Oncoimmunology*, *5*(1), e1049803. https://doi.org/10.1080/2162402X.2015.1049803

Durbin, H., Milligan, E. M., Mather, S. J., Tucker, D. F., Raymond, R., & Bodmer, W. F. (1988). Monoclonal antibodies to placental alkaline phosphatase: preclinical evaluation in a human xenograft tumour model of F(ab')2 and Fab fragments. *International Journal of Cancer. Supplement = Journal International Du Cancer. Supplement*, *2*(2 S), 59–66. https://doi.org/10.1002/IJC.2910410715

Durbin, H., Rodrigues, N., & Bodmer, W. F. (1990a). Further characterization, isolation and identification of the epithelial cell-surface antigen defined by monoclonal antibody aua1. *International Journal of Cancer*, *45*(3), 562–565. https://doi.org/10.1002/IJC.2910450331

Durbin, H., Rodrigues, N., & Bodmer, W. F. (1990b). Further characterization, isolation and identification of the epithelial cell-surface antigen defined by monoclonal antibody AUA1. *International Journal of Cancer*, *45*(3), 562–565. https://doi.org/10.1002/IJC.2910450331

Durbin, H., Tucker, D. F., Milligan, E. M., Bobrow, L. G., Warne, P. H., Pookim, Y. L., & Bodmer, W. F. (1988). Production of monoclonal antibodies to placental alkaline phosphatase: preliminary characterisation includes identification of one antibody reactive with routinely fixed histological preparations. *International Journal of Cancer. Supplement = Journal International Du Cancer. Supplement*, *2*(2 S), 50–58. https://doi.org/10.1002/IJC.2910410714

Elmore, S. (2007a). Apoptosis: A Review of Programmed Cell Death. *Toxicologic Pathology*, *35*(4), 495. https://doi.org/10.1080/01926230701320337

Elmore, S. (2007b). Apoptosis: A Review of Programmed Cell Death. *Toxicologic Pathology*, *35*(4), 495. https://doi.org/10.1080/01926230701320337

Elmore, S. (2007c). Apoptosis: A Review of Programmed Cell Death. *Toxicologic Pathology*, *35*(4), 495. https://doi.org/10.1080/01926230701320337

Epenetos, A. A., Hooker, G., Durbin, H., Bodmer, W. F., Snook, D., Begent, R., Oliver, R. T. D., & Lavender, J. P. (1985). Indium-111 labelled monoclonal antibody to placental alkaline phosphatase in in the detection of neoplasms of testis, ovary, and cervix. *Lancet (London, England)*, *2*(8451), 350–353. https://doi.org/10.1016/S0140-6736(85)92495-X

Ferrari, F., Bellone, S., Black, J., Schwab, C. L., Lopez, S., Cocco, E., Bonazzoli, E., Predolini, F., Menderes, G., Litkouhi, B., Ratner, E., Silasi, D. A., Azodi, M., Schwartz, P. E., & Santin, A. D. (2015). Solitomab, an EpCAM/CD3 bispecific antibody construct (BiTE®), is highly active against primary uterine and ovarian carcinosarcoma cell lines in vitro. *Journal of Experimental & Clinical Cancer Research : CR*, *34*(1). https://doi.org/10.1186/S13046-015-0241-7

Fidler, I. J. (1989). Origin and biology of cancer metastasis. *Cytometry*, *10*(6), 673–680. https://doi.org/10.1002/cyto.990100602

Fischer, N., Riechmann, L., & Winter, G. (2004). A native-like artificial protein from antisense DNA. *Protein Engineering, Design and Selection*, *17*(1), 13–20. https://doi.org/10.1093/PROTEIN/GZH002

Fontenot, J. D., Gavin, M. A., & Rudensky, A. Y. (2003). Foxp3 programs the development and function of CD4+CD25+ regulatory T cells. *Nature Immunology 2003 4:4*, *4*(4), 330–336. https://doi.org/10.1038/ni904

Frieling, G. W., Al-Zaid, T., & Prieto, V. G. (2014). Placental alkaline phosphatase positivity in metastatic melanoma. *The American Journal of Dermatopathology*, *36*(2), 189–190. https://doi.org/10.1097/DAD.0B013E318284A586

Gao, H., Liang, J., Duan, J., Chen, L., Li, H., Zhen, T., Zhang, F., Dong, Y., Shi, H., & Han, A. (2021). A Prognosis Marker SLC2A3 Correlates With EMT and Immune Signature in Colorectal Cancer. *Frontiers in Oncology*, *11*. https://doi.org/10.3389/FONC.2021.638099

Geginat, J., Paroni, M., Maglie, S., Alfen, J. S., Kastirr, I., Gruarin, P., de Simone, M., Pagani, M., & Abrignani, S. (2014). Plasticity of human CD4 T cell subsets. *Frontiers in Immunology*, *5*(DEC), 121514. https://doi.org/10.3389/FIMMU.2014.00630/BIBTEX

Gerlinger, M., & Swanton, C. (2010a). How Darwinian models inform therapeutic failure initiated by clonal heterogeneity in cancer medicine. *British Journal of Cancer*, *103*(8), 1139. https://doi.org/10.1038/SJ.BJC.6605912

Gerlinger, M., & Swanton, C. (2010b). How Darwinian models inform therapeutic failure initiated by clonal heterogeneity in cancer medicine. *British Journal of Cancer*, *103*(8), 1139. https://doi.org/10.1038/SJ.BJC.6605912

Gires, O., Pan, M., Schinke, H., Canis, M., & Baeuerle, P. A. (2020). Expression and function of epithelial cell adhesion molecule EpCAM: where are we after 40 years? *Cancer Metastasis Reviews*, *39*(3), 969. https://doi.org/10.1007/S10555-020-09898-3

Golubovskaya, V., Sienkiewicz, J., Sun, J., Huang, Y., Hu, L., Zhou, H., Harto, H., Xu, S., Berahovich, R., Bodmer, W., & Wu, L. (2023a). mRNA-Lipid Nanoparticle (LNP) Delivery of Humanized EpCAM-CD3 Bispecific Antibody Significantly Blocks Colorectal Cancer Tumor Growth. *Cancers*, *15*(10). https://doi.org/10.3390/CANCERS15102860

Golubovskaya, V., Sienkiewicz, J., Sun, J., Huang, Y., Hu, L., Zhou, H., Harto, H., Xu, S., Berahovich, R., Bodmer, W., & Wu, L. (2023b). mRNA-Lipid Nanoparticle (LNP) Delivery of Humanized EpCAM-CD3 Bispecific Antibody Significantly Blocks Colorectal Cancer Tumor Growth. *Cancers*, *15*(10). https://doi.org/10.3390/CANCERS15102860

Golubovskaya, V., & Wu, L. (2016). Different Subsets of T Cells, Memory, Effector Functions, and CAR-T Immunotherapy. *Cancers*, *8*(3), 36. https://doi.org/10.3390/CANCERS8030036

Graham, T. A., & Sottoriva, A. (2017). Measuring cancer evolution from the genome. *The Journal of Pathology*, *241*(2), 183–191. https://doi.org/10.1002/PATH.4821

Guy, C. S., & Vignali, D. A. A. (2009). Organization of proximal signal initiation at the TCR:CD3 complex. *Immunological Reviews*, *232*(1), 7. https://doi.org/10.1111/J.1600-065X.2009.00843.X

Haffner, M. C., Zwart, W., Roudier, M. P., True, L. D., Nelson, W. G., Epstein, J. I., De Marzo, A. M., Nelson, P. S., & Yegnasubramanian, S. (2020). Genomic and phenotypic heterogeneity in prostate cancer. *Nature Reviews. Urology*, *18*(2), 79. https://doi.org/10.1038/S41585-020-00400-W

Hanahan, D., & Weinberg, R. A. (2011). Hallmarks of Cancer: The Next Generation. *Cell*, *144*(5), 646–674. https://doi.org/10.1016/J.CELL.2011.02.013

Harjes, U. (2020). Tumour-reactive T cells work remotely using IFNγ. *Nature Reviews Cancer 2020 20:5*, *20*(5), 261–261. https://doi.org/10.1038/s41568-020-0255-0

Harmenberg, U., Koha, M., Makiya, R., Koshida, K., Brismar, B., Stigbrand, T., & Wahren, B. (1991a). Identification and characterization of alkaline phosphatase isozymes in human colorectal adenocarcinomas. *Tumour Biology : The Journal of the International Society for Oncodevelopmental Biology and Medicine*, *12*(4), 237–248. https://doi.org/10.1159/000217710

Harmenberg, U., Koha, M., Makiya, R., Koshida, K., Brismar, B., Stigbrand, T., & Wahren, B. (1991b). Identification and characterization of alkaline phosphatase isozymes in human colorectal adenocarcinomas. *Tumour Biology : The Journal of the International Society for Oncodevelopmental Biology and Medicine*, *12*(4), 237–248. https://doi.org/10.1159/000217710

Hayday, A., Dechanet-Merville, J., Rossjohn, J., & Silva-Santos, B. (2024). Cancer immunotherapy by γδ T cells. *Science (New York, N.Y.)*, *386*(6717), eabq7248. https://doi.org/10.1126/SCIENCE.ABQ7248

Hengartner, M. O. (2001). Apoptosis: Corralling the Corpses. *Cell*, *104*(3), 325–328. https://doi.org/10.1016/S0092-8674(01)00219-7

Henrikson, N. B., Webber, E. M., Goddard, K. A., Scrol, A., Piper, M., Williams, M. S., Zallen, D. T., Calonge, N., Ganiats, T. G., Janssens, A. C. J. W., Zauber, A., Lansdorp-Vogelaar, I., Van Ballegooijen, M., & Whitlock, E. P. (2015). Family history and the natural history of colorectal cancer: systematic review. *Genetics in Medicine : Official Journal of the American College of Medical Genetics*, *17*(9), 702–712. https://doi.org/10.1038/GIM.2014.188

Herlyn, M., Steplewski, Z., Herlyn, D., & Koprowski, H. (1979). Colorectal carcinoma-specific antigen: detection by means of monoclonal antibodies. *Proceedings of the National Academy of Sciences of the United States of America*, *76*(3), 1438–1442. https://doi.org/10.1073/PNAS.76.3.1438

Herrera, M., Pretelli, G., Desai, J., Garralda, E., Siu, L. L., Steiner, T. M., & Au, L. (2024). Bispecific antibodies: advancing precision oncology. *Trends in Cancer*, *10*(10), 893–919. https://doi.org/10.1016/J.TRECAN.2024.07.002/ATTACHMENT/5CCE5164-6903-4220-A0F7-5FCEEAF788FB/MMC1.DOCX

Hosseini, S. S., Khalili, S., Baradaran, B., Bidar, N., Shahbazi, M. A., Mosafer, J., Hashemzaei, M., Mokhtarzadeh, A., & Hamblin, M. R. (2021a). Bispecific monoclonal antibodies for targeted immunotherapy of solid tumors: Recent advances and clinical trials. *International Journal of Biological Macromolecules*, *167*, 1030–1047. https://doi.org/10.1016/J.IJBIOMAC.2020.11.058

Hosseini, S. S., Khalili, S., Baradaran, B., Bidar, N., Shahbazi, M. A., Mosafer, J., Hashemzaei, M., Mokhtarzadeh, A., & Hamblin, M. R. (2021b). Bispecific monoclonal antibodies for targeted immunotherapy of solid tumors: Recent advances and clinical trials. *International Journal of Biological Macromolecules*, *167*, 1030–1047. https://doi.org/10.1016/J.IJBIOMAC.2020.11.058

Hosseini, S. S., Khalili, S., Baradaran, B., Bidar, N., Shahbazi, M. A., Mosafer, J., Hashemzaei, M., Mokhtarzadeh, A., & Hamblin, M. R. (2021c). Bispecific monoclonal antibodies for targeted immunotherapy of solid tumors: Recent advances and clinical trials. *International Journal of Biological Macromolecules*, *167*, 1030–1047. https://doi.org/10.1016/J.IJBIOMAC.2020.11.058

How to Cite FlowJo for Publication | FlowJo, LLC. (n.d.). Retrieved June 13, 2024, from https://www.flowjo.com/citing-flowjo

Huehls, A. M., Coupet, T. A., & Sentman, C. L. (2014a). Bispecific T cell engagers for cancer immunotherapy. *Immunology and Cell Biology*, *93*(3), 290. https://doi.org/10.1038/ICB.2014.93

Huehls, A. M., Coupet, T. A., & Sentman, C. L. (2014b). Bispecific T cell engagers for cancer immunotherapy. *Immunology and Cell Biology*, *93*(3), 290. https://doi.org/10.1038/ICB.2014.93

Hurwitz, H., Fehrenbacher, L., Novotny, W., Cartwright, T., Hainsworth, J., Heim, W., Berlin, J., Baron, A., Griffing, S., Holmgren, E., Ferrara, N., Fyfe, G., Rogers, B., Ross, R., & Kabbinavar, F. (2004). Bevacizumab plus Irinotecan, Fluorouracil, and Leucovorin for Metastatic Colorectal Cancer. *New England Journal of Medicine*, *350*(23), 2335–2342. https://doi.org/10.1056/NEJMOA032691/ASSET/60859BCD-95A2-40AF-B3BA-9692B062B704/ASSETS/IMAGES/LARGE/NEJMOA032691_T4.JPG

Igney, F. H., & Krammer, P. H. (2002). Death and anti-death: tumour resistance to apoptosis. *Nature Reviews Cancer 2002 2:4*, *2*(4), 277–288. https://doi.org/10.1038/nrc776

Iwai, Y., Ishida, M., Tanaka, Y., Okazaki, T., Honjo, T., & Minato, N. (2002). Involvement of PD-L1 on tumor cells in the escape from host immune system and tumor immunotherapy by PD-L1 blockade. *Proceedings of the National Academy of Sciences of the United States of America*, *99*(19), 12293. https://doi.org/10.1073/PNAS.192461099

Jacobsen, G. K., & Norgaard-Pedersen, B. (1984). Placental alkaline phosphatase in testicular germ cell tumours and in carcinoma-in-situ of the testis. An immunohistochemical study. *Acta Pathologica, Microbiologica, et Immunologica Scandinavica. Section A, Pathology*, *92*(5), 323–329. https://doi.org/10.1111/J.1699-0463.1984.TB04411.X

Janeway, C. A., & Medzhitov, R. (2002). Innate immune recognition. *Annual Review of Immunology*, *20*(Volume 20, 2002), 197–216. https://doi.org/10.1146/ANNUREV.IMMUNOL.20.083001.084359/CITE/REFWORKS

Jiang, M., Jia, K., Wang, L., Li, W., Chen, B., Liu, Y., Wang, H., Zhao, S., He, Y., & Zhou, C. (2021). Alterations of DNA damage response pathway: Biomarker and therapeutic strategy for cancer immunotherapy. *Acta Pharmaceutica Sinica. B*, *11*(10), 2983. https://doi.org/10.1016/J.APSB.2021.01.003

Juno, J. A., Bockel, D. van, Kent, S. J., Kelleher, A. D., Zaunders, J. J., & Munier, C. M. L. (2017). Cytotoxic CD4 T Cells—Friend or Foe during Viral Infection? *Frontiers in Immunology*, *8*(JAN), 1. https://doi.org/10.3389/FIMMU.2017.00019

Kaech, S. M., & Cui, W. (2012). Transcriptional control of effector and memory CD8+ T cell differentiation. *Nature Reviews. Immunology*, *12*(11), 749. https://doi.org/10.1038/NRI3307

Kailayangiri, S., Altvater, B., Wiebel, M., Jamitzky, S., & Rossig, C. (2020). Overcoming Heterogeneity of Antigen Expression for Effective CAR T Cell Targeting of Cancers. *Cancers*, *12*(5). https://doi.org/10.3390/CANCERS12051075

Kantarjian, H., Stein, A., Gökbuget, N., Fielding, A. K., Schuh, A. C., Ribera, J.-M., Wei, A., Dombret, H., Foà, R., Bassan, R., Arslan, Ö., Sanz, M. A., Bergeron, J., Demirkan, F., Lech-Maranda, E., Rambaldi, A., Thomas, X., Horst, H.-A., Brüggemann, M., … Topp, M. S. (2017). Blinatumomab versus Chemotherapy for Advanced Acute Lymphoblastic Leukemia. *The New England Journal of Medicine*, *376*(9), 836–847. https://doi.org/10.1056/NEJMOA1609783

Kaplan, E. L., & Meier, P. (1958). Nonparametric Estimation from Incomplete Observations. *Journal of the American Statistical Association*, *53*(282), 457–481. https://doi.org/10.1080/01621459.1958.10501452

Kashyap, D., Garg, V. K., & Goel, N. (2021). Intrinsic and extrinsic pathways of apoptosis: Role in cancer development and prognosis. *Advances in Protein Chemistry and Structural Biology*, *125*, 73–120. https://doi.org/10.1016/BS.APCSB.2021.01.003

Ke, N., Wang, X., Xu, X., & Abassi, Y. A. (2011a). The xCELLigence system for real-time and label-free monitoring of cell viability. *Methods in Molecular Biology (Clifton, N.J.)*, *740*, 33–43. https://doi.org/10.1007/978-1-61779-108-6_6

Ke, N., Wang, X., Xu, X., & Abassi, Y. A. (2011b). The xCELLigence system for real-time and label-free monitoring of cell viability. *Methods in Molecular Biology (Clifton, N.J.)*, *740*, 33–43. https://doi.org/10.1007/978-1-61779-108-6_6

Klinger, M., Benjamin, J., Kischel, R., Stienen, S., & Zugmaier, G. (2016a). Harnessing T cells to fight cancer with BiTE® antibody constructs--past developments and future directions. *Immunological Reviews*, *270*(1), 193–208. https://doi.org/10.1111/IMR.12393

Klinger, M., Benjamin, J., Kischel, R., Stienen, S., & Zugmaier, G. (2016b). Harnessing T cells to fight cancer with BiTE® antibody constructs--past developments and future directions. *Immunological Reviews*, *270*(1), 193–208. https://doi.org/10.1111/IMR.12393

Köhler, G., & Milstein, C. (1975). Continuous cultures of fused cells secreting antibody of predefined specificity. *Nature 1975 256:5517*, *256*(5517), 495–497. https://doi.org/10.1038/256495a0

Koshida, K., Yokoyama, K., Imao, T., Konaka, H., Hirano, K., Uchibayashi, T., & Namiki, M. (1998). Immunolocalization of anti-placental alkaline phosphatase monoclonal antibody in mice with testicular tumors and lymph node metastasis. *Urological Research*, *26*(1), 23–28. https://doi.org/10.1007/S002400050018/METRICS

Kuhla, A., Eipel, C., Abshagen, K., Siebert, N., Menger, M. D., & Vollmar, B. (2009). Role of the perforin/granzyme cell death pathway in D-Gal/LPS-induced inflammatory liver injury. *American Journal of Physiology - Gastrointestinal and Liver Physiology*, *296*(5), 1069–1076. https://doi.org/10.1152/AJPGI.90689.2008/ASSET/IMAGES/LARGE/ZH30050953780007.JPEG

Kuipers, E. J., Grady, W. M., Lieberman, D., Seufferlein, T., Sung, J. J., Boelens, P. G., Van De Velde, C. J. H., & Watanabe, T. (2015). COLORECTAL CANCER. *Nature Reviews. Disease Primers*, *1*, 15065. https://doi.org/10.1038/NRDP.2015.65

Kulis, M., & Esteller, M. (2010). DNA Methylation and Cancer. *Advances in Genetics*, *70*(C), 27–56. https://doi.org/10.1016/B978-0-12-380866-0.60002-2

Kwak, E. L., Ahronian, L. G., Siravegna, G., Mussolin, B., Godfrey, J. T., Clark, J. W., Blaszkowsky, L. S., Ryan, D. P., Lennerz, J. K., John Iafrate, A., Bardelli, A., Hong, T. S., & Corcoran, R. B. (2015). Molecular heterogeneity and receptor co-amplification drive resistance to targeted therapy in MET-amplified esophagogastric cancer. *Cancer Discovery*, *5*(12), 1271. https://doi.org/10.1158/2159-8290.CD-15-0748

Kyriakidis, I., Vasileiou, E., Rossig, C., Roilides, E., Groll, A. H., & Tragiannidis, A. (2021). Invasive Fungal Diseases in Children with Hematological Malignancies Treated with Therapies That Target Cell Surface Antigens: Monoclonal Antibodies, Immune Checkpoint Inhibitors and CAR T-Cell Therapies. *Journal of Fungi (Basel, Switzerland)*, *7*(3), 1–29. https://doi.org/10.3390/JOF7030186

Lange PH, M. J. (1990). Placental-like alkaline phosphatase in seminoma. *Urological Research*, *18*(2), 87–92. https://doi.org/10.1007/BF00302465

Le, D. T., Uram, J. N., Wang, H., Bartlett, B. R., Kemberling, H., Eyring, A. D., Skora, A. D., Luber, B. S., Azad, N. S., Laheru, D., Biedrzycki, B., Donehower, R. C., Zaheer, A., Fisher, G. A., Crocenzi, T. S., Lee, J. J., Duffy, S. M., Goldberg, R. M., de la Chapelle, A., … Diaz, L. A. (2015). PD-1 Blockade in Tumors with Mismatch-Repair Deficiency. *The New England Journal of Medicine*, *372*(26), 2509–2520. https://doi.org/10.1056/NEJMOA1500596

Le Du, M. H., Stigbrand, T., Taussig, M. J., Ménez, A., & Stura, E. A. (2001). Crystal Structure of Alkaline Phosphatase from Human Placenta at 1.8 Å Resolution: IMPLICATION FOR A SUBSTRATE SPECIFICITY. *Journal of Biological Chemistry*, *276*(12), 9158–9165. https://doi.org/10.1074/JBC.M009250200

Leach, D. R., Krummel, M. F., & Allison, J. P. (1996). Enhancement of antitumor immunity by CTLA-4 blockade. *Science (New York, N.Y.)*, *271*(5256), 1734–1736. https://doi.org/10.1126/SCIENCE.271.5256.1734

Li, D., Bentley, C., Yates, J., Salimi, M., Greig, J., Wiblin, S., Hassanali, T., & Banham, A. H. (2017a). Engineering chimeric human and mouse major histocompatibility complex (MHC) class I tetramers for the production of T-cell receptor (TCR) mimic antibodies. *PLOS ONE*, *12*(4), e0176642. https://doi.org/10.1371/JOURNAL.PONE.0176642

Li, D., Bentley, C., Yates, J., Salimi, M., Greig, J., Wiblin, S., Hassanali, T., & Banham, A. H. (2017b). Engineering chimeric human and mouse major histocompatibility complex (MHC) class I tetramers for the production of T-cell receptor (TCR) mimic antibodies. *PLOS ONE*, *12*(4), e0176642. https://doi.org/10.1371/JOURNAL.PONE.0176642

Li, D., Guo, X., Yang, K., Yang, Y., Zhou, W., Huang, Y., Liang, X., Su, J., Jiang, L., Li, J., Fu, M., He, H., Yang, J., Shi, H., Yang, H., Tong, A., Chen, N., Hu, J., Xu, Q., … Wang, W. (2023). EpCAM-targeting CAR-T cell immunotherapy is safe and efficacious for epithelial tumors. *Science Advances*, *9*(48), eadg9721. https://doi.org/10.1126/SCIADV.ADG9721

Li, J., Chen, S., Xiao, X., Zhao, Y., Ding, W., & Li, X. C. (2017). IL-9 and Th9 cells in health and diseases—from tolerance to immunopathology. *Cytokine & Growth Factor Reviews*, *37*, 47. https://doi.org/10.1016/J.CYTOGFR.2017.07.004

Li, X., Berahovich, R., Zhou, H., Liu, X., Li, F., Xu, S., Wei, Y., Ouaret, D., Bodmer, W., Wu, L., & Golubovskaya, V. (2020a). PLAP -CAR T cells mediate high specific cytotoxicity against colon cancer cells. *Frontiers in Bioscience - Landmark*, *25*(9), 1765–1786. https://doi.org/10.2741/4877/4877/FIG7.JPG

Li, X., Berahovich, R., Zhou, H., Liu, X., Li, F., Xu, S., Wei, Y., Ouaret, D., Bodmer, W., Wu, L., & Golubovskaya, V. (2020b). PLAP -CAR T cells mediate high specific cytotoxicity against colon cancer cells. *Frontiers in Bioscience (Landmark Edition)*, *25*(9), 1765–1786. https://doi.org/10.2741/4877

Li, X., Berahovich, R., Zhou, H., Liu, X., Li, F., Xu, S., Wei, Y., Ouaret, D., Bodmer, W., Wu, L., & Golubovskaya, V. (2020c). PLAP -CAR T cells mediate high specific cytotoxicity against colon cancer cells. *Frontiers in Bioscience (Landmark Edition)*, *25*(9), 1765–1786. https://doi.org/10.2741/4877

Lin, S., Sartori, M. J., Mezzano, L., & de Fabro, S. P. (2005). Placental Alkaline Phosphatase (PLAP) Enzyme Activity and Binding to IgG in Chagas' Disease. *Placenta*, *26*(10), 789–795. https://doi.org/10.1016/J.PLACENTA.2004.08.014

Linnenbach, A. J., Seng, B. A., Wu, S., Robbins, S., Scollon, M., Pyrc, J. J., Druck, T., & Huebner2, K. (1993). Retroposition in a Family of Carcinoma-Associated Antigen Genes. *MOLECULAR AND CELLULAR BIOLOGY*, *13*(3), 1507–1515.

Liu, N., Du, J., Ge, J., & Liu, S. B. (2024). DNA damage-inducing endogenous and exogenous factors and research progress. *Nucleosides, Nucleotides & Nucleic Acids*. https://doi.org/10.1080/15257770.2024.2428436

Liu, S., Mao, Q., Xue, W., Zhang, X., Qi, Y., Wang, Y., Chen, P., & Zhou, Q. (2019). High expression of ALPPL2 is associated with poor prognosis in gastric cancer. *Human Pathology*, *86*, 49–56. https://doi.org/10.1016/J.HUMPATH.2018.11.019

Liu, T. C., Kalugin, P. N., Wilding, J. L., & Bodmer, W. F. (2022). GMMchi: gene expression clustering using Gaussian mixture modeling. *BMC Bioinformatics*, *23*(1). https://doi.org/10.1186/S12859-022-05006-0

Lonsdale, J., Thomas, J., Salvatore, M., Phillips, R., Lo, E., Shad, S., Hasz, R., Walters, G., Garcia, F., Young, N., Foster, B., Moser, M., Karasik, E., Gillard, B., Ramsey, K., Sullivan, S., Bridge, J., Magazine, H., Syron, J., … Moore, H. F. (2013). The Genotype-Tissue Expression (GTEx) project. *Nature Genetics 2013 45:6*, *45*(6), 580–585. https://doi.org/10.1038/ng.2653

Lozano-Ojalvo, D., López-Fandiño, R., & López-Expósito, I. (2015). PBMC-Derived T Cells. *The Impact of Food Bioactives on Health: In Vitro and Ex Vivo Models*, 169–180. https://doi.org/10.1007/978-3-319-16104-4_16

Macdonald, J., Henri, J., Roy, K., Hays, E., Bauer, M., Veedu, R. N., Pouliot, N., & Shigdar, S. (2018). EpCAM Immunotherapy versus Specific Targeted Delivery of Drugs. *Cancers*, *10*(1). https://doi.org/10.3390/CANCERS10010019

Maida, M., Macaluso, F. S., Ianiro, G., Mangiola, F., Sinagra, E., Hold, G., Maida, C., Cammarota, G., Gasbarrini, A., & Scarpulla, G. (2017). Screening of colorectal cancer: present and future. *Expert Review of Anticancer Therapy*, *17*(12), 1131–1146. https://doi.org/10.1080/14737140.2017.1392243

Majno, G., & Joris, I. (1995). Review Apoptosis, Oncosis, and Necrosis An Overview of Cell Death. *American Journal OfPathology*, *146*(1).

Martínez-Lostao, L., Anel, A., & Pardo, J. (2015). How Do Cytotoxic Lymphocytes Kill Cancer Cells? *Clinical Cancer Research : An Official Journal of the American Association for Cancer Research*, *21*(22), 5047–5056. https://doi.org/10.1158/1078-0432.CCR-15-0685

Maus, M. V., Grupp, S. A., Porter, D. L., & June, C. H. (2014). Antibody-modified T cells: CARs take the front seat for hematologic malignancies. *Blood*, *123*(17), 2625. https://doi.org/10.1182/BLOOD-2013-11-492231

Medzhitov, R. (2007). Recognition of microorganisms and activation of the immune response. *Nature 2007 449:7164*, *449*(7164), 819–826. https://doi.org/10.1038/nature06246

Mellman, I., Chen, D. S., Powles, T., & Turley, S. J. (2023). The cancer-immunity cycle: Indication, genotype, and immunotype. *Immunity*, *56*(10), 2188–2205. https://doi.org/10.1016/J.IMMUNI.2023.09.011

Millán, J. L. (2006). Mammalian Alkaline Phosphatases: From Biology to Applications in Medicine and Biotechnology. *Mammalian Alkaline Phosphatases: From Biology to Applications in Medicine and Biotechnology*, 1–322. https://doi.org/10.1002/3527608060

Moertel, C. G., Fleming, T. R., Macdonald, J. S., Haller, D. G., Laurie, J. A., Goodman, P. J., Ungerleider, J. S., Emerson, W. A., Tormey, D. C., Glick, J. H., Veeder, M. H., & Mailliard, J. A. (1990). Levamisole and Fluorouracil for Adjuvant Therapy of Resected Colon Carcinoma. *New England Journal of Medicine*, *322*(6), 352–358. https://doi.org/10.1056/NEJM199002083220602/ASSET/63B85BD4-B6D7-4473-9C84-59B1F36845EE/ASSETS/IMAGES/LARGE/NEJM199002083220602_T6.JPG

Mouradov, D., Sloggett, C., Jorissen, R. N., Love, C. G., Li, S., Burgess, A. W., Arango, D., Strausberg, R. L., Buchanan, D., Wormald, S., O'Connor, L., Wilding, J. L., Bicknell, D., Tomlinson, I. P. M., Bodmer, W. F., Mariadason, J. M., & Sieber, O. M. (2014a). Colorectal cancer cell lines are representative models of the main molecular subtypes of

primary cancer. *Cancer Research*, *74*(12), 3238–3247. https://doi.org/10.1158/0008-5472.CAN-14-0013

Mouradov, D., Sloggett, C., Jorissen, R. N., Love, C. G., Li, S., Burgess, A. W., Arango, D., Strausberg, R. L., Buchanan, D., Wormald, S., O'Connor, L., Wilding, J. L., Bicknell, D., Tomlinson, I. P. M., Bodmer, W. F., Mariadason, J. M., & Sieber, O. M. (2014b). Colorectal cancer cell lines are representative models of the main molecular subtypes of primary cancer. *Cancer Research*, *74*(12), 3238–3247. https://doi.org/10.1158/0008-5472.CAN-14-0013

Mueckler, M., & Thorens, B. (2013). The SLC2 (GLUT) Family of Membrane Transporters. *Molecular Aspects of Medicine*, *34*(0), 121. https://doi.org/10.1016/J.MAM.2012.07.001

Murphy, K. C. W. (2017). Janeway 's: Immunobiology. *Garland Science, Taylor & Francis Group, LLC*, 1–277.

Netea, M. G., Quintin, J., & Van Der Meer, J. W. M. (2011). Trained Immunity: A Memory for Innate Host Defense. *Cell Host & Microbe*, *9*(5), 355–361. https://doi.org/10.1016/J.CHOM.2011.04.006

Neumann, A., Keller, T., Jocham, D., & Doehn, C. (2011). [Human placental alkaline phosphatase (hPLAP) is the most frequently elevated serum marker in testicular cancer]. *Aktuelle Urologie*, *42*(5), 311–315. https://doi.org/10.1055/S-0031-1271545

Nicholson, D. W., Ali, A., Thornberry, N. A., Vaillancourt, J. P., Ding, C. K., Gallant, M., Gareau, Y., Griffin, P. R., Labelle, M., Lazebnik, Y. A., Munday, N. A., Raju, S. M., Smulson, M. E., Yamin, T. T., Yu, V. L., & Miller, D. K. (1995). Identification and inhibition of the ICE/CED-3 protease necessary for mammalian apoptosis. *Nature*, *376*(6535), 37–43. https://doi.org/10.1038/376037A0

Nisonoff, A., & Rivers, M. M. (1961). Recombination of a mixture of univalent antibody fragments of different specificity. *Archives of Biochemistry and Biophysics*, *93*(2), 460–462. https://doi.org/10.1016/0003-9861(61)90296-X

Ntouroupi, T. G., Ashraf, S. Q., McGregor, S. B., Turney, B. W., Seppo, A., Kim, Y., Wang, X., Kilpatrick, M. W., Tsipouras, P., Tafas, T., & Bodmer, W. F. (2008). Detection of circulating tumour cells in peripheral blood with an automated scanning fluorescence microscope. *British Journal of Cancer*, *99*(5), 789. https://doi.org/10.1038/SJ.BJC.6604545

O'Donnell, J. S., Teng, M. W. L., & Smyth, M. J. (2018). Cancer immunoediting and resistance to T cell-based immunotherapy. *Nature Reviews Clinical Oncology 2018 16:3*, *16*(3), 151–167. https://doi.org/10.1038/s41571-018-0142-8

Orsaria, M., Londero, A. P., Marzinotto, S., DI Loreto, C., Marchesoni, Di., & Mariuzzi, L. (2016). Placental type alkaline phosphatase tissue expression in ovarian serous carcinoma. *Cancer Biomarkers : Section A of Disease Markers*, *17*(4), 479–486. https://doi.org/10.3233/CBM-160665

Papamichael, D., Audisio, R. A., Glimelius, B., de Gramont, A., Glynne-Jones, R., Haller, D., Köhne, C. H., Rostoft, S., Lemmens, V., Mitry, E., Rutten, H., Sargent, D., Sastre, J., Seymour, M., Starling, N., van Cutsem, E., & Aapro, M. (2015). Treatment of colorectal cancer in older patients: International Society of Geriatric Oncology (SIOG) consensus recommendations 2013. *Annals of Oncology*, *26*(3), 463–476. https://doi.org/10.1093/ANNONC/MDU253

Pardoll, D. M. (2012). The blockade of immune checkpoints in cancer immunotherapy. *Nature Reviews Cancer 2012 12:4*, *12*(4), 252–264. https://doi.org/10.1038/nrc3239

Parkin, J., & Cohen, B. (2001a). An overview of the immune system. *The Lancet*, *357*(9270), 1777–1789. https://doi.org/10.1016/S0140-6736(00)04904-7

Parkin, J., & Cohen, B. (2001b). An overview of the immune system. *Lancet (London, England)*, *357*(9270), 1777–1789. https://doi.org/10.1016/S0140-6736(00)04904-7

Paul, S., Konig, M. F., Pardoll, D. M., Bettegowda, C., Papadopoulos, N., Wright, K. M., Gabelli, S. B., Ho, M., van Elsas, A., & Zhou, S. (2024). Cancer therapy with antibodies. *Nature Reviews. Cancer*, *24*(6), 399. https://doi.org/10.1038/S41568-024-00690-X

Peper, J. K., Schuster, H., Löffler, M. W., Schmid-Horch, B., Rammensee, H. G., & Stevanović, S. (2014a). An impedance-based cytotoxicity assay for real-time and label-free assessment of T-cell-mediated killing of adherent cells. *Journal of Immunological Methods*, *405*, 192–198. https://doi.org/10.1016/J.JIM.2014.01.012

Peper, J. K., Schuster, H., Löffler, M. W., Schmid-Horch, B., Rammensee, H. G., & Stevanović, S. (2014b). An impedance-based cytotoxicity assay for real-time and label-free assessment of T-cell-mediated killing of adherent cells. *Journal of Immunological Methods*, *405*, 192–198. https://doi.org/10.1016/J.JIM.2014.01.012

Pervez, S., Epenetos, A. A., Mooi, W. J., Evans, D. J., Rowlinson, G., Dhokia, B., & Krausz, T. (1988). Localization of monoclonal antibody auai and its F(ab')2 fragments in human tumour xenografts: An autoradiographic and immunohistochemical study. *International Journal of Cancer*, *41*(3 S), 23–29. https://doi.org/10.1002/IJC.2910410806

Pistoia, V., Tumino, N., Vacca, P., Veneziani, I., Moretta, A., Locatelli, F., & Moretta, L. (2018). Human γδ T-Cells: From Surface Receptors to the Therapy of High-Risk Leukemias. *Frontiers in Immunology*, *9*(MAY), 984. https://doi.org/10.3389/FIMMU.2018.00984

Pistritto, G., Trisciuoglio, D., Ceci, C., Alessia Garufi, & D'Orazi, G. (2016). Apoptosis as anticancer mechanism: function and dysfunction of its modulators and targeted therapeutic strategies. *Aging (Albany NY)*, *8*(4), 603. https://doi.org/10.18632/AGING.100934

Polyak, K. (2007). Breast cancer: origins and evolution. *The Journal of Clinical Investigation*, *117*(11), 3155–3163. https://doi.org/10.1172/JCI33295

Prager, I., Liesche, C., Van Ooijen, H., Urlaub, D., Verron, Q., Sandström, N., Fasbender, F., Claus, M., Eils, R., Beaudouin, J., Önfelt, B., & Watzl, C. (2019). NK cells switch from granzyme B to death receptor–mediated cytotoxicity during serial killing. *The Journal of Experimental Medicine*, *216*(9), 2113. https://doi.org/10.1084/JEM.20181454

Prestwich, R. J., Errington, F., Hatfield, P., Merrick, A. E., Ilett, E. J., Selby, P. J., & Melcher, A. A. (2008). The Immune System — is it Relevant to Cancer Development, Progression and Treatment? *Clinical Oncology*, *20*(2), 101–112. https://doi.org/10.1016/J.CLON.2007.10.011

Prinz, I., Silva-Santos, B., & Pennington, D. J. (2013a). Functional development of γδ T cells. *European Journal of Immunology*, *43*(8), 1988–1994. https://doi.org/10.1002/EJI.201343759

Prinz, I., Silva-Santos, B., & Pennington, D. J. (2013b). Functional development of γδ T cells. *European Journal of Immunology*, *43*(8), 1988–1994. https://doi.org/10.1002/EJI.201343759

Putnam, C. M., Kondeti, L., Kesler, M. B. A., & Varney, M. E. (2023). Modulating the immune system as a therapeutic target for myelodysplastic syndromes and acute myeloid leukemia. *Biochemistry and Cell Biology*, *101*(6), 481–495. https://doi.org/10.1139/BCB-2022-0374/ASSET/IMAGES/BCB-2022-0374_TAB4.GIF

Raimondi, E., Talarico, D., Moro, L., Rutter, W. J., Della Valle, G., & Decarli, L. (1988). Regional mapping of the human placental alkaline phosphatase gene (ALPP) to 2q37 by in situ hybridization. *Cytogenetics and Cell Genetics*, *47*(1–2), 98–99. https://doi.org/10.1159/000132518

Ransohoff, D. F. (2005). Colon Cancer Screening in 2005: Status and Challenges. *Gastroenterology*, *128*(6), 1685–1695. https://doi.org/10.1053/J.GASTRO.2005.04.005

Ray, A., Das, D. S., Song, Y., Richardson, P., Munshi, N. C., Chauhan, D., & Anderson, K. C. (2015). Targeting PD1–PDL1 immune checkpoint in plasmacytoid dendritic cell interactions with T cells, natural killer cells and multiple myeloma cells. *Leukemia*, *29*(6), 1441. https://doi.org/10.1038/LEU.2015.11

Reina-Campos, M., Scharping, N. E., & Goldrath, A. W. (2021). CD8+ T cell metabolism in infection and cancer. *Nature Reviews. Immunology*, *21*(11), 718. https://doi.org/10.1038/S41577-021-00537-8

Reiswich, V., Gorbokon, N., Luebke, A. M., Burandt, E., Menz, A., Kluth, M., Hube-Magg, C., Wittmer, C., Weidemann, S., Fraune, C., Möller, K., Lebok, P., Sauter, G., Simon, R., Uhlig, R., Wilczak, W., Jacobsen, F., Minner, S., Krech, R., … Krech, T. (2021). Pattern of placental alkaline phosphatase (PLAP) expression in human tumors: a tissue microarray study on 12,381 tumors. *The Journal of Pathology. Clinical Research*, *7*(6), 577–589. https://doi.org/10.1002/CJP2.237

Ribas, A. (2015). Adaptive immune resistance: How cancer protects from immune attack. *Cancer Discovery*, *5*(9), 915. https://doi.org/10.1158/2159-8290.CD-15-0563

Ross, S. L., Sherman, M., McElroy, P. L., Lofgren, J. A., Moody, G., Baeuerle, P. A., Coxon, A., & Arvedson, T. (2017a). Bispecific T cell engager (BiTE®) antibody constructs can mediate bystander tumor cell killing. *PLOS ONE*, *12*(8), e0183390. https://doi.org/10.1371/JOURNAL.PONE.0183390

Ross, S. L., Sherman, M., McElroy, P. L., Lofgren, J. A., Moody, G., Baeuerle, P. A., Coxon, A., & Arvedson, T. (2017b). Bispecific T cell engager (BiTE®) antibody constructs can mediate bystander tumor cell killing. *PloS One*, *12*(8). https://doi.org/10.1371/JOURNAL.PONE.0183390

Runcie, K., Budman, D. R., John, V., & Seetharamu, N. (2018a). Bi-specific and tri-specific antibodies- the next big thing in solid tumor therapeutics. *Molecular Medicine*, *24*(1), 1–15. https://doi.org/10.1186/S10020-018-0051-4/TABLES/5

Runcie, K., Budman, D. R., John, V., & Seetharamu, N. (2018b). Bi-specific and tri-specific antibodies- the next big thing in solid tumor therapeutics. *Molecular Medicine*, *24*(1), 1–15. https://doi.org/10.1186/S10020-018-0051-4/TABLES/5

Sallusto, F., Geginat, J., & Lanzavecchia, A. (2004). CENTRAL MEMORY AND EFFECTOR MEMORY T CELL SUBSETS: Function, Generation, and Maintenance. *Annu. Rev. Immunol*, *22*, 745–763. https://doi.org/10.1146/annurev.immunol.22.012703.104702

Samaranayake, H., Wirth, T., Schenkwein, D., Räty, J. K., & Ylä-Herttuala, S. (2009). Challenges in monoclonal antibody-based therapies. *Annals of Medicine*, *41*(5), 322–331. https://doi.org/10.1080/07853890802698842

Saura-Esteller, J., de Jong, M., King, L. A., Ensing, E., Winograd, B., de Gruijl, T. D., Parren, P. W. H. I., & van der Vliet, H. J. (2022). Gamma Delta T-Cell Based Cancer Immunotherapy: Past-Present-Future. *Frontiers in Immunology*, *13*, 915837. https://doi.org/10.3389/FIMMU.2022.915837

Schindelin, J., Arganda-Carreras, I., Frise, E., Kaynig, V., Longair, M., Pietzsch, T., Preibisch, S., Rueden, C., Saalfeld, S., Schmid, B., Tinevez, J. Y., White, D. J., Hartenstein, V., Eliceiri, K., Tomancak, P., & Cardona, A. (2012). Fiji: an open-source platform for biological-image analysis. *Nature Methods 2012 9:7*, *9*(7), 676–682. https://doi.org/10.1038/nmeth.2019

Seimetz, D., Lindhofer, H., & Bokemeyer, C. (2010). Development and approval of the trifunctional antibody catumaxomab (anti-EpCAM x anti-CD3) as a targeted cancer

immunotherapy. *Cancer Treatment Reviews*, *36*(6), 458–467. https://doi.org/10.1016/J.CTRV.2010.03.001

Sharma, U., Pal, D., & Prasad, R. (2014). Alkaline Phosphatase: An Overview. *Indian Journal of Clinical Biochemistry*, *29*(3), 269. https://doi.org/10.1007/S12291-013-0408-Y

Shi, J., Sun, Z., Gao, Z., Huang, D., Hong, H., & Gu, J. (2023). Radioimmunotherapy in colorectal cancer treatment: present and future. *Frontiers in Immunology*, *14*, 1105180. https://doi.org/10.3389/FIMMU.2023.1105180

Silberstein, S., Lenz, R., & Xu, C. (2015). Therapeutic Monoclonal Antibodies: What Headache Specialists Need to Know. *Headache*, *55*(8), 1171–1182. https://doi.org/10.1111/HEAD.12642

Smyth, M. J., Dunn, G. P., & Schreiber, R. D. (2006). Cancer Immunosurveillance and Immunoediting: The Roles of Immunity in Suppressing Tumor Development and Shaping Tumor Immunogenicity. *Advances in Immunology*, *90*, 1–50. https://doi.org/10.1016/S0065-2776(06)90001-7

Sonar, S., Nyahatkar, S., Kalele, K., & Adhikari, M. D. (2024). Role of DNA methylation in cancer development and its clinical applications. *Clinical and Translational Discovery*, *4*(1), e279. https://doi.org/10.1002/CTD2.279

Sonnemann, H. M., Pazdrak, B., Antunes, D. A., Roszik, J., & Lizée, G. (2023). Vestigial-like 1 (VGLL1): An ancient co-transcriptional activator linking wing, placenta, and tumor development. *Biochimica et Biophysica Acta (BBA) - Reviews on Cancer*, *1878*(3), 188892. https://doi.org/10.1016/J.BBCAN.2023.188892

Spiess, C., Zhai, Q., & Carter, P. J. (2015). Alternative molecular formats and therapeutic applications for bispecific antibodies. *Molecular Immunology*, *67*(2), 95–106. https://doi.org/10.1016/J.MOLIMM.2015.01.003

Spurr, N. K., Durbin, H., Sheer, D., Parkar, M., Bobrow, L., & Bodmer, W. F. (1986). Characterization and chromosomal assignment of a human cell surface antigen defined by the monoclonal antibody AUAI. *International Journal of Cancer*, *38*(5), 631–636. https://doi.org/10.1002/IJC.2910380503

Sterner, R. C., & Sterner, R. M. (2021). CAR-T cell therapy: current limitations and potential strategies. *Blood Cancer Journal*, *11*(4), 69. https://doi.org/10.1038/S41408-021-00459-7

Su, Y., Zhang, X., Bidlingmaier, S., Behrens, C. R., Lee, N. K., & Liu, B. (2020a). ALPPL2 Is a Highly Specific and Targetable Tumor Cell Surface Antigen. *Cancer Research*, *80*(20), 4552–4564. https://doi.org/10.1158/0008-5472.CAN-20-1418

Su, Y., Zhang, X., Bidlingmaier, S., Behrens, C. R., Lee, N. K., & Liu, B. (2020b). ALPPL2 is a highly specific and targetable tumor cell surface antigen. *Cancer Research*, *80*(20), 4552. https://doi.org/10.1158/0008-5472.CAN-20-1418

Su, Y., Zhang, X., Bidlingmaier, S., Behrens, C. R., Lee, N. K., & Liu, B. (2020c). ALPPL2 Is a Highly Specific and Targetable Tumor Cell Surface Antigen. *Cancer Research*, *80*(20), 4552–4564. https://doi.org/10.1158/0008-5472.CAN-20-1418

Su, Y., Zhang, X., Bidlingmaier, S., Behrens, C. R., Lee, N. K., & Liu, B. (2020d). ALPPL2 is a highly specific and targetable tumor cell surface antigen. *Cancer Research*, *80*(20), 4552. https://doi.org/10.1158/0008-5472.CAN-20-1418

Su, Y., Zhang, X., Bidlingmaier, S., Behrens, C. R., Lee, N. K., & Liu, B. (2020e). ALPPL2 is a highly specific and targetable tumor cell surface antigen. *Cancer Research*, *80*(20), 4552. https://doi.org/10.1158/0008-5472.CAN-20-1418

Sulaiman, S., & Marciani, L. (2019). MRI of the Colon in the Pharmaceutical Field: The Future before us. *Pharmaceutics*, *11*(4), 146. https://doi.org/10.3390/PHARMACEUTICS11040146

Sun, L., Su, Y., Jiao, A., Wang, X., & Zhang, B. (2023a). T cells in health and disease. *Signal Transduction and Targeted Therapy*, *8*(1). https://doi.org/10.1038/S41392-023-01471-Y

Sun, L., Su, Y., Jiao, A., Wang, X., & Zhang, B. (2023b). T cells in health and disease. *Signal Transduction and Targeted Therapy*, *8*(1), 235. https://doi.org/10.1038/S41392-023-01471-Y

Sun, L., Su, Y., Jiao, A., Wang, X., & Zhang, B. (2023c). T cells in health and disease. *Signal Transduction and Targeted Therapy*, *8*(1). https://doi.org/10.1038/S41392-023-01471-Y

Sutton, V. R., Davis, J. E., Cancilla, M., Johnstone, R. W., Ruefli, A. A., Sedelies, K., Browne, K. A., & Trapani, J. A. (2000). Initiation of Apoptosis by Granzyme B Requires Direct Cleavage of Bid, but Not Direct Granzyme B–Mediated Caspase Activation. *The Journal of Experimental Medicine*, *192*(10), 1403. https://doi.org/10.1084/JEM.192.10.1403

Suurs, F. V., Lub-de Hooge, M. N., de Vries, E. G. E., & de Groot, D. J. A. (2019a). A review of bispecific antibodies and antibody constructs in oncology and clinical challenges. *Pharmacology & Therapeutics*, *201*, 103–119. https://doi.org/10.1016/J.PHARMTHERA.2019.04.006

Suurs, F. V., Lub-de Hooge, M. N., de Vries, E. G. E., & de Groot, D. J. A. (2019b). A review of bispecific antibodies and antibody constructs in oncology and clinical challenges. *Pharmacology & Therapeutics*, *201*, 103–119. https://doi.org/10.1016/J.PHARMTHERA.2019.04.006

Thakur, A., Huang, M., & Lum, L. G. (2018). Bispecific antibody based therapeutics: Strengths and challenges. *Blood Reviews*, *32*(4), 339–347. https://doi.org/10.1016/J.BLRE.2018.02.004

Thanikachalam, K., & Khan, G. (2019). Colorectal Cancer and Nutrition. *Nutrients 2019, Vol. 11, Page 164*, *11*(1), 164. https://doi.org/10.3390/NU11010164

Thrift, A. P., Gong, J., Peters, U., Chang-Claude, J., Rudolph, A., Slattery, M. L., Chan, A. T., Locke, A. E., Kahali, B., Justice, A. E., Pers, T. H., Gallinger, S., Hayes, R. B., Baron, J. A., J.caan, B., Ogino, S., Berndt, S. I., Chanock, S. J., Casey, G., … Campbell, P. T. (2015). Mendelian Randomization Study of Body Mass Index and Colorectal Cancer Risk. *Cancer Epidemiology, Biomarkers & Prevention : A Publication of the American Association for Cancer Research, Cosponsored by the American Society of Preventive Oncology*, *24*(7), 1024–1031. https://doi.org/10.1158/1055-9965.EPI-14-1309

Tomar, N., & De, R. K. (2014). A brief outline of the immune system. *Methods in Molecular Biology*, *1184*, 3–12. https://doi.org/10.1007/978-1-4939-1115-8_1/TABLES/3

Travers, P., & Bodmer, W. (1984a). Preparation and characterization of monoclonal antibodies against placental alkaline phosphatase and other human trophoblast-associated determinants. *International Journal of Cancer*, *33*(5), 633–641. https://doi.org/10.1002/IJC.2910330514

Travers, P., & Bodmer, W. (1984b). Preparation and characterization of monoclonal antibodies against placental alkaline phosphatase and other human trophoblast-associated determinants. *International Journal of Cancer*, *33*(5), 633–641. https://doi.org/10.1002/IJC.2910330514

Tucker, D. F., Oliver, R. T. D., Travers, P., & Bodmer, W. F. (1985). Serum marker potential of placental alkaline phosphatase-like activity in testicular germ cell tumours evaluated by H17E2 monoclonal antibody assay. *British Journal of Cancer*, *51*(5), 631. https://doi.org/10.1038/BJC.1985.95

Vacca, P., Munari, E., Tumino, N., Moretta, F., Pietra, G., Vitale, M., Del Zotto, G., Mariotti, F. R., Mingari, M. C., & Moretta, L. (2018). Human natural killer cells and other innate lymphoid cells in cancer: Friends or foes? *Immunology Letters*, *201*, 14–19. https://doi.org/10.1016/J.IMLET.2018.11.004

van der Gun, B. T. F., Melchers, L. J., Ruiters, M. H. J., de Leij, L. F. M. H., McLaughlin, P. M. J., & Rots, M. G. (2010). EpCAM in carcinogenesis: the good, the bad or the ugly. *Carcinogenesis*, *31*(11), 1913–1921. https://doi.org/10.1093/CARCIN/BGQ187

Vengerov, Y. Y., Gudima, S. O., Voronov, A. V., & Votrin, I. I. (1988). Immunochemical studies of human placental alkaline phosphatase in normal and neoplastic tissues. *Advances in Enzyme Regulation*, *27*(C), 345–352. https://doi.org/10.1016/0065-2571(88)90025-8

Vieira, L. M., Jorge, N. A. N., de Sousa, J. B., Setubal, J. C., Stadler, P. F., & Walter, M. E. M. T. (2021). Competing Endogenous RNA in Colorectal Cancer: An Analysis for Colon, Rectum, and Rectosigmoid Junction. *Frontiers in Oncology*, *11*, 681579. https://doi.org/10.3389/FONC.2021.681579

Volpe, E., Sambucci, M., Battistini, L., & Borsellino, G. (2016). Fas–Fas Ligand: Checkpoint of T Cell Functions in Multiple Sclerosis. *Frontiers in Immunology*, *7*(SEP), 27. https://doi.org/10.3389/FIMMU.2016.00382

Wang, C., Ye, Y., Hu, Q., Bellotti, A., & Gu, Z. (2017). Tailoring Biomaterials for Cancer Immunotherapy: Emerging Trends and Future Outlook. *Advanced Materials*, *29*(29), 1606036. https://doi.org/10.1002/ADMA.201606036

Wang, C., Zhang, Y., & Dong, Y. (2021). Lipid Nanoparticle-mRNA Formulations for Therapeutic Applications. *Accounts of Chemical Research*, *54*(23), 4283–4293. https://doi.org/10.1021/ACS.ACCOUNTS.1C00550

Weinstein, J. N., Collisson, E. A., Mills, G. B., Shaw, K. R. M., Ozenberger, B. A., Ellrott, K., Sander, C., Stuart, J. M., Chang, K., Creighton, C. J., Davis, C., Donehower, L., Drummond, J., Wheeler, D., Ally, A., Balasundaram, M., Birol, I., Butterfield, Y. S. N., Chu, A., … Kling, T. (2013). The Cancer Genome Atlas Pan-Cancer analysis project. *Nature Genetics 2013 45:10*, *45*(10), 1113–1120. https://doi.org/10.1038/ng.2764

Went, P. T., Lugli, A., Meier, S., Bundi, M., Mirlacher, M., Sauter, G., & Dirnhofer, S. (2004). Frequent EpCam protein expression in human carcinomas. *Human Pathology*, *35*(1), 122–128. https://doi.org/10.1016/J.HUMPATH.2003.08.026

Wik, J. A., & Skålhegg, B. S. (2022). T Cell Metabolism in Infection. *Frontiers in Immunology*, *13*. https://doi.org/10.3389/FIMMU.2022.840610

Williams, G. H., McLaughlin, P. J., & Johnson, P. M. (1986). Tissue origin of serum placental-like alkaline phosphatase in cigarette smokers. *Clinica Chimica Acta*, *155*(3), 329–333. https://doi.org/10.1016/0009-8981(86)90252-4

Wu, L., Wang, W., Tian, J., Qi, C., Cai, Z., Yan, W., Xuan, S., & Shang, A. (2021). Engineered mRNA-expressed bispecific antibody prevent intestinal cancer via lipid nanoparticle delivery. *Bioengineered*, *12*(2), 12383. https://doi.org/10.1080/21655979.2021.2003666

Wu, Z., & Cheung, N. V. (2017). T cell engaging bispecific antibody (T-BsAb): from technology to therapeutics. *Pharmacology & Therapeutics*, *182*, 161. https://doi.org/10.1016/J.PHARMTHERA.2017.08.005

Wu, Z., & Cheung, N. V. (2018). T cell engaging bispecific antibody (T-BsAb): from technology to therapeutics. *Pharmacology & Therapeutics*, *182*, 161. https://doi.org/10.1016/J.PHARMTHERA.2017.08.005

Yatim, K. M., & Lakkis, F. G. (2015). A Brief Journey through the Immune System. *Clinical Journal of the American Society of Nephrology : CJASN*, *10*(7), 1274. https://doi.org/10.2215/CJN.10031014

Yekehfallah, V., Pahlavanneshan, S., Sayadmanesh, A., Momtahan, Z., Ma, B., & Basiri, M. (2022a). Generation and Functional Characterization of PLAP CAR-T Cells against Cervical Cancer Cells. *Biomolecules*, *12*(9). https://doi.org/10.3390/BIOM12091296/S1

Yekehfallah, V., Pahlavanneshan, S., Sayadmanesh, A., Momtahan, Z., Ma, B., & Basiri, M. (2022b). Generation and Functional Characterization of PLAP CAR-T Cells against Cervical Cancer Cells. *Biomolecules*, *12*(9), 1296. https://doi.org/10.3390/BIOM12091296/S1

Zajac, P., Schultz-Thater, E., Tornillo, L., Sadowski, C., Trella, E., Mengus, C., Iezzi, G., & Spagnoli, G. C. (2017). MAGE-A antigens and cancer immunotherapy. *Frontiers in Medicine*, *4*(MAR), 18. https://doi.org/10.3389/FMED.2017.00018/FULL

ZEISS Axioscan 7 Microscope Slide Scanner. (n.d.). Retrieved June 13, 2024, from https://www.zeiss.com/microscopy/en/products/imaging-systems/axioscan-for-biology.html?utm_source=google&utm_medium=cpc&utm_campaign=C-00011305&utm_content=global&gad_source=1&gclid=EAIaIQobChMI44bGkuTYhgMV3o1QBh3QJAAVEAAYAyAAEgIBmfD_BwE

Zellmer, V. R., & Zhang, S. (2014). Evolving concepts of tumor heterogeneity. *Cell and Bioscience*, *4*(1), 1–8. https://doi.org/10.1186/2045-3701-4-69/FIGURES/2

Zhao, W., Jin, L., Chen, P., Li, D., Gao, W., & Dong, G. (2022a). Colorectal cancer immunotherapy-Recent progress and future directions. *Cancer Letters*, *545*, 215816. https://doi.org/10.1016/J.CANLET.2022.215816

Zhao, W., Jin, L., Chen, P., Li, D., Gao, W., & Dong, G. (2022b). Colorectal cancer immunotherapy-Recent progress and future directions. *Cancer Letters*, *545*, 215816. https://doi.org/10.1016/J.CANLET.2022.215816

Zhao, Y., Niu, C., & Cui, J. (2018). Gamma-delta (γδ) T cells: friend or foe in cancer development? *Journal of Translational Medicine*, *16*(1), 3. https://doi.org/10.1186/S12967-017-1378-2

Zhao, Z., Li, T., Yuan, Y., & Zhu, Y. (2023). What is new in cancer-associated fibroblast biomarkers? *Cell Communication and Signaling : CCS*, *21*(1). https://doi.org/10.1186/S12964-023-01125-0

Zhu, J., Yamane, H., & Paul, W. E. (2010). Differentiation of Effector CD4 T Cell Populations. *Annual Review of Immunology*, *28*, 445. https://doi.org/10.1146/ANNUREV-IMMUNOL-030409-101212